Molecular Mechanisms of Drug-Induced Hepatic Steatosis

Inauguraldissertation

zur

Erlangung der Würde eines Doktors der Philosophie

vorgelegt der

Philosophisch-Naturwissenschaftlichen Fakultät

der Universität Basel

von

David Alexander Grünig

aus Burgistein, Bern

Basel, 2019

Genehmigt von der Philosophisch-Naturwissenschaftlichen Fakultät

auf Antrag von

Prof. Stephan Krähenbühl

Prof. Jörg Huwyler

Basel, den 26. Juni 2018

Prof. Martin Spiess (Dekan)

TABLE OF CONTENTS

SUMMARY

Steatosis of the liver is defined by an excess accumulation of intracellular triglycerides within the hepatocytes. Nonalcoholic fatty liver disease ranges from simple steatosis to nonalcoholic steatohepatitis. It is a serious health problem worldwide, reported to affect 15 – 30 % of the population in developed countries. Inordinate accumulation of fat is damaging to the liver, because high levels of triglycerides, free fatty acids, or intermediates of lipid metabolism are extremely problematic for a cell. A further problem is that nonalcoholic fatty liver disease can be a risk factor for developing adverse reactions to drugs, interfering with hepatic lipid metabolism, leading to idiosyncratic drug-induced liver injury. Drug-induced liver injury has been the major cause of drugs failing market-approval or for later withdrawal from the market. An improved preclinical detectability of such adverse reactions would therefore be highly appreciated by the industry, as well as by patients.

The present work consists of three projects investigating molecular mechanisms of drug-induced hepatic steatosis *in vitro*, and is emphasizing on the application of an optimized method to measure the acylcarnitine pattern of cells, treated with toxicants. We focused on the measurement of acylcarnitines, because they are known to reflect the cellular acyl-CoA pattern, allowing us to make interpretations on the specific location of inhibition by a substance. Furthermore, the liquid chromatography-tandem mass spectrometry method, used for this determination, allows for a fast and economic workup and analysis of a high number of samples, applicable for high-throughput screenings. Additionally, the small sample volume needed for the analysis allows this assay to be linked together with many other 96-well format assays. An important finding in our study was that the acylcarnitine method repeatedly turned out to be a more sensitive approach to identify drugs inhibiting fatty acid oxidation, as the older, well-established methods, such as radio-enzymatic determination of β-oxidation inhibition, or lipid accumulation experiments.

In the first paper, we aimed to establish and optimize the semi-quantitative acylcarnitine measurement with three specific and well-characterized inhibitors of fatty acid oxidation. We compared, as well as supplemented, the results of the new method with older, well-established methods. In a second step of the study, we applied the same methods on three compounds, of which adverse reactions are not well understood, to obtain new insights about their steatogenic mechanisms.

In the two following papers, investigating the catechol-*O*-methyl-transferase inhibitors tolcapone and entacapone, we aimed to expand the knowledge of tolcapone-associated steatosis and liver toxicity observed in clinics. Entacapone was included as well, because of its structural similarity. We studied in detail effects on lipid metabolism, as well as on their actions on mitochondrial respiration and cell death, for a comprehensive toxicological study about the two drugs.

An accumulation of effects are compiled in the following graphical abstract (**Fig. 1).**

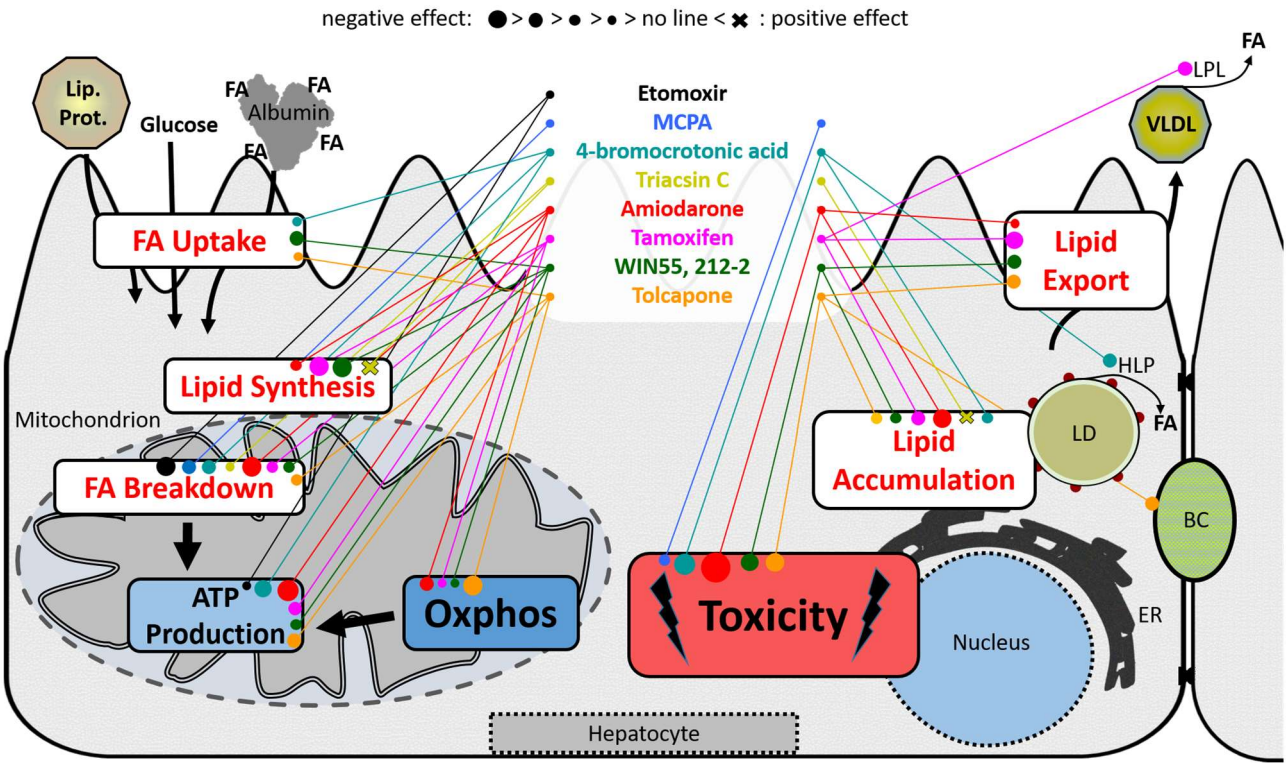

Fig. 1. Graphical abstract. Shown are the cumulated effects linked to the induction of hepatic steatosis of the substances used in this thesis from our own investigations as well as from literature. Negative effects can be upregulation of FA uptake, upregulation of lipid synthesis, decrease in FA breakdown, or decrease in lipid excretion. Furthermore, disruption of oxphos and cytotoxic potential on our cell models are displayed. Effects on ATP production, as well as lipid accumulation, both from measurements of our studies, may be secondary responses to effects of upstream processes. Negative effect (●) intensities are interpreted as overall relations of a compounds effects, such as lipid accumulation vs. cytotoxicity, or β-oxidation inhibition vs. lipid accumulation, and may therefore seem subjective. Furthermore, these intensities are chosen in relation to each other, neglecting substances outside the thesis. Missing connections indicate the lack of measurements or the lack in literature, incorporated in this thesis. Abbreviations: FA: fatty acid, Lip. Prot.: lipoprotein, VLDL: very-low densitiy lipoprotein, LD: lipid droplet, BC: bile canaliculus, oxphos: oxidative phosphorylation, ATP: adenosine triphosphate, ER: endoplasmic reticulum, LPL: lipoprotein lipase, HLP: hormone sensitive lipase.

ABBREVIATIONS

ACC:	Acetyl-CoA carboxylase
ACSL:	Acetyl-CoA synthetase
ADP:	Adenosine diphosphate
ADRP:	Adipose differentiation-related protein
ALT:	Alanine amino transferase
AMP:	Adenosine monophosphate
AMPK:	AMP-activated protein kinase
ApoB:	Apolipoprotein B
AST:	Aspartate amino transferase
ATP:	Adenosine triphosphate
CB:	Cannabinoid
COT:	Carnitine-octanoyl transferase
CPT:	Carnitine-palmitoyl transferase
DAG:	Diacylglycerol
DGAT:	Diacylglycerol acyltransferase
DILI:	Drug induced liver injury
DMSO:	Dimethyl sulfoxide
ER:	Endoplasmic reticulum
ESR:	Estrogen receptor
ETC:	Electron transfer chain
ETF:	Electron transferring flavoprotein
ETFDH:	ETF dehydrogenase
FABP:	Fatty acid binding protein
FADH:	Flavin adenine dinucleotide

FAS:	Fatty acid synthetase
FATP:	Fatty acid transport protein
FFA:	Free fatty acid
GPAM:	Mitochondrial glycerol-3-phosphate acyltransferase
GPAT:	Glyerol-3-phosphate acyltransferase
GSH:	Glutathione
LCFA:	Long-chain fatty acid
LD:	Lipid droplet
LPL:	Lipoprotein lipase
mtDNA:	Mitochondrial DNA
MTTP:	Microsomal triglyceride transfer protein
NADH:	Nicotinamide adenine dinucleotide
oxphos:	Oxidative phosphorylation
PHH:	Primary human hepatocytes
PKA:	Protein kinase A
PPAR:	Peroxisome proliferator activated receptor
ROS:	Reactive oxygen species
TCA:	Tricarboxylic acid cycle
TG:	Triglyceride
VLDL:	Very-low density lipoprotein

1. INTRODUCTION

1.1 Fat

This thesis is revolved around lipids. Fat, oil, lard, dripping, butter, blubber, schmaltz, lard, ghee, grease, smen, or any other form or name it appears in our diet or physiology, they practically accompany us and every other animal throughout our life.

Essentially, fats (solid at room temperature) and oils (liquid at room temperature) are mainly composed of fatty acids (FAs) and glycerol linked by an ester bond, so called triglycerides (TGs) **(Fig. 2)**. Lipids, however, are not only TGs. They are defined as any class of organic compounds that are insoluble in water [4]. In our diet the predominant dietary lipids are TGs, phospholipids, and cholesterol [5]. They provide 30 – 40 % of our total food energy intake [6,7], which is not surprising, as fat has the highest energy density (kcal/g) of all foods. As comparison, pure sugar has approximately half of the calories per gram than olive oil [8].

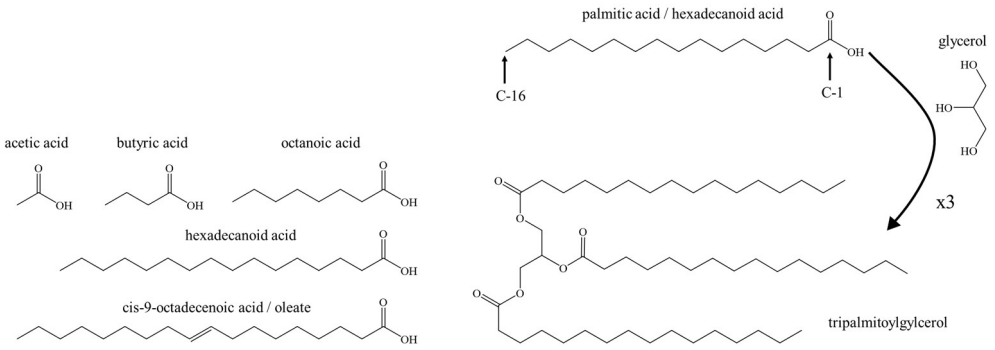

Fig. 2. Nomenclature and chemical structures of fatty acids, triglycerides and relevant precursors.

The main bulk of energy originates from FAs, which derive from lipids through efficient breakdown, as discussed in detail in further sections. FAs are not only weighty regarding calories, but they also have many other functions in our bodies. They are first and foremost integral components of all cellular membranes. They affect signal transductions and protein binding [9] and also act as precursors for hormones and substrates in signaling pathways [10]. Therefore, it is unsurprising that the body has to tightly regulate the metabolism of such biologically important substances.

1.1.1 Digestion and Uptake

Lipid absorption and subsequent systemic distribution, as well as storage, have been extensively investigated early on [7,11,12]. Currently, numerous articles are published on the topic, giving a more comprehensive overview over the fate of dietary lipids [3,5,10,13]. As they are water insoluble compounds, they have to be markedly altered prior to uptake. Fat absorption requires a complex series of events involving gastric, intestinal, biliary, and pancreatic functions [7].

Already the first contact with our body, when long-chain FAs come in contact with our tongue, prepares the digestive system for lipid intake. The FA transporter CD36 is expressed on the taste buds of the tongue, leading to a cephalic response, in order to prepare the gastrointestinal tract for optimal absorption. These FA-sensing receptors are expressed throughout the upper gastro intestinal tract, as well as in numerous other tissues. The actual digestion of TGs starts also in the mouth and stomach, where a lingual lipase and gastric lipase are expressed and secreted.

Lipases are the main enzymes responsible for making lipids suitable for uptake. They hydrolyze the ester bonds of two acyl-chains of a TG to yield free FAs and monoacyl glycerol. The main share of lipase action on dietary lipids, however, is done by the pancreatic lipase. Bile acids, originating from the liver, have a central role in the digestion of lipids as well. They help to form micelles that disperse the water-insoluble lipids and make them more available for protein-digestion as well as for uptake by enterocytes in the small intestine. Free FAs, monoacyl glycerols, free cholesterol, cholesterol esters, plant sterols, and phospholipids, upon uptake by the enterocyte, are either degraded for resynthetization or directly packed into lipid droplets (LDs) at the apical side of the cells for further use.

1.1.2 Distribution and Storage

The lipids within the enterocytes are eventually excreted to the lymph over complex mechanisms. This export starts with the synthesis of apolipoprotein B48 (ApoB48), which is rapidly loaded with TGs. After initial lipid loading, membrane formation with free cholesterol and phospholipids occurs, following a secondary core expansion with more TGs and cholesteryl esters. After subsequent budding from the endoplasmic reticulum (ER), this early form of a chylomicron fuses with the Golgi, where this vesicle undergoes further modifications, such as addition of other lipoproteins and protein glycosylation. Mature chylomicrons are finally released from the basolateral side via exocytosis and enter the circulation at the thoracic duct **(Fig. 3)**.

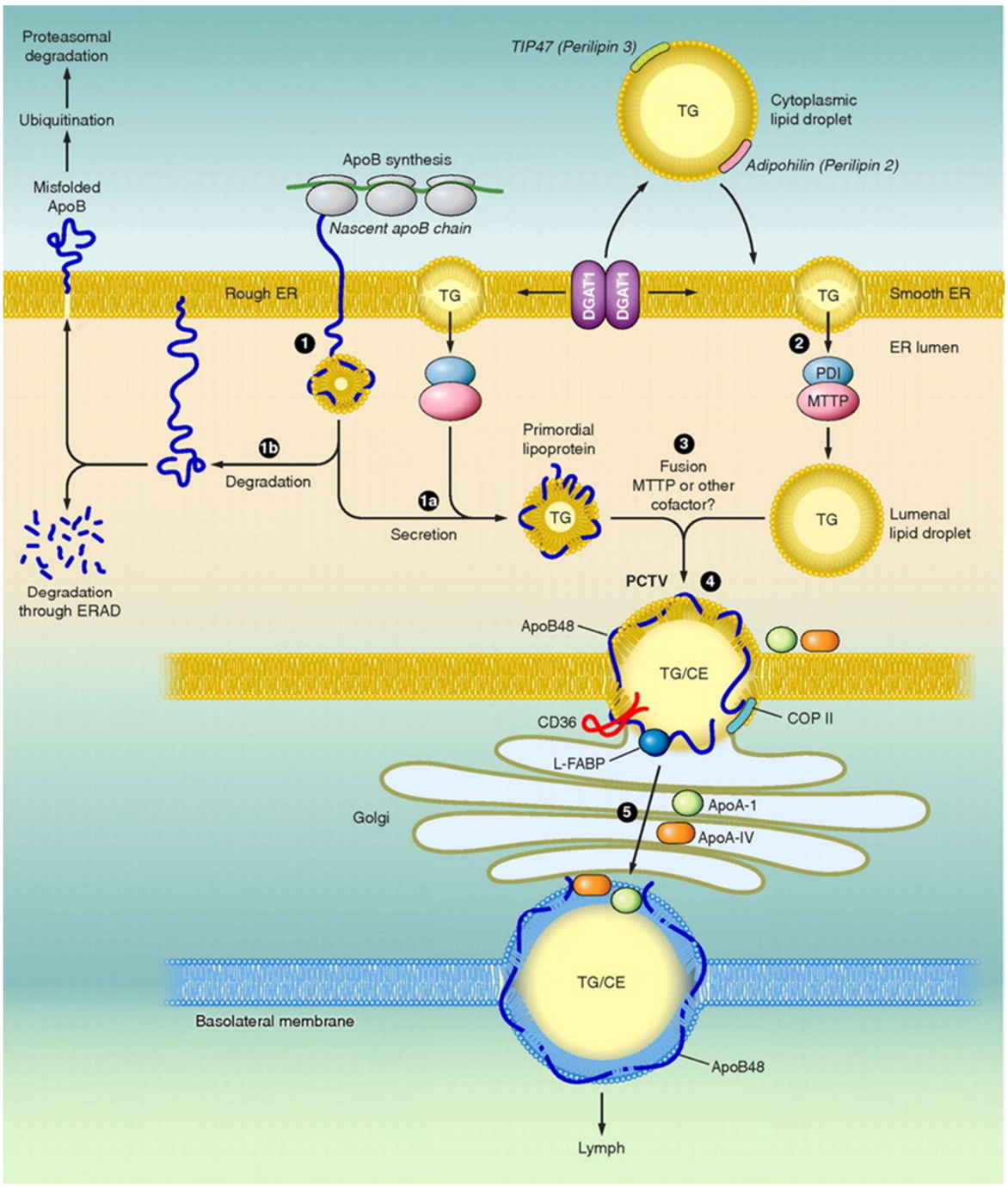

Fig. 3. Schematic representation of intestinal lipoprotein assembly. In a first step, the nascent ApoB48 polypeptide is co-translationally translocated across the rough ER membrane (1). When lipids are available within the ER membrane, physical interactions between ApoB48 and MTTP promote optimal folding and biogenesis of a primordial lipoprotein particle (1a). MTTP resides as a heterodimeric complex with the chaperone protein PDI. MTTP also promotes mobilization of TG-rich lipid droplets from the smooth ER membrane into the lumen of the ER, to emerge as luminal lipid droplets (2). When TG availability is limited or MTTP function is impaired, nascent ApoB becomes misfolded and is degraded (1b). During the second step of lipoprotein assembly, the primordial particle fuses with luminal lipid droplets, resulting in a core expansion, which gives so called pre-chylomicron transport vesicles (PCTVs) (3). Other proteins, including CD36 and L-FABP, participate in the TG loading of PCTV as well. After fusion with vesicular transport proteins, like COP II, the pre-chylomicron particles are incorporated into a vesicular complex that buds from the ER and fuses with the Golgi apparatus. Vectorial transport of these pre-chylomicron particles (4) results in their continued maturation by the addition of further proteins and glycosylation. Eventually, mature chylomicron particles are secreted into the lymphatic capillaries (5). The scheme is adapted from Abumrand and Davidson [3]. Abbreviations: Apo: apolipoprotein, CD36: fatty acid translocase / cluster of differentiation 36, CE: cholesterol ester, COP II: coat protein 2, ER: endoplasmic reticulum, ERAD: ER-associated degradation pathways, L-FABP: fatty acid binding protein 1, MTTP: microsomal triglyceride transfer protein, PCTV: pre-chylomicron transport vesicle, PDI: protein disulfide isomerase, TG: triglyceride.

The synthesis, maturation and excretion of chylomicrons is very similar to the pathway of hepatocytes excreting TGs, using very-low-density lipoprotein (VLDL), which is discussed in more detail below. Chylomicrons, as VLDL, are lipoproteins in the circulation for the purpose of distributing energy-rich TGs to different tissues. As explained above, chylomicrons originate from the intestine and VLDL from the liver, two tissues with highly active lipid metabolism. A key player of lipoprotein metabolism is the lipoprotein lipase (LPL), which is synthesized in skeletal muscle, heart, and adipose tissue [14]. After export from the aforementioned tissues, the LPL is attached to the endothelium of adjacent blood capillaries. LPL binds to circulating lipoproteins and hydrolyzes the TGs, they carry in their cores, into FAs. These are then taken up by the cells through fatty acid transport proteins (FATPs), like for example by the CD36 transporter.

During the loss of about 50% of lipids from the core of chylomicrons or VLDL vesicles, a series of specific apolipoprotein exchanges take place, as well as the enrichment of cholesteryl esters. One important lipoprotein exchange is the acquisition of ApoE, originating from the interaction with high-density lipoprotein (HDL). These changes lead chylomicrons and VLDL vesicles to change in appearance and nomenclature. Chylomicrons mature to chylomicron remnants and VLDL to intermediate-density lipoprotein (IDL) and further to low-density lipoprotein (LDL). These matured lipoproteins are then targets for the liver, which removes them from the circulation [14,15].

The majority of new chylomicrons reach the adipose tissue for storage until times of negative energy balance [16]. Although enterocytes and hepatocytes have a high capacity to store TGs, the main location of fat storage are the adipocytes within the fatty tissue. This tissue is able to fine-tune uptake and release of lipids, in order to adapt precisely to various metabolic states. Many different signals can affect lipolysis and export activity of adipocytes, as for example the stimulation by the autonomic nervous system, insulin, catecholamines, or cytokines [17]. In order to supply extra-adipose tissue with energy, the adipocyte has to mobilize and excrete these TGs, which are stored in the huge LDs within the cell. This pathway is considerably simpler than the lipoprotein-pathway, which is the predominant export-pathway of hepato- and enterocytes. In adipocytes, TGs are hydrolyzed on the surface of LDs through well-controlled mechanisms, mainly involving the enzyme hormone-sensitive lipase. After hydrolysis of TGs, free FAs are finally transported by the fatty acid binding protein 4 (FABP4) out of the cell [18]. Free FAs have an abysmal solubility in water at 37° C (in the nM range for palmitate and oleate [19]), however, levels in the circulation are around 0.3 mM. This enhanced solubility is possible because of the plasma protein albumin. This protein is responsible for many transport functions, like the distribution of free FAs, of which it can bind 0.1 – 2 moles per mole protein [20]. These two different mechanisms of lipid distribution (by lipoproteins or bound to albumin) throughout the circulation ensure proper supply of tissues that are in need of energy.

1.2 Hepatic Energy Metabolism

Located under the rib cage and below the diaphragm in the upper-right abdominal cavity, the liver resides just above the small intestine. In the adult body it weighs about 1.5 – 2 kg and is made up of two main lobes (left and right), which are subdivided into smaller hepatic lobules. The liver is not only supplied with blood by the hepatic artery but also by the portal vein, making up 30% and 70% of the blood flow, respectively. About 25% of the cardiac output is received by the liver, mostly due to its high oxygen requirements and relative desaturation of oxygen in the portal venous blood [21]. This organ has many essential functions, such as production of bile acids, protein synthesis, iron homeostasis, filtering of nutrients and antigens, and of course carbohydrate and lipid metabolism [22]. A specific hepatic function, for example, is to supply extrahepatic tissues with energy. This is especially important for the brain, which heavily relies on the liver under low glucose conditions. For this purpose, it not only excretes VLDL, but hepatic tissue also oxidizes FAs to synthetize ketone bodies over the HMG-CoA pathway for further secretion. Acetoacetate and 3-hydroxybutyrate are the two predominant products of hepatic ketogenesis. After uptake in extrahepatic tissue, they are metabolized back into acetyl-CoA within the cells and are then ready to be used for adenosine triphosphate (ATP) production [23].

1.2.1 Liver Mitochondria

Like in most other tissues, energy metabolism in liver cells are closely linked to their mitochondria. Not without reason, they are called “the powerhouse of the cell”. Mitochondria are organelles within eukaryotic cells and originate from free living proteobacteria by endosymbiosis [24]. They retained some of their circular DNA, of which they contain several copies. In humans the mitochondrial DNA encodes for 37 genes, of which 13 are polypeptides, located in the electron transfer chain (ETC) [25]. The remaining 24 genes are used for a functional translation of the 13 mitochondrially encoded proteins. Within the cell mitochondria are arranged as a network (**Fig. 4a**) and they orchestrate energy metabolism by substrate catabolism, as well as anabolism.

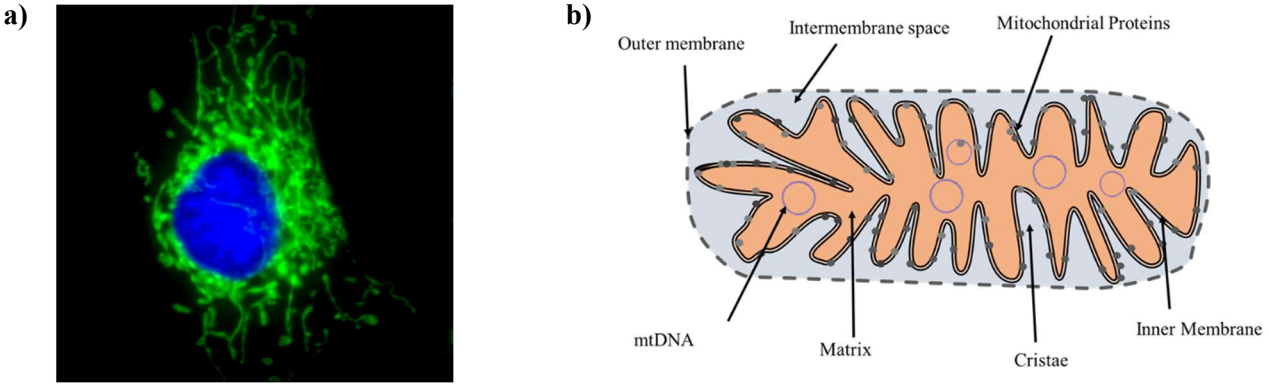

Fig. 4. Mitochondrial structure and network. a) Fluorescent staining of mitochondrial network in HepG2 cells. Green color represents Mito Tracker green dye for mitochondria, blue color represents Hoechst 33342 dye for DNA (nucleus). The mitochondrial network, as well as single mitochondria are visible, with highest density around the nucleus. The picture was taken on an Olympus IX83 microscope, using a 100x objective. b) Schematic representation of mitochondrial morphology.

The mitochondrial network in hepatocytes is closely regulated in response to the metabolic state and other intracellular or environmental signals. Within the cell, the network of mitochondria undergoes constant change, as biogenesis and selective autophagy (mitophagy) adapt the mitochondrial content in the cell. This promotes, when under stress, a pool of functionally intact mitochondria [26,27]. These processes are very complex and rely on many interactions of nuclear and mitochondrial factors.

A way for the cell to produce ATP without mitochondria is glycolysis. Necessary enzymes are located in the cytosol, converting glucose to pyruvate, which yields two ATP per molecule glucose. In mitochondria, however, one glucose molecule, used for oxidative phosphorylation, yields 36 ATP. Therefore, it is not surprising that mitochondria make up a significant amount of the cell's volume. In such a metabolically active cell, like the hepatocyte, the mean volume density is an impressive 27% [28]. Ultimately, mitochondria are the main energy-supply, in form of ATP, for the cell.

Each mitochondrion is enclosed by two membranes. The outer mitochondrial membrane smoothly envelopes and separates the organelles from the cytosol. Channels (porins) spanning through the outer mitochondrial membrane enable compounds under 5000 Da to pass freely into the inter-membrane space [29]. The inner mitochondrial membrane, on the other hand, is a folded membrane, forming multiple invaginations, the so called cristae, into the mitochondrial matrix **(Fig. 4b)**. Unlike the outer, the inner membrane is tight, which is especially important for retaining a proton-gradient across it. The proton gradient is built by the ETC, which actively pumps protons out of the mitochondria.

Oxidative phosphorylation (oxphos) is an indispensable process for energy production in the cell. It consists of two linked processes, consisting of five complexes in total. Firstly, Complexes I - IV constitute the ETC, which produces a proton-gradient by oxidation of reduced substrates. This oxidation of substrates leads Complexes I, III, and IV to pump H^+ out of the mitochondrial matrix, establishing a transmembrane potential. In a second step, this proton gradient is then used by the ATP-synthase, also called Complex V, for phosphorylation of ADP by inorganic phosphate. Proton influx through the membrane spanning part of the enzyme causes rotation of the catalytic part. Ultimately, this rotation-energy is used for the phosphorylation of ADP **(Fig. 5)**.

Accordingly, the maintenance of the mitochondrial membrane potential ($\Delta\Psi$) is of utmost importance for a functional energy production by mitochondria. Several compounds are known to interfere with this potential by channeling protons through the membrane. These so-called uncouplers are usually lipophilic weak acids, which get protonated in the inter-membrane space, where the pH is low, then diffusing across the membrane. In the matrix, where the pH is higher, they lose the proton and thus circumvent the translocation of protons by Complex V, ultimately stimulating respiration by Complex I-IV, however, without the synthesis of ATP. The first known uncoupler, 2,4-dinitrophenol, was observed in 1885 by French scientists, showing acceleration of metabolism and increase in body temperature in dogs [30]. It then was investigated thoroughly during the First World War, because of increased numbers of dying workers in explosive factories, manufacturing shells and

hand grenades containing this substance. Poisoned workers showed very high body temperatures (up to 45° C), gastro-intestinal disturbances, anorexia, nausea, loss of weight, and immediate rigor mortis after death, which led to preventive measures, like the placing of asbestos curtains, washable gloves, daily baths and change of clothes, or other sanitary- and also eating-regulations. Furthermore, 2,4-dinitrophenol also caused many casualties in the 1930s, when it was observed, that women were taking the compound to induce weight loss [31].

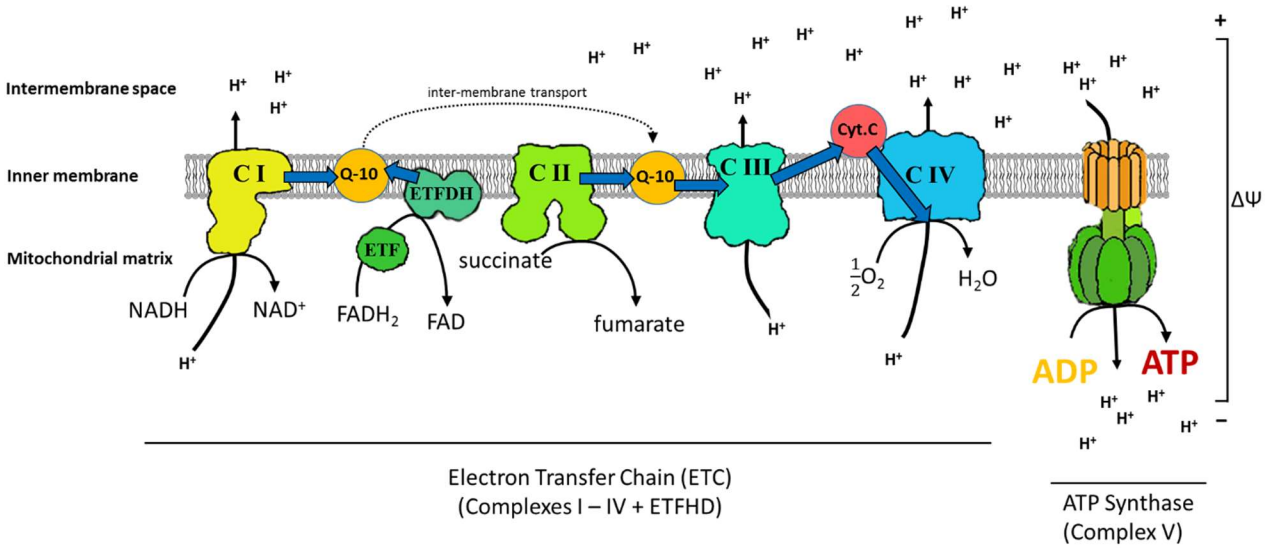

Fig. 5. Oxidative phosphorylation pathway (oxphos). The process of oxidative phosphorylation is the main pathway within the cell to produce ATP. It consist of two distinct processes embedded into the inner mitochondrial membrane, the ETC and the ATP synthase (Complex V). In the ETC reduced substrates, such as NADH, FADH2, and succinate are oxidized by the NADH-ubiquinone oxidoreductase (Complex I), ETFDH, and succinate-CoenzymeQ reductase (Complex II), respectively. These proteins transfer electrons from their substrates onto Q-10, which is substrate for the CoenzymeQ-cytochrome c oxidoreductase (Complex III). Q-10 is a highly lipophilic substance, able to diffuse within the inner mitochondrial membrane. Complex III transfers the electrons from Q-10 onto cytochrome c, a water-soluble electron carrier, located at the surface of the inner mitochondrial membrane, in the inter-membrane space. In the final step of the ETC, cytochrome c oxidase (Complex IV) uses the electrons from reduced Q-10 to reduce molecular oxygen to water. In the process of transferring electrons Complex I, III, and IV actively move protons (H+) from the mitochondrial matrix to the inter-membrane space, forming the mitochondrial membrane potential (ΔΨ). This potential is ultimately used by the ATP Synthase (Complex V) to form ATP from ADP and an inorganic phosphate. The reverse proton pumping action of this enzyme leads to a rotation of the subunit facing into the mitochondrial matrix. This rotational energy causes conformational changes in the catalytic sites of the enzyme, allowing it to bind ADP and a phosphate, fusing the two, and finally releasing ATP. The shapes of the enzymes in this scheme are based on crystal-structures, however, in reality the enzymes of oxphos are arranged together as supercomplexes. Abbreviations: ETC: electron transfer chain, ETFDH: electron-transferring-flavoprotein dehydrogenase, Q-10: coenzymeQ10.

Naturally, for their proton translocation, Complexes I-V are therefore integrated in the inner mitochondrial membrane. Complex II, the succinate-coenzyme Q reductase, links the oxphos pathway with the Krebs-cycle, which is also called tricarboxylic acid cycle (TCA). Located in the mitochondrial matrix, the TCA connects the protein, carbohydrate and lipid metabolism. Eight enzymes carry out a series of reactions that completely oxidize acetate (as acetyl-CoA) into two molecules of carbon dioxide and water. One cycle yields three NADH and one $FADH_2$, further fueling the ETC.

Lastly, long-chain FAs catabolism yields a notable amount of acetyl-CoA for further metabolism and energy production. Relevant pathways and connections concerning lipids are discussed in detail in the next section.

1.2.2 Hepatic Lipid Metabolism in Detail

Besides enterocytes and adipose tissue, the liver is the main organ for metabolism of lipids. Within the liver, which harbors many different cell types, the hepatocytes are responsible for the bulk of lipid metabolism in this organ. On a cellular level, the organelles, most involved in the metabolism of lipids, are the mitochondria, wherein the most important lipid metabolism pathways take place. High levels of unesterified FAs within the cell can pose a serious problem and cause lipotoxicity. In order to avoid overload as well as deprivation, lipid metabolism has to be closely coordinated by the cell. There are five major ways with which the hepatocyte can adapt levels of intracellular TG, free FAs, and intermediates: **Uptake, degradation, synthesis, storage, and excretion**.

1.2.2.1 Uptake and Activation

FAs circulate in plasma mostly bound to serum albumin. The cellular uptake mechanism is quite complex involving dissociation of FAs from serum albumin and transport across the cell membrane. Although not the only uptake mechanism for lipoproteins, the low-density lipoprotein receptor (LDLR) expressed on hepatocytes recognizes and binds ApoE for subsequent uptake by the cell. When ApoE is present on former VLDL or chylomicron particles, one speaks of remnant-lipoproteins, for which the liver has a high affinity for clearance from the circulation [15].

Free short- and medium-chain FAs are able to pass the hepatocyte membrane by passive diffusion, while FAs with longer chain length (>C12) rely on active transport [32,33]. FATPs, responsible for this transport, are integral membrane proteins with six isoforms of high homology (FATP1 – FATP6). In the liver, FATP5 is the FATP with the highest expression and importance. FATP5, like its other isoforms, exhibits acyl-CoA synthetase activity after translocation of the FAs across the plasma membrane. This so called activation, the esterification of a FA to coenzyme A (CoA), is a step imperative for functional metabolism within the cell. About 4% of known enzymes utilize the acyl carrier CoA as an obligate cofactor [34-36]. The activation process of FAs can not only be executed by the FATPs, but is predominantly carried out by acyl-CoA synthetases (ACSLs). After the initial report of ACSL1 in 1953, 26 different isoforms (encoded by five genes) were subsequently identified in humans and mice. These ACSLs differ in tissue expression, cellular localization, substrate specificity, as well as on the metabolic destination (e.g. breakdown vs. synthesis) of their product. The situation, therefore, is very complex and still open for elucidation. What is known, however, is that in the liver the most expressed isoforms, responsible for the activation of long-chain FAs are ACSL1 (50% of hepatic activity), ACSL4, and ACSL5. ACSL1 and ACSL5 are reported to channel their activated FAs mostly towards TG synthesis, while the direction of channeling for other ACSLs are mostly speculative [34,37-39].

1.2.2.2 Degradation

The mitochondrial β-oxidation pathway is the central pathway to break down FAs within the cell, constituting up to 95% of overall FA-oxidation activity [40] in the liver. As stated above, mitochondrial β-oxidation is located

within the mitochondrial matrix. Activated FAs (acyl-CoAs), however, are too polar to cross the inner mitochondrial membrane. Therefore they have to be actively transported into the mitochondrial matrix. This import is carried out by three consecutive proteins: carnitine palmitoyltransferase 1 (CPT1), carnitine-acylcarnitine transferase (CACT), and CPT2 (carnitine shuttle).

CPT1 catalyzes the formation of long-chain acylcarnitines from acyl-CoAs and free carnitine. Localized at the outer mitochondrial membrane, it is the committing and rate-limiting step for mitochondrial β-oxidation. As acylcarnitine-entity, they are targets for the CACT, which imports one acylcarnitine and exports one free carnitine. Inside the mitochondrial matrix CPT2 carries out the reverse reaction of CPT1 – the transfer of the FA from carnitine to a free CoA. As FA-CoA, inside the mitochondrion, it can then undergo β-oxidation [41,42].

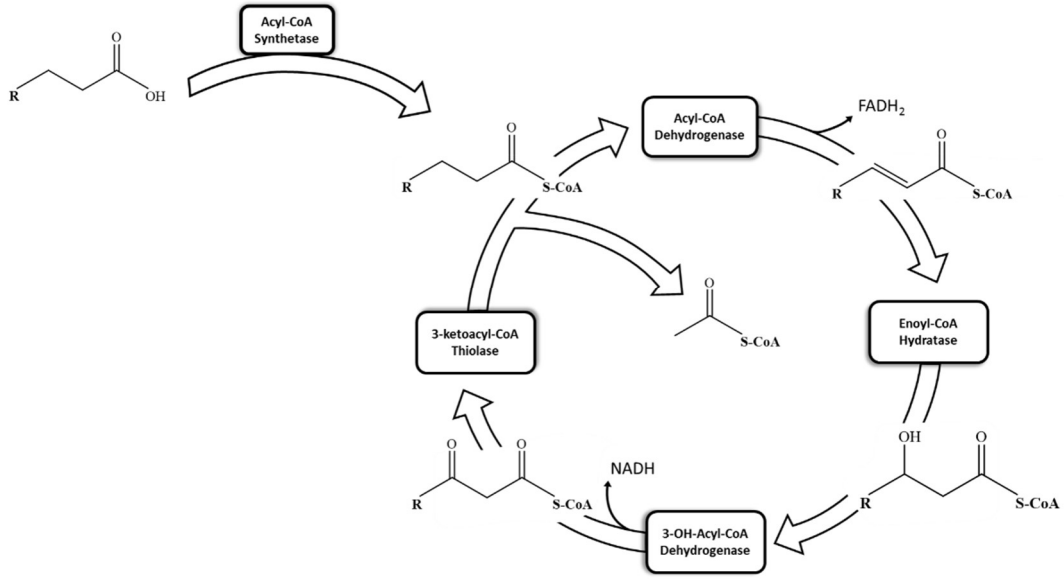

Fig. 6. Simplified four-step reaction cycle of mitochondrial β-oxidation of saturated straight-chain FAs.

Fully saturated straight chain FAs undergo β-oxidation until their full degradation to a final acetyl-CoA or propionyl-CoA, yielding acetyl-CoA, $FADH_2$, and NADH, for every two-carbon-shortening of the FA [42]. Omitting chain length specificities and unsaturated/branched FAs, β-oxidation proceeds in four reiterating steps, as shown in **Fig. 6.** Of the aforementioned products of the β-oxidation cycle, NADH and $FADH_2$ are oxidized as cofactors in the ETC. NADH is used by Complex I and $FADH_2$ is transported over the electron-transferring-flavoprotein (ETF) to the electron-transferring-flavoprotein dehydrogenase (ETFDH). ETFDH feeds the electrons from $FADH_2$ to the coenzyme Q pool, to ultimately contribute to the Complex III activity [41,43] **(Fig. 7)**. Although over 90% of FA oxidation is carried out by β-oxidation in the mitochondrial matrix, there is an alternative pathway by which the cell can break down FAs. The so-called ω-oxidation starts with the hydroxylation on the ω-carbon (carbon at the opposite site of the preexisting carboxyl group) by members of the cytochrome P450 (CYP) 4A and 4F subfamilies, which are associated with the membrane of the ER. After further oxidation to dicarboxylic acids by an alcohol- and aldehyde-dehydrogenase, they are translocated to peroxisomes, where they undergo peroxisomal β-oxidation [40].

Peroxisomal β-oxidation, however, can only metabolize very long- and long-chain FAs and not medium- nor short-chain FAs or respective dicarboxylic acids. For complete breakdown, they have to be transported into mitochondria [44]. Furthermore, peroxisomal β-oxidation enzymes differ slightly from the mitochondrial forms. Breakdown in peroxisomes only produces one NADH and is directly coupled to O_2 and not to the ETC [45]. The product of FA oxidation, acetyl-CoA, has many fates in the cell. For instance, it can be used right in the mitochondria for feeding into the citric acid cycle, for protein acetylation, for ketone body synthesis, but also as building block for many other pathways of the cell. Namely, it is the precursor for FA synthesis [46-48].

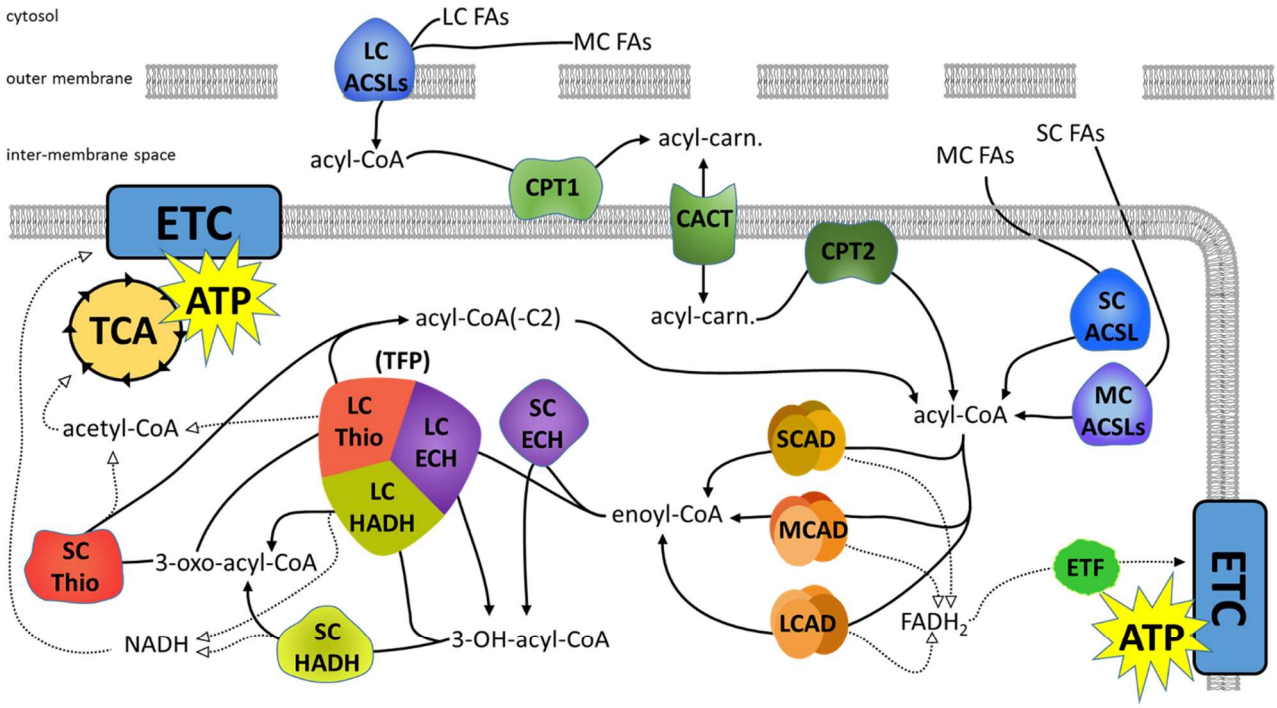

Fig. 7. β-oxidation pathway in humans. Overview of proteins and reactions involved in the mitochondrial breakdown of short-, medium-, and long-chain FAs. After activation of the FA to FA-CoA, by an ACSL and the use of one ATP, long-chain acyl-CoAs are translocated into the mitochondrial matrix by the carnitine shuttle. Short- and medium-chain FAs can also cross the inner mitochondrial membrane by diffusion and get activated by ACSLs, present in the matrix. The carnitine shuttle consists of three proteins: CPT1, CACT and CPT2. CPT1 catalyzes the formation of long-chain acylcarnitines from acyl-CoAs and free carnitine. Localized at the outer mitochondrial membrane, it is the committing and rate-limiting step for mitochondrial β-oxidation. As acylcarnitines, they are targets for the CACT, which imports one acylcarnitine and exports one free carnitine. Inside the mitochondrial matrix CPT2 carries out the reverse reaction of CPT1 – transfer of the FA from carnitine to a CoA. Inside the mitochondrion as acyl-CoA, it then can undergo β-oxidation. The first reaction involves a FAD-linked dehydrogenation of acyl-CoA to yield trans-2-enoyl-CoA, which is catalysed by chain-length specific acyl-CoA dehydrogenases. For the next step, one of the two ECHs hydrates the carbon double-bond, which is followed by a NAD^+-linked dehydrogenation, carried out by one of the two HADHs, to yield 3-keto-acyl-CoA. The final step is carried out by the LC Thio for longer forms, and for shorter forms by SC Thio. They cleave 3-keto-acyl-CoAs by the thiol group and transfer the remaining acyl-chain to a free CoA, finally producing an acetyl-CoA and a two-carbon shortened acyl-CoA, which can undergo the cycle again. The LC ECH, LC HADH and LC Thio are aggregated to one protein complex, called the TFP. Abbreviations: ACSL: acyl-CoA synthase, ATP: adenosine triphosphate, CACT: carnitine-acylcarnitine translocase, carn.: carnitine, CPT: carnitine-palmitoyl transferase, ECH: enoyl-CoA hydratase, ETC: electron transfer chain, ETF: electron transfer flavoprotein, FA: fatty acid, HADH: 3-hydroxyacyl-CoA dehydrogenase, LC: long-chain, LCAD: long-chain acyl-CoA dehydrogenase, MC: medium-chain, MCAD: medium-chain acyl-CoA dehydrogenase, SC: short-chain, SCAD: short-chain acyl-CoA dehydrogenase, TCA: tricarboxylic acid cycle, TFP: trifunctional protein, Thio: 3-keto-thiolase.

1.2.2.3 Fatty Acid and Triglyceride Synthesis

De novo lipogenesis is the combined metabolic pathway, consisting of glycolysis and the biosynthesis of new FAs to produce TGs. FA-synthesis is started by the irreversible carboxylation of acetyl-CoA to malonyl-CoA by acetyl-CoA carboxylase (ACC). In a next step, the multifunctional enzymatic complex, the fatty acid synthetase (FAS), made up of six enzymes functionally fused together, catalyzes the formation of palmitate by the elongation of one acetyl-CoA with seven malonyl-CoAs, with the use of one NADPH per elongation step [49,50]. The liver, like other lipogenic tissues, is greatly capable of synthesizing TGs from FAs and glycerol, a product from glycolysis. After formation of glycerol-3-phosophate by glycerol kinase, the first, committing and rate-limiting step of TG-synthesis is catalyzed by glycerol-3-phosphate acyltransferase (GPAT), which transfers a free FA to the phosphorylated glycerol. In the liver, two isoforms essentially share the bulk of this first acylation step, the microsomal GPAT and the mitochondrial GPAT (GPAM). Lysophosphatidic acid (single-acyl glycerol-phosphate) is then acylated again to form diacyl glycerol (DAG), which is the branch point between phospholipid and TG synthesis. In order to finally form a TG, DAG is acylated one more time by diacylglycerol acyltransferase-1 (DGAT) [46].

1.2.2.4 Trafficking and Storage

In order to avoid toxic levels of intracellular free FAs, the cell possesses several strategies to react. One way is the notably high content of fatty acid binding protein (FABP) in hepatocytes. In the liver, approximately 10% of cellular protein consists of FABP1, which binds and therefore “detoxifies” free FAs, FA-CoAs, FA-carnitines, as well as other intermediates of lipid acid metabolism. Furthermore, FABP is of great importance for the intracellular transport of its ligands, as it is believed, that through protein-protein interactions of FABP and other proteins, substrates are moved in a targeted way within the cell. One example is FABP-dependent translocation to the nucleus, in order to deliver peroxisome proliferator-activated receptor (PPAR)α or PPARγ agonists, which often have a high binding-rate to FABP [51-53].

Synthesis of neutral TGs is also a way for the cell to limit levels of free FAs. Besides binding to proteins like FABP, TGs are normally stored in LDs within the cell. Those LDs are stabilized vesicles, filled with mainly TGs, and enveloped by a mono-layer of phospholipids, which are complemented with numerous proteins, important for the handling of this energy-rich storage. LD-proteins are important for the stabilization, as well as for intracellular displacement of LDs for specific functions, as for example for excretion purposes [54].

Adipose differentiation-related protein (ADRP), also known as Perilipin 2, is an important protein on the surface of LDs. One function of it, for example, is to regulate membrane dynamics and lipolysis on the surface of LDs. As an integral LD-protein it is positively correlated with cellular lipid droplet content, and therefore also TG content [55,56]. A similar group of LD-associated proteins is the CIDE (cell death-inducing DNA fragmentation factor-α-like effector) family. They are localized on the LD surface and are particularly enriched at LD-LD contact sites, controlling LD fusion and size. Like ADRP, Cidea and Cidec are positively correlated

with the LD content of the cells, however their specific roles in promotion of TG accumulation are still controversial [57,58].

1.2.2.5 Export

Finally, the hepatocyte can also actively excrete the TGs within the cell to the system. For anabolic and energy requirements VLDL is synthetized in the liver and excreted for the supply of extrahepatic tissue, very similar to the situation in enterocytes, described above. VLDL consists of a core of TGs and cholesteryl esters, which is surrounded by a monolayer of phospholipids and cholesterol with specific apolipoproteins embedded. The full length ApoB, ApoB100, is a structural protein, essential for the formation and stability of VLDL vesicles, as well recognition thereof by extrahepatic tissue [59,60].

The mechanism of the whole VLDL synthesis is quite complex and not yet fully understood, however, very similar to the synthesis and excretion of chylomicrons (**Fig. 3**). Briefly, it starts at the ER membrane, the location of ApoB-synthesis. After translation to the luminal side of the ER, various lipids and multiple copies of other apolipoproteins are a recruited to the ApoB. The microsomal triglyceride transfer protein (MTTP), an enzyme crucial for the pathway, then transfers the bulk of TGs from the ER-TG pool to the newly forming VLDL particle [59,61,62]. If the ApoB is not properly lapidated, it is degraded again, before exiting the ER [60]. After translocation to the Golgi and subsequent modification, it is excreted to the circulation via exocytosis [63].

Through a mostly unknown mechanism, hepatocytes are also able to excrete FAs through the cell membrane, in the form of acyl-carnitines [64]. Since acyl-CoAs are too polar for crossing biological membranes by diffusion, and there is no efficient transport system in place, they cannot leave hepatocytes in this form. Acyl-CoAs, however, can be converted to the corresponding acyl-carnitines. As acyl-carnitines they can not only leave the mitochondria over the carnitine shuttle, but also the cell, thus reaching the bloodstream and also urine. Consequently, in addition to its role in the mitochondrial β-oxidation pathway, carnitine is important for the protection of the cellular CoA pool. It provides the cell with a mechanism to maintain CoA availability for CoA-dependent reactions under conditions of acyl-CoA accumulation [65].

1.2.3 Regulation of Hepatic Lipid Metabolism

Hepatic lipid metabolism has to be capable to respond to various situations, such as postprandial spikes in FA availability or the need for *de novo* lipogenesis. Also the distribution of energy-rich substrates, like ketone bodies for extrahepatic tissue during fasting or prolonged exercise, needs responsive mechanisms. Therefore, many regulatory pathways are in place, able to alter metabolic rates and protein expressions of enzymes involved.

Above all, adaption of mitochondrial mass is a major way for the cell to adapt to metabolism-related changes [26]. Mitochondrial biogenesis and degradation, still under much needed investigation, are mainly regulated by

nuclear factors. Peroxisome proliferator-activated receptor gamma coactivator 1-alpha (PGC1α) is described as master regulator in this pathway. It is a transcriptional coactivator, which induces the activity of the transcription factors nuclear respiratory factor 1 and 2 (NRF1 and 2). They, themselves, regulate the transcription of the mitochondrial transcription factor A (TFAM), which is responsible for the replication of mitochondrial DNA, and the expression of many other genes, linked to mitochondrial biogenesis and metabolic activity [26,66,67].

FAs are ligands of PPARα, which is the most important control element for FAs oxidation. It has been shown, that strong agonists for this adopted orphan receptor are mostly dietary polyunsaturated FAs and newly synthesized FAs [68]. When activated, PPARα upregulates almost all of the enzymes connected to FA degradation. Examples are CPT1, FABP, CYP4A11, or the medium-chain acyl-CoA dehydrogenase (MCAD), as well as genes for carnitine biosynthesis [69,70]. Such nuclear receptors consist besides of a ligand binding site also of a central DNA-binding domain that binds to specific sequences within a gene promotor. Binding of ligands will lead to recruitment of coactivators, resulting in chromatin remodeling with subsequent DNA transcription [68]. Besides from its ligands, PPARα is also regulated by various other stimuli, which are associated, for example, with dietary status (**Fig. 8**).

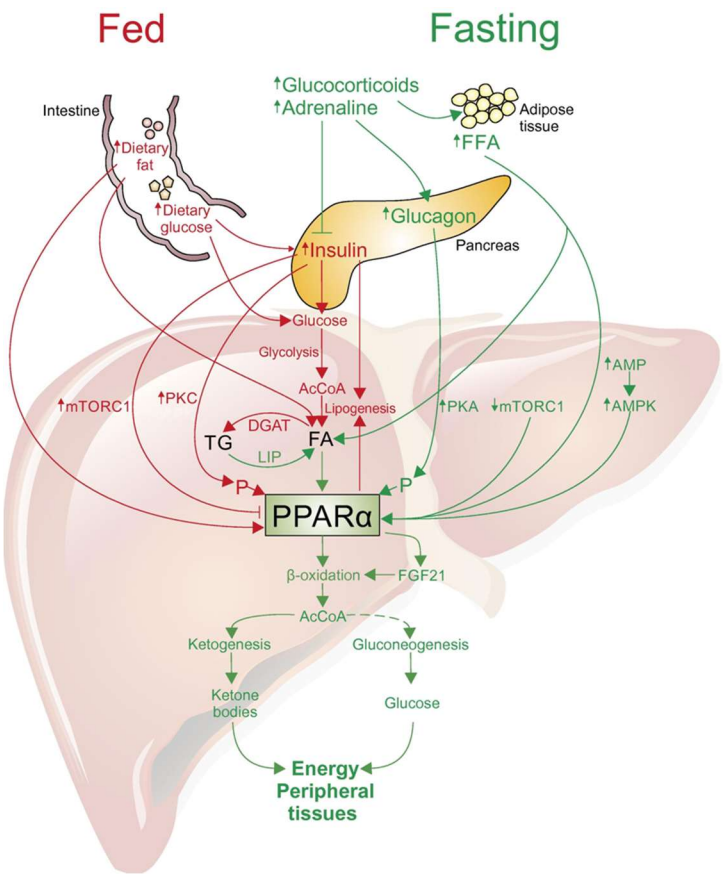

Fig. 8. PPARα as molecular switch directing energy metabolism. Shown are influences of fed states (red arrows) and fasting states (green arrows) on the activity of PPARα and its downstream control. Postprandial glucose leads to production and secretion of insulin by the pancreas, which induces hepatic glucose uptake and glycolysis, yielding AcCoA, which induces FA synthesis. Insulin leads to phosphorylation of PPARα via PKC and thereby enhances its transcriptional activity. Insulin-activated mTORC1 blocks PPARα activity. FAs and FA-derivatives are direct activators of PPARα. During fasting, hormones such as adrenaline and glucocorticoids are synthesized together with glucagon. Glucagon sustains hepatic gluconeogenesis and increases cAMP levels, triggering PKA-dependent PPARα phosphorylation and activity. Fasting leads to decreased mTOR1C activation, thus stimulating PPARα-dependent FA oxidation and ketogenesis. The fasting-induced release of FAs from adipose tissue raises plasma levels of free FAs that are subsequently taken up and stored in the liver as TGs. LIP-dependent hydrolysis of hepatic TGs provides FA-ligands for PPARα activation, which leads to increased β-oxidation rates directly and via FGF21-activation, to provide substrates for ketone body synthesis and gluconeogenesis, thus maintaining energy supply for extrahepatic tissues. The scheme is adapted from Pawlak et al. [1]. Abbreviations: AcCoA: acetyl-Coenzyme, AMP: adenosine monophosphate, AMPK: AMP-activated protein kinase, DGAT: diglyceride acyltransferase, FA: fatty acid, FFA: free fatty acid, FGF21: fibroblast growth factor 21, LIP: lipase, mTORC1: mammalian target of rapamycin complex 1, P: phosphorylation, PKA: protein kinase A, PKC: protein kinase C, PPARα: Peroxisome proliferator-activated receptor α, TG: triglyceride.

Effects on transcriptional regulations are usually long-term adaptions, however, acute activity-regulations are possible by substrate-feedback. Most importantly, CPT1, the rate limiting step in the catabolism of FAs, is negatively regulated by levels of malonyl-CoA, the substrate for FA-synthesis [41]. Therefore, under conditions with high availability of energy in the form of acetyl-CoA, ACC is increasingly building malonyl-CoA, which inhibits CPT1 by binding to a high-affinity binding site [71]. Accordingly, the cell downregulates the usage of FAs for ATP production under this condition.

Acetyl-CoA levels can also acutely affect the metabolism over the AMP-activated protein kinase (AMPK). If energy levels are low and adenosine monophosphate (AMP) levels are high, AMPK phosphorylates ACC, which decreases its activity and therefore decreasing malonyl-CoA levels. This leads to a shift in metabolism away from lipogenesis and towards breakdown [41,42,48]. Furthermore, acetyl-CoA availability also affects the acetylation-status of mitochondrial proteins, and therefore their activity [72]. One example thereof is the activation of PGC1α by deacetylation, carried out by sirtuin-1 [73].

The regulation of TG synthesis is equally complex and alters greatly in different tissues. The most important players are the transcription factors sterol regulatory element-binding protein 1c (SERBP-1c) and PPARγ, as well as hormonal and nutritional regulators [46]. SREBP-1c is mainly activated by insulin and repressed by high levels of polyunsaturated FAs [74]. When activated, for example by the insulin pathway, it translocates from the ER to the nucleus and upregulates the transcription of lipogenic proteins such as ACC, GPAM, and FAS [75].

PPARγ, like other PPARs is a nuclear receptor belonging to the steroid receptor superfamily, which are activated by FAs [76]. When an agonist binds, corepressors around the PPAR disassociate and it can then form a complex with the retinoid X receptor. Together they recruit different coactivators, like PGC1α, and induce transcription of specific genes. PPARγ controlled genes are in the hundreds and include Cidec, LPL, cytochrome C, CD36, FATP1, ADRP, FAS, Glut4 (glucose transporter type 4), and many more [77]. Activation therefore mostly leads to increased glucose metabolism and TG storage.

Estrogen receptors (ESRs) are not only important for female traits and development, but also for general energy metabolism in vertebrates. Upon activation, ESRs can initiate biological events within days and hours, but over the cell membrane, even in seconds [78]. There are two types of ESRs: nuclear ESRs and membrane ESRs. However, they are not only present in the cell membrane and the nucleus, but also reported in mitochondria [79,80]. Most of the known transcriptional effects of estrogen, however, are nuclear-initiated. When activated, ESRs translocate from the plasma to the nucleus, where they recruit transcriptional machinery and other cofactors to specific DNA sequences [81]. It is known that estrogen benefits insulin sensitivity and lipid metabolism, the mechanism behind it, however, is still poorly understood [82,83].

Another emerging pathway involved in lipid metabolism is the endocannabinoid system. It is clear that the endogenous cannabinoids arachidonoylethanolamine (anandamide) and 2-arachidonoylglycerol have an important role in food intake and body weight as they have effects on appetite and response to diet [84,85]. There are two types of cannabinoid receptors present in the body, with quite different effects. Endocannabinoids,

synthesized in the liver from essential FAs like linoleic acid [84], exert their effects over the following two receptors: cannabinoid-receptor 1 and 2 (CB1 & CB2) [86,87]. CB2 activation is mostly expressed on cells of the immune system and is attributed to positive effects regarding inflammation and lipid homeostasis [88]. CB1 activation, on the other hand, is closely linked to a greater steatogenic risk potential in humans [89]. Furthermore, animal studies in mice and rats clearly showed the necessity of CB1 expression for developing hepatic steatosis under high fat or high alcohol diet [90,91]. CB1 activation not only results in an upregulation of the lipogenic transcription factor SREBP1c and its target enzymes, but also appears to regulate hepatic FA oxidation by decreasing the activity of CPT1[90,92]. Finally, cannabinoids not only exert their effects through CB receptors on the cell membrane, but also through receptor-independent mechanisms [93,94], as well as through CB receptors located in the mitochondrial membrane [95]. The understanding of mechanistics behind the CB receptor mediated effects, unfortunately, is still incomplete, especially in regard to the role of cannabinoids on mitochondria [96-99].

Apparent from the examples of regulations of hepatic lipid metabolism above, multiple regulatory pathways are connected in different ways for the fine-tuning of hepatic energy homeostasis. Similarly, these regulatory mechanisms generally affect other metabolic pathways as well, such as glycolysis or oxphos, which is comprehensible, since almost all ATP-producing pathways are in some way interlinked. These pathways are not only linked over identical upstream master-regulators, such as PPARs, but also over substrate interchange **(Fig. 9)** or feedback mechanisms.

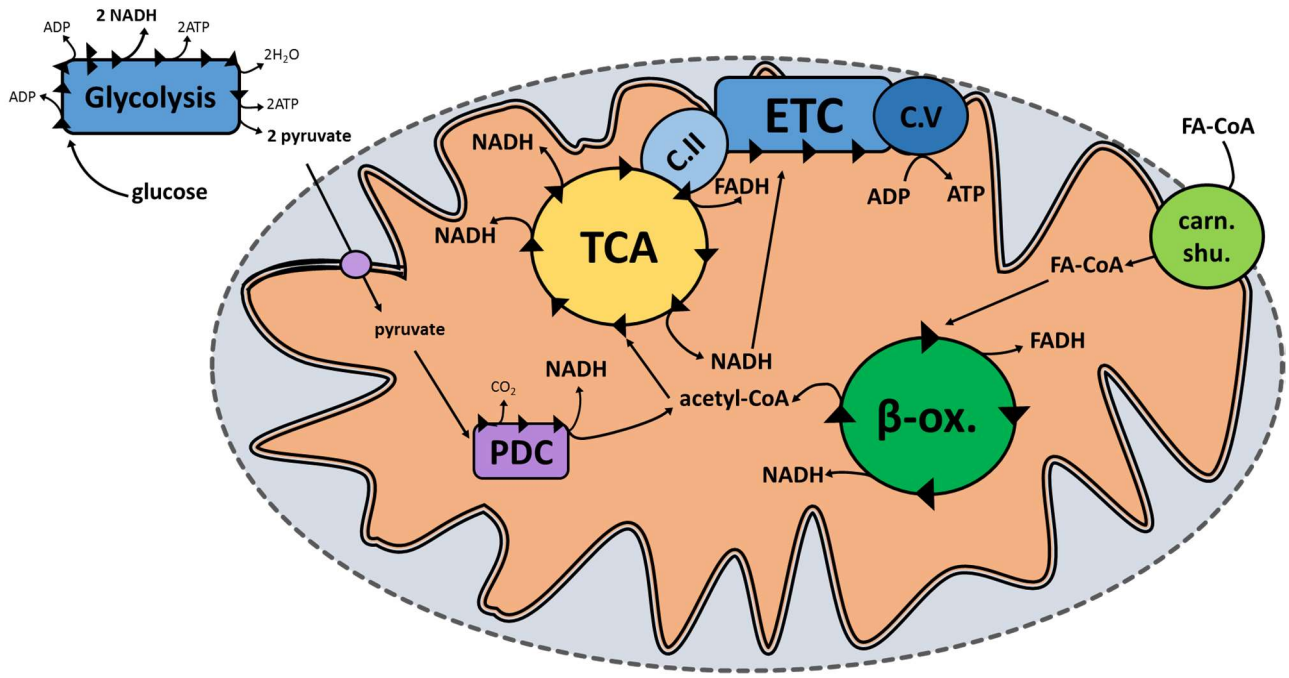

Fig. 9. Overview of interlinked metabolic pathways. Shown is a mitochondrion, with respective intra-mitochondrial metabolic pathways and the glycolysis, which is located in the cytosol. Abbreviations: ADP: adenosine diphosphate, ATP: adenosine triphosphate, C.II: Complex II, C.V: ATP synthase, ETC: electron transfer chain, FA-CoA: fatty acid-Coenzyme A, FADH: flavin adenine dinucleotide, NADH: nicotinamide adenine dinucleotide, PDC: pyruvate dehydrogenase complex, TCA: tricarboxylic acid cycle, β-ox.: β-oxidation.

1.3 Liver Injury and Metabolic Imbalance

The liver is a site, which receives multiple xenobiotics and waste products to detoxify. Under normal circumstances, it is perfectly able to carry out this task. However, in some cases, it cannot cope with the demand and is damaged in the process, if the burden goes on. Typical challenges for the liver, which lead to injury, are cholestasis [100], chronic alcoholism, ischemia, autoimmune or viral hepatitis, as well as toxic liver injury [101]. For clinicians the first indication of liver injury is often the pattern of liver enzyme alterations. The eminent thereof are alanine amino transferase (ALT) and aspartate amino transferase (AST). Both are cytoplasmic enzymes found in hepatocytes. When found elevated in the blood of patients, it therefore suggests damaged hepatocytes [102]. Other relevant biomarkers for liver injury are elevated serum bilirubin, gamma-glutamyl transferase, alkaline phosphatase, or low serum albumin.

In view of xenobiotics, the liver is especially at risk of damage. Nowadays, most drugs are lipophilic and undergo extensive hepatic metabolism to render them more hydrophilic, in order to excrete them via the urine. The lipophilicity of drugs and the fact that those drugs reach the liver right after gastrointestinal uptake, can lead to a much higher drug and metabolite concentration in the liver, compared to other tissues. For instance, these membrane partitioning and accumulation effects are well known for tamoxifen [103,104] or also for tyrosine kinase inhibitors [105,106].

Drug-induced liver injury (DILI) can be classified into two types regarding their predictability. Intrinsic toxicity causes liver injury in a dose-dependent fashion and is predictable [107]. The most used example thereof is the toxicity of acetaminophen (paracetamol), of which the mechanism of toxicity is known very well, as well as the dose- and time dependency. Idiosyncratic toxicity, on the other hand, is unexpected and not strictly dose-dependent. Furthermore, it only affects a small proportion of patients and also cannot be predicted by its pharmacological action [108]. Due to the low incidence and unpredictability, it is evident that patients developing idiosyncratic DILI possess or acquired underlying factors, making them susceptible for these currently unknown mechanisms of toxicity.

In this thesis, the focus lies on the elucidation of molecular mechanisms of drugs causing idiosyncratic hepatotoxicity. More precisely, the drugs chosen for investigation have all a common type of outcome: hepatic steatosis.

1.3.2 Hepatic Steatosis

Steatosis of the liver is defined by an excess accumulation of intracellular TGs within the hepatocytes. One differs between two types of steatosis, the macrovesicular and microvesicular form.

The histological representation of macrovesicular steatosis is described as fatty hepatocytes, which contain a large droplet of fat with peripheral displacement of the nucleus. Microvesicular steatosis, on the other hand, is characterized by an abnormal accumulation of multiple small LDs without nucleus displacement [109] **(Fig. 10)**. Diagnosis relies on liver function tests and imaging with the exclusion of other liver diseases. The gold standard, however, still is to perform a liver biopsy with subsequent histological evaluation, where at least five percent of cells have to show lipid accumulation [110].

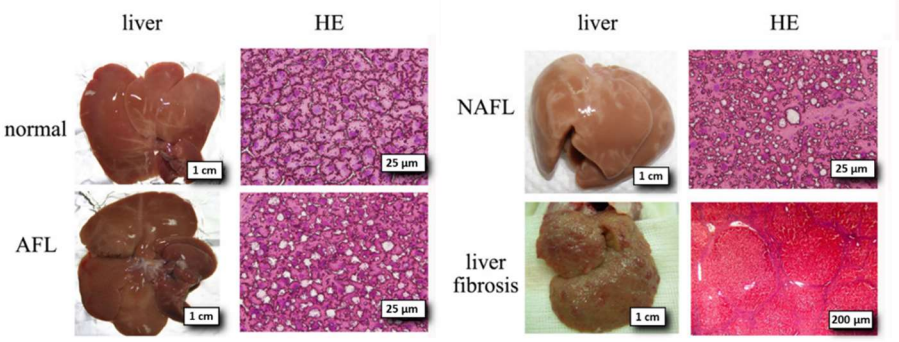

Fig. 10. Tissue- and histologic representation of hepatic steatosis and fibrosis. Shown are livers from rats. On the left excised livers are shown. On the right hematoxylin and HE stained sections are shown with different magnifications. Abbreviations: AFL: alcoholic fatty liver, NAFL: non-alcoholic fatty liver, HE: hematoxylin and eosin. The figure is adapted from Liu et al. [2].

Hepatic steatosis, which is not a result of excessive alcohol intake, is also called nonalcoholic fatty liver disease (NAFLD). It ranges from simple steatosis to nonalcoholic steatohepatitis. NAFLD is a serious health problem worldwide, reported to affect 15 – 30 % of the population in developed countries [111]. Macrovesicular steatosis, often associated with excess alcohol exposure or treatment with glucocorticoids, usually, is a form of injury, which is reversible. The microvesicular form, however, is a more severe injury of the liver, typically associated with mitochondrial dysfunction and can aggravate significantly [112]. If not managed in a timely manner, steatosis can worsen to steatohepatitis, cirrhosis, and also to liver failure. Ultimately, severe liver injury with microvesicular steatosis often ends fatally in the absence of liver transplantation [113].

As NAFLD is directly associated with obesity, the management of this disease typically lies, in a first approach, on changes in lifestyle and diet. The treatment for more progressed forms can include supplementation of antioxidants like vitamin E, drugs to increase insulin sensitivity, fibrates against dyslipidemias, and statins. Liver transplantation, as a last resort, is increasingly used as well [114,115].

Inordinate accumulation is damaging to the liver, because high levels of TGs, free FAs, or intermediates of lipid metabolism are extremely problematic for a cell. Especially excessive free FA concentrations pose a serious problem. Not only can the detergent-like effect of FAs damage membranes, but also peroxidased FAs

are a grave consequence of FA overload. FA peroxidation occurs mainly on unsaturated FAs at the location of double bonds [116]. It is initiated, when a hydrogen atom is abstracted form a CH_2 group of a FA. Reactive oxygen species (ROS), which are able to abstract a hydrogen, are for example superoxide- and hydroxyl radicals, produced in the mitochondria. Superoxide anions ($O_2^{\cdot-}$) can arise from the activities of Complexes I and III of the ETC. The greatest portion of ROS is produced by Complex I of the respiratory chain. ROS formation occurs, when unpaired electrons escape the respiration chain and are accepted by O_2 [117]. Superoxide dismutase 2, localized in the mitochondria, scavenges superoxide radicals by catalyzing two $O_2^{\cdot-}$ to a hydrogen peroxide. Hydrogen peroxide is then catalyzed into water and O_2 by the enzyme catalase. Alternatively, due to iron ligands present in the mitochondrial matrix, which allow for redox-cycling, hydroxyl radicals can be formed through the Fenton reaction [118]. Not only FAs can get peroxidised, but also cholesterols and phospholipids. Lipid peroxidation gives complex products, such as aldehydes, polymeric materials, and lipid radicals, which all are cytotoxic [116]. Under normal circumstances, the cell is able to detoxify radicals promptly through binding to the antioxidant glutathione (GSH), however, if oxidative stress surpasses the antioxidative capacity, membranes, proteins, and DNA can get damaged through these highly reactive molecules.

In the case of palmitate, the most abundant endogenous FA[119], an excess of C16-ceramide formation can occur in the cells [35,51]. Ceramides belong to the structurally diverse class of sphingolipids, which make up a significant amount of membrane lipids. When there is a disproportionate ceramide formation it leads to membrane permeability, pore formation, and altered cell signaling of membrane proteins. These changes ultimately will lead to programmed cell death (apoptosis) [120].

The exact mechanism behind the accumulation of excess lipids in the liver is complex and multifactorial. Different theories have been formulated on the topic, assenting on the "two-hit hypothesis" [121]. Accordingly, pathological lipid accumulation in the liver occurs after a second hit, meaning a further insult to hepatic metabolism, after it has already been sensitized from the first hit. The case report of a patient, who died after treatment with valproate is a good example thereof [122]. This patient was treated for epilepsy with valproate, which is known to interfere with FA metabolism[123], upon which he died. This was the second hit. After postmortem investigation in cultured fibroblasts, it was found that the patient had an underlying deficiency in an enzyme, which is important for the metabolism of medium-chain FAs, which represents the first hit in this case. First hits, or in other words underlying susceptibilities, can also be insulin resistance, sedentary lifestyle, high fat diets, or many forms of mitochondrial dysfunction [121].

Lastly, a "hit" to increase FA content can be caused by disruption of one or more of the pathways, which are involved in the regulation of FA and TG levels in the hepatocyte. Namely, the **uptake and activation** of free FAs can be increased, *de novo* **lipogenesis** can be elevated, FA **degradation** in mitochondria and peroxisomes can be reduced, or finally TG **export** by VLDL secretion can be decreased **(Fig. 11)**.

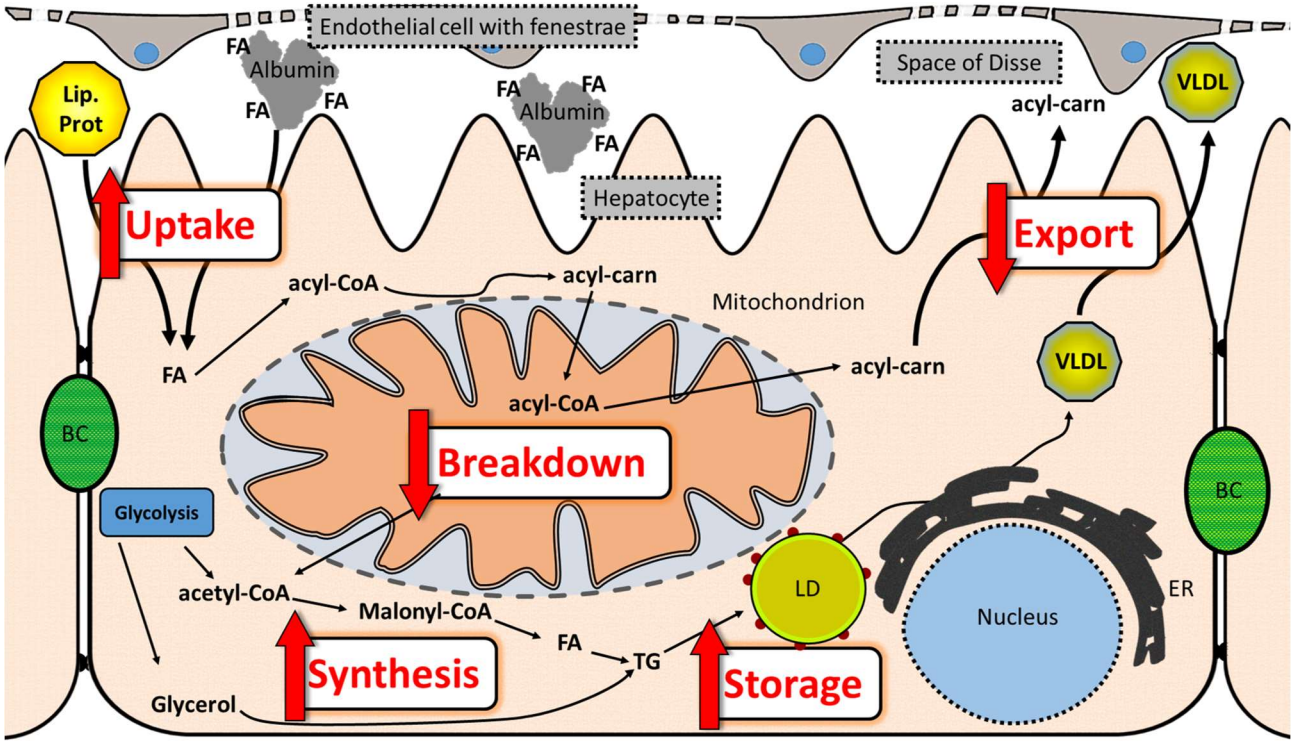

Fig. 11. Graphical representation of pathways, with which the cell can regulate lipid content. Abbreviations: BC: bile canaliculus, carn: carnitine, CoA: coenzyme A, ER: endoplasmic reticulum, FA: fatty acid, LD: lipid droplet, Lip.Prot: lipoprotein, TG: triglyceride, VLDL: very-low density lipoprotein.

1.4 Investigation

1.4.1 Why Study Hepatic Lipid Metabolism?

Globally, NAFLD is the most common cause of liver disease, affecting up to 58% of overweight individuals [111]. The problem of obesity in the general population has tremendously gained importance over the last century. In most western countries chronic diseases, related to diet, represent the largest cause of morbidity and mortality. An obvious component of this multifactorial problem is the steadily increasing consumption of refined vegetable oils, with high contents of fully saturated- and trans-fats [6] and a sedentary lifestyle. A further problem is that NAFLD can obviously be a risk factor for developing adverse reactions to drugs, interfering with hepatic lipid metabolism, leading to idiosyncratic DILI.

Furthermore, DILI has been the major cause of drugs failing approval, black box warnings, as well as withdrawal from the market over the last 50 years [124,125]. DILI usually appears in a small population of patients, often missed in clinical phases 1 and 2. The pharmaceutical industry, therefore, makes great efforts to find and establish safe biomarkers for the preclinical assessment of possible toxicity [124].

Many mechanisms are known that can cause hepatic steatosis. In the case of drug-induced hepatic steatosis, however, a lot of questions still remain unanswered. Consequently, in order to save both lives and money, elucidations of mechanisms leading to adverse reactions on the liver are needed for better disease prevention and handling, ultimately increasing quality of life in affected individuals.

1.4.2 Models for Investigation

Whether it is the use of animal models, tissue cultures, cell cultures, microsomes, homogenate fractions, single enzyme preparations, or in silico modeling, every model of investigation has advantages and disadvantages. It is up to a systematic decision process for choosing the model best applied for respective scientific investigations. Today, besides clinical studies, animal models are viewed as closest to the situation in human, in most cases. The high costs, labor intensity, availability of animal facilities, and ethical considerations, however, lead most scientific work to remain *in vitro*. Testing in cell cultures also has its advantages over studies *in vivo*. Testing *in vitro* is highly reproducible, reduces the costs of investigation tremendously and allows for a very high number of experiments. Moreover, it allows for the use of human material, as species differences could render findings in animals hard to interpret.

Fig. 12. Vivisection of a pig. Picture from the cover of the 1565 version of Galens (129 AD – ca. 210 AD) *Opera Omnia*.

There has been a long way from first observations in nature, over early animal vivisections and experiments on criminals, to the situation today, where we scientists are blessed with uncountable models of investigations to choose from. Still, in the second half of the nineteenth century with the beginning of scientifically meaningful animal research[126], experiments were mostly performed for physiological knowledge. Scientific studies on toxicity began in 1920, when J.W. Trevan proposed the use of the 50% lethal dose (LD50), followed by methods for testing eye and skin irritation in rabbits [127]. In the same time, work on first continuous primary cell cultures started. Based on early works, like the experiments 1882 by Sydney Ringer[128], who developed the Ringer's solution for keeping excised tissues functional for a short period of time, or 1885 work by Wilhelm Roux[129], who managed the first sustained maintenance of tissues *ex vivo*. Eventually in the 1943s the first permanent cell line emerged from subcutaneous mouse tissue[130]. February 1 1951, was the day when Henrietta Lacks visited the Johns Hopkins Gynecology Clinic in Baltimore, Maryland, where her cervical tumor was diagnosed. This tumor gave rise to the first transformed human cell line, the world-renowned HeLa cells [131]. From there on the number of different stable cell lines almost exploded. There are currently 1252 stable cell lines from human origin available at ATCC (Manassas, VA, USA), one of the biggest suppliers for cell lines today (May 2018).

1.4.2.1 Hepatic Cell Cultures

Regarding the liver, primary human hepatocytes (PHH) are nowadays still considered as the closest cell model to the situation *in vivo*[132-134]. As these cells freshly derive from the environment of a whole body, they still highly express the majority of important functions for the first several days in their new habitat [135-137]. This main advantage of this model keeps the PHH remaining as gold standard in the field of pharmacology and toxicology.

Arguably, the main disadvantage of PHHs is their intrinsic variability, as they are obtained from different individuals with possible genetic polymorphisms, different hormonal status, diet, age, social habits, and exposure to different xenobiotics. Moreover, it is difficult to retain their expression levels of proteins for a longer period. Lastly, a problem mostly affecting academic researchers is their high cost and the limited accessibility to fresh cultures [138]. Today, cryopreservation is the only method for long-term storage and therefore permanent availability. This method, however, can influence the cells negatively for the purpose of drug metabolism studies [139].

The development of cell lines derived from tumors gave a highly reproducible and cheaper method to the hands of scientists. These cell lines grow continuously with a very high proliferation capacity in a highly reproducible manner and have a virtually unlimited life span [140]. They are therefore extensively used for countless investigations and applications. Despite those economic and simplicity advantages, tumor derived cells have limited or altered functions in many ways, as for example liver hepatoma cell lines, which have significant lower performances in drug metabolism [132,137].

1.4.2.2 Models Used in this Thesis

The work in this thesis was done exclusively with material derived from livers. Two liver cell lines, discussed below, as well as isolated mitochondria from mouse livers were used. The cell lines are from human origin and well-established within our own lab. Mitochondria, on the other hand, were retrieved from mouse livers. Although mice exhibit significant species-dependent differences to humans, this model factually proofs to be practical, as FA metabolism is highly conserved throughout mammalians [41].

1.4.2.2.1 HepG2 Cells

HepG2 cells are likely one of the most used hepatoma cell lines, to date [141]. It is the best-characterized hepatoma cell line from human origin with an enormous number of data on the effects of hepatotoxic compounds [142]. Notably, this cell line is very often used in FA metabolism studies because of its expression of many differentiated hepatic functions [143]. Other than a high mitochondrial activity, this includes substantial activities of crucial elements in the metabolism of lipids, like synthesis and excretion of lipoproteins and bile acids[144], other plasma proteins[145],

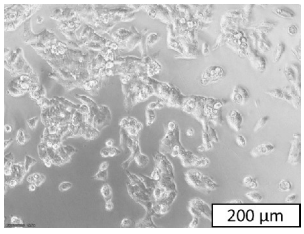

Fig. 13. Light microscope picture of HepG2 cells in a culture flask, one day after seeding.

intact insulin-signaling[146], as well as lipid-storage [147]. Gómez-Lechón et al. could nicely show the very similar behavior in lipid accumulation of HepG2 cells and PHH [148]. The mayor drawback of these cells, however, is the poor expression of phase I and phase II drug metabolizing enzymes[137,141] often leading to false predictions about metabolism-dependent toxicity. Nevertheless, HepG2 cells are a very convenient and powerful tool under the right conditions and investigations.

1.4.2.2.2 HepaRG Cells

HepaRG cells are a more sophisticated, well-known human hepatoma cell line, derived from a liver tumor of a female patient. The researchers **R**umin and **G**ripon (hence the name Hepa**RG**) isolated and characterized the cells, starting in 1999 [149]. A remarkable feature is that these cells, when seeded at low density, transdifferentiate into bi-potent hepatic progenitor cells under the right conditions, as used in this work. They then actively divide before acquiring typical morphological characteristics of hepatocytes in primary culture. After two weeks at confluence and the presence of corticosteroids and dimethyl sulfoxide (DMSO), they build hepatocyte-like colonies, which are surrounded by biliary-like cells [150,151]. HepaRG cells express 81 – 92% of genes active in PHH[152] and have a much higher cytochrome P450-activity compared to other hepatoma cell lines [137,150,153]. Although, this model is more labor- and time-intensive, it gains more and more importance. Because of its similar response to PHHs, it is one of the most useful hepatoma cell lines to date for the research of hepatotoxic compounds [132,153].

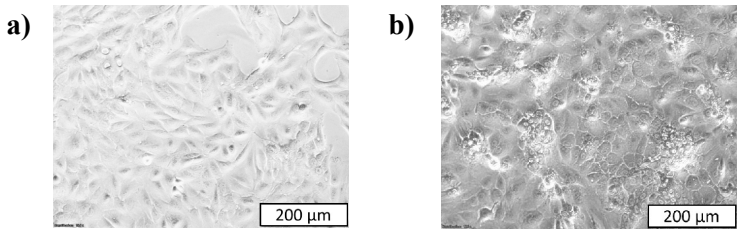

Fig. 14. Light microscope picture of HepaRG cells in culture plates. a) Undifferentiated HepaRG cells three days after seeding. b) Fully differentiated HepaRG culture four weeks after seeding, with differentiated structures visible.

1.4.2.2.3 Isolated Liver Mitochondria

As described earlier, mitochondria are in constant interaction with the intracellular matrix. Therefore, the separation of mitochondria from other cell components can be a useful way to assess effects purely on mitochondria under precisely controlled conditions [154]. This allows for example to show direct effect on the activity of oxidative phosphorylation[155], β-oxidation[156], mitochondrial membrane potential[157], or mitochondrial superoxide production[158], to give a few examples. Furthermore, mitochondria can be isolated from different tissue and species, as for example from genetically modified animal models [159]. Considering mitochondria derived from liver tissue, there are several advantageous circumstances. It is a soft tissue with high mitochondrial content, which makes the isolation procedure relatively easy and results in a good yield. Furthermore, availability

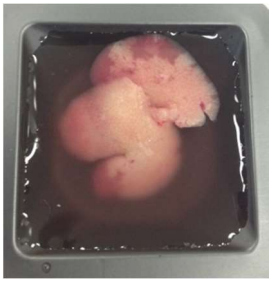

Fig. 15. Excised liver of a mouse. In preparation for the isolation procedure of mitochondria, the liver was previously flushed with ice-cold isolation buffer, for fast temperature decrease and in order to remove blood. Hexagonal liver lobules are therefore nicely visible.

of liver tissue from experimental animals is usually assured, when an animal facility is present. Once isolated, mitochondria can be used in two ways. When using the mitochondria on the same day of isolation, they retain coupling and integrity over several hours, allowing studies reliant on the membrane potential and transport mechanisms. Freezing and thawing mitochondria will disrupt said integrity, allowing the study of effects on single enzymes separated from eventual dependence on other factors.

The most used way to isolate mitochondria is through differential centrifugation. The method was developed in the 1950s and has been modified in many ways [160]. Nowadays, additional methods have been developed, such as preparation of an isopycnic gradient, followed by ultracentrifugation or isolation by magnetic microbeads. Although the differential centrifugation method results in a good yield of functionally intact mitochondria, contaminations of other organelles, which are mostly peroxisomal[161], can interfere with proteomic analyses, for example [162]. For FA metabolism studies or measurements of oxidative phosphorylation, the crude mitochondrial fractions obtained, using differential centrifugation, however, are qualitatively sufficient [160].

1.5 Drugs

During the work on this thesis, several compounds – pharmaceutical drugs, as well as compounds intended for scientific investigations – were used and will be described in this section.

1.5.1 Model Inhibitors

As described in Paper 1 and 3, the four following compounds were solely used as models to compare because of their well characterized properties. All of them are active as inhibitors in a step of FA breakdown. Important for our investigations, using these compounds, was that they were reported in literature to be specific inhibitors for only one enzyme type [163].

1.5.1.1 Etomoxir

Etomoxir, or (2-[6-(4-chlorophenoxy) hexyl]-oxirane-2-carboxylate, is a specific and powerful inhibitor of CPT1. It first has to be activated to etomoxiryl-CoA, before it can bind and irreversibly inhibits its target protein. Reported IC_{50} values are in the nM range for CPT1 and around 100 times higher for other acyl transferases [164,165]. Because etomoxir works on CPT1, it only inhibits FA oxidation in intact mitochondria.

Etomoxir was originally developed for its hypoglycemic properties. By inhibiting FA oxidation, it shifts the metabolism towards glucose oxidation. After failing for the treatment of diabetes mellitus, it was recognized for the treatment of congestive heart failure, however, it was

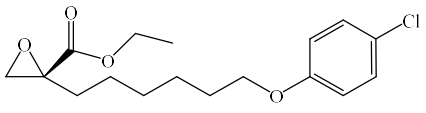

Fig. 16. Chemical structure of etomoxir.

not pursued further. A reconfirmation study with 360 subjects had to be stopped because of suspected hepatotoxicity [166].

1.5.1.2 Methylene Cyclopropyl Acetic Acid

Jamaican vomiting sickness is an endemically occurring poisoning with a high mortality rate. The poisoning leads to pronounced hypoglycemia with symptoms of severe vomiting, usually followed by convulsion, and coma. The toxin responsible, hypoglycin, is found in the unripe fruits of the local akee tree, which are mostly ingested by children [167].

Methylene cyclopropyl acetic acid (MCPA) is the active metabolite of hypoglycin and is also activated to its CoA-form within cells. After its identification, MCPA was studied on its ability of lipid metabolism inhibition. It was found that MCPA irreversibly inhibits acyl-CoA dehydrogenases, which are responsible for the first step in β-oxidation. Specifically, MCPA is able to inhibit short-chain and medium-chain acyl-CoA dehydrogenase, as well as isovaryl-CoA dehydrogenase to a lesser extend [168-170].

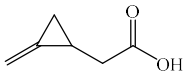

Fig. 17. Chemical structure of methylene cyclopropyl acetic acid.

1.5.1.3 4-Bromocrotonic Acid

Similar to MCPA, 4-bromocrotonic acid (4bc) was synthesized and studied for its potential as hypoglycemic drug, as well as for the use as research tool for studying β-oxidation [171,172].

4bc enters mitochondria directly, is then activated to its CoA-form and metabolized to 3-keto-4-bromobutyryl-CoA by acyl-CoA hydratase and 3-OH acyl-CoA dehydrogenase. This metabolite, then, irreversibly inhibits 3-ketoacyl-CoA thiolase, as well as acetoacetyl-CoA thiolase [172,173], therefore stopping β-oxidation at its last step.

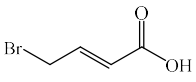

Fig. 18. Chemical structure of 4-bromocrotonic acid.

1.5.1.4 Triacsin C

Triacsin C was included in Paper 3, after it was observed that the drugs of investigation were inhibitors for ACSLs. Triacsins were found during a screening of bioactive compounds from microorganisms. Their strong inhibitory activity on ACSLs was found in 1986 after isolation from a *Streptomyces* species, originating from a Japanese soil sample [174]. Of all triacsin compounds (A –D), triacsin C was found to be the strongest inhibitor, with an IC_{50} value of 9 µM on isolated rat liver ACSLs [175]. In human tissues, however, triacsin C seems to be even more potent, as effective treatment concentrations range around 1 - 5 µM [176-178].

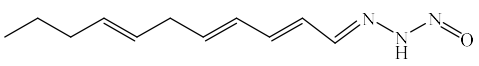

Fig. 19. Chemical structure of triacsin C.

Since its discovery, triacsin C has often been used as model compound for the inhibition of ACSL [179-182]. During these studies, it was found that triacsin C is not affecting all ACSL isoforms the same. It is reported,

that mostly lipogenic ACSL isoforms are affected (ACSL1, ACSL3, and ACSL4), resulting in the inhibition of *de novo* synthesis of TGs by around 75% and β-oxidation only by around 35% [38]. Additionally, unlike the other model inhibitors used in this thesis, triacsin C is a competitive inhibitor.

1.5.2 Selected Compounds for Comparison Investigations

The following drugs were chosen for Paper 1 for proof of concept and also the elucidation of mechanisms leading to steatosis in patients, which come in contact with these compounds.

1.5.2.1 Amiodarone

Amiodarone was approved in the US in 1985 as an effective agent for the treatment of tachyarrhythmias [183]. It showed toxicities on several tissues and received a black box warning in the US after some years [184]. Amiodarone is a well-known hepatic toxicant with multiple actions, mainly affecting mitochondria.

Approximately 25% of treated patients show elevation of ALT levels, with 1- 3% of patients developing severe hepatotoxicity. Hepatic steatosis is a common finding in such patients [185,186]. This kind of injury can be explained by its numerous adverse effects on the liver, where amiodarone is reported to uncouple oxphos, leading to accumulation of superoxide anions, inhibiting β-oxidation, inhibiting ETC proteins, and also inhibiting several CYPs [157,187,188]. Furthermore, the liver may be a preferential target for amiodarone-induced toxicity, because higher concentrations in hepatic tissue are reported, due to accumulation of this lipophilic compound in membranes [189]. Plasma levels can reach 2.5 µM or more[190], which makes the toxic effects, seen with an only two fold higher concentration in *in vitro* experiments, highly translatable [157,187].

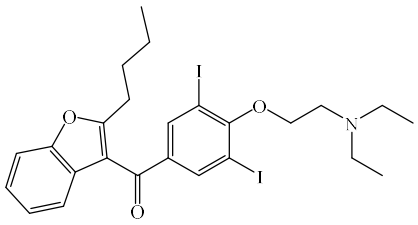

Fig. 20. Chemical structure of amiodarone.

1.5.2.2 Tamoxifen

In the late 1950s tamoxifen, then ICI 46 474, was developed in the laboratories of Imperial Chemical Industries Ltd. (now AstraZeneca) for the use as a contraceptive [191]. Years later, after failing in the intended indication and after extensive trials, tamoxifen was finally approved by the FDA for the treatment of breast cancer in 1977. Because of its availability and inexpensiveness it eventually gained worldwide popularity as a miracle drug for breast cancer [191,192]. As stated above, tamoxifen, although a first generation SERM, is still used extensively in clinics [191].

Despite being generally well tolerated, it has an extensive list of adverse reactions, such as higher risk for developing endometrial cancers, hot flushes, problems with metabolism and eating, elevation of serum TG, headaches, liver cholestasis and also steatosis, just to name a few [193]. In Paper 1, the focus, among others, lied on the hepatotoxicity of tamoxifen. The most encountered form of tamoxifen-induced hepatotoxicity is the development of steatosis. It is even reported that 43% of patients develop hepatic steatosis within the first two years of treatment [194]. The investigations on the mechanism behind it, however, are still ongoing.

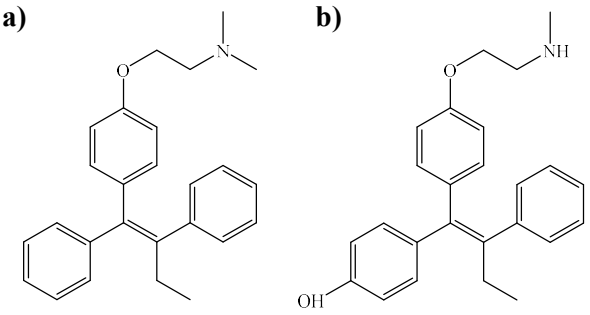

Fig. 21. Chemical structures of a) tamoxifen and its metabolite b) N-desmethyl-4-hydroxytamoxifen (endoxifen).

Pharmacological studies of tamoxifen suggested that it gets metabolized to three active metabolites, two of which are 100 times more potent than the parent drug [191]. Cytochrome P450 3A4 and 2D6 are involved in this conversions [104]. It is indicated that the pharmacological and toxicological activity of tamoxifen mainly occurs via the metabolite 4-hydroxy tamoxifen and its desmethyl analogue endoxifen (**Fig. 21b**) [191]. This is of importance for the interpretation of concentration-toxicity correlations and translatability to the *in vivo* situation, as HepG2, which were used for this study, have almost no activity of CYP 2D6.

1.5.2.3 WIN55, 212-2

The third test compound, we included in Paper 1, was WIN55, 212-2 (WIN55). It is an aminoalkylindole-type CB receptor agonist, developed by Sterling-Winthrop Inc. As explained earlier, the endocannabinoid system has an important function in the regulation of hepatic lipid metabolism and is reliant on signaling by endocannabinoids like anandamide. There are several xenobiotics affecting this system. One of them is WIN55, which is about five times more potent, than trans-Δ9-tetrahydrocannabinol (THC) or Cannabidiol [87], the main active substances in *Cannabis sativa*.

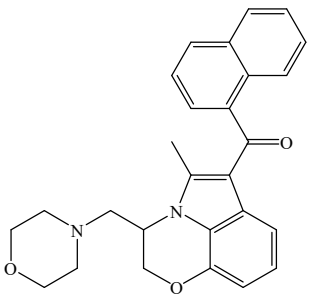

Fig. 22. Chemical structure of WIN55,212-2.

Marijuana (*Cannabis Sativa* and preparations from it) is the most commonly used illicit drug consumed in the US [195], as well as in other western countries, like Switzerland [196]. In 2007 11.2% of adults were consuming this drug at least every six months, with 31.7% of them consuming every week and 9.3% every day[197]. In recent years, new insights were made on the consequences of altered CB signaling on lipid metabolism. CB1 receptor activation has been consistently linked to the initiation and progression of steatosis [90,92,198,199]. A study by Hezode et al., for example, identified daily cannabis smoking as a novel independent predictor of steatosis severity during chronic hepatitis.[89] Furthermore, CB1 receptor activation was shown to dose-dependently increase the lipid accumulation in HepG2 cells and immortalized primary human hepatocytes in the presence of oleic acid [200].

WIN55 binds both to CB1 and CB2 receptors in the nM range and can therefore be a good surrogate for THC, which is only available with special permissions in Switzerland.

1.5.4 COMT Inhibitors

Parkinson's disease is the second most common neurodegenerative disorder, affecting almost exclusively the elderly population. It is characterized by the degeneration and loss of dopaminergic neurons, which results in disruption of motor functions, leading to tremor, bradykinesia, and rigidity [201].

The intracellular enzyme catechol-*O*-methyltransferase (COMT), which is widely distributed in the body, is responsible for the elimination of catechol compounds, like dopamine, adrenaline and related substances. Inhibition of this enzyme in conjunction with levodopa treatment effectively increases dopamine levels in the brain, improving symptoms of Parkinson's disease. COMT inhibitors are beneficial for Parkinson's treatment, because they decrease the overall elimination of levodopa, improve the delivery to the brain, and prolong the clinical response to levodopa treatment [202]. These inhibitors are always used in combination with levodopa and a DOPA decarboxylase inhibitor [203].

1.5.3.1 Tolcapone

The second generation COMT inhibitor tolcapone was developed in the late 1980s, after the first generation compounds had failed clinical implementation because of their toxicity. Tolcapone, currently on the market in many countries, has a nitrocatechol structure and inhibits COMT reversibly in the periphery and the brain. It has a bioavailability of 60% and is always given three times daily to reach steady state, as it has a relatively short half-life of 2.1 h [204].

In preclinical safety studies, tolcapone proved to be safe after toxicity testing in several animal species. Clinical trials showed side effects, mainly associated with levodopa treatment, meaning dopaminergic adverse events. After about one year on the market, tolcapone was finally found to induce liver toxicity, with three fatal cases reported. Thereafter it was taken from the market in many countries and only reintroduced with restricted use and simultaneous therapeutic drug monitoring [205].

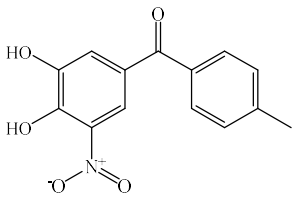

Fig. 23. Chemical structure of tolcapone.

To this date, available research articles connect tolcapone-associated hepatotoxicity mainly to mitochondrial energy metabolism, focusing on uncoupling of oxphos [206-209]. Two studies, a biomarker screening[210] and a capture compound mass spectrometry study[211], have implemented the toxicity of tolcapone not only with enzymes of oxphos, but also the lipid metabolism. As there are reports of hepatic steatosis in patients with adverse reactions under tolcapone therapy [209,212], investigations on possible adverse reactions on hepatic lipid metabolism seemed compelling.

1.5.3.2 Entacapone

Entacapone was developed together with tolcapone and is also a second generation, reversible COMT inhibitor. It has a lower bioavailability (35%), longer half-life (3.4 h) and in contrast to tolcapone, only inhibits COMT in the periphery. Entacapone is better tolerated in patients, however, has a greater variability of plasma levels during the day (up to ten fold [213]), because of its low bioavailability, higher clearance, and smaller volume of distribution [204].

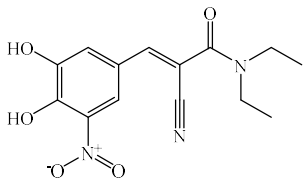

Fig. 24. Chemical structure of entacapone.

While tolcapone leads to elevated liver enzymes in 3% of treated patients, entacapone only affects 0.2% [202,214]. It is, however, also associated with interactions with proteins of oxphos and lipid metabolism [210,211]. Furthermore, entacapone was also associated with mitochondrial uncoupling, but at higher concentrations than tolcapone [207].

Even though entacapone has a lower incidence of toxicity than tolcapone, it is clearly linked to possible adverse effects on mitochondrial energy metabolism. Additionally, because of its similar chemical structure, we also included this compound in our studies for toxicological comparison to tolcapone.

1.6 Aims of the Thesis

1.6.1 General Aims

The main goal of the thesis was to contribute to the understanding of idiosyncratic drug-induced steatosis observed in clinics. Therefore, we aimed to create a cell model for impaired hepatocellular FA metabolism and to evaluate biomarkers for FA metabolism inhibition. Secondly, we aimed to elucidate mechanisms behind the idiosyncratic adverse reactions of drugs, leading to steatosis, using the methods established in the first step of Paper 1.

To achieve this goals, three major work packages were defined as followed.

1.6.2 Paper 1 (Acylcarnitines as Biomarkers)

In the first step, we wanted to find and characterize biomarkers for changes in FA metabolism by evaluating acylcarnitines as specific biomarkers for distinguishable locations of inhibitions within the FA catabolism pathways. We aimed to establish and optimize a semi-quantitative acylcarnitine measurement using LC-MS/MS, with three specific and well-established inhibitors of FA oxidation. We compared, as well as

supplemented, the results of the new method with older, well established methods. In a second step of the study, we applied the same methods on three compounds, of which adverse reactions are not well understood, to obtain new insights about their steatogenic mechanisms.

1.6.3 Paper 2 (Tolcapone and Entacapone – Fatty Acid Metabolism)

The purpose of the second project was the detailed study on the mechanistic bases of the steatogenic effect, exerted by tolcapone treatment, to further increase the understanding of its adverse reactions on the FA metabolism. Entacapone, also a second generation COMT inhibitor, was included as well, because of its structural similarity. Also, we used HepaRG cells in this investigation to further establish the acylcarnitine measurement from Paper 1, as means for a detailed analysis of FA metabolism changes in an additional cell line.

1.6.4 Paper 3 (Tolcapone and Entacapone – Electron Transfer Chain)

The focus of Paper 3 was to expand the knowledge of tolcapone-associated steatosis and liver toxicity observed in clinics. Entacapone was included as well, as in the previous Paper. Tolcapone, a known mitochondrial uncoupler, was shown to also interact with proteins of the ETC besides its impact on FA metabolism. To study this additional important effects, we therefore aimed to additionally investigate their actions in regard to their effect on mitochondrial respiration, as well as cell death for a comprehensive study about the drugs.

2. RESULTS

2.1 Paper 1

Effect of Toxicants on Fatty Acid Metabolism in HepG2 Cells

frontiers in Pharmacology

ORIGINAL RESEARCH
published: 23 April 2018
doi: 10.3389/fphar.2018.00257

Effect of Toxicants on Fatty Acid Metabolism in HepG2 Cells

David Grünig[1,2], *Urs Duthaler*[1,2] *and Stephan Krähenbühl*[1,2,3]*

[1] Division of Clinical Pharmacology and Toxicology, University Hospital Basel, Basel, Switzerland, [2] Department of Biomedicine, University of Basel, Basel, Switzerland, [3] Swiss Centre for Applied Human Toxicology, Basel, Switzerland

Impairment of hepatic fatty acid metabolism can lead to liver steatosis and injury. Testing drugs for interference with hepatic fatty acid metabolism is therefore important. To find out whether HepG2 cells are suitable for this purpose, we investigated the effect of three established fatty acid metabolism inhibitors and of three test compounds on triglyceride accumulation, palmitate metabolism, the acylcarnitine pool and dicarboxylic acid accumulation in the cell supernatant and on ApoB-100 excretion in HepG2 cells. The three established inhibitors [etomoxir, methylenecyclopropylacetic acid (MCPA), and 4-bromocrotonic acid (4-BCA)] depleted mitochondrial ATP at lower concentrations than cytotoxicity occurred, suggesting mitochondrial toxicity. They inhibited palmitate metabolism at similar or lower concentrations than ATP depletion, and 4-BCA was associated with cellular fat accumulation. They caused specific changes in the acylcarnitine pattern and etomoxir an increase of thapsic (C18 dicarboxylic) acid in the cell supernatant, and did not interfere with ApoB-100 excretion (marker of VLDL export). The three test compounds (amiodarone, tamoxifen, and the cannabinoid WIN 55,212-2) depleted the cellular ATP content at lower concentrations than cytotoxicity occurred. They all caused cellular fat accumulation and inhibited palmitate metabolism at similar or higher concentrations than ATP depletion. They suppressed medium-chain acylcarnitines in the cell supernatant and amiodarone and tamoxifen impaired thapsic acid production. Tamoxifen and WIN 55,212-2 decreased cellular ApoB-100 excretion. In conclusion, the established inhibitors of fatty acid metabolism caused the expected effects in HepG2 cells. HepG cells proved to be useful for the detection of drug-associated toxicities on hepatocellular fatty acid metabolism.

Keywords: liver steatosis, fatty acids, biomarkers, ApoB-100, acylcarnitines, dicarboxylic acids

OPEN ACCESS

Edited by:
Eleonore Fröhlich, Medizinische Universität Graz, Austria

Reviewed by:
Alberto Mantovani, Istituto Superiore di Sanità, Italy
Anna Alisi, Ospedale Pediatrico Bambino Gesù (IRCCS), Italy
Kamal Niaz, Università degli Studi di Teramo, Italy
Francesco Paolo Busardò, Sapienza Università di Roma, Italy

***Correspondence:**
Stephan Krähenbühl
stephan.kraehenbuehl@usb.ch

Specialty section:
This article was submitted to Predictive Toxicology, a section of the journal Frontiers in Pharmacology

Received: *20 October 2017*
Accepted: *07 March 2018*
Published: *23 April 2018*

Citation:
Grünig D, Duthaler U and Krähenbühl S (2018) Effect of Toxicants on Fatty Acid Metabolism in HepG2 Cells. Front. Pharmacol. 9:257. doi: 10.3389/fphar.2018.00257

INTRODUCTION

Hepatocellular metabolism of fatty acids is a complex function of hepatocytes. During starvation, when fatty acids become the most important fuel, activated fatty acids are mainly transported into the mitochondrial matrix for subsequent β-oxidation (Soeters et al., 2012). After ingestion of a meal, the high insulin concentration blocks transport of fatty acids into the mitochondrial matrix by inhibiting carnitine palmitoyltransferase (CPT) 1A, thereby shifting activated fatty acids into triglyceride synthesis (Foster, 2012). Triglycerides can be stored in lipid vesicles or be excreted as very low-density lipoprotein (VLDL).

Several drugs have been shown to interfere with hepatic metabolism of fatty acids. Well-known examples are for instance valproic acid, tamoxifen, amiodarone and methotrexate (Fromenty and Pessayre, 1995; Amacher, 2014; Ress and Kaser, 2016). Since interference with hepatic fatty acid

metabolism can be associated with liver injury, possible effects on fatty acid metabolism of drug candidates should be assessed in the preclinical and clinical phases of drug development. Fatty acid oxidation can be determined reliably in isolated liver mitochondria, cultured hepatocytes and in experimental animals (Krahenbuhl et al., 1994; Knapp et al., 2008; Felser et al., 2013). The methods usually used involve metabolism of radioactive substrates as well as spectrophotometric or radioenzymatic determination of enzyme activities. These methods are time-consuming and complicated and therefore difficult to use as biomarkers in cell cultures, experimental animals or humans. In order to be able to detect the potential for interference with hepatic lipid metabolism early, suitable cell models and, importantly, biomarkers that can also be used *in vivo*, are necessary.

Hepatic mitochondrial fatty acid breakdown starts with the activation of a given fatty acid at the outer mitochondrial membrane and ends with the formation of acetyl-CoA (and propionyl-CoA from odd-chain fatty acids) in the mitochondrial matrix. When this process is impaired, substrates proximal to the affected enzyme or transporter accumulate within the hepatocyte. After the initial activation step, accumulating substrates are acyl-CoAs of different chain lengths of the acyl group, depending on the location of the block. Since acyl-CoAs are too polar for crossing biological membranes by diffusion and efficient transport systems do not exist, they cannot leave hepatocytes and do not reach the blood. Acyl-CoAs can be converted to the corresponding acylcarnitines, however, which can be transported out of mitochondria and hepatocytes and reach the blood. This is well-established in patients with defects in hepatic fatty acid oxidation such as medium-chain acyl-CoA dehydrogenase deficiency, who typically have elevated medium-chain acylcarnitine plasma and urine concentrations (Minkler and Hoppel, 1993; Vernez et al., 2003). Acylcarnitines in plasma or urine of patients or in the supernatant of cell cultures could therefore be used as biomarkers for impaired hepatic β-oxidation. In addition, when mitochondrial β-oxidation of fatty acids is impaired, cytochrome P450 (CYP) 4A1 (CYP4A11 in humans) is induced, which catalyzes the formation of dicarboxylic acids (Kaikaus et al., 1993; Wanders et al., 2011). Dicarboxylic acids represent therefore also a potential biomarker for detecting inhibition of hepatic fatty acid metabolism in cell cultures and *in vivo*.

The principle aims of the current study were to investigate the effect of different compounds known to be associated with liver steatosis on a human hepatocyte cell line, to find out underlying mechanisms and to assess the suitability of the different assays used to determine fatty acid metabolism. Based on our own experience (Felser et al., 2013) and on reports from others (Guo et al., 2006; Donato et al., 2009), we decided to use HepG2 cells. HepG2 cells are a hepatoma cell line used widely for toxicological studies. They are easy to culture and are well-suited for studying mitochondrial functions (Felser et al., 2014a; Kamalian et al., 2015), but have only a minor expression of hepatocyte specific functions such as for instance expression of CYP enzymes (Berger et al., 2016). In the current study, we first investigated the effect of three established inhibitors of hepatic fatty acid metabolism on different aspects of fatty acid metabolism in HepG2 cells (see Supplementary Figure 1 for chemical structures). In a second step, we used the findings obtained in the first part of the study to investigate the effect of three compounds (amiodarone, tamoxifen, and WIN 55,212-2; all of them known to cause hepatocellular triglyceride accumulation) on fatty acid metabolism in HepG2 cells.

MATERIALS AND METHODS

Chemicals

4-bromocrotonic acid (4-BCA) was purchased from TCI Chemicals (Eschborn, Germany). WIN 55, 212-2 was purchased from Cayman Chemical (Ann Arbor, MI, United States). Etomoxir, methylenecyclopropylacetic acid (MCPA), amiodarone, and tamoxifen were obtained from Sigma-Aldrich (Buchs, Switzerland). If not stated otherwise, all other chemicals were also purchased from Sigma-Aldrich (Buchs, Switzerland). Stock solutions were prepared in DMSO and kept at −20°C for cell treatment (in general at 1:1000 dilution).

Cell Culture

The human hepatocellular carcinoma cell line HepG2 was purchased from ATCC (Molsheim Cedex, France). Cells were cultured in Dulbecco's modified Eagle low glucose medium (1 g/L) (DMEM) supplemented with 10% (v/v) heat inactivated fetal bovine serum (FBS), 1% 1 M HEPES buffer, 1% 200 mM GlutaMAX^{TM}-I supplement and 1% MEM non-essential amino acids (100×). Cells were kept in a humidified incubator at 37°C and 5% CO_2. TrypLE express trypsin was used for passaging cells and a Neubauer hemacytometer for cell counting.

Plasma Membrane Integrity

Plasma membrane integrity was assessed by the detection of adenylate kinase (AK) release into supernatant of the incubations. AK was determined with the ToxiLight assay kit (Lonza, Basel, Switzerland) and as described previously (Felser et al., 2013).

Intracellular ATP Content

The intracellular ATP content was measured using the CellTiter-Glo Luminescent cell viability assay (Lonza, Basel, Switzerland) according to the manufacturer's protocol as described previously (Felser et al., 2013).

Protein Content

We assessed the protein content of the samples after dissolving the cells in RIPA-buffer (50 mM Tris–HCl, 150 mM NaCl, 1% Triton X-100, 0.5% sodium deoxycholate, 0.1% sodium dodecyl sulfate and 1 mM EDTA in MilliQ water, pH 7.4) using the Pierce BCA Protein Assay Kit (Thermo Scientific, Wohlen, Switzerland) according to the manufacturer's instructions. Samples were measured at 562 nm using the Tecan plate reader.

Intracellular Lipid Accumulation

We used the method described by Donato et al. (2009) with some modifications. HepG2 cells were incubated in the presence of

drugs and exogenous lipids (DMEM containing 500 μM of a 2:1 mixture of oleate and palmitate). Oleate and palmitate were kept as stock solutions containing 667 μM oleate or 333 μM palmitate in DMEM containing 1% fatty acid free bovine serum albumin. After 24 h exposure, cells were detached using Trypsin-EDTA (Thermo Scientific, Wohlen, Switzerland) and washed with PBS. Afterwards, cells were stained with 10 μg/mL propidium iodide to exclude dead cells and 250 ng/mL BODIPY 493/503 (Thermo scientific, Wohlen, Switzerland) in PBS for 30 min at 37°C. Stained cells were examined by flow cytometry.

Fluorescence Microscopy

HepG2 cells were seeded in black corning CellBIND 96 well assay plates with clear flat bottom purchased from Corning Inc. (Corning, NY, United States). After treatment with the toxicants, the cells were washed and fixed for 4 min with 4% paraformaldehyde solution. After an additional washing step, the cells were stained for 30 min with 0.5 μg/mL BODIPY 493/503 Thermo Scientific (Wohlen, Switzerland) and 1 μM of DAPI Thermo Scientific (Wohlen, Switzerland) in PBS. After washing twice with PBS and addition of antifade-mounting medium (1 mg/mL p-phenylenediamine in 90% glycerol, pH 9), cells were imaged using an Olympus IX83 microscope (Olympus, Tokyo, Japan).

β-Oxidation of ^{14}C-Palmitate

Metabolism of 1-^{14}C-palmitic acid (60 mCi/mmol; PerkinElmer, Schwerzenbach, Switzerland) was determined as the formation of ^{14}C-acid-soluble β-oxidation products in HepG2 cells treated for 24 h with test compounds. Measurements were performed as previously described (Kaufmann et al., 2005) with some modifications. HepG2 cells were permeabilized (10 μg digitonin/million cells), incubations contained 2 mM 1-^{14}C-palmitate (10 nCi/assay) and the incubation lasted 15 min.

Mitochondrial Isolation

Male C57BL/6 mice were kept in the animal facility of the University Hospital Basel (Basel, Switzerland) in a temperature-controlled environment with a 12-h light/dark cycle and food and water *ad libitum*. Animal procedures were conducted in accordance with the institutional guidelines for the care and use of laboratory animals. Mice were sacrificed by cervical dislocation. Before the liver was removed, it was flushed with 5 mL of ice cold isolation buffer (200 mM mannitol, 50 mM sucrose, 1 mM Na_4EDTA, 20 mM HEPES, pH 7.4) and then immersed in ice-cold isolation buffer. Mitochondria were isolated by differential centrifugation as described by Hoppel et al. (1979). The mitochondrial protein content was determined using the Pierce BCA Protein Assay Kit (Thermo Scientific, Wohlen, Switzerland).

Activity of Carnitine Palmitoyltransferase (CPT) 1

Carnitine palmitoyltransferase 1 activity was assessed by the formation of palmitoyl-^{14}C-carnitine from palmitoyl-CoA and ^{14}C-carnitine as described previously (Felser et al., 2014b). One hundred and twenty-five micrograms of previously frozen mitochondrial protein was the enzyme source. The substrate concentrations were 400 μM ^{14}C-L-carnitine (25 pCi per assay) and 200 μM palmitoyl-CoA. The reaction was followed for 10 min.

Mitochondrial Metabolism of Palmitoylcarnitine

The metabolism of 1-^{14}C palmitoylcarnitine was assessed as described by Felser et al. (2014b). Freshly isolated mitochondria (125 μg mitochondrial protein) were incubated with 200 μM [1-^{14}C]-palmitoylcarnitine (25 pCi per assay). The reaction was stopped after 4 min.

Activity of Acyl-CoA Dehydrogenases

The activity of the respective acyl-CoA dehydrogenase was determined by the method of Hoppel et al. (1979). In a 24-well plate, 50 μg of previously frozen mitochondrial protein was preincubated in the presence of test compounds for 3 min in assay buffer (34 mM potassium phosphate, 1.5 mM KCN, 3.75 μM rotenone, 1.5 mM cytochrome C, 3 mM phenazine ethosulfate, pH 7.2). The reaction was started by the addition of palmitoyl-CoA or octanoyl-CoA (final concentrations were 50 and 100 μM, respectively) and monitored at 550 nm over 2 min using a Tecan plate reader.

Acylcarnitines

Acylcarnitines were analyzed by liquid chromatography tandem mass spectrometry (LC-MS/MS) according to Morand et al. (2013) with some adaptions. In brief, the supernatants of cells were mixed with internal standard solution containing acetylcarnitine-d3 (10 μM), octanoylcarnitine-d3 (1 μM), and palmitoylcarnitine-d3 (1 μM) in methanol in a ratio of 1:3 (v/v). The mixture was centrifuged at 3220 × *g* for 30 min (Eppendorf Centrifuge 5810R) and the supernatant transferred to an autosampler tube and diluted 1:1 with water before analysis. The LC-MS/MS system consisted of a Nexera SIL-30AC autosampler, a column-oven (CTO-20A), four HPLC pumps (2× LC-20AD and 2× LC-ADXR) and a system controller (CBM-20A), all acquired from Shimadzu (Kyoto, Japan). The HPLC system was coupled to an API 4000 triple quadrupole mass spectrometer from AB Sciex (Concord, Canada), equipped with a turbo electrospray ionization source.

Samples were separated on a Luna C8 5 μM column (150 mm × 2 mm) using a C8 (4 mm × 2.0 mm) precolumn (Phenomenex, Torrance, CA, United States) at 50°C. Mobile phase A was an aqueous solution of 5 mmol/L heptafluorobutyric acid and 6 mmol/L ammonium acetate. Mobile B was methanol with the same additives. Samples were loaded onto the analytical column using 20% mobile phase B. After 0.5 min, the gradient was linearly increased within 3 min to 95% mobile phase B. The column was washed for 2 min at 95% mobile phase B and thereafter reconditioned for another 0.5 min at 20% mobile phase B. The retention times of acetylcarnitine, C3-carnitine, C4-carnitine, C5-carnitine,

C6-carnitine, C8-carnitine, C10-carnitine, C12-carnitine, C14-carnitine, palmitoylcarnitine, and 3-oxo-palmitoylcarnitine were 1.24, 1.44, 2.09, 2.48, 2.82, 3.18, 3.45, 3.64, 3.82, 3.98, and 3.78 min, respectively.

Acylcarnitines of interest were analyzed in the positive mode by multiple reaction monitoring (MRM). Acylcarnitines build a characteristic fragment of 85 m/z, which corresponds to a McLafferty rearrangement of the butyric acid side chain with loss of the trimethylamine moiety (Zuniga and Li, 2011). The following mass transitions (m/z) were used: acetylcarnitine, 204→85; acetylcarnitine-d3, 207→85; C3-carnitine, 218→85; C4-carnitine, 232→85; C5-carnitine, 246→85; C6-carnitine, 260→85; C8-carnitine, 288→85; C8-carnitine-d3, 291→85; C10-carnitine, 316→85; C12-carnitine, 344→85; C14-carnitine, 372→85; palmitoylcarnitine, 400→85; palmitoylcarnitine-d3, 403→85; 3-oxo-palmitoylcarnitine, 414→85. Reference substances were obtained for acetylcarnitine, octanoylcarnitine, and palmitoylcarnitine and used as standards and for quality control. The ion spray voltage was 5,500 eV, the probe temperature was 450°C, and the dwell time was 20 ms for each analyte.

Dicarboxylic Acids

After treatment of the cells with the toxicants in 12-well plates, the cell suspensions (500 μL) were frozen and thawed before the addition of 500 μL of internal standard solution (methanol containing 1 μM sebacic acid-d16). Samples were diluted further with 1000 μL internal standard solution for protein precipitation and then centrifuged at 15,500 × *g* for 10 min at 15°C. The supernatant was transferred to an autosampler tube and analyzed using the LC-MS/MS system described for the analysis of acylcarnitines. Samples were separated on a Symmetry C18 3.5 μM (4.6 mm × 75 mm) column (Waters Corporation, Milford, MA, United States). Mobile phase A was water containing 0.1% formic acid and mobile B was methanol containing 0.1% formic acid. Samples were loaded onto the analytical column using 50% mobile phase B. After 0.25 min, the gradient was linearly increased within 1.25 min to 95% mobile phase B. The column was washed for 1.5 min at 95% mobile phase B and thereafter reconditioned for another 0.5 min at 50% mobile phase B. The retention times of suberic acid, sebacic acid, and thapsic acid were 1.35, 1.78, and 2.45 min, respectively. Dicarboxylic acids of interest were analyzed in the negative mode by MRM. The following mass transitions (m/z) were used: suberic acid, 173→111; sebacic acid-d16, 217→153; thapsic acid, 285→267. The ion spray voltage was −4,500 eV, the probe temperature was 500°C, and the dwell time was 25 ms for each analyte.

Export of ApoB-100

HepG2 cells were grown in a 96-well plate (25,000 cells/well) and exposed to the toxicants for 24 h. The ApoB-100 concentration was measured as a surrogate of the export of triglycerides as VLDL in 100 μL of cell supernatant using the ApoB Quantikine® ELISA Kit from R&D Systems (Minneapolis, MN, United States) according to the manufacturer's protocol.

Statistical Methods

All results are expressed as mean ± standard error of the mean (SEM). Statistical analysis and calculation of IC_{50} values were performed with the statistics program Prism 7 from GraphPad Software (La Jolla, CA, United States). Differences between groups were determined by one-way-ANOVA followed by a Dunnett post-test. P-values < 0.05 were considered as significant and marked with *.

RESULTS

We included six compounds in our study; three established inhibitors of hepatic fatty acid metabolism [etomoxir as an inhibitor of CPT1A (Lilly et al., 1992; Ceccarelli et al., 2011), MCPA as an inhibitor of medium chain acyl-CoA dehydrogenase (Ikeda and Tanaka, 1990; Tserng et al., 1991) and 4-BCA as an inhibitor of 3-keto-acyl-CoA thiolase (Olowe and Schulz, 1982)] and three test compounds known to interfere with hepatic fatty acid metabolism and to be associated with liver steatosis (amiodarone, tamoxifen, and WIN 55,212-2) (Purohit et al., 2010; Amacher, 2014) (Supplementary Figure 1). The idea was to study first the effect of the well characterized inhibitors (etomoxir, MCPA, and 4-BCA) on the assays used in order to find out whether we obtained the expected results. The experience gained in this first step could then be used to judge the results obtained by the less characterized compounds (amiodarone, tamoxifen, and WIN 55,212-2) in order to find out mechanisms how these compounds inhibit fatty acid metabolism.

Membrane Integrity and Cellular ATP

First, we investigated plasma membrane integrity and effect on the cellular ATP content of the three established inhibitors. For that, we exposed HepG2 cells for 24 h to different concentrations of the three inhibitors. The concentration-toxicity relationships are shown in Supplementary Figure 2 and the corresponding IC_{50} values are listed in **Table 1**. All established inhibitors tested significantly decreased the cellular ATP content and impaired membrane integrity. The depletion of the cellular ATP content occurred at lower concentrations than impairment of membrane integrity, which is an indicator of mitochondrial

TABLE 1 | IC_{50} values for AK release, ATP content, and β-oxidation.

	AK release	ATP content	$\frac{IC_{50}\ AK}{IC_{50}\ ATP}$	β-oxidation
Etomoxir	>200	177 ± 27	>1.1	0.02 ± 0.001
MCPA	>500	>500	n.d.	28.0 ± 4.6
4-BCA	1340 ± 410	262 ± 18	5.11	113 ± 10
Amiodarone	80.0 ± 1.0	36.1 ± 1.5	2.22	29.5 ± 3.5
Tamoxifen	24.0 ± 1.0	14.8 ± 2.1	1.62	30.4 ± 3.5
WIN 55,212-2	>10	9.2 ± 0.2	>1.1	2.0 ± 0.1

The IC_{50} values [μM] of the compounds investigated were calculated based on the experiments shown in Supplementary Figures 2, 3 and in ***Figure 2****. Calculations were performed using Prism 7 from GraphPad Software (La Jolla, CA, United States). Data are presented as are presented as mean ± SEM of at least 3 independent experiments. n.d. not determinable.*

toxicity (Kamalian et al., 2015). Etomoxir depleted the cellular ATP content most potently, whereas 4-BCA was the most potent compound regarding impairment of membrane integrity.

The concentration-toxicity curves and the corresponding IC_{50} values of the three test compounds are shown in Supplementary Figure 3 and **Table 1**, respectively. All three test compounds significantly depleted the cellular ATP pool and impaired membrane integrity. Similar to the established inhibitors, the test compounds depleted the cellular ATP pool at lower concentrations than impairment of membrane integrity occurred (**Table 1**).

Intracellular Lipid Accumulation

In order to demonstrate the effect on hepatic fatty acid metabolism of the toxicants studied, we first investigated their potential for cellular accumulation of neutral lipids (mainly triglycerides) by staining with BODIPY 493/503. As shown in **Figure 1**, with the exception of etomoxir and MCPA, all substances tested were associated with lipid accumulation in a concentration-dependent fashion, starting at concentrations in the range of the IC_{50} values for ATP depletion. The results obtained with FACS were confirmed by the determination of lipid accumulation using the fluorescence microscope (**Figure 1G**).

Effect on ^{14}C-Palmitate Metabolism in HepG2 Cells

The quantification of the metabolism of ^{14}C-palmitate represents a specific way to assess the effect of toxicants on activation, intracellular transport and β-oxidation of long-chain fatty acids. All compounds investigated significantly inhibited palmitate metabolism. The concentration-toxicity curves are shown in **Figure 2**, and the corresponding IC_{50} values in **Table 1**. The most potent established inhibitor was etomoxir, with an IC_{50} in the nanomolar range. With the exception of tamoxifen, the IC_{50} values were either lower (etomoxir, MCPA, 4-BCA, and WIN 55,212-2) or similar (amiodarone) as the IC_{50} values for cellular ATP depletion. Similar results were obtained in isolated mouse liver mitochondria (data not shown).

Analysis of Acylcarnitines

Another possibility to assess effects on fatty acid metabolism is by analyzing the acylcarnitine pool in the supernatant of the incubations. The cellular carnitine pool is much larger than the CoA pool and acyl-CoAs can be converted to the corresponding acylcarnitines by carnitine acyltransferases. In

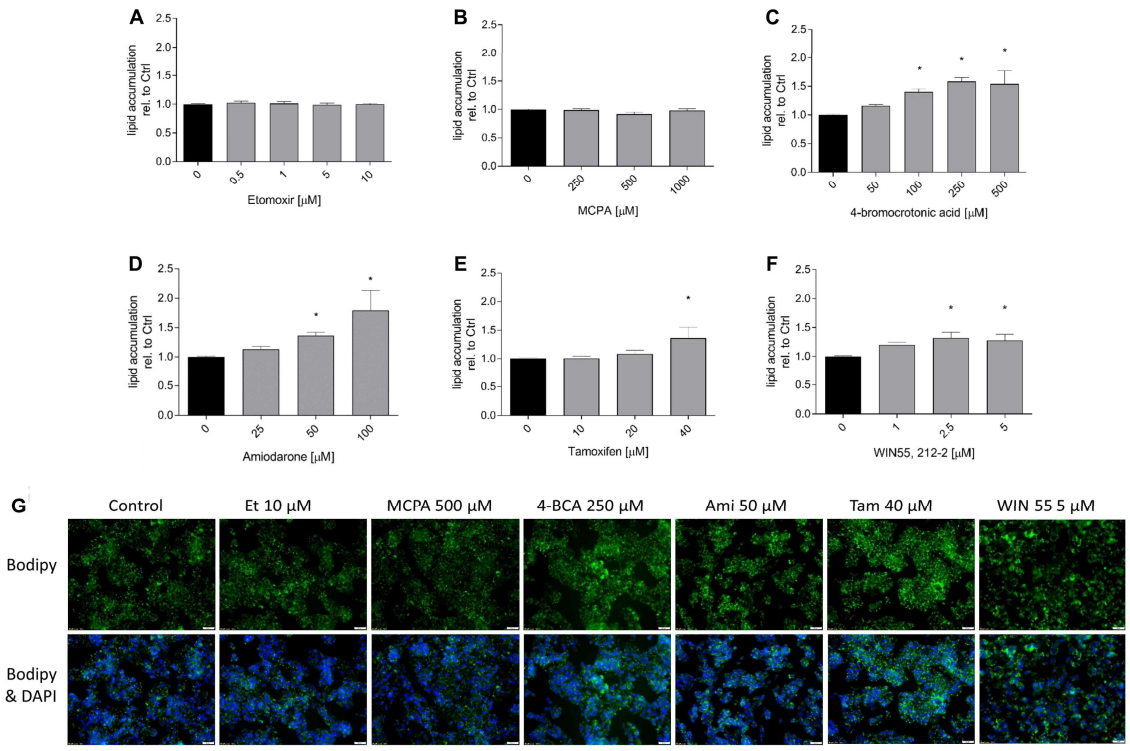

FIGURE 1 | Effect on intracellular lipid accumulation in HepG2 cells. HepG2 cells were cultured in a medium containing palmitate and oleate and treated with the compounds of interest for 24 h. After treatment, cells were stained with 10 µg/mL propidium iodide and BODIPY, and eventually analyzed by FACS. **(A)** etomoxir, **(B)** MCPA, **(C)** 4-BCA, **(D)** amiodarone, **(E)** tamoxifen, and **(F)** WIN 55,212-2. Below the columns there are representative fluorescence microscopy pictures **(G)**. These HepG2 cells were treated as described above and stained with BODIPY (green for fat) and DAPI (blue for nuclei). Results were normalized to control values (DMSO 0.1%) and are presented as mean ± SEM. *$p < 0.05$ vs. DMSO 0.1% control.

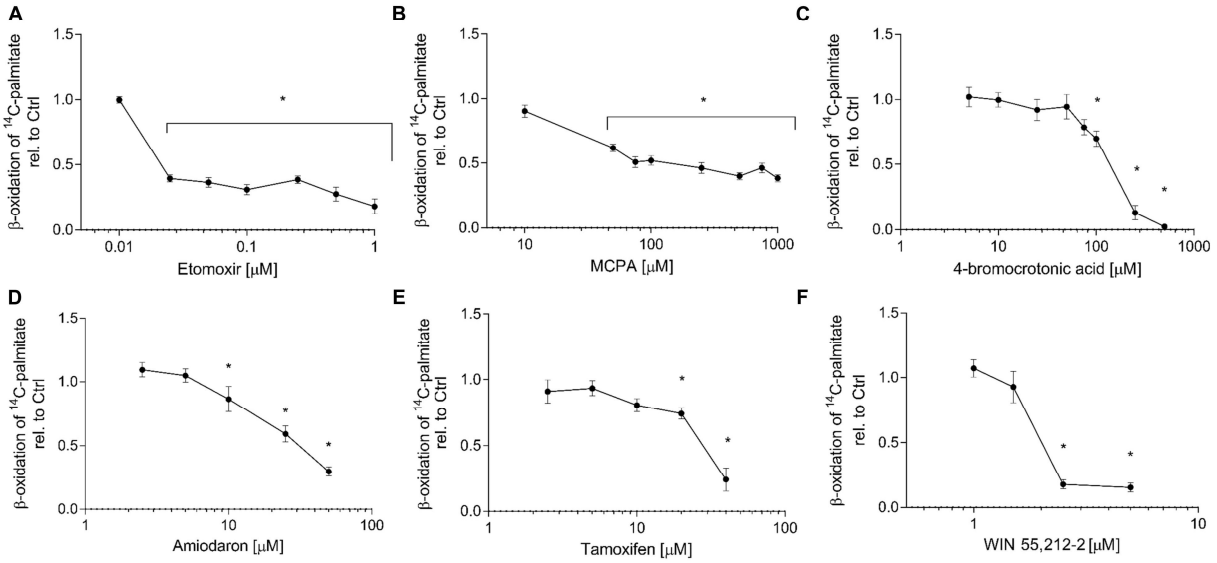

FIGURE 2 | Effect on 1-^{14}C-palmitate metabolism in HepG2 cells. HepG2 cells were exposed to **(A)** etomoxir, **(B)** MCPA, **(C)** 4-bromocrotonic acid, **(D)** amiodarone, **(E)** tamoxifen, or **(F)** WIN 55,212-2 for 24 h and metabolism of 1-^{14}C-palmitic acid was determined in permeabilized cells. Basal rates of palmitate oxidation for control incubations (0.1% DMSO) were 5.9 ± 0.5 nmol palmitate × min^{-1} × mg protein^{-1}. Results are expressed relative to DMSO 0.1% exposed control values and are presented as mean ± SEM. *$p < 0.05$ vs. DMSO 0.1% control.

contrast to acyl-CoAs, acylcarnitines can leave mitochondria and cells by specific transport systems and can therefore be detected in cell supernatants and body fluids. Since acylcarnitines reflect the cellular CoA pool, they can be used for the detection and the characterization of disturbances in fatty acid metabolism (Minkler and Hoppel, 1993; Vernez et al., 2003).

As shown in **Figure 3**, the established inhibitors were associated with the predicted changes in the acylcarnitine pool of the cell supernatant. As expected, HepG2 cells exposed to increasing concentrations of the CPT1 inhibitor etomoxir showed a decrease in C8 to C16 acylcarnitines in the supernatant (**Figure 3A**). Fatty acids with less than 8 carbons can be transported independently of CPT1 into the mitochondrial matrix (Rinaldo, 2001). The medium-chain acyl-CoA dehydrogenase inhibitor MCPA was associated with a massive increase in the medium-chain acylcarnitine concentration in the cell supernatant (C4–C10 acylcarnitines, **Figure 3B**) (Zschocke et al., 2001; Okun et al., 2002). The 3-keto-acyl-CoA thiolase inhibitor 4-BCA was associated with a concentration-dependent increase in β-keto C16 acylcarnitine (**Figure 3C**).

Regarding the test compounds (**Figure 4**), amiodarone showed a clear, concentration-dependent decrease in medium-chain acylcarnitines (C6–C14) (**Figure 4A**). Also tamoxifen (**Figure 4B**) and WIN 55,212-2 (**Figure 4C**) showed concentration dependent decreases in C6–C10 acylcarnitines, but the decreases were less accentuated than those for amiodarone.

For etomoxir and tamoxifen, similar data were obtained in HepaRG cells (data not shown).

Analysis of Dicarboxylic Acids

Acylcarnitines exported from mitochondria can also reach the endoplasmic reticulum, where they can undergo hydrolysis and ω-oxidation by for instance CYP4A11. The end product is the corresponding ω-aldehyde of the carboxylic acid, which can be oxidized to the corresponding dicarboxylic acid in peroxisomes (Wanders et al., 2011). Dicarboxylic acids of different chain lengths may therefore serve as indirect markers for inhibition of mitochondrial fatty acid metabolism. As shown in Supplementary Figure 4, we found a significant increase in the formation of thapsic acid (Supplementary Figure 4A), which is the dicarboxylic acid corresponding to palmitate, in the presence of 10 μM etomoxir. In comparison, amiodarone (50 μM) and tamoxifen (40 μM) significantly decreased the formation of thapsic acid. In contrast to thapsic acid, the formation of suberic acid (C8) was not affected by any of the toxicants investigated (Supplementary Figure 4B).

Effect on Lipid Metabolism in Isolated Mitochondria

In order to confirm the results obtained by quantification of palmitate metabolism and the acylcarnitine and dicarboxylic acid pools in the cell supernatant, we determined the activity of the enzymes that were predicted to be affected by the toxicants investigated in isolated and previously frozen mouse liver mitochondria. As shown in **Figure 5A**, the activity of CPT1A was significantly inhibited by amiodarone and tamoxifen in a dose-dependent manner. Etomoxir did not inhibit CPT1A under these conditions, because it inhibits CPT1

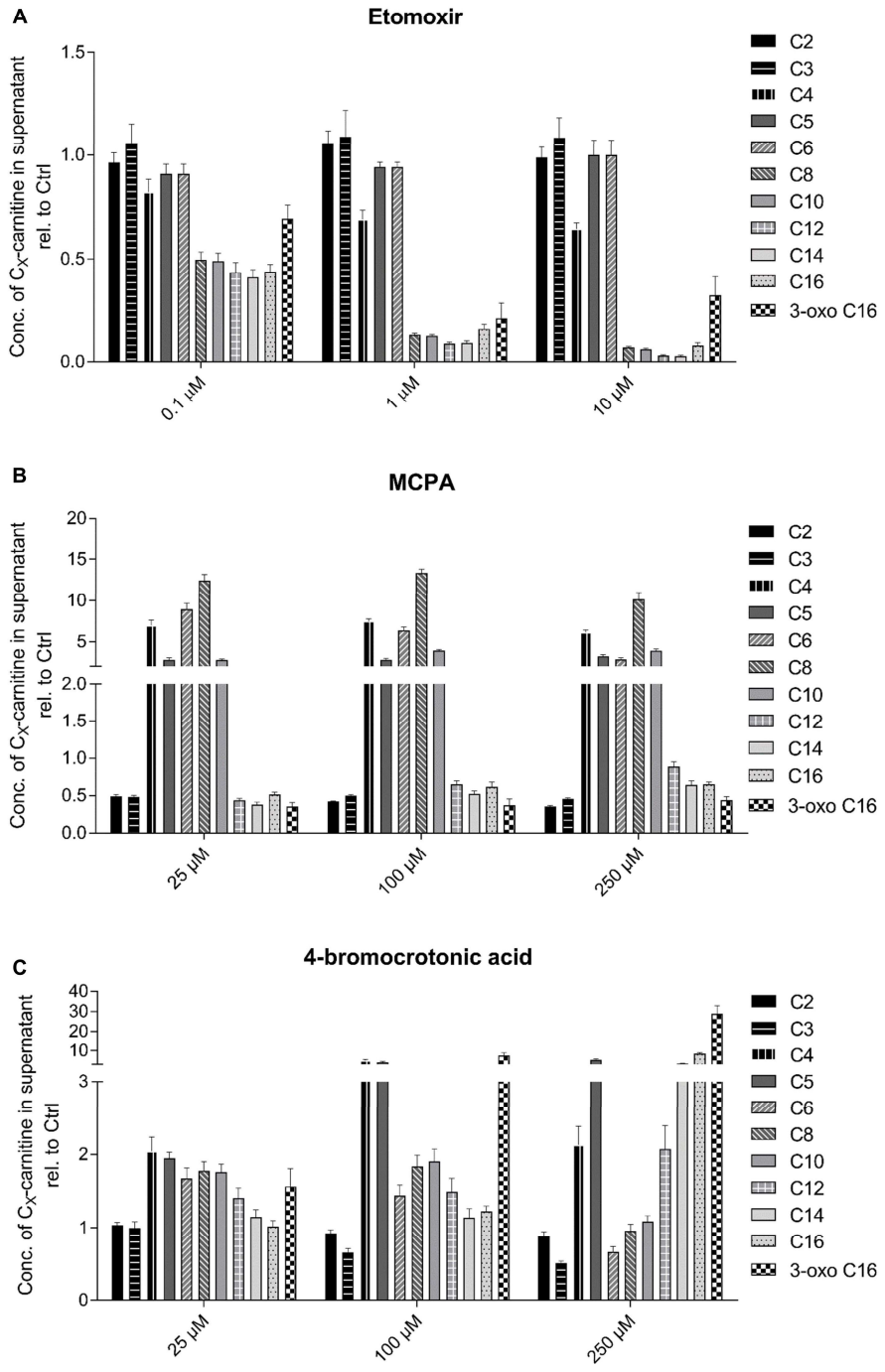

FIGURE 3 | Effect of **(A)** etomoxir, **(B)** MCPA, and **(C)** 4-BCA on the acylcarnitine pattern in the supernatant of HepG2 cells. Acylcarnitines were analyzed in the supernatant of HepG2 cells treated with the compounds of interest for 24 h using LC-MS/MS as described in the section "Materials and Methods." Results were normalized to the values obtained in DMSO 0.1% exposed control cells. Values are expressed as mean ± SEM.

after formation of the CoA derivative and CoASH was not present in the assay. The metabolism of palmitoylcarnitine, which reflects the import of fatty acids into mitochondria as well as β-oxidation (**Figure 5B**), was significantly inhibited by 4-BCA and by the higher concentrations of amiodarone (50 and 100 µM). The activity of the long-chain acyl-CoA dehydrogenase (**Figure 5C**) was significantly inhibited by amiodarone 50 and 100 µM, and the activity of the medium-chain acyl-CoA

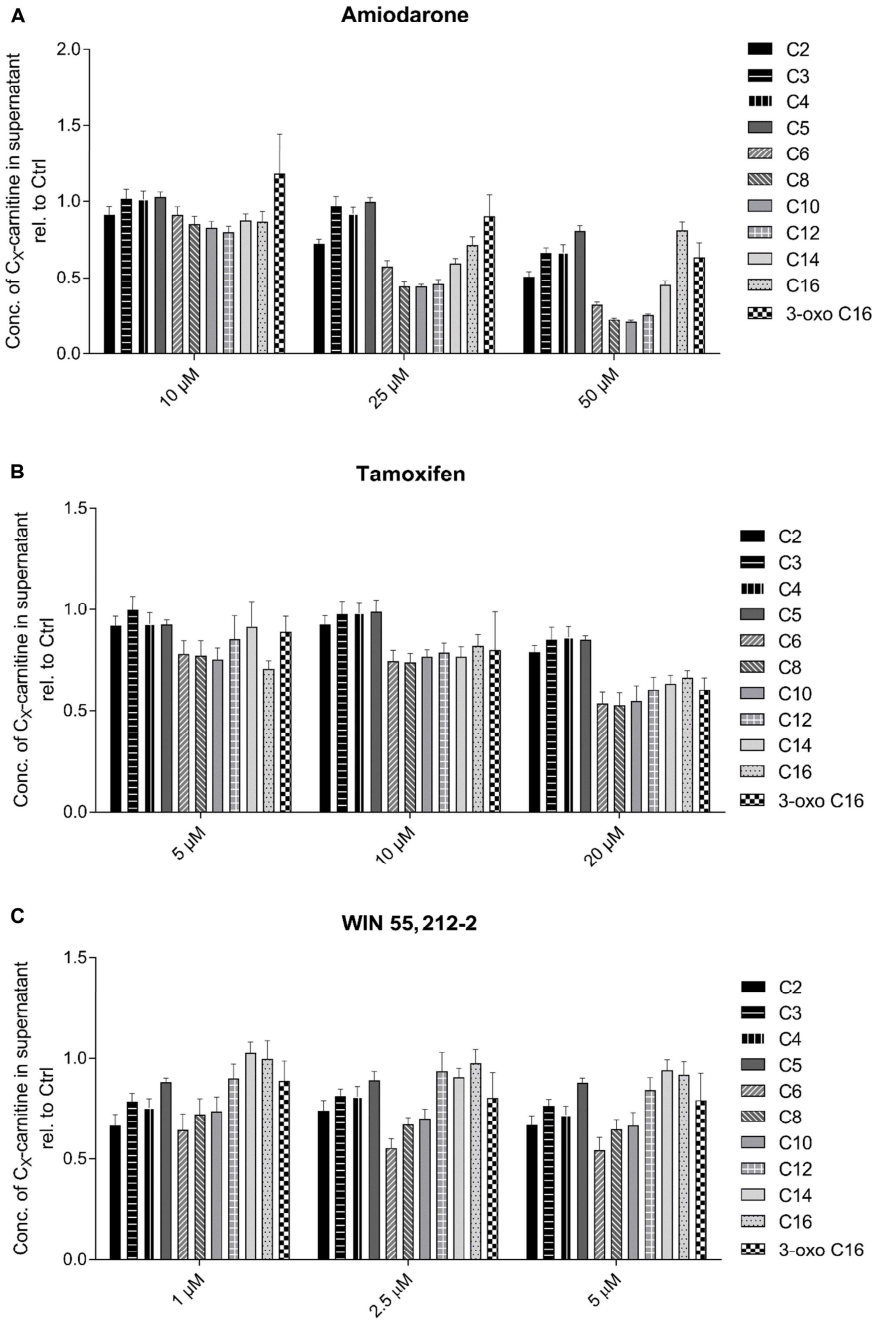

FIGURE 4 | Effect of **(A)** amiodarone, **(B)** tamoxifen, and **(C)** WIN 55,212-2 on the acylcarnitine pattern in the supernatant of HepG2 cells. Acylcarnitines were analyzed in the supernatant of HepG2 cells treated with the compounds of interest for 24 h using LC-MS/MS as described in the section "Materials and Methods." Results were normalized to the values obtained in DMSO 0.1% exposed control cells. Values are expressed as mean ± SEM.

dehydrogenase was decreased by MCPA and amiodarone (**Figure 5D**).

The results show that amiodarone and tamoxifen inhibit CPT1A (as predicted from the acylcarnitine pattern in the cell supernatant) and that amiodarone additionally inhibits long-chain and medium-chain acyl-CoA dehydrogenase.

ApoB-100 Excretion

In hepatocytes, activated fatty acids can either be transported into the mitochondrial matrix for β-oxidation or be used for triglyceride synthesis. Triglycerides can be transported out of the cells in the form of VLDL. To assess VLDL excretion, we determined the concentration of ApoB-100 in

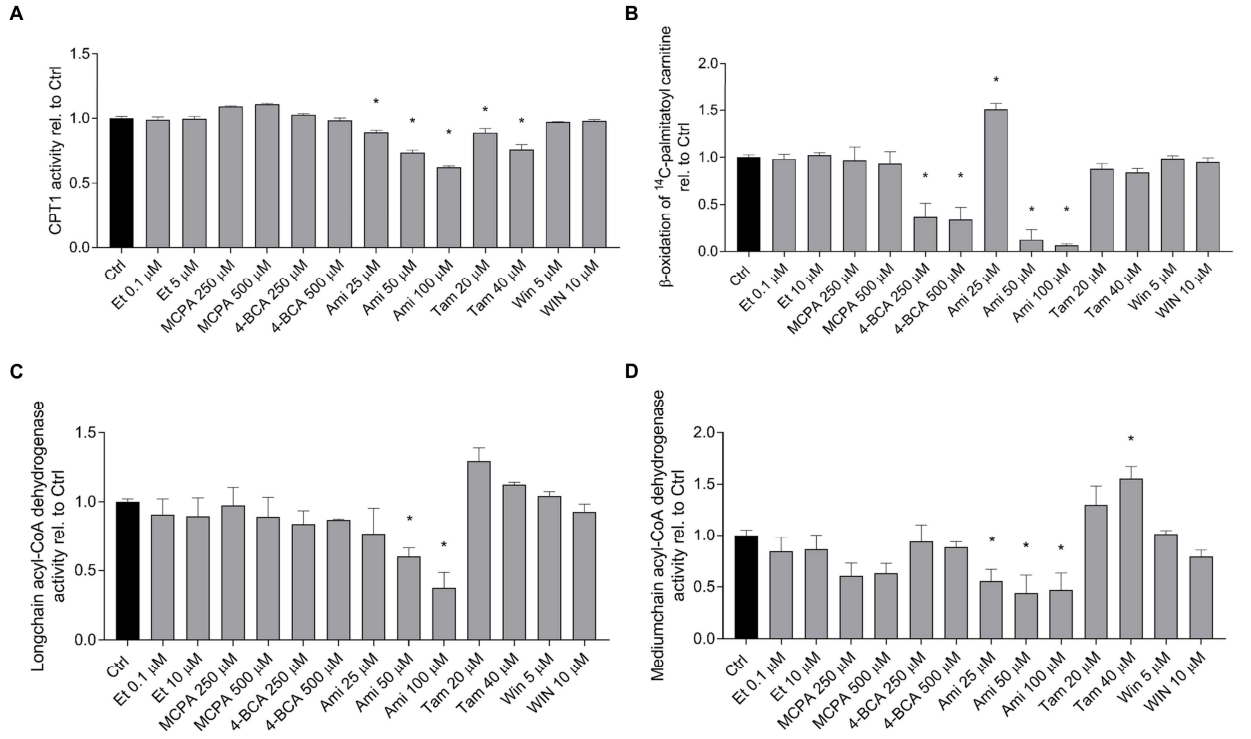

FIGURE 5 | Effect on fatty acid metabolism in isolated mouse liver mitochondria. Isolated, previously frozen mouse liver mitochondria were used as enzyme source. **(A)** Effect on CPT1A activity. Formation of ^{14}C-palmitoylcarnitine from ^{14}C-palmitoyl-CoA was assessed after incubation with the toxicants for 10 min. Basal rates of palmitoyl-CoA formation for control incubations (0.1% DMSO) were 3.0 ± 0.25 nmol palmitoyl-CoA × min^{-1} × mg protein^{-1}. **(B)** Effect on 1-^{14}C-palmitoylcarnitine metabolism. Mitochondria were treated with the toxicants for 10 min before formation of acid soluble products was determined. Basal rates of palmitoylcarnitine oxidation for control incubations (0.1% DMSO) were 213 ± 22 nmol palmitoylcarnitine × min^{-1} × mg protein^{-1}. **(C,D)** Effect on long-chain and medium-chain acyl-CoA dehydrogenases. After pretreatment with the toxicants for 3 min, reduction of cytochrome c by FADH produced by the acyl-CoA dehydrogenases was determined spectrophotometrically. Basal rates of cytochrome c oxidation by long- and medium-chain acyl-CoA dehydrogenases in control incubations (0.1% DMSO) were 53.7 ± 2.2 nmol × min^{-1} × mg protein^{-1} and 32.3 ± 1.2 nmol × min^{-1} × mg protein^{-1}, respectively. Results were normalized to the values obtained in DMSO 0.1% exposed controls and are expressed as mean ± SEM. *$p < 0.05$ vs. DMSO 0.1% control.

the cell supernatant, which is the protein backbone of VLDL (Fisher and Ginsberg, 2002). As shown in **Figure 6**, etomoxir, MCPA, 4-BCA, and amiodarone did not affect the ApoB-100 concentration in the cell supernatant after an incubation period of 24 h. In contrast, tamoxifen (20 μM) and WIN 55,212-2 (5 μM) significantly decreased the excretion of ApoB after 24 h of treatment, suggesting inhibition of VLDL excretion.

DISCUSSION

The principle aims of the current study were to investigate the suitability of HepG2 cells for studying the effect of toxicants on fatty acid metabolism and to test new methods for assessing toxic effects on hepatocellular lipid metabolism, which could also provide information about the associated mechanisms. Therefore, we first investigated the effects of three established inhibitors of fatty acid metabolism; etomoxir as an inhibitor of CPT1A (Lilly et al., 1992; Ceccarelli et al., 2011), MCPA as an inhibitor of medium chain acyl-CoA dehydrogenase (Ikeda and Tanaka, 1990; Tserng et al., 1991) and 4-BCA as an inhibitor of 3-keto-acyl-CoA thiolase (Olowe and Schulz, 1982; Yao et al., 1994). In a second step, we investigated the effects of three less characterized test compounds (amiodarone, tamoxifen, and WIN 55,212-2) in order to find out if and how they inhibit fatty acid metabolism by HepG2 cells.

With the exception of etomoxir and MCPA, all compounds investigated were associated with cellular triglyceride accumulation. Regarding etomoxir and MCPA, this finding is surprising, since both compounds strongly inhibited palmitate metabolism with an IC_{50} clearly lower than the highest concentrations used in the experiments with fat accumulation. Hepatic lipid droplets are formed in the endoplasmic reticulum and have a core of triglycerides and sterol esters, which is surrounded by phospholipids. Importantly, they contain a number of proteins on their surface, which are responsible for their formation and degradation (Khan et al., 2015; Mashek et al., 2015). Regarding the complexity of the composition and the metabolism of hepatic lipid droplets, it can be imagined that inhibition of fatty acid breakdown by etomoxir and MCPA is not sufficient for lipid droplet formation. This notion

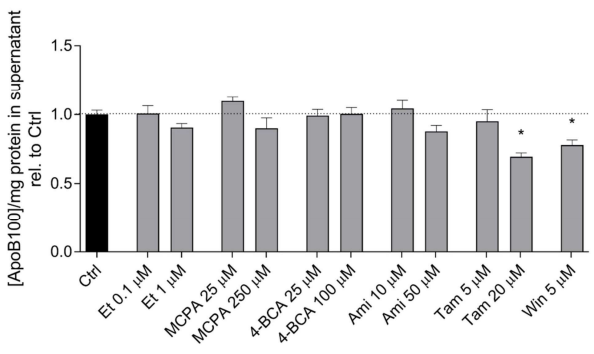

FIGURE 6 | Effect on the ApoB-100 concentration in the supernatant of HepG2 cells. The ApoB concentration in the supernatant of HepG2 cells treated with the compounds of interest for 24 h was measured using an ELISA as described in the section "Materials and Methods." The mean ApoB-100 concentration in the supernatant of control cells exposed to 0.1% DMSO was 3.10 ± 0.12 µg × mg protein^{-1}. Results are normalized to control cells exposed to 0.1% DMSO and are presented as mean ± SEM. *$p < 0.05$ vs. DMSO 0.1% control. Ctrl, control; Et, etomoxir; MCPA, methylenecyclopropylacetic acid; 4-BCA, 4-bromocrotonic acid; Ami, amiodarone; Tam, tamoxifen; Win, WIN 55,212-2.

is in line with the multiple parallel hit hypothesis of lipid droplet formation proposed by Tilg and Moschen (2010), which states that multiple factors are necessary for lipid droplet formation. Importantly, this means that impairment of hepatic fatty acid metabolism can be missed, if lipid droplet accumulation is used as the only assay of fatty acid metabolism.

In comparison, the determination of palmitate metabolism using ^{14}C-palmitate proved to be a reliable assay for detecting an impairment of fatty acid metabolism in HepG2 cells. All compounds investigated inhibited ^{14}C-palmitate metabolism at relevant concentrations. The assay is simple and works in both cells and isolated mitochondria (Krahenbuhl et al., 1994; Kaufmann et al., 2005; Felser et al., 2013). The product measured consists of water-soluble degradation compounds, which, in the case of hepatocytes and HepG2 cells, may mainly be acetyl-CoA, acetylcarnitine and ketone bodies. In permeabilized cells, the assay can detect impaired activation, transport into the mitochondrial matrix and β-oxidation. In comparison to the determination of the acylcarnitine pool in the cell supernatant, the determination of the palmitate metabolism provides no information about the location where long-chain fatty acid metabolism is inhibited.

Similar to palmitate metabolism, also the investigation of the acylcarnitine pattern in the supernatant yielded the expected results for the three established inhibitors. Based on the experience with this assay in patients with fatty acid oxidation disorders (Ensenauer et al., 2012), this result could be expected. The CPT1 inhibitor etomoxir decreased the C8 to C16 acylcarnitine concentrations due to a block of the transport of palmitate into the mitochondrial matrix (Lilly et al., 1992). The medium-chain acyl-CoA dehydrogenase inhibitor MCPA was associated with a massive increase in the C4 to C10 acylcarnitines, demonstrating the specificity of this inhibitor toward medium-chain acyl-CoA dehydrogenase. In comparison, 4-BCA showed a more complex pattern. As expected, 3-oxo-palmitate was increased, demonstrating the block of the long-chain β-ketoacyl-CoA thiolase. Since also C10 to C12 and C4 and C5 acylcarnitines were increased, the block appears not to be specific for the long-chain β-keto acyl-CoAs, but probably includes also medium- and short-chain β-ketoacyl-CoAs (Kamijo et al., 1997).

The test compounds did not show such a clear picture. Amiodarone was associated with a decrease in C6 to C16 acylcarnitines, which is compatible with CPT1A inhibition. Inhibition of CPT1A by amiodarone was shown directly in the current study using isolated liver mitochondria (**Figure 5**) and has been described previously in rat liver (Kennedy et al., 1996). Interestingly, C14 and C16 acylcarnitine concentrations were increased compared to C6 to C12 acylcarnitines and also compared to the CPT1A inhibitor etomoxir, suggesting that amiodarone inhibited β-oxidation of long-chain fatty acids in addition to CPT1A. This was confirmed directly in isolated mitochondria where amiodarone inhibited the long- and medium-chain acyl-CoA dehydrogenase (**Figure 5**).

Tamoxifen showed a decrease in C6 to C16 acylcarnitines, compatible with an inhibition of the import of long-chain fatty acids into the mitochondrial matrix. This was confirmed by inhibition of CPT1A in isolated liver mitochondria (**Figure 5**). Finally, WIN 55,212-2 exhibited a decrease of C2 to C10 acylcarnitines but normal concentrations of C12 to C16 acylcarnitines. Similar to amiodarone, this pattern could have been explained by impaired mitochondrial import of long-chain fatty acids combined with impaired β-oxidation. However, in contrast to amiodarone and tamoxifen, WIN 55,212-2 did not impair the function of CPT1A or of β-oxidation (**Figure 5**). The mechanism by which WIN 55,212-2 inhibits palmitate metabolism could therefore not be explained by the assays used in the current study. Inhibition of fatty acid activation is a possibility that we did not test.

Acylcarnitines cannot only be excreted, but can also be converted to the corresponding dicarboxylic acids by the ω-oxidation pathway, which involves members of microsomal enzymes of the CYP4A- and 4F-family as well as the peroxisomal fatty aldehyde dehydrogenase (FALHD) (Kelson et al., 1997; Wanders et al., 2011). Dicarboxylic acids are therefore potential biomarkers for impaired mitochondrial fatty acid metabolism that could also be used *in vivo*. Etomoxir was the only compound of the toxicants studied that caused an increase in thapsic (C16 dicarboxylic) acid in the cell supernatant. The finding that CPT1A inhibitors can induce the formation of dicarboxylic acids has been described previously and has been explained by induction of CYP4A1, a microsomal enzyme responsible for ω-oxidation of fatty acids (Kaikaus et al., 1993). Interestingly, amiodarone and tamoxifen inhibited the formation of thapsic acid (Supplementary Figure 4). At least amiodarone and its N-deethylated metabolites are known CYP inhibitors (Ohyama et al., 2000), which may explain this finding.

The excretion of ApoB-100 was determined as a marker of the excretion of VLDL, which is a lipoprotein rich in triglycerides (Tiwari and Siddiqi, 2012). Both tamoxifen and WIN 55,212-2 inhibited the excretion of ApoB-100, whereas the other compounds had no significant effect. The steatogenic effect of tamoxifen has been attributed in previous studies to increased fatty acid synthesis (Cole et al., 2010; Zhao et al., 2014) and impaired fatty acid β-oxidation (Tuquet et al., 2000; Zhou et al., 2012). The results of the current study are in agreement with these studies and additionally suggest that tamoxifen also affects VLDL secretion. This has recently been demonstrated directly in a study in humans (Birzniece et al., 2017). In comparison, no mechanistic studies are so far available for WIN 55,212-2. Studies for other cannabinoids suggest, that the steatogenic effect of these compounds is due to stimulation of the CB1 receptors, which is associated with a downregulation of CPT1 expression and an increased expression of the transcription factor SREBP-1c (Purohit et al., 2010; Regnell, 2013; Zhang et al., 2014). The results of the current study suggest that WIN 55,212-2 affects both fatty acid breakdown and triglyceride excretion.

The current study has strengths and weaknesses. A strength is certainly that most alterations in the acylcarnitine patterns were confirmed by determination of the respective enzyme activities in isolated mouse liver mitochondria. A weakness is that we did not use primary human hepatocytes for comparison of the findings in HepG2 cells. Since we obtained the predicted results for the established inhibitors in HepG2 cells and since we confirmed the most important findings in mouse liver mitochondria, we believe that the results obtained in HepG2 cells are reliable. In support of this statement, HepG2 cells have been proposed as an *in vitro* model for assessing hepatocellular fatty acid metabolism by other researchers (Amacher, 2011; Donato and Gomez-Lechon, 2012).

CONCLUSION

The current study shows that amiodarone impairs fatty acid metabolism by inhibiting CPT1A and long- and medium-chain acyl-CoA dehydrogenase, whereas tamoxifen and WIN 55,212-2 inhibit fatty acid degradation and ApoB-100 excretion, compatible with impaired VLDL excretion. HepG2 cells are a suitable human cell line for studying certain aspects of fatty acid metabolism *in vitro*. The determination of the acylcarnitine pool provides valuable information about the location of inhibition of fatty acid degradation and may be a useful *in vivo* biomarker in future studies.

AUTHOR CONTRIBUTIONS

DG: data generation, data interpretation, and writing manuscript. UD: data generation, data interpretation, and correction of final manuscript. SK: study design, data interpretation, and writing of manuscript.

FUNDING

The study was supported by a grant from the Swiss National Science Foundation to SK (SNF 31003A_156270).

SUPPLEMENTARY MATERIAL

The Supplementary Material for this article can be found online at: https://www.frontiersin.org/articles/10.3389/fphar.2018.00257/full#supplementary-material

REFERENCES

Amacher, D. E. (2011). Strategies for the early detection of drug-induced hepatic steatosis in preclinical drug safety evaluation studies. *Toxicology* 279, 10–18. doi: 10.1016/j.tox.2010.10.006

Amacher, D. E. (2014). Female gender as a susceptibility factor for drug-induced liver injury. *Hum. Exp. Toxicol.* 33, 928–939. doi: 10.1177/0960327113512860

Berger, B., Donzelli, M., Maseneni, S., Boess, F., Roth, A., Krahenbuhl, S., et al. (2016). Comparison of liver cell models using the basel phenotyping cocktail. *Front. Pharmacol.* 7:443. doi: 10.3389/fphar.2016.00443

Birzniece, V., Barrett, P. H. R., and Ho, K. K. Y. (2017). Tamoxifen reduces hepatic VLDL production and GH secretion in women: a possible mechanism for steatosis development. *Eur. J. Endocrinol.* 177, 137–143. doi: 10.1530/EJE-17-0151

Ceccarelli, S. M., Chomienne, O., Gubler, M., and Arduini, A. (2011). Carnitine palmitoyltransferase (CPT) modulators: a medicinal chemistry perspective on 35 years of research. *J. Med. Chem.* 54, 3109–3152. doi: 10.1021/jm100809g

Cole, L. K., Jacobs, R. L., and Vance, D. E. (2010). Tamoxifen induces triacylglycerol accumulation in the mouse liver by activation of fatty acid synthesis. *Hepatology* 52, 1258–1265. doi: 10.1002/hep.23813

Donato, M. T., and Gomez-Lechon, M. J. (2012). Drug-induced liver steatosis and phospholipidosis: cell-based assays for early screening of drug candidates. *Curr. Drug Metab.* 13, 1160–1173. doi: 10.2174/138920012802850001

Donato, M. T., Martinez-Romero, A., Jimenez, N., Negro, A., Herrera, G., Castell, J. V., et al. (2009). Cytometric analysis for drug-induced steatosis in HepG2 cells. *Chem. Biol. Interact.* 181, 417–423. doi: 10.1016/j.cbi.2009.07.019

Ensenauer, R., Fingerhut, R., Schriever, S. C., Fink, B., Becker, M., Sellerer, N. C., et al. (2012). In situ assay of fatty acid beta-oxidation by metabolite profiling following permeabilization of cell membranes. *J. Lipid Res.* 53, 1012–1020. doi: 10.1194/jlr.D022608

Felser, A., Blum, K., Lindinger, P. W., Bouitbir, J., and Krahenbuhl, S. (2013). Mechanisms of hepatocellular toxicity associated with dronedarone–a comparison to amiodarone. *Toxicol. Sci.* 131, 480–490. doi: 10.1093/toxsci/kfs298

Felser, A., Lindinger, P. W., Schnell, D., Kratschmar, D. V., Odermatt, A., Mies, S., et al. (2014a). Hepatocellular toxicity of benzbromarone: effects on mitochondrial function and structure. *Toxicology* 324, 136–146. doi: 10.1016/j.tox.2014.08.002

Felser, A., Stoller, A., Morand, R., Schnell, D., Donzelli, M., Terracciano, L., et al. (2014b). Hepatic toxicity of dronedarone in mice: role of mitochondrial β-oxidation. *Toxicology* 323, 1–9. doi: 10.1016/j.tox.2014.05.011

Fisher, E. A., and Ginsberg, H. N. (2002). Complexity in the secretory pathway: the assembly and secretion of apolipoprotein B-containing lipoproteins. *J. Biol. Chem.* 277, 17377–17380. doi: 10.1074/jbc.R100068200

Foster, D. W. (2012). Malonyl-CoA: the regulator of fatty acid synthesis and oxidation. *J. Clin. Invest.* 122, 1958–1959. doi: 10.1172/JCI63967

Fromenty, B., and Pessayre, D. (1995). Inhibition of mitochondrial beta-oxidation as a mechanism of hepatotoxicity. *Pharmacol. Ther.* 67, 101–154. doi: 10.1016/0163-7258(95)00012-6

Guo, W., Huang, N., Cai, J., Xie, W., and Hamilton, J. A. (2006). Fatty acid transport and metabolism in HepG2 cells. *Am. J. Physiol. Gastrointest. Liver Physiol.* 290, G528–G534. doi: 10.1152/ajpgi.00386.2005

Hoppel, C., DiMarco, J. P., and Tandler, B. (1979). Riboflavin and rat hepatic cell structure and function. Mitochondrial oxidative metabolism in deficiency states. *J. Biol. Chem.* 254, 4164–4170.

Ikeda, Y., and Tanaka, K. (1990). Selective inactivation of various acyl-CoA dehydrogenases by (methylenecyclopropyl)acetyl-CoA. *Biochim. Biophys. Acta* 1038, 216–221. doi: 10.1016/0167-4838(90)90208-W

Kaikaus, R. M., Sui, Z., Lysenko, N., Wu, N. Y., Ortiz de Montellano, P. R., Ockner, R. K., et al. (1993). Regulation of pathways of extramitochondrial fatty acid oxidation and liver fatty acid-binding protein by long-chain monocarboxylic fatty acids in hepatocytes. Effect of inhibition of carnitine palmitoyltransferase I. *J. Biol. Chem.* 268, 26866–26871.

Kamalian, L., Chadwick, A. E., Bayliss, M., French, N. S., Monshouwer, M., Snoeys, J., et al. (2015). The utility of HepG2 cells to identify direct mitochondrial dysfunction in the absence of cell death. *Toxicol. In Vitro* 29, 732–740. doi: 10.1016/j.tiv.2015.02.011

Kamijo, T., Indo, Y., Souri, M., Aoyama, T., Hara, T., Yamamoto, S., et al. (1997). Medium chain 3-ketoacyl-coenzyme A thiolase deficiency: a new disorder of mitochondrial fatty acid beta-oxidation. *Pediatr. Res.* 42, 569–576. doi: 10.1203/00006450-199711000-00002

Kaufmann, P., Torok, M., Hanni, A., Roberts, P., Gasser, R., and Krahenbuhl, S. (2005). Mechanisms of benzarone and benzbromarone-induced hepatic toxicity. *Hepatology* 41, 925–935. doi: 10.1002/hep.20634

Kelson, T. L., Secor McVoy, J. R., and Rizzo, W. B. (1997). Human liver fatty aldehyde dehydrogenase: microsomal localization, purification, and biochemical characterization. *Biochim. Biophys. Acta* 1335, 99–110. doi: 10.1016/S0304-4165(96)00126-2

Kennedy, J. A., Unger, S. A., and Horowitz, J. D. (1996). Inhibition of carnitine palmitoyltransferase-1 in rat heart and liver by perhexiline and amiodarone. *Biochem. Pharmacol.* 52, 273–280. doi: 10.1016/0006-2952(96)00204-3

Khan, S. A., Wollaston-Hayden, E. E., Markowski, T. W., Higgins, L., and Mashek, D. G. (2015). Quantitative analysis of the murine lipid droplet-associated proteome during diet-induced hepatic steatosis. *J. Lipid Res.* 56, 2260–2272. doi: 10.1194/jlr.M056812

Knapp, A. C., Todesco, L., Beier, K., Terracciano, L., Sagesser, H., Reichen, J., et al. (2008). Toxicity of valproic acid in mice with decreased plasma and tissue carnitine stores. *J. Pharmacol. Exp. Ther.* 324, 568–575. doi: 10.1124/jpet.107.131185

Krahenbuhl, S., Talos, C., and Reichen, J. (1994). Mechanisms of impaired hepatic fatty acid metabolism in rats with long-term bile duct ligation. *Hepatology* 19, 1272–1281. doi: 10.1016/0270-9139(94)90877-X

Lilly, K., Chung, C., Kerner, J., VanRenterghem, R., and Bieber, L. L. (1992). Effect of etomoxiryl-CoA on different carnitine acyltransferases. *Biochem. Pharmacol.* 43, 353–361. doi: 10.1016/0006-2952(92)90298-W

Mashek, D. G., Khan, S. A., Sathyanarayan, A., Ploeger, J. M., and Franklin, M. P. (2015). Hepatic lipid droplet biology: getting to the root of fatty liver. *Hepatology* 62, 964–967. doi: 10.1002/hep.27839

Minkler, P. E., and Hoppel, C. L. (1993). Quantification of free carnitine, individual short- and medium-chain acylcarnitines, and total carnitine in plasma by high-performance liquid chromatography. *Anal. Biochem.* 212, 510–518. doi: 10.1006/abio.1993.1361

Morand, R., Donzelli, M., Haschke, M., and Krahenbuhl, S. (2013). Quantification of plasma carnitine and acylcarnitines by high-performance liquid chromatography-tandem mass spectrometry using online solid-phase extraction. *Anal. Bioanal. Chem.* 405, 8829–8836. doi: 10.1007/s00216-013-7309-z

Ohyama, K., Nakajima, M., Suzuki, M., Shimada, N., Yamazaki, H., and Yokoi, T. (2000). Inhibitory effects of amiodarone and its N-deethylated metabolite on human cytochrome P450 activities: prediction of in vivo drug interactions. *Br. J. Clin. Pharmacol.* 49, 244–253. doi: 10.1046/j.1365-2125.2000.00134.x

Okun, J. G., Kolker, S., Schulze, A., Kohlmuller, D., Olgemoller, K., Lindner, M., et al. (2002). A method for quantitative acylcarnitine profiling in human skin fibroblasts using unlabelled palmitic acid: diagnosis of fatty acid oxidation disorders and differentiation between biochemical phenotypes of MCAD deficiency. *Biochim. Biophys. Acta* 1584, 91–98. doi: 10.1016/S1388-1981(02)00296-2

Olowe, Y., and Schulz, H. (1982). 4-Bromocrotonic acid, an effective inhibitor of fatty acid oxidation and ketone body degradation in rat heart mitochondria. On the rate-determining step of beta-oxidation and ketone body degradation in heart. *J. Biol. Chem.* 257, 5408–5413.

Purohit, V., Rapaka, R., and Shurtleff, D. (2010). Role of cannabinoids in the development of fatty liver (steatosis). *AAPS J.* 12, 233–237. doi: 10.1208/s12248-010-9178-0

Regnell, S. E. (2013). Cannabinoid 1 receptor in fatty liver. *Hepatol. Res.* 43, 131–138. doi: 10.1111/j.1872-034X.2012.01085.x

Ress, C., and Kaser, S. (2016). Mechanisms of intrahepatic triglyceride accumulation. *World J. Gastroenterol.* 22, 1664–1673. doi: 10.3748/wjg.v22.i4.1664

Rinaldo, P. (2001). Fatty acid transport and mitochondrial oxidation disorders. *Semin. Liver Dis.* 21, 489–500. doi: 10.1055/s-2001-19037

Soeters, M. R., Soeters, P. B., Schooneman, M. G., Houten, S. M., and Romijn, J. A. (2012). Adaptive reciprocity of lipid and glucose metabolism in human short-term starvation. *Am. J. Physiol. Endocrinol. Metab.* 303, E1397–E1407. doi: 10.1152/ajpendo.00397.2012

Tilg, H., and Moschen, A. R. (2010). Evolution of inflammation in nonalcoholic fatty liver disease: the multiple parallel hits hypothesis. *Hepatology* 52, 1836–1846. doi: 10.1002/hep.24001

Tiwari, S., and Siddiqi, S. A. (2012). Intracellular trafficking and secretion of VLDL. *Arterioscler. Thromb. Vasc. Biol.* 32, 1079–1086. doi: 10.1161/atvbaha.111.241471

Tserng, K. Y., Jin, S. J., and Hoppel, C. L. (1991). Spiropentaneacetic acid as a specific inhibitor of medium-chain acyl-CoA dehydrogenase. *Biochemistry* 30, 10755–10760. doi: 10.1021/bi00108a021

Tuquet, C., Dupont, J., Mesneau, A., and Roussaux, J. (2000). Effects of tamoxifen on the electron transport chain of isolated rat liver mitochondria. *Cell Biol. Toxicol.* 16, 207–219. doi: 10.1023/A:1007695308257

Vernez, L., Hopfgartner, G., Wenk, M., and Krahenbuhl, S. (2003). Determination of carnitine and acylcarnitines in urine by high-performance liquid chromatography-electrospray ionization ion trap tandem mass spectrometry. *J. Chromatogr. A* 984, 203–213. doi: 10.1016/S0021-9673(02)01838-1

Wanders, R. J., Komen, J., and Kemp, S. (2011). Fatty acid omega-oxidation as a rescue pathway for fatty acid oxidation disorders in humans. *FEBS J.* 278, 182–194. doi: 10.1111/j.1742-4658.2010.07947.x

Yao, K. W., Mao, L. F., Luo, M. J., and Schulz, H. (1994). The relationship between mitochondrial activation and toxicity of some substituted carboxylic acids. *Chem. Biol. Interact.* 90, 225–234. doi: 10.1016/0009-2797(94)90012-4

Zhang, Y. F., Yuan, Z. Q., Song, D. G., Zhou, X. H., and Wang, Y. Z. (2014). Effects of cannabinoid receptor 1 (brain) on lipid accumulation by transcriptional control of CPT1A and CPT1B. *Anim. Genet.* 45, 38–47. doi: 10.1111/age.12078

Zhao, F., Xie, P., Jiang, J., Zhang, L., An, W., and Zhan, Y. (2014). The effect and mechanism of tamoxifen-induced hepatocyte steatosis in vitro. *Int. J. Mol. Sci.* 15, 4019–4030. doi: 10.3390/ijms15034019

Zhou, Z., Zhou, J., and Du, Y. (2012). Estrogen receptor alpha interacts with mitochondrial protein HADHB and affects beta-oxidation activity. *Mol. Cell. Proteomics* 11:M111.011056. doi: 10.1074/mcp.M111.011056

Zschocke, J., Schulze, A., Lindner, M., Fiesel, S., Olgemoller, K., Hoffmann, G. F., et al. (2001). Molecular and functional characterisation of mild MCAD deficiency. *Hum. Genet.* 108, 404–408. doi: 10.1007/s004390100501

Zuniga, A., and Li, L. (2011). Ultra-high performance liquid chromatography tandem mass spectrometry for comprehensive analysis of urinary acylcarnitines. *Anal. Chim. Acta* 689, 77–84. doi: 10.1016/j.aca.2011.01.018

Conflict of Interest Statement: The authors declare that the research was conducted in the absence of any commercial or financial relationships that could be construed as a potential conflict of interest.

Legends to supplementary Figures

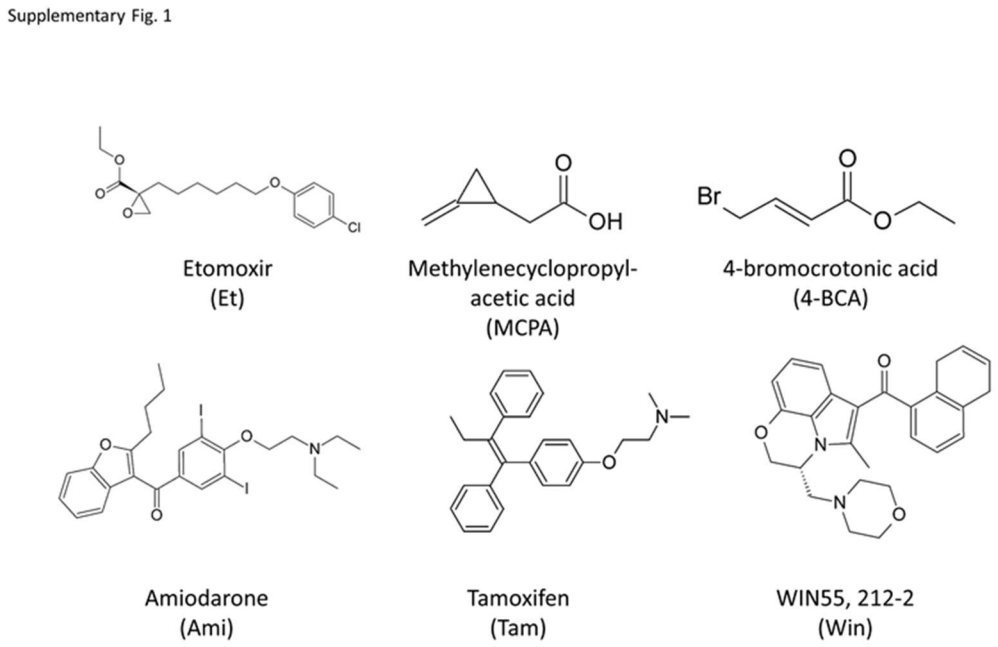

Supplementary Figure 1

Chemical structures of etomoxir, methylenecyclopropylacetic acid (MCPA), 4-bromocrotonic acid (4-BCA), amiodarone, tamoxifen, and WIN55,212-2.

Supplementary Fig. 2

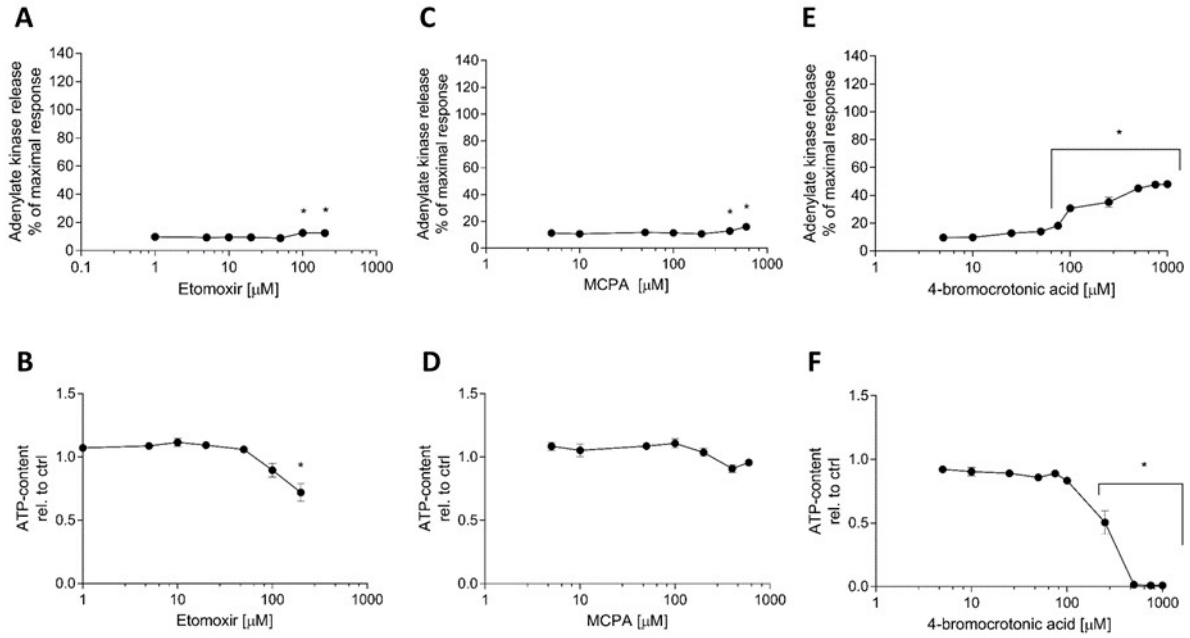

Supplementary Figure 2

Effect of etomoxir, methylenecyclopropylacetic acid (MCPA) and 4-bromocrotonic acid (4-BCA) on plasma membrane integrity and on the cellular ATP content. HepG2 cells were exposed to the toxicants for 24 h. Membrane integrity is expressed as the percentage of dead cells with Triton X set at 100%. ATP content is displayed as the percentage in relation to control incubations (DMSO 0.1%) set at 100%. (**A,B**) etomoxir, (**C,D**) MCPA, (**E,F**) 4-BCA. Results are given as mean ± SEM in relation to control incubations (DMSO 0.1%).*$p<0.05$ vs. DMSO 0.1% control.

Supplementary Fig. 3

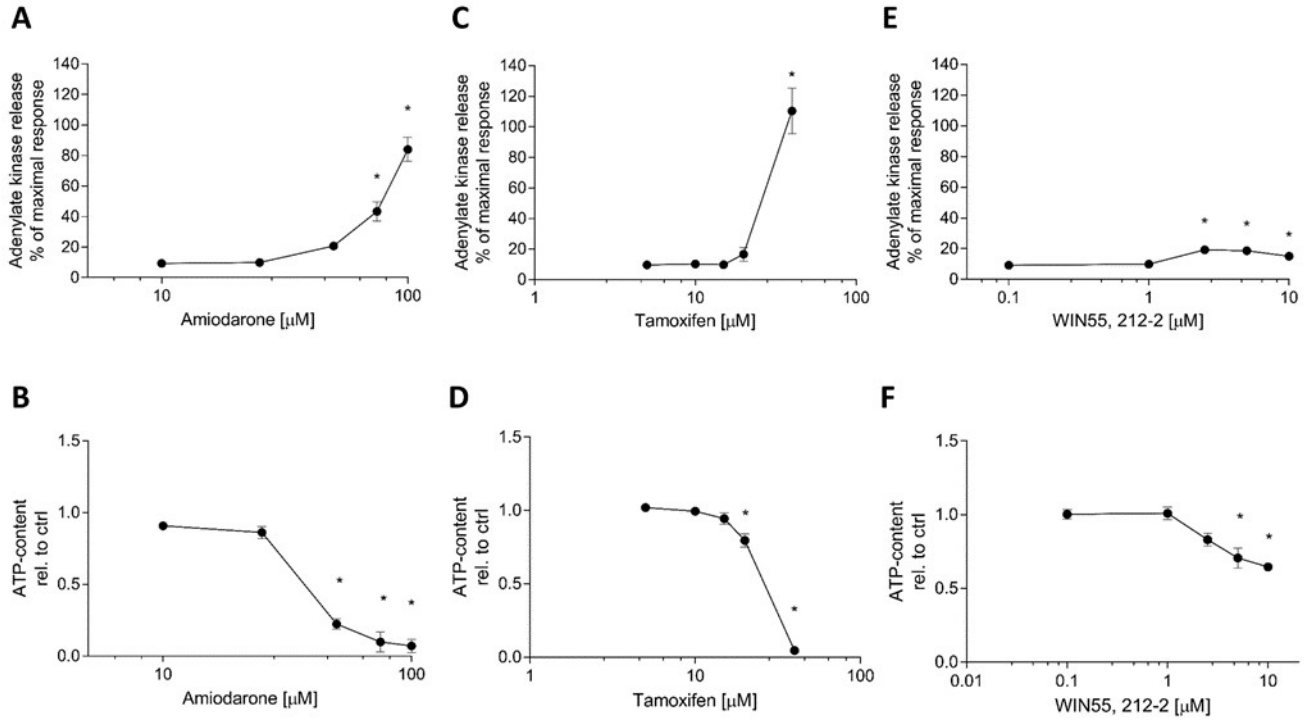

Supplementary Figure 3

Effect of amiodarone, tamoxifen and WIN55,212-2 on plasma membrane integrity and on the cellular ATP content. HepG2 cells were exposed to the compounds of interest for 24 h. Membrane integrity is expressed as the percentage of dead cells with Triton X set at 100%. ATP content is displayed as the percentage in relation to control incubations (DMSO 0.1%) set at 100%. (**A,B**) amiodarone, (**C,D**) tamoxifen, (**E,F**) 4-WIN55,212-2. Results are given as mean ± SEM in relation to control incubations (DMSO 0.1%).*$p<0.05$ vs. DMSO 0.1% control.

Supplementary Fig. 4

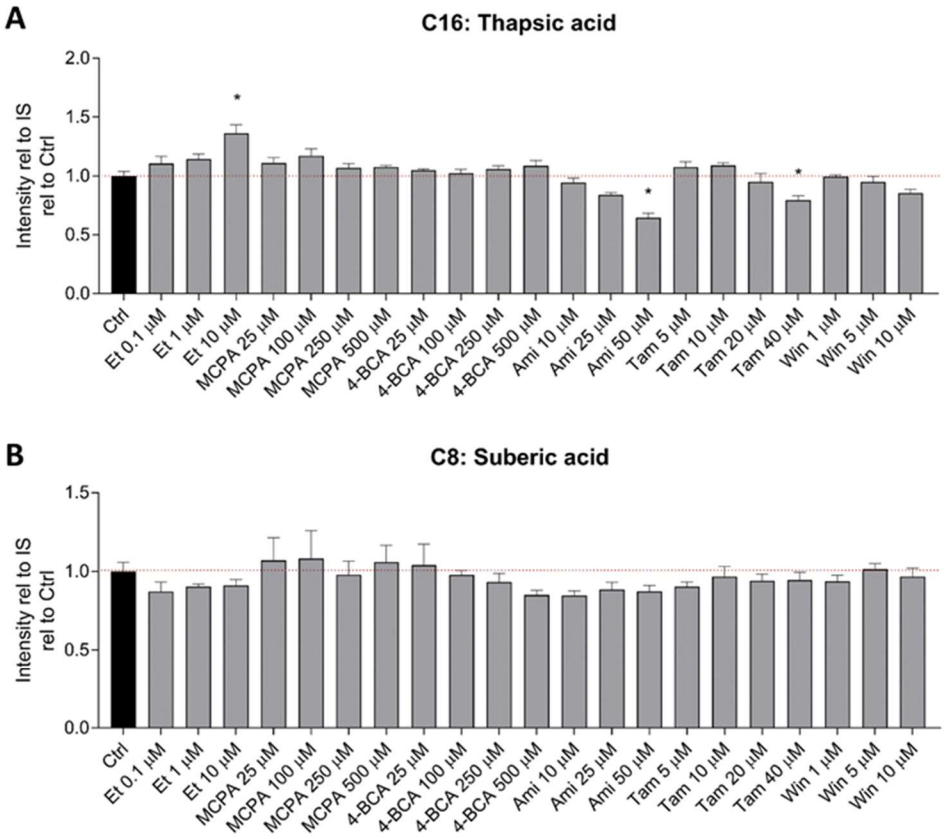

Supplementary Figure 4

Effect on the dicarboxylic acid concentration in HepG2 cells. Dicarboxylic acids were analyzed in HepG2 cells treated with the compounds of interest for 24 h using LC-MS/MS as described in Methods. Results were normalized to the values obtained in DMSO 0.1% exposed control cells. Values are expressed as mean ± SEM. *$p<0.05$ vs. DMSO 0.1% control.

2.2 Paper 2

Effect of the Catechol-*O*-Methyltransferase Inhibitors Tolcapone and Entacapone on Fatty Acid Metabolism in HepaRG Cells

TOXICOLOGICAL SCIENCES, 2018, 1–12

doi: 10.1093/toxsci/kfy101
Advance Access Publication Date: April 23, 2018
Research Article

Effect of the Catechol-O-Methyltransferase Inhibitors Tolcapone and Entacapone on Fatty Acid Metabolism in HepaRG Cells

David Grünig[*,†], Andrea Felser,[*,†,1] Urs Duthaler,[*,†,1] Jamal Bouitbir,[*,†,‡] and Stephan Krähenbühl[*,†,‡,2]

[*]Division of Clinical Pharmacology & Toxicology, University Hospital Basel, 4031 Basel, Switzerland; [†]Department of Biomedicine, University of Basel, 4031 Basel, Switzerland; and [‡]Swiss Center for Applied Human Toxicology (SCAHT), 4055 Basel, Switzerland

[1]These authors contributed equally to this study.
[2]To whom correspondence should be addressed. Fax: +41-61-265-4560. E-mail: kraehenbuehl@uhbs.ch.

ABSTRACT

Tolcapone and entacapone are catechol-O-methyltransferase inhibitors used in patients with Parkinson's disease. For tolcapone, patients with liver failure have been reported with microvesicular steatosis observed in the liver biopsy of 1 patient. We therefore investigated the impact of tolcapone and entacapone on fatty acid metabolism in HepaRG cells exposed for 24 h and on acutely exposed mouse liver mitochondria. In HepaRG cells, tolcapone induced lipid accumulation starting at 100 μM, whereas entacapone was ineffective up to 200 μM. In HepaRG cells, tolcapone-inhibited palmitate metabolism and activation starting at 100 μM, whereas entacapone did not affect palmitate metabolism. In isolated mouse liver mitochondria, tolcapone inhibited palmitate metabolism starting at 5 μM and entacapone at 50 μM. Inhibition of palmitate activation could be confirmed by the acylcarnitine pattern in the supernatant of HepaRG cell cultures. Tolcapone-reduced mRNA and protein expression of long-chain acyl-CoA synthetase 1 (ACSL1) and protein expression of ACSL5, whereas entacapone did not affect ACSL expression. Tolcapone increased mRNA expression of the fatty acid transporter CD36/FAT, impaired the secretion of ApoB100 by HepaRG cells and reduced the mRNA expression of ApoB100, but did not relevantly affect markers of fatty acid binding, lipid droplet formation and microsomal lipid transfer. In conclusion, tolcapone impaired hepatocellular fatty acid metabolism at lower concentrations than entacapone. Tolcapone increased mRNA expression of fatty acid transporters, inhibited activation of long-chain fatty acids and impaired very low-density lipoprotein secretion, causing hepatocellular triglyceride accumulation. The findings may be relevant in patients with a high tolcapone exposure and preexisting mitochondrial dysfunction.

Key words: COMT inhibitors; HepaRG cells; fatty acid metabolism; long-chain acyl-CoA synthetase; VLDL secretion.

Tolcapone and entacapone are catechol-O-methyltransferase (COMT) inhibitors used for the treatment of patients with Parkinson's disease. COMT inhibitors act mainly in the periphery and block O-methylation of DOPA, thereby increasing the availability of DOPA for transport into the brain and decreasing the formation 3-O-methyl-DOPA, which may impair DOPA transport into the brain (Kaakkola, 2000). Treatment with COMT inhibitors usually allows a reduction of the DOPA dose and leads to an increase in the on-time as well as to a decrease in DOPA-associated dyskinesias (Kaakkola, 2000).

In humans, both compounds are almost completely absorbed and have bioavailabilities in the range of 60% (tolcapone) and 35% (entacapone), indicating a significant first liver-pass effect. They are rapidly eliminated with half-lives of 2–3 h. Entacapone is mainly glucuronidated and eliminated almost completely over the bile/feces as the glucuronide or the parent

compound. In comparison, only approximately 30% of tolcapone is glucuronidated and 40% eliminated by the bile/feces (Jorga *et al.*, 2001). In contrast to entacapone, tolcapone can also be O-methylated and undergo oxidative metabolism by cytochrome P450 (CYP) 3A4 and other CYPs. Entacapone is approximately 98% bound to serum proteins and tolcapone >99%. The dosage of entacapone is usually 200 mg together with every dose of L-DOPA (mostly 3 times a day) and of tolcapone 100–200 mg 3 times daily. Maximal plasma concentrations were approximately 6 μM after a single dose of 200 mg entacapone and 17 μM after a single dose of 100 mg tolcapone (Kaakkola, 2000). The liver concentration is not known, but may be higher than in plasma after oral ingestion taking into account the first liver-pass effect.

The most prevalent adverse reactions of the COMT inhibitors mainly reflect dopamine toxicity such as hypotension, nausea, hallucinations and dyskinesias (Haasio, 2010; Kaakkola, 2000). Nondopaminergic adverse reactions mainly include diarrhea and abdominal pain. Hepatocellular liver injury (increased transaminases) has been observed in clinical studies in approximately 3% and 0.2% of patients treated with tolcapone and entacapone, respectively (Haasio, 2010; Kaakkola, 2000; Lew and Kricorian, 2007). Regarding tolcapone, hepatocellular injury is dose-dependent and usually occurs during the first 6 months of treatment (Olanow, 2000). Increased transaminases typically return rapidly to normal after stopping tolcapone, but can also normalize over time in patients with continuous treatment. Four patients with liver failure associated with tolcapone have been described, and 3 of these patients died (Olanow, 2000). In 2 of these patients, a liver biopsy was performed. One of these biopsies revealed centroacinar necrosis with an inflammatory infiltrate in the portal tracts and microvesicular steatosis in adjacent hepatocytes (Assal *et al.*, 1998; Spahr *et al.*, 2000). Electron microscopy of hepatocytes showed proliferation of swollen mitochondria, reduction in matrix density and loss of cristae (Borges, 2003; Spahr *et al.*, 2000), suggesting that tolcapone is a mitochondrial toxicant.

We recently described the toxicity of tolcapone and entacapone on the respiratory chain of mitochondria in HepaRG cells exposed for 24 h and acutely exposed mouse liver mitochondria in detail (Grunig *et al.*, 2017). In that study, tolcapone inhibited the function of enzyme complexes of the electron transport chain and uncoupled oxidative phosphorylation in a concentration-dependent manner. Entacapone showed similar toxic effects, but at clearly higher concentrations. These findings were in agreement with previous studies showing that tolcapone uncouples oxidative phosphorylation of liver mitochondria, leading to a drop in the membrane potential of isolated rat liver mitochondria (Haasio, 2010), and to increased body temperature, weight loss, and hepatotoxicity in rats (Haasio *et al.*, 2001, 2002b). Mitochondrial toxicity of tolcapone was also suggested in a capture compound mass spectrometry study, in which tolcapone interacted preferentially with proteins of the mitochondrial respiratory chain and of fatty acid metabolism (Fischer *et al.*, 2010).

During our recent investigations of mitochondrial function in HepaRG cells (Grunig *et al.*, 2017), we also observed that tolcapone and entacapone inhibited the metabolism of palmitate, suggesting impairment of hepatic fatty acid metabolism. This finding was in agreement with microvesicular steatosis described in the liver biopsy of a patient with tolcapone-associated liver injury (Spahr *et al.*, 2000) and with the interaction of tolcapone and/or tolcapone metabolites with enzymes involved in fatty acid metabolism (Fischer, *et al.*, 2010). We therefore decided to study the effect of the COMT inhibitors tolcapone and entacapone on fatty acid metabolism using HepaRG cells and isolated mouse liver mitochondria in more detail. The studies showed that tolcapone mainly inhibited activation of fatty acids and excretion of very low-density lipoprotein (VLDL), causing hepatocellular lipid accumulation.

MATERIALS AND METHODS

Chemicals. Triacsin C (TC), entacapone (Enta), 4-bromocrotonic acid (4bc) were acquired from Santa Cruz Biotechnology (Dallas, Texas), Toronto Research Chemicals (Toronto, CAN) and TCI Chemicals (Eschborn, Germany), respectively. Tolcapone (Tol), etomoxir (Et), and methylenecyclopropylacetic acid (MCPA) were obtained from Sigma-Aldrich (Buchs, Switzerland). If not stated otherwise, all other chemicals were also purchased from Sigma-Aldrich. Drug or toxicant stock solutions were dissolved in DMSO and kept at −20° C for cell treatment (in general at 1:1000 dilution).

Cell cultures. All cells were kept at 37°C in a humidified 5% CO_2 cell culture incubator and were passaged using trypsin. Cell culture supplements were all purchased from GIBCO (Paisley, GBR).

HepaRG cells, purchased from Thermo Scientific (Wohlen, Switzerland), were cultured and differentiated as described before (Grunig *et al.*, 2017; Guillouzo *et al.*, 2007).

HepG2 cells, purchased from ATCC (Manassas, Virginia), were maintained in Dulbecco's Modified Eagle Medium (1.0 g/l glucose, 4 mM L-glutamine and 1 mM pyruvate) supplemented with 10% heat-inactivated fetal calf serum, 2 mM GlutaMAX, 10 mM 4-(2-hydroxyethyl)-1-piperazineethanesulfonic acid (HEPES) buffer, 1% MEM nonessential amino acids solution, and penicillin-streptomycin (10 000 U/ml).

Intracellular lipid accumulation. In order to load cells with exogenous fatty acids, cell culture media were supplemented with 1% BSA, 334 μM palmitic acid and 666 μM oleic acid. HepG2 cells were loaded with 50% fatty acid supplemented medium and HepaRG cells with 25%. After 24 h, the medium containing fatty acids was replaced by fatty acid free medium and cells exposed to toxicants for 24 h. Before FACS analysis, cells were detached using trypsin-EDTA (Thermo Scientific), washed with PBS, and then stained with 5 ng/ml BODIPY 493/503 and 10 μg/ml propidium iodide (PI) for 30 min at 37°C. After incubation, samples were kept on ice until analysis by flow cytometry.

Fluorescence microscopy. HepG2 and HepaRG cells were seeded in Poly-L-Lysine coated μ-Slide plates, purchased from Ibidi (Martinsried, Germany). Cells were treated with culture medium containing fatty acids (2:1 oleate:palmitate bound to BSA as described in the preceding section) followed by toxicants for 24 h, and then washed and fixed for 4 min with 4% paraformaldehyde at 37°C. After an additional washing step, cells were stained for 30 min with 0.5 μg/ml BODIPY 493/503 from Thermo Scientific and 1 μM DAPI (Thermo Scientific) in PBS at 37°C. After washing twice with PBS and the addition of antifade-mounting medium (1 mg/ml p-phenylene diamine in 90% glycerol, pH 9.2), the cells were imaged on an Olympus IX83 microscope, purchased from Olympus (Shinjuku, Japan).

Isolation of mitochondria. Mouse liver mitochondria were freshly isolated as originally described by Hoppel et al. for rats (Hoppel *et al.*, 1979) with the modifications described previously in Felser *et al.* (2013).

Oxidation of 1-^{14}C palmitic acid, 1-^{14}C palmitoylcarnitine, and 1-^{14}C palmitoyl-CoA. Metabolism of fatty acid oxidation substrates was assessed using permeabilized HepaRG cells and isolated mouse liver mitochondria by the methods described earlier in Felser *et al.* (2013, 2014). The reactions were started by the addition of 25 µl radioactive substrate mix, with final concentrations of 200 µM for palmitic acid, palmitoylcarnitine, or palmitoyl-CoA, containing also the radioactive substrate (0.1 pCi/assay for 1-^{14}C-palmitic acid, 25 pCi/assay for 1-^{14}C-palmitoylcarnitine, and 25 pCi/assay for 1-^{14}C-palmitoyl-CoA).

Activity of long-chain acyl-CoA synthetase and carnitine palmitoyltransferase 1. Long-chain acyl-CoA synthetase (ACSL) activity was assessed by the rate of ^{14}C-palmitoyl-CoA formation, as described previously (Felser *et al.*, 2014).

Carnitine palmitoyltransferase (CPT) 1 activity was measured as the formation of palmitoyl-^{14}C-carnitine from palmitoyl-CoA and ^{14}C-carnitine as described previously in Felser *et al.* (2014).

Acyl-CoA dehydrogenase activities. Activities of the respective acyl-CoA dehydrogenase isoforms were determined by the method published by Hoppel *et al.* (1979). In a 48-well plate, 50 µg of mitochondrial protein (previously frozen) was preincubated in the presence of test compounds for 5 min in the assay buffer (34 mM potassium phosphate, 1.5 mM KCN, 3.75 µM rotenone, 1.5 mM cytochrome C, 3 mM phenazine ethosulfate, pH 7.2). The reaction was started by the addition of palmitoyl-CoA or octanoyl-CoA (final concentrations 50 and 100 µM, respectively) and monitored at 550 nm over 2 min in a Tecan microplate reader (Männedorf, Switserland).

Formation of acylcarnitines. Acylcarnitines of interest were analyzed by liquid chromatography tandem mass spectrometry (LC-MS/MS) based on the method of Morand *et al.* (2013) with minor modifications. In brief, the supernatants of cells were mixed with internal standard solution, containing deuterated standards in methanol, in a ratio of 1:3 (v/v). The mixtures were centrifuged before they were transferred to an autosampler tube and diluted 1:1 with water. For analysis we used a LC-MS/MS system consisting of a Nexera SIL-30AC autosampler, a column-oven (CTO-20A), 4 HPLC pumps (2× LC-20AD and 2× LC-ADXR) and a system controller (CBM-20A), all acquired from Shimadzu (Kyoto, Japan). The HPLC system was coupled to an API 4000 triple quadrupole mass spectrometer from AB Sciex (Concord, California), equipped with a turbo electrospray ionization source.

For sample separation a Luna C8 5 µM column (150 × 2 mm) was used at 50°C. Reference substances were obtained for acetylcarnitine, octanoylcarnitine, and palmitoylcarnitine and used as standards and for quality control.

Western blotting. After 24 h of incubation with the drugs, the cells were washed with PBS and lysed with RIPA buffer (50 nM Tris-HCL, pH 7.4, 150 mM NaCl, 1% Triton X-100, 0.5% sodium deoxycholate, 0.1% sodium dodecylsulfate, and 1 mM EDTA in water), containing 1 tablet of complete Mini Protease inhibitor cocktail from Roche Diagnostics (Rotkreuz, Switzerland) per 10 ml of buffer. Lysates were incubated with RIPA buffer under constant agitation for 15 min and then centrifuged at 15 700 × g for 10 min at 4°C. After determining the protein content with Pierce BCA Protein Assay Kit (Thermo Scientific) 15 µg of protein was separated on 4%–12% bis-tris gradient gel (Invitrogen, Carlsbad, California), and transferred to polyvinylidene difluoride membranes, using the Trans-Blot Turbo Transfer System (Bio-Rad, Hercules, Califronia). All primary antibodies were obtained from Abcam (Cambridge, UK) and diluted 1:1000. Exceptions were antibodies against adipose differentiation-related protein (ADRP) and glyceraldehyde 3-phosphate dehydrogenase (GAPDH), which were obtained from Santa Cruz Biotechnology and diluted 1:250 and 1:5000, respectively, as well as ACSL1 antibody, which was obtained from Cell Signaling Technology (Danvers) and diluted 1:1000. The secondary antibodies were from Santa Cruz Biotechnology and used at a dilution of 1:2000. Protein bands were normalized to GPDH.

mRNA quantification. For RNA extraction and purification, the Qiagen RNeasy Mini Extraction Kit (Qiagen, Hilden, Germany) was used and for RNA quality evaluation a NanoDrop 2000 (Thermo Scientific) was used. cDNA was synthesized from 1 µg RNA, using the Qiagen Omniscript system. mRNA quantification was conducted using FastStart Universal SYBR Green Master from Roche in a ViiA 7 Real Time PCR System from Applied Biosystems (Waltham, Massachusetts). The relative quantity of specifically amplified cDNA was calculated by the comparative-threshold cycle method. As endogenous reference, GAPDH was used and no-template and no-reverse-transcription controls ensured the absence of nonspecific amplification. The specific primers used are given in Supplementary Table 1.

Hepatocellular export of ApoB100. Levels of ApoB100 in the supernatants of the cells were measured in order to assess the excretion of triglycerides. The ApoB Quantikine ELISA Kit from R&D Systems (Minneapolis, Minnesota) was used according to the manufacturer's protocol with some modifications. For that, 145 µl assay diluent RD1-113 plus 5 µl calibrator diluent RD-61 were added to each well before the addition of 100 µl cell supernatant.

Statistical analysis. Data are given as the mean ± SEM of at least 3 independent experiments. Statistical analyses were performed using GraphPad Prism 6 (GraphPad Software, La Jolla, California). For the comparison of treatment groups to the 0.1% DMSO control group, 1-way ANOVA was used followed by the Dunnett's posttest procedure. The p-values $< .05$ (*) were considered significant.

RESULTS

Intracellular Lipid Accumulation

We first investigated the potential of tolcapone and entacapone for cellular neutral lipid accumulation using the dye BODIPY 493/503 and flow cytometric analysis in HepaRG and in HepG2 cells. Both HepaRG cells (Figure 1B) as well as HepG2 cells (Figure 1C) treated with tolcapone for 24 h showed a concentration-dependent increase in intracellular lipid content. For tolcapone, this increase started at 50 µM and reached statistical significance at 100 and 200 µM in both cell types. In comparison, entacapone caused a significant accumulation of lipids only in HepG2 (200 µM), but not in HepaRG cells. TC, an efficient inhibitor of fatty acid activation (Igal *et al.*, 1997), did not affect lipid accumulation in HepaRG cells (Figure 1B) and decreased lipid accumulation in HepG2 cells (Figure 1C).

The results obtained by flow cytometry were qualitatively confirmed using fluorescence microscopy (Figure 1D for HepaRG and Supplementary Figure 2 for HepG2 cells). Both cell lines showed accumulation of small lipid droplets in green

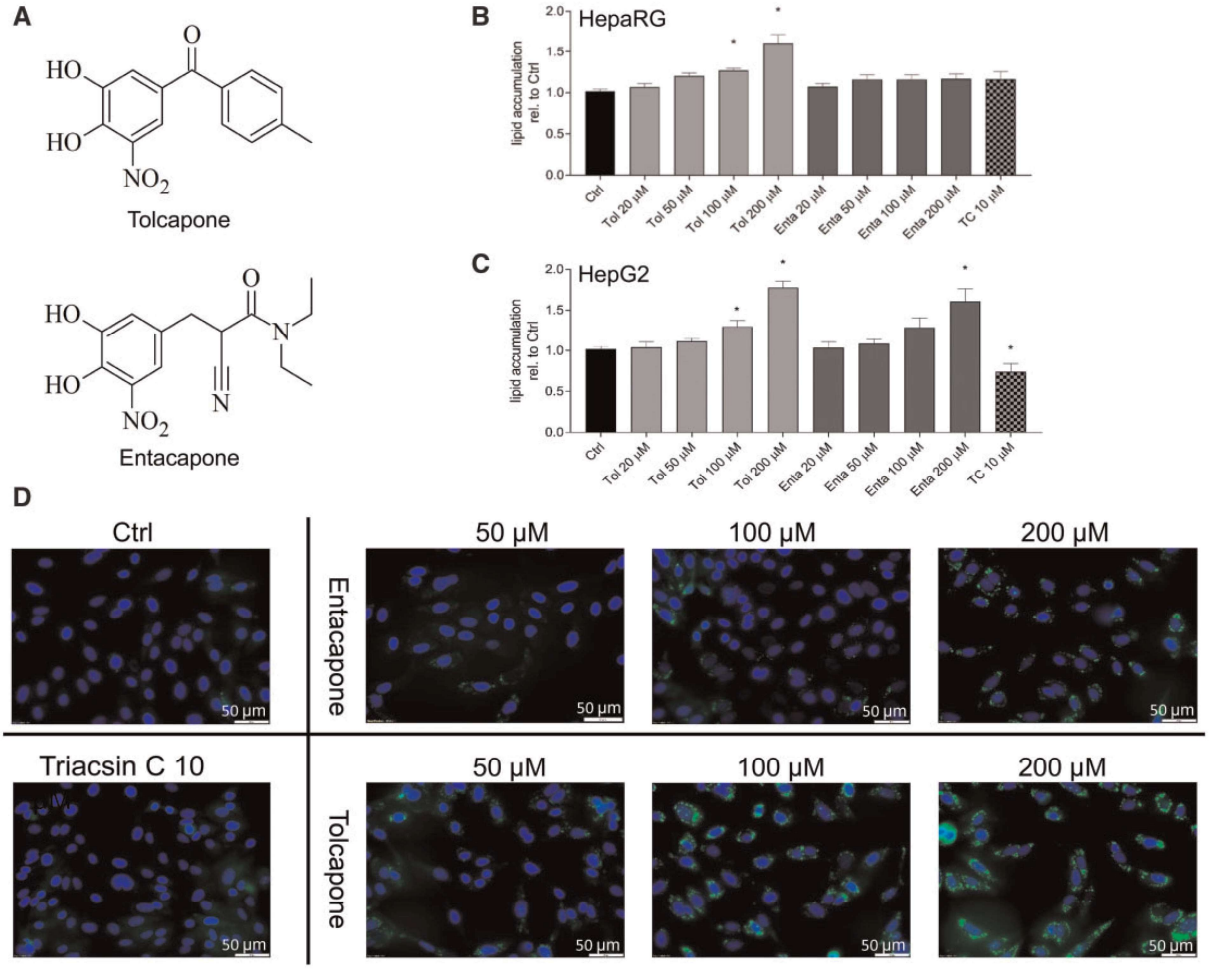

Figure 1. Effect on intracellular lipid accumulation in HepaRG cells. Cells were first cultured for 24 h in a medium containing BSA-bound palmitate and oleate before treatment with the compounds of interest. A, Chemical structure of tolcapone and entacapone. B, Fold change in lipid accumulation in HepaRG cells. After treatment with the compounds of interest for 24 h, cells were stained with PI and BODIPY493/503 and analyzed by FACS. Results are presented as mean ± SEM of 6 independent experiments. $^{*}p < .05$ versus DMSO 0.1% control. C, Fold change in lipid accumulation in treated HepG2 cells. HepG2 cells were treated and analyzed as described for HepaRG cells. Results are presented as mean ± SEM of 6 independent experiments. $^{*}p < .05$ versus DMSO 0.1% control. D, Representative fluorescence microscopy pictures of HepaRG cells treated with the compounds of interest for 24 h. After treatment, cells were stained with PI for nuclei and BODIPY493/503 for neutral lipids.

around the nucleus in blue when treated with tolcapone. Similar to the flow cytometric analysis, also entacapone (200 µM) produced an increased number of lipid droplets in HepG2 cells, but, in contrast to cytometry, also in HepaRG cells. Treatment with TC led to a decrease of triglyceride incorporation into lipid droplets in both cell lines, as suggested by dissemination of a faint BODIPY signal throughout the cells with very small lipid droplets.

Cellular Fatty Acid Metabolism In Vitro

To elucidate the mechanism leading to lipid accumulation, we assessed the metabolism of various fatty acid oxidation substrates in HepaRG cells treated for 24 h. We could observe a decrease in β-oxidation capacity of palmitate (Figure 2A) after treatment with tolcapone starting at 100 µM but not entacapone. CPT1 activity (Figure 2B), which is considered the rate-limiting step in lipid oxidation (Bonnefont *et al.*, 2004), was not affected by tolcapone or entacapone treatment. Moreover, the metabolism of palmitoyl-CoA was unchanged (Figure 2C), indicating that transport of fatty acids into mitochondria and mitochondrial β-oxidation were not affected. These findings suggested an inhibition of fatty acid metabolism by tolcapone before entry into mitochondria, pointing towards an effect on fatty acid activation (synthesis of acyl-CoAs). This was confirmed directly for tolcapone, which inhibited activation of palmitate starting at 50 µM (Figure 2D). In contrast, entacapone did not inhibit palmitate activation in HepaRG cells.

Mitochondrial Fatty Acid Metabolism

Next, we determined the inhibitory capability of the drugs on freshly isolated mouse liver mitochondria. Similar to the findings in HepaRG cells, we observed inhibition of palmitate metabolism by tolcapone (Supplementary Figure 2A), but starting at lower concentrations (at 5 µM) compared with HepaRG cells (where inhibition started at 100 µM, see Figure 2A). Interestingly, also entacapone-inhibited palmitate metabolism in isolated mouse liver mitochondria, starting at 50 µM. As we had observed already in HepaRG cells, metabolism of palmitoyl-carnitine (Supplementary Figure 3B) and palmitoyl-CoA (Supplementary Figure 3C) was affected neither by tolcapone,

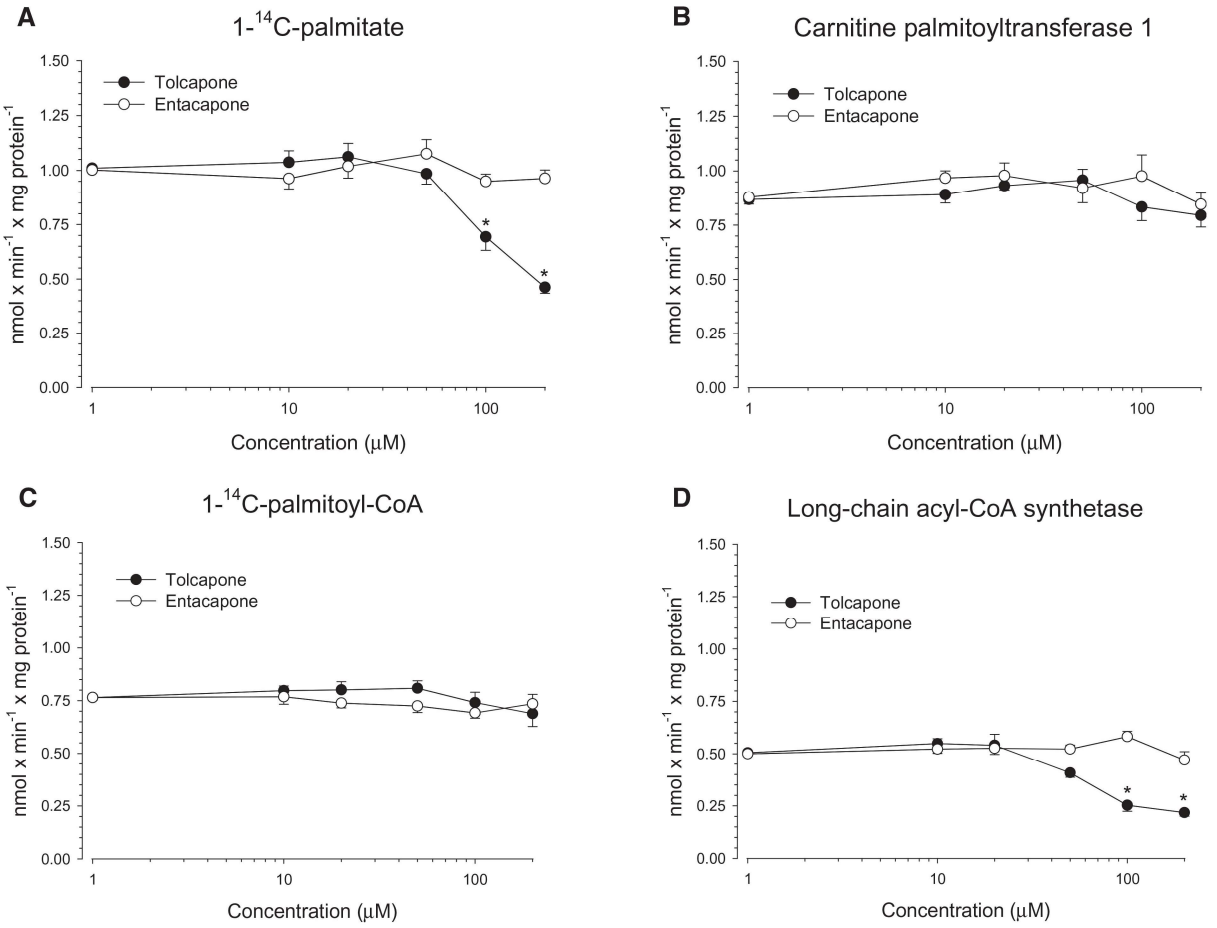

Figure 2. Effect of tolcapone and entacapone on fatty acid metabolism in HepaRG cells. Cells were treated with the compounds of interest for 24 h, before determining (A) metabolism of ^{14}C-palmitic acid (control activity 0.98 ± 0.06 nmol × min^{-1} × mg protein^{-1}), (B) activity of CPT1 (control activity 0.82 ± 0.06 nmol × min^{-1} × mg protein^{-1}), (C) metabolism of 1-^{14}C-palmitoyl-CoA (control activity 0.75 ± 0.05 nmol × min^{-1} × mg protein^{-1}) and (D) activity of ACSL (control activity 0.51 ± 0.03 nmol × min^{-1} × mg protein^{-1}). Results are presented as mean ± SEM of at least 8 independent experiments. *$p < .05$ versus DMSO 0.1% control.

nor by entacapone. Similar to HepaRG cells, inhibition of palmitate activation (synthesis of palmitoyl-CoA) by tolcapone was also detectable for isolated mitochondria (Supplementary Figure 3D), while entacapone did not affect palmitate activation under these conditions.

Changes in Acylcarnitine Pattern

As published recently, the pattern of acylcarnitines excreted by cells can be useful for the detection of specific inhibitions in fatty acid metabolism (Grünig *et al.*, 2018). Treatment with tolcapone was associated with a concentration-dependent decrease in medium-chain acylcarnitine formation (C5 to C10 acylcarnitines; starting at 50 µM) with a concomitant increase in 3-oxo-palmitoylcarnitine (starting at 50 µM) and an increase in C12–C16 acylcarnitines at higher concentrations (starting at 100 µM) (Figure 3A). In comparison, entacapone treated HepaRG cells showed a similar, but less pronounced depression of medium-chain acylcarnitine formation (Figure 3B), starting at 100 µM. Moreover, the effects on long-chain-acylcarnitines (C14 and C16) and 3-oxo-palmitoylcarnitine were less pronounced compared with tolcapone.

For the purpose of pattern comparison and proof of concept, we also studied the effect of the acyl-CoA synthesis inhibitor TC (Igal *et al.*, 1997), the CPT1 inhibitor etomoxir (Ceccarelli *et al.*, 2011), the medium-chain acyl-CoA dehydrogenase inhibitor methylenecyclopropyl acetic acid (MCPA) (Tserng *et al.*, 1991), and the 3-keto-acyl-CoA thiolase inhibitor 4-bromocrotonic acid (Olowe and Schulz, 1982) on the acylcarnitine pattern in the supernatant of HepaRG cells. As shown in Figure 3C, the established inhibitors affected the acylcarnitine pattern in predictable fashion. TC and etomoxir decreased all acylcarnitines determined, showing the importance of fatty acid activation and acylcarnitine formation for mitochondrial hepatocellular long-chain fatty acid metabolism. MCPA was associated with an increase in the medium-chain acylcarnitines, demonstrating the block of medium-chain acyl-CoA dehydrogenase and 4-bromocrotonic acid with the expected increase in 3-oxo-palmitoylcarnitine.

Activity of Acyl-CoA Dehydrogenases

Because of the increase in excreted long-chain acylcarnitines after tolcapone treatment (Figure 3A), we determined the effect of tolcapone and entacapone on the activity of acyl-CoA dehydrogenases in liver mitochondria. Tolcapone showed a concentration-dependent decrease in the activity of the long-chain acyl-CoA dehydrogenase, reaching statistical significance at the highest concentration investigated (400 µM). In contrast, tolcapone did not affect medium-chain acyl-CoA dehydrogenase (Supplementary Figure3B) and entacapone did affect the

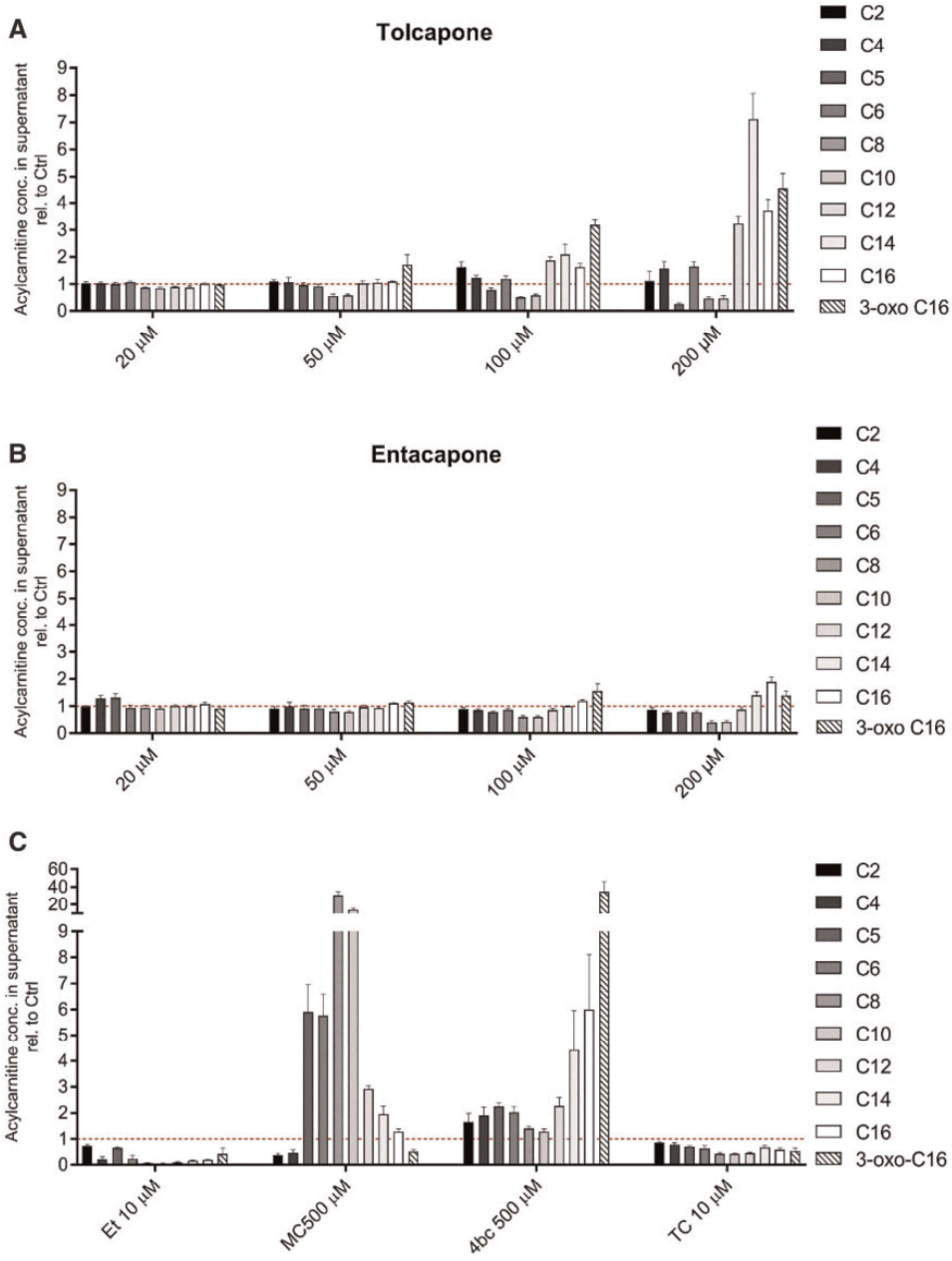

Figure 3. Effect of tolcapone, entacapone, TC, etomoxir, methylenecyclopropaneacetic acid, and 4-bromocrotonic acid on the acylcarnitine pattern in the supernatant of HepaRG cells. HepaRG cells were treated with the toxicants for 24 h in the presence of oleate, palmitate and L-carnitine. The supernatant was analyzed using LC-MS/MS as described in the Methods section. Results were normalized to the values of DMSO 0.1% exposed control cells and are expressed as mean ± SEM of 3 independent experiments. Abbreviations: TC, triacsin C; Et, etomoxir; MC, methylene-cyclopropane acetic acid; 4bc, 4-bromocrotonic acid.

activity of neither long- nor medium-chain acyl-CoA dehydrogenase (Supplementary Figs. 3A and 3B).

Effects on mRNA and Protein Expression of ACSL

To elucidate potential mechanisms how tolcapone could inhibit palmitate activation, we investigated mRNA and protein expression ACSL1 and ACSL5, which are considered to be associated with mitochondria (Soupene and Kuypers, 2008).

As shown in Figures 4A and 4B, tolcapone decreased mRNA expression of ACSL1 starting at 100 µM, but had no significant effect on ACSL5 mRNA expression. In comparison, entacapone and TC did not affect mRNA expression of ACSL1 and ACSL5. As shown in Figures 4C and 4D, and Supplementary Figure 4, tolcapone decreased protein expression of ACSL1 and 5 at the highest concentration investigated (200 µM), whereas entacapone and TC did not affect protein expression of ACSL1 and 5.

Effects on Markers of Fatty Acid Import, Synthesis and Trafficking, Lipid Storage, and Lipid Excretion

Hepatocytes can maintain their fatty acid pool by import and by de novo synthesis. As shown in Figures 5A and 5B, tolcapone was associated with a significant increase in the mRNA expression of CD36/FAT and with a numerical increase in the mRNA expression of fatty acid transport protein 5 (FATP5), 2 proteins

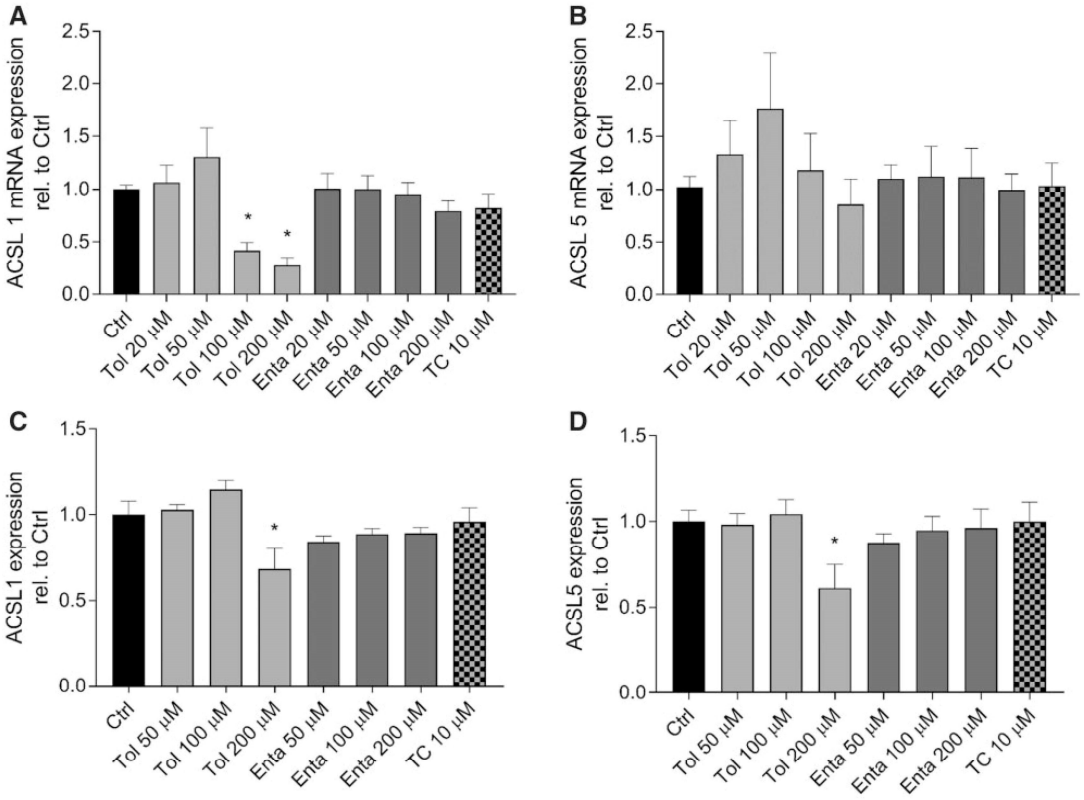

Figure 4. Effect of tolcapone and entacapone on mRNA and protein expression of ACSLs in HepaRG cells. Cells were treated for 24 h with the drugs before determination of mRNA and protein content of ACSL. A, Fold change in mRNA expression of ACSL1 and (B) fold change in mRNA expression of ACSL5. C, Quantification of a Western blot showing fold change in ACSL1 expression and (D) fold change in ACSL5 expression. Results are normalized to control cells exposed to 0.1% DMSO and are presented as mean ± SEM of 4 independent experiments. $^{*}p < .05$ versus DMSO 0.1% control. Abbreviations: Ctrl, control (DMSO 0.1%); Tol, tolcapone; Enta, entacapone; TC, triacsin C.

involved in fatty acid import (Bechmann *et al.*, 2012; Kazantzis and Stahl, 2012). In comparison, entacapone did not affect mRNA expression of CD36/FAT (Figure 5A) and decreased FATP5 mRNA expression (Figure 5B). As shown in Figure 5C and Supplementary Figure 4, the liver fatty acid-binding protein (FABP), which is important for intracellular binding and transport of fatty acids and intermediates (Wang *et al.*, 2015), was not significantly affected by tolcapone, entacapone or TC.

Tolcapone reduced mRNA expression of the sterol regulatory element-binding protein-1c (SREBP-1c), which is a regulator of fatty acid synthesis (Eberle *et al.*, 2004) (Figure 5D). Accordingly, tolcapone reduced also the mRNA expression of acetyl-CoA carboxylase (ACC, Figure 5E) and fatty acid synthase (FAS, Figure 5F), which encode 2 essential proteins in fatty acid synthesis (Bechmann *et al.*, 2012). In comparison, entacapone and triacsin did not affect the mRNA expression of the corresponding genes.

Next, we investigated triglyceride synthesis and lipid droplet formation. The protein expression of glycerol-3-phosphate acyltransferase 1 (GPAT1), which catalyzes the first step in glycerolipid (eg, triglyceride) synthesis (Wendel *et al.*, 2009), was not affected by tolcapone or TC, whereas entacapone decreased the expression of GPAT1 concentration-dependently, reaching statistical significance at 200 µM (Figure 6A and Supplementary Figure 4).

Protein expression of perilipin-2, also known as ADRP, which is involved in lipid droplet formation (Brasaemle *et al.*, 1997), was not affected by entacapone or TC (Figure 6B and Supplementary Figure 4), whereas tolcapone numerically decreased ADRP protein expression at 200 µM. In contrast, mRNA expression of the cell death-inducing DNA fragmentation factor-alpha-like effector a (cidea), encoding a protein involved in lipid droplet formation (Zhou *et al.*, 2012), was significantly increased by tolcapone (100 µM) (Figure 6C). In comparison, entacapone and triacsin did not affect cidea mRNA expression.

The protein content of the microsomal triglyceride transfer protein (MTTP), which is essential for lipidation of ApoB100 (Mason, 1998), was not affected by entacapone or TC (Figure 6D and Supplementary Figure 4). In comparison, tolcapone increased the protein expression of MTTP concentration-dependently, reaching statistical significance at 200 µM.

Hepatocytes can export triglycerides in the form of VLDL. Since ApoB100 is the protein core of VLDL, we determined the ApoB concentration in the supernatant of HepaRG cells exposed to the toxicants. Treatment with tolcapone was associated with a concentration-dependent decrease in the ApoB100 concentration, reaching statistical significance at 100 µM (Figure 6E), whereas entacapone and TC did not significantly affect ApoB100 secretion. As shown in Figure 6F, tolcapone decreased mRNA expression of ApoB starting at 100 µM, suggesting that impaired transcription of the ApoB100 gene could be the reason for the observed decrease in ApoB100 secretion. Entacapone did not affect ApoB100 secretion or mRNA expression, whereas TC increased ApoB100 mRNA expression without affecting ApoB100 secretion (Figs. 6E and 6F).

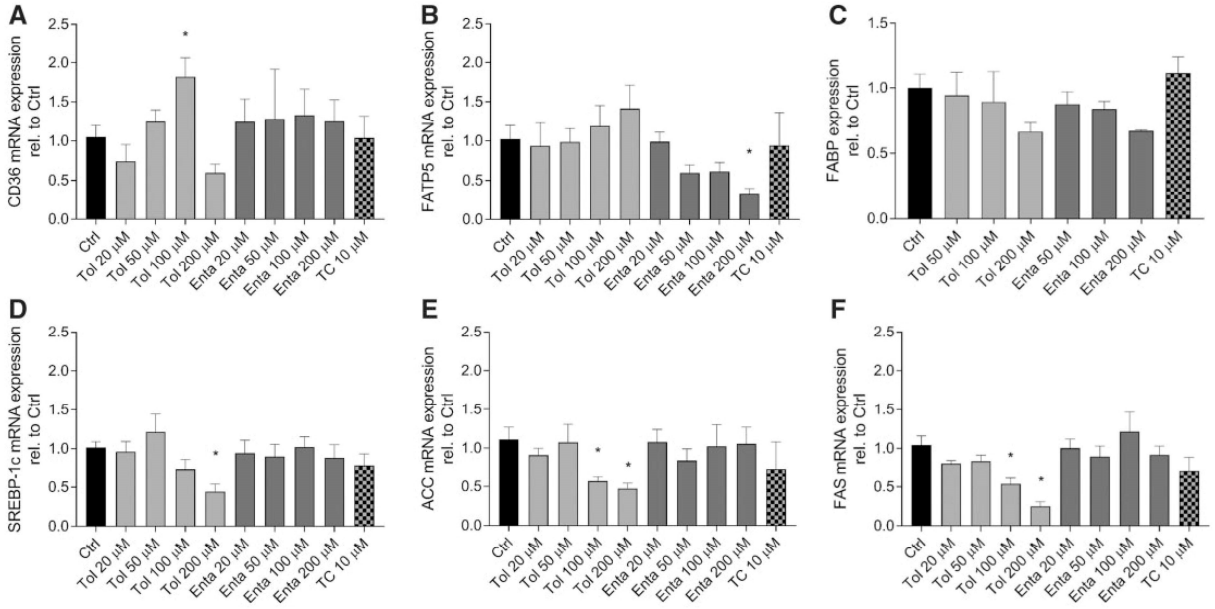

Figure 5. Effect of tolcapone and entacapone on mRNA or protein expression of fatty acid transporters, transport proteins and proteins involved in fatty acid synthesis in HepaRG cells. Cells were treated for 24 h with the drugs before determination of the mRNA or protein content. A, Fold change in mRNA expression of CD36/FAT, (B) fold change in mRNA expression of FATP5, (C) fold change in the protein content of FABP, (D) fold change in mRNA expression of SREBP-1c, (E) fold change in mRNA expression of ACC, and (F) fold change in FAS mRNA expression. Results are normalized to control cells exposed to 0.1% DMSO and are presented as mean ± SEM of 4 independent experiments. $^*p < .05$ versus DMSO 0.1% control. Abbreviations: Ctrl, control (DMSO 0.1%); Tol, tolcapone; Enta, entacapone; TC, triacsin C; FATP, fatty acid transport protein; FABP, fatty acid-binding protein; SREBP, sterol regulatory element-binding protein; ACC, acetyl-CoA carboxylase; FAS, fatty acid synthase.

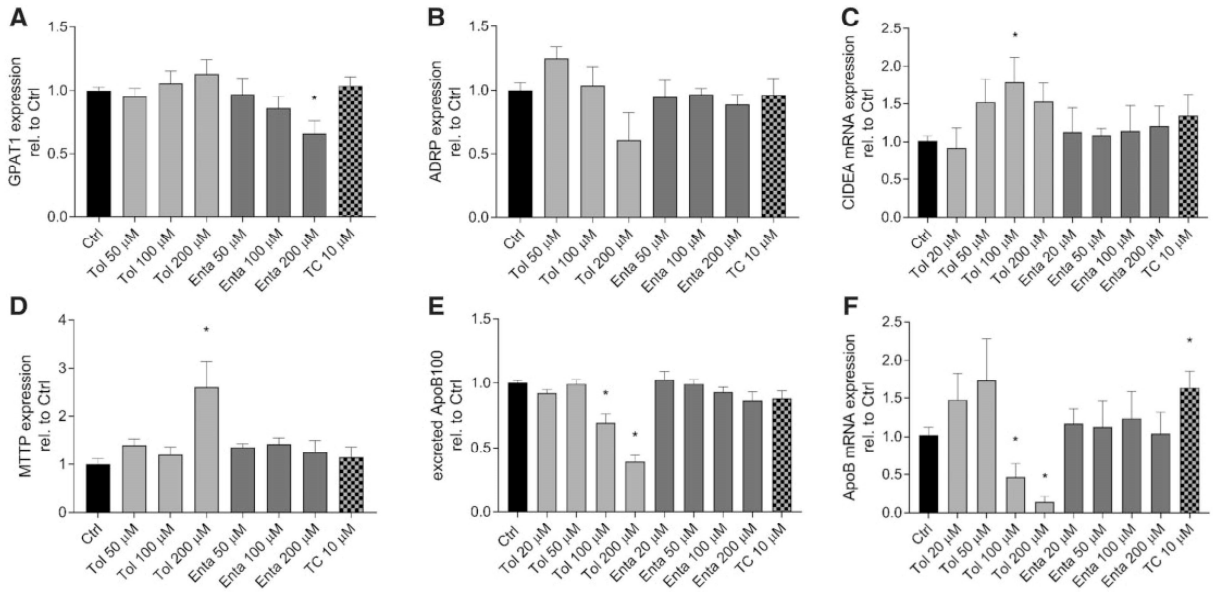

Figure 6. Effect of tolcapone and entacapone on mRNA or protein expression of proteins involved in triglyceride synthesis, lipid droplet formation or VLDL formation and export in HepaRG cells. Cells were treated for 24 h with the drugs before determination of the mRNA or protein content. A, Fold change in GPAT1 protein expression. B, Fold change in ADRP protein expression. C, Fold change in cidea mRNA expression. D, Fold change in MTTP protein expression. E, Fold change in ApoB100 protein excreted into the supernatant of HepaRG cell cultures. The mean concentration of ApoB100 in the supernatant of control cells (exposed to 0.1% DMSO) was 26.2 ± 1.3 ng × mL^{-1}. F, Fold change in mRNA ApoB100 expression. Results were normalized to control incubations exposed to 0.1% DMSO and are presented as mean ± SEM of $n = 5$ independent experiments. $^*p < .05$ versus DMSO 0.1% control. Abbreviations: Ctrl, control (DMSO 0.1%); Tol, tolcapone; Enta, entacapone; TC, triacsin C; GPAT, glycerol-3-phosphate acyltransferase; ADRP, adipose differentiation-related protein; cidea, cell death-inducing DNA fragmentation factor-alpha-like effector a; MTTP, microsomal triglyceride transfer protein; ApoB, apolipoprotein B.

DISCUSSION

This study illustrates that tolcapone is associated with lipid accumulation in HepaRG and HepG2 cells, which, as shown HepaRG cells, can be explained by increased fatty acid import, impaired mitochondrial fatty acid metabolism and impaired secretion of VLDL.

After having entered the hepatocytes, fatty acids are activated and can subsequently undergo degradation by

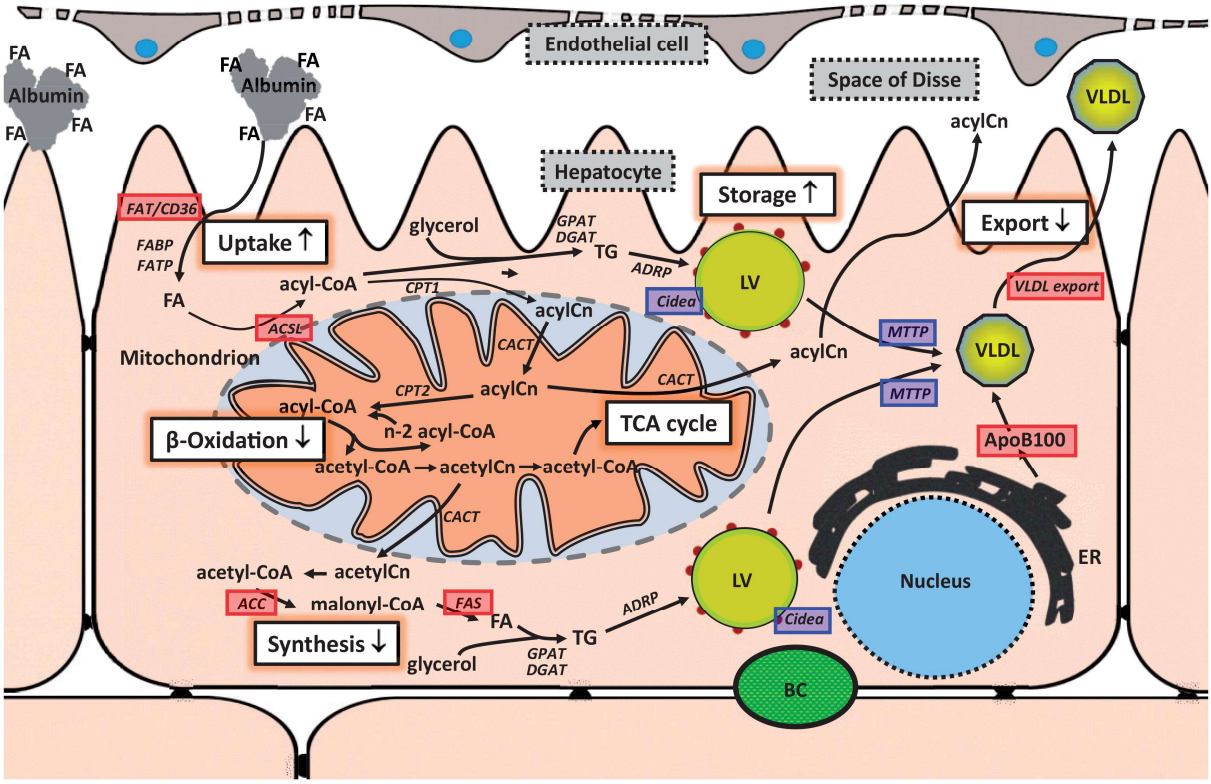

Figure 7. Hepatocellular fatty acid metabolism. Long-chain fatty acids (FA) are imported into hepatocytes by mainly active transport and diffusion (Uptake). Subsequently, they can be activated to the corresponding CoA derivative by ACSLs. The activated fatty can be converted to the carnitine (Cn) derivative by CPT1, imported into the mitochondrial matrix by COCT and reconverted to the corresponding CoA derivative by CPT2. This is followed by β-oxidation, which produces acetyl-CoA, NADH, and $FADH_2$ (not shown). Acyl-CoAs can be converted to the corresponding carnitine derivatives, which can be exported from mitochondria (and cells) by COCT. Hepatocytes can also synthesize fatty acids starting from malonyl-CoA (Synthesis), which is regulated by SREBP-1c (not shown). Depending on the metabolic conditions, activated fatty acids can also be used for triglyceride (TG) synthesis. Triglycerides can be stored in lipid vesicles (LV) (Storage). ADRP and cidea are 2 proteins involved in lipid droplet formation. Triglycerides can also be used for the synthesis of VLDL, which can be exported (Export). Effects of tolcapone are indicated with arrows and with red (decrease) or blue boxes (increase) around critical proteins or activities. Abbreviations: ACC, acetyl-CoA carboxylase; ACSL, long-chain acyl-CoA synthetase; ADRP, adipose differentiation-related protein; ApoB, apolipoprotein B; BC, bile canaliculus; CACT, carnitine-acylcarnitine translocase; cidea, cell death-inducing DNA fragmentation factor-alpha-like effector a; CPT, carnitine palmitoyltransferase; DGAT, diacylglycerol-O-acyltransferase; ER, endoplasmic reticulum; FA, long-chain fatty acids; FABP, fatty acid binding protein; GPAT, glycerol-3-phosphate acyltransferase; LV, lipid vesicle; MTTP, microsomal triglyceride transfer protein; SREBP-1c, sterol regulatory element-binding protein 1c; VLDL, very low-density lipoprotein.

β-oxidation or can be used for triglyceride production. Triglycerides can be stored in lipid droplets or can be incorporated into VLDL particles that are exported from hepatocytes (Figure 7). In order to find out possible reasons why tolcapone is associated with lipid accumulation in hepatocytes, we assessed these pathways using different approaches. First, we confirmed that tolcapone (and less so entacapone) is associated with hepatocellular lipid accumulation. For that we chose 2 frequently used cell models, HepG2 cells and the better differentiated HepaRG cells (Berger *et al.*, 2016). In both cell models, tolcapone was associated with lipid accumulation starting at 100 μM, whereas entacapone reached a significant accumulation only in HepG2 cells at 200 μM. Although better differentiated, HepaRG cells seem to be slightly less sensitive to inhibition of fatty acid metabolism than HepG2 cells. The suitability of HepG2 cells for studying fatty acid metabolism has been demonstrated previously in Donato *et al.* (2009) and Felser *et al.* (2013). Nevertheless, since we wanted to study the mechanisms and not the extent of lipid accumulation, we chose the better differentiated HepaRG cells for our investigations.

The mRNA expression of CD36/FAT and FATP5 was concentration-dependently increased by tolcapone, indicating an augmentation in transcription and possibly also in protein expression and activity of these transporters. These findings offered 1 possible explanation for the observed lipid droplet accumulation by tolcapone in HepaRG cells.

Considering the description of microvesicular steatosis in a patient with tolcapone-associated liver injury (Spahr *et al.*, 2000), impairment of mitochondrial fatty acid metabolism could be expected (Fromenty and Pessayre, 1995). Furthermore, we and others have reported that tolcapone impairs the function of the mitochondrial electron transport chain (Grunig *et al.*, 2017; Haasio *et al.*, 2002a), which can disturb mitochondrial fatty acid metabolism. In agreement with these reports, palmitate metabolism was reduced in HepaRG cells and in acutely exposed isolated mouse liver mitochondria. To our surprise, however, β-oxidation (metabolism of palmitoylcarnitine and palmitoyl-CoA) was intact and we could localize the defect in mitochondrial fatty acid metabolism in the activation of long-chain fatty acids. There are several acyl-CoA synthases performing activation of fatty acids, depending on the chain-length of the fatty acids to be activated and with different subcellular localization (Soupene and Kuypers, 2008). ACSLs localized on the outer mitochondrial membrane, which are responsible for the activation

of long-chain fatty acids undergoing mitochondrial metabolism, are mainly ACSL1 and ACSL5 (Soupene and Kuypers, 2008). Based on our findings, we can propose 2 mechanisms how tolcapone affects the mitochondrial ACSLs. The data in isolated mitochondria indicate an acute inhibition, which is most probably the result of a direct interaction of tolcapone with the mitochondrial ACSLs. The second mechanism was detected in HepaRG cells exposed for 24 h. In these experiments, we observed a decrease in the mRNA and protein expression of mainly ACSL1, the most active ACSL in liver (Yan *et al.*, 2015), suggesting an inhibition of the transcription of the gene encoding ACSL1.

TC, which was used as a positive control, is an inhibitor of ACSL1, ACSL3, and ACSL4 (Tomoda *et al.*, 1991). In contrast to tolcapone, TC was not associated with hepatocellular accumulation of lipids (Figure 1). This difference compared with tolcapone may be explained by inhibition of nonmitochondrial ACSLs, which are important for triglyceride synthesis (Soupene and Kuypers, 2008).

We determined the acylcarnitine pool in the HepaRG culture supernatant as an additional marker of mitochondrial fatty acid metabolism (see Figure 7). We have shown previously that the acylcarnitine pool in cell culture supernatant can be used for localizing defects in mitochondrial fatty acid metabolism (Grünig *et al.*, 2018). Acylcarnitines are formed from the respective acyl-CoAs by carnitine acyltransferases (Brass and Hoppel, 1980) and can be transported out of mitochondria and cells into the circulation (Vernez *et al.*, 2003) or into cell culture supernatants. The acylcarnitine pattern in cell culture supernatants describes therefore the cellular (and mitochondrial) acyl-CoA pattern, which can reflect alterations in fatty acid metabolism (Ensenauer *et al.*, 2012). In this study, treatment of HepaRG cells was associated with a decrease in medium-chain acylcarnitines starting at 50 μM and an increase in long-chain acylcarnitines starting at 100 μM. The decrease in medium-chain acylcarnitines was less accentuated as observed with TC, but can be explained by inhibition of fatty acid activation. The concomitant increase in the long-chain acylcarnitines, which occurred at higher concentrations, can be explained by the observed inhibition of the long-chain acyl-CoA dehydrogenase. The results of the acylcarnitine pattern are therefore in agreement with the findings obtained with direct determination of enzyme activities.

A third mechanism for the observed increase in lipid droplet accumulation in HepaRG cells treated with tolcapone was an impaired export of VLDL (and therefore triglycerides) out of hepatocytes as suggested by impaired ApoB100 excretion (see Figure 7). Every LDL particle contains 1 ApoB100 molecule, which is the structural protein of the LDL particle and essential for VLDL formation (Fisher, 2012; Mason, 1998). We also observed reduced ApoB100 mRNA levels in HepaRG cells treated with tolcapone, suggesting that the reason for reduced ApoB100 in tolcapone-treated cells may be impaired ApoB100 synthesis. In addition, degradation of ApoB100 has been reported to be important for the cellular ApoB100 levels and to involve ApoB100 oxidation followed by autophagy (Fisher, 2012). Since tolcapone was associated with mitochondrial ROS production (Grunig *et al.*, 2017), ApoB100 degradation could be increased in the presence of tolcapone. Since the protein expression of important factors in FABP, triglyceride synthesis (GPAT1), lipid droplet formation (ADRP), and MTTP were either not significantly affected or increased by tolcapone, lipid trafficking and lipid loading of ApoB100 appear not the be the principle reasons for impaired VLDL secretion by tolcapone-treated HepaRG cells.

In isolated mouse liver mitochondria, we observed a decrease in palmitate metabolism at 5 μM for tolcapone and at 50 μM for entacapone. In HepaRG cells, long-chain fatty acid metabolism (based on the acylcarnitine pattern in the cell culture supernatant) started to be disturbed at a tolcapone concentration of 50 μM, whereas most other alterations in fatty acid metabolism started at 100 μM. Similar concentrations were also needed to disturb the function of the mitochondrial respiratory chain of HepaRG cells in a previous study (Grunig *et al.*, 2017). The difference between mitochondria and HepaRG cells is most likely a consequence of better accessibility of mitochondria and lack of protein in the incubations with mitochondria. A recent in silico study suggested that both hepatic exposure and preexisting mitochondrial dysfunction are the key factors determining the occurrence of liver injury in patients treated with tolcapone (Longo *et al.*, 2016). The estimated liver concentrations that can be reached with therapeutic doses of tolcapone were 1–3 and 0.3–1.3 μM for entacapone. In comparison, maximal plasma concentrations reached after single doses of 200-mg entacapone (6 μM) and 100-mg tolcapone (17 μM) were higher (Kaakkola, 2000), but still lower than the lowest concentrations associated with toxicity in HepaRG cells. A suitable explanation for severe hepatic toxicity in patients treated with tolcapone is therefore that such patients must have high hepatic exposures and a preexisting mitochondrial disease. This concept has been illustrated recently in an *in vitro* study investigating the toxicity of different mitochondrial toxicants in HepG2 cells (Haegler *et al.*, 2015) and explains the infrequence of severe hepatotoxicity in patients treated with tolcapone. For entacapone, exposures reached and mitochondrial toxicity are not pronounced enough to result in liver toxicity.

In conclusion, tolcapone increases mRNA expression of fatty acid transporting proteins, inhibits activation of long-chain fatty acids and impairs VLDL secretion by hepatocytes, leading to hepatocellular triglyceride accumulation. Entacapone exhibits similar toxic effects than olcapone but at higher concentrations.

SUPPLEMENTARY DATA

Supplementary data are available at *Toxicological Sciences* online.

FUNDING

This study was supported by a grant from the Swiss National Science Foundation to S.K. (SNF 31003A-132992).

REFERENCES

Assal, F., Spahr, L., Hadengue, A., Rubbici-Brandt, L., and Burkhard, P. R. (1998). Tolcapone and fulminant hepatitis. *Lancet* **352**, 958.

Bechmann, L. P., Hannivoort, R. A., Gerken, G., Hotamisligil, G. S., Trauner, M., and Canbay, A. (2012). The interaction of hepatic lipid and glucose metabolism in liver diseases. *J. Hepatol.* **56**, 952–964.

Berger, B., Donzelli, M., Maseneni, S., Boess, F., Roth, A., Krahenbuhl, S., and Haschke, M. (2016). Comparison of Liver Cell Models Using the Basel Phenotyping Cocktail. *Front. Pharmacol.* **7**, 443–410. 3389/fphar.2016.00443.

Bonnefont, J. P., Djouadi, F., Prip-Buus, C., Gobin, S., Munnich, A., and Bastin, J. (2004). Carnitine palmitoyltransferases 1 and 2:

Biochemical, molecular and medical aspects. *Mol. Aspects Med.* **25**, 495–520.

Borges, N. (2003). Tolcapone-related liver dysfunction: Implications for use in Parkinson's disease therapy. *Drug Saf.* **26**, 743–747.

Brasaemle, D. L., Barber, T., Wolins, N. E., Serrero, G., Blanchette-Mackie, E. J., and Londos, C. (1997). Adipose differentiation-related protein is an ubiquitously expressed lipid storage droplet-associated protein. *J. Lipid Res.* **38**, 2249–2263.

Brass, E. P., and Hoppel, C. L. (1980). Relationship between acid-soluble carnitine and coenzyme A pools in vivo. *Biochem. J.* **190**, 495–504.

Ceccarelli, S. M., Chomienne, O., Gubler, M., and Arduini, A. (2011). Carnitine palmitoyltransferase (CPT) modulators: A medicinal chemistry perspective on 35 years of research. *J. Med. Chem.* **54**, 3109. 10.1021/jm100809g.

Donato, M. T., Martínez-Romero, A., Jiménez, N., Negro, A., Herrera, G., Castell, J. V., O'Connor, J.-E., and Gómez-Lechón, M. J. (2009). Cytometric analysis for drug-induced steatosis in HepG2 cells. *Chemico-Biol. Interact.* **181**, 417–423.

Eberle, D., Hegarty, B., Bossard, P., Ferre, P., and Foufelle, F. (2004). SREBP transcription factors: Master regulators of lipid homeostasis. *Biochimie* **86**, 839–848.

Ensenauer, R., Fingerhut, R., Schriever, S. C., Fink, B., Becker, M., Sellerer, N. C., Pagel, P., Kirschner, A., Dame, T., Olgemoller, B., *et al.* (2012). In situ assay of fatty acid beta-oxidation by metabolite profiling following permeabilization of cell membranes. *J. Lipid Res.* **53**, 1012–1020.

Felser, A., Blum, K., Lindinger, P. W., Bouitbir, J., and Krahenbuhl, S. (2013). Mechanisms of hepatocellular toxicity associated with dronedarone–A comparison to amiodarone. *Toxicol. Sci.* **131**, 480–490.

Felser, A., Stoller, A., Morand, R., Schnell, D., Donzelli, M., Terracciano, L., Bouitbir, J., and Krahenbuhl, S. (2014). Hepatic toxicity of dronedarone in mice: Role of mitochondrial beta-oxidation. *Toxicology* **323**, 1–9.

Fischer, J. J., Michaelis, S., Schrey, A. K., Graebner, O. G., Glinski, M., Dreger, M., Kroll, F., and Koester, H. (2010). Capture compound mass spectrometry sheds light on the molecular mechanisms of liver toxicity of two Parkinson drugs. *Toxicol. Sci.* **113**, 243–253.

Fisher, E. A. (2012). The degradation of apolipoprotein B100: Multiple opportunities to regulate VLDL triglyceride production by different proteolytic pathways. *Biochim. Biophys. Acta* **1821**, 778–781.

Fromenty, B., and Pessayre, D. (1995). Inhibition of mitochondrial beta-oxidation as a mechanism of hepatotoxicity. *Pharmacol. Ther.* **67**, 101–154.

Grünig, D., Duthaler, U., and Krahenbuhl, S. (2018). Effect of toxicants on fatty acid metabolism in HepG2 cells. *Front. Pharmacol.* in press.

Grunig, D., Felser, A., Bouitbir, J., and Krahenbuhl, S. (2017). The catechol-O-methyltransferase inhibitors tolcapone and entacapone uncouple and inhibit the mitochondrial respiratory chain in HepaRG cells. *Toxicol. In Vitro* **42**, 337–347.

Guillouzo, A., Corlu, A., Aninat, C., Glaise, D., Morel, F., and Guguen-Guillouzo, C. (2007). The human hepatoma HepaRG cells: A highly differentiated model for studies of liver metabolism and toxicity of xenobiotics. *Chemico-Biol. Interact.* **168**, 66–73.

Haasio, K. (2010). Toxicology and safety of COMT inhibitors. *Int. Rev. Neurobiol.* **95**, 163–189.

Haasio, K., Koponen, A., Penttila, K. E., and Nissinen, E. (2002a). Effects of entacapone and tolcapone on mitochondrial membrane potential. *Eur. J. Pharmacol.* **453**, 21–26.

Haasio, K., Nissinen, E., Sopanen, L., and Heinonen, E. H. (2002b). Different toxicological profile of two COMT inhibitors in vivo: The role of uncoupling effects. *J. Neural Trans.* **109**, 1391–1401.

Haasio, K., Sopanen, L., Vaalavirta, L., Linden, I. B., and Heinonen, E. H. (2001). Comparative toxicological study on the hepatic safety of entacapone and tolcapone in the rat. *J. Neural Trans.* **108**, 79–91.

Haegler, P., Grünig, D., Berger, B., Krähenbühl, S., and Bouitbir, J. (2015). Impaired mitochondrial function in HepG2 cells treated with hydroxy-cobalamin[c-lactam]: A cell model for idiosyncratic toxicity. *Toxicology* **336**, 48–58.

Hoppel, C., DiMarco, J. P., and Tandler, B. (1979). Riboflavin and rat hepatic cell structure and function. Mitochondrial oxidative metabolism in deficiency states. *J. Biol. Chem.* **254**, 4164–4170.

Igal, R. A., Wang, P., and Coleman, R. A. (1997). Triacsin C blocks de novo synthesis of glycerolipids and cholesterol esters but not recycling of fatty acid into phospholipid: Evidence for functionally separate pools of acyl-CoA. *Biochem. J.* **324**, 529–534.

Jorga, K., Fotteler, B., Heizmann, P., and Gasser, R. (2001). Metabolism and excretion of tolcapone, a novel inhibitor of catechol-O-methyltransferase. *Br. J. Clin. Pharmacol.* **48**, 513–520.

Kaakkola, S. (2000). Clinical pharmacology, therapeutic use and potential of COMT inhibitors in Parkinson's disease. *Drugs* **59**, 1233–1250.

Kazantzis, M., and Stahl, A. (2012). Fatty acid transport proteins, implications in physiology and disease. *Biochim. Biophys. Acta* **1821**, 852–857.

Lew, M. F., and Kricorian, G. (2007). Results from a 2-year centralized tolcapone liver enzyme monitoring program. *Clin. Neuropharmacol.* **30**, 281–286. 10.1097/WNF.0b013e318149f290.

Longo, D. M., Yang, Y., Watkins, P. B., Howell, B. A., and Siler, S. Q. (2016). Elucidating differences in the hepatotoxic potential of tolcapone and entacapone with DILIsym((R)), a mechanistic model of drug-induced liver injury. *CPT Pharmacometrics Syst. Pharmacol.* **5**, 31–39.

Mason, T. M. (1998). The role of factors that regulate the synthesis and secretion of very-low-density lipoprotein by hepatocytes. *Crit. Rev. Clin. Lab. Sci.* **35**, 461–487.

Morand, R., Donzelli, M., Haschke, M., and Krahenbuhl, S. (2013). Quantification of plasma carnitine and acylcarnitines by high-performance liquid chromatography-tandem mass spectrometry using online solid-phase extraction. *Anal. Bioanal. Chem.* **405**, 8829–8836.

Olanow, C. W. (2000). Tolcapone and hepatotoxic effects. Tasmar Advisory Panel. *Arch. Neurol.* **57**, 263–267.

Olowe, Y., and Schulz, H. (1982). 4-Bromocrotonic acid, an effective inhibitor of fatty acid oxidation and ketone body degradation in rat heart mitochondria. On the rate-determining step of beta-oxidation and ketone body degradation in heart. *J. Biol. Chem.* **257**, 5408–5413.

Soupene, E., and Kuypers, F. A. (2008). Mammalian long-chain acyl-CoA synthetases. *Exp. Biol. Med. (Maywood, N.J.)* **233**, 507–521.

Spahr, L., Rubbia-Brandt, L., Burkhard, P. R., Assal, F., and Hadengue, A. (2000). Tolcapone-related fulminant hepatitis: Electron microscopy shows mitochondrial alterations. *Digest. Dis. Sci.* **45**, 1881–1884.

Tomoda, H., Igarashi, K., Cyong, J. C., and Omura, S. (1991). Evidence for an essential role of long chain acyl-CoA synthetase in animal cell proliferation. Inhibition of long chain acyl-CoA synthetase by triacsins caused inhibition of Raji cell proliferation. *J. Biol. Chem.* **266**, 4214–4219.

Tserng, K. Y., Jin, S. J., and Hoppel, C. L. (1991). Spiropentaneacetic acid as a specific inhibitor of medium-chain acyl-CoA dehydrogenase. *Biochemistry* **30**, 10755–10760.

Vernez, L., Hopfgartner, G., Wenk, M., and Krahenbuhl, S. (2003). Determination of carnitine and acylcarnitines in urine by high-performance liquid chromatography-electrospray ionization ion trap tandem mass spectrometry. *J. Chromatogr. A* **984**, 203–213.

Wang, G., Bonkovsky, H. L., de Lemos, A., and Burczynski, F. J. (2015). Recent insights into the biological functions of liver fatty acid binding protein 1. *J. Lipid Res.* **56**, 2238–2247. 10.1194/jlr.R056705.

Wendel, A. A., Lewin, T. M., and Coleman, R. A. (2009). Glycerol-3-phosphate acyltransferases: Rate limiting enzymes of triacylglycerol biosynthesis. *Biochim. Biophys. Acta* **1791**, 501–506.

Yan, S., Yang, X. F., Liu, H. L., Fu, N., Ouyang, Y., and Qing, K. (2015). Long-chain acyl-CoA synthetase in fatty acid metabolism involved in liver and other diseases: An update. *World J. Gastroenterol.* **21**, 3492–3498.

Zhou, L., Xu, L., Ye, J., Li, D., Wang, W., Li, X., Wu, L., Wang, H., Guan, F., and Li, P. (2012). Cidea promotes hepatic steatosis by sensing dietary fatty acids. *Hepatology* **56**, 95–107,

Supplement

Effect of the catechol-O-methyltransferase inhibitors tolcapone and entacapone on fatty acid metabolism in HepaRG cells

Running title: COMT inhibitors and hepatocellular fatty acid metabolism

[1,2]David Grünig *, [1,2]Andrea Felser*, [1,2,3]Jamal Bouitbir, [1,2,3]Stephan Krähenbühl

*contributed equally

[1]Division of Clinical Pharmacology & Toxicology, University Hospital Basel, Switzerland;

[2]Department of Biomedicine, University of Basel, Switzerland;

[3]Swiss Center of Applied Human Toxicology (SCAHT)

Correspondence

Stephan Krähenbühl, MD, PhD

Clinical Pharmacology & Toxicology

University Hospital

4031 Basel

Switzerland

Phone: +41 61 265 4715

Fax: +41 61 265 4560

E-mail:kraehenbuehl@uhbs.ch

Supplementary Tables

Supplementary Table 1

Primers used for mRNA quantification.

ACC: forward 5'-CGA GGG AGA AGG TAG CAC TG-3', backward 5'-GAA ACC ACG GAG CAG AAG AG-3'

ACSL1: forward 5'-GGA GTG GGC TGC AGT GAC -3', reverse 5'-GGG CTT GCA TTG TCC CTG T-3'

ACSL5: forward 5'-GCT CCT TTG AGG AAC TGT GC-3', reverse 5'-ATC CCC GAG TCC CAT AAA AC-3'

ApoB: forward 5'- AAG GCT TCA AGC ACA TTG GT-3', reverse 5'- CTG AGC CTC CAG ACC CAT C-3'

CD36/FAT: forward 5'- TGC TAG AGA CCC TGG CTG AT -3', backward 5'- CAG CGT CCT GGG TTA CAT TT -3'

Cidea: forward 5'-GCG TCC TTC CAA CCA CTT TT-3', backward 5'-ACA GAG ACC CCA CAC AGA TG-3'

FAS: forward 5'-AAC TCC TGC AAG TTC TCC GA-3', backward 5'-GCT CCA GCC TCG CTC TC-3'

FATP5: forward 5'- ACG GGG AGA AGT TGT ACC AG -3', backward 5'- CAG TTT GAA CGT GCT GGT GA -3'

GAPDH: forward 5'-AGC CAC ATC GCT CAG ACA C-3', reverse 5'-GCC CAA TAC GAC CAA ATC C-3'

SREBP-1c: forward 5'-TGT TTC CGT CTG CCT CTT CT-3', backward 5'-GTG AGC CTG TCT CCT TCT GG-3'

Legends to supplementary Figures

Suppl. Fig. 1

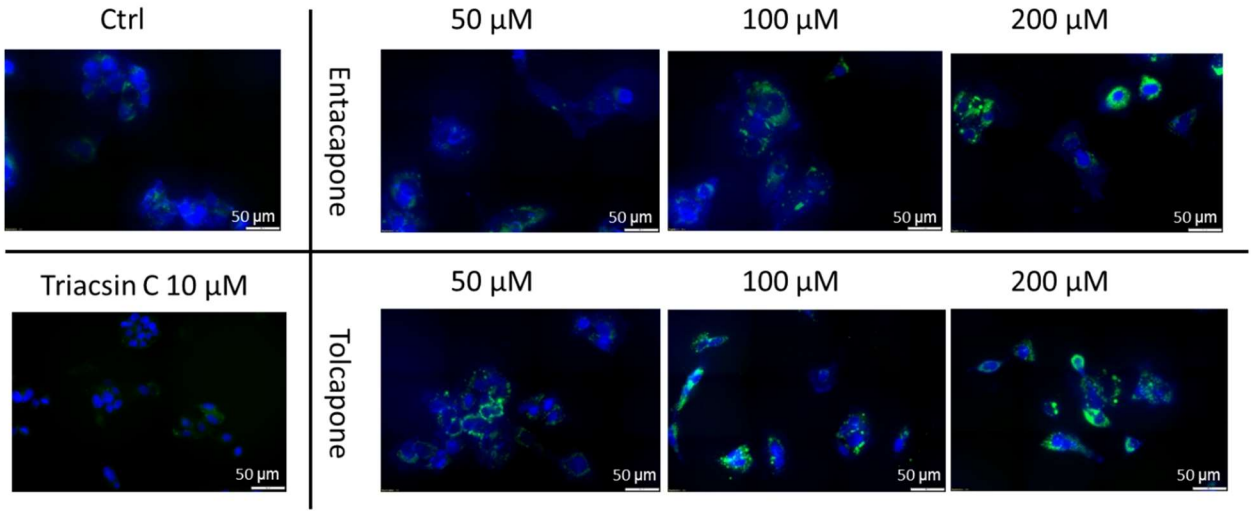

Supplementary Fig. 1.

Effect on intracellular lipid accumulation in HepG2 cells. Cells were first cultured for 24 h in a medium containing BSA-bound palmitate and oleate before treatment with the compounds of interest for 24 h. After treatment, cells were fixed, stained with DAPI for nuclei (blue) and BODYPI 493/503 for neutral lipids (green), and analyzed with fluorescence microscopy. Abbreviation: Ctrl: control (DMSO 0.1%).

Suppl. Fig. 2

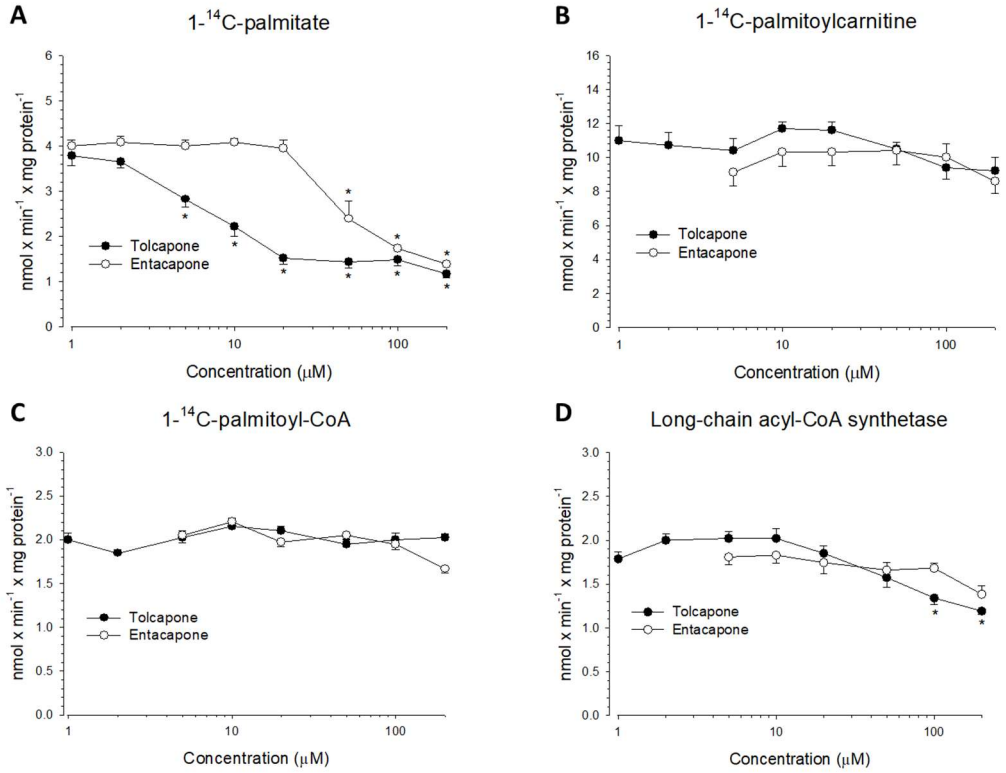

Supplementary Fig. 2

Effect of tolcapone and entacapone on fatty acid metabolism in freshly isolated mouse liver mitochondria. Mitochondria were treated with the toxicants for 10 min before determining **(A)** metabolism of ^{14}C-palmitic acid (control activity 3.85±0.2 nmol x min^{-1} x mg protein^{-1}), **(B)** ^{14}C-palmitoyl-carnitine (control activity 11.0±0.7 nmol x min^{-1} x mg protein^{-1}), **(C)** ^{14}C-palmitoyl-CoA (control activity 1.96±0.10 nmol x min^{-1} x mg protein^{-1}) and **(D)** the activity of long-chain acyl-CoA synthetase (ACSL) (control activity 1.72±0.09 nmol x min^{-1} x mg protein^{-1}). Results are presented as mean ± SEM of at least 6 independent experiments. *p<0.05 vs. DMSO 0.1% control.

Suppl. Fig. 3

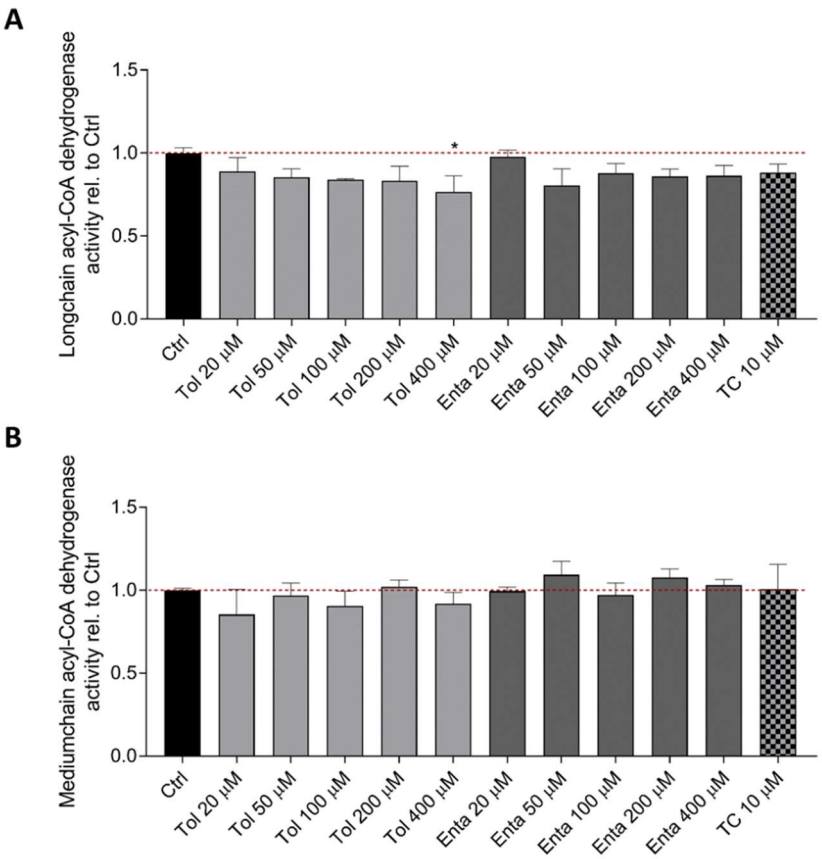

Supplementary Fig. 3.

Activities of long-chain- and medium-chain-acyl-CoA dehydrogenase in mouse liver mitochondria. Disrupted mitochondria were acutely treated for 5 min before assessing the activities of **(A)** long-chain-acyl-CoA dehydrogenase and **(B)** medium-chain-acyl-CoA dehydrogenase. Basal activities were 40.2 ± 1.4 nmol x·min^{-1} x·mg protein^{-1} for the long-chain-acyl-CoA dehydrogenase and 19.2 ± 1.1 nmol x min^{-1} x·mg protein^{-1} for the medium-chain-acyl-CoA dehydrogenase. Results were normalized to control values (DMSO 0.1%) and are presented as mean ± SEM. *$p<0.05$ vs. DMSO 0.1% control. Abbreviations: Ctrl: control (DMSO 0.1%), Tol: tolcapone, Enta: entacapone, TC: triacsin C.

Suppl. Fig. 4

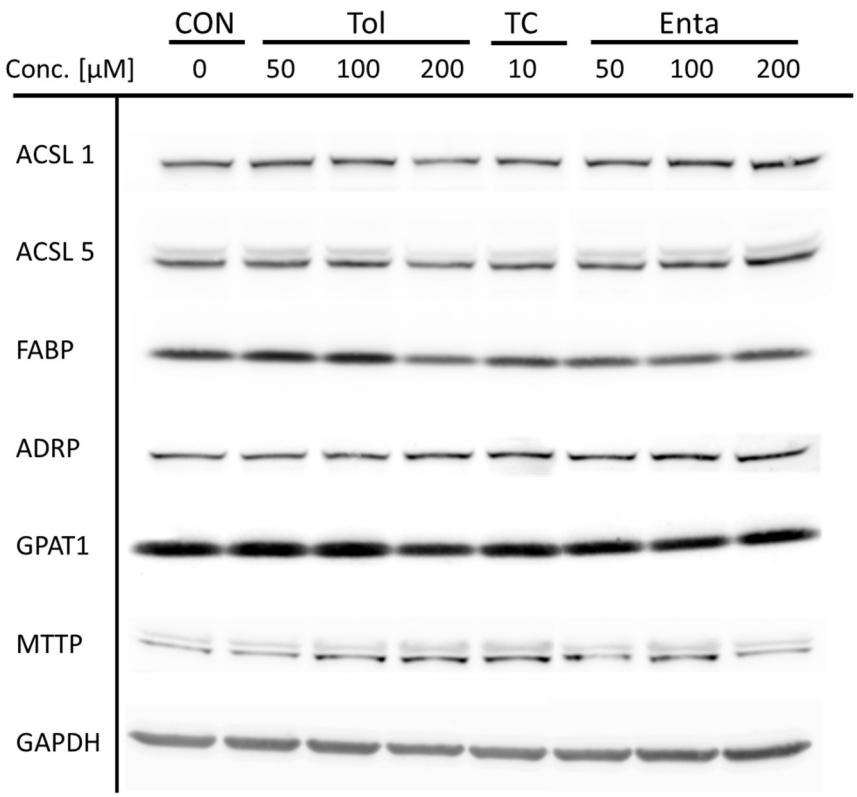

Supplementary Fig. 4.

Western blots of proteins involved I hepatic lipid metabolism. Whole cell lysates were subjected to western blot analysis as described in Methods. Shown are representative blots of the investigated proteins. Glyceraldehyde 3-phosphate dehydrogenase (GAPDH) was used for normalization and loading control. Abbreviations: CON: control (DMSO 0.1%), Tol: tolcaptone, TC: triacsin C, Enta: entacapone, ACSL: long-chain acyl-CoA synthetase, FABP: fatty acid binding protein, ADRP: adipose differentiation-related protein, GPAT1: glycerol-3-phosphate acyltransferase 1, MTTP: microsomal triglyceride transfer protein.

2.3 Paper 3

The catechol-*O*-methyltransferase inhibitors tolcapone and entacapone uncouple and inhibit the mitochondrial respiratory chain in HepaRG cells

Toxicology in Vitro 42 (2017) 337–347

Contents lists available at ScienceDirect

Toxicology in Vitro

journal homepage: www.elsevier.com/locate/toxinvit

The catechol-*O*-methyltransferase inhibitors tolcapone and entacapone uncouple and inhibit the mitochondrial respiratory chain in HepaRG cells

David Grünig[a,b,1], Andrea Felser[a,b,1], Jamal Bouitbir[a,b,c], Stephan Krähenbühl[a,b,c,*]

[a] Division of Clinical Pharmacology & Toxicology, University Hospital Basel, Switzerland
[b] Department of Biomedicine, University of Basel, Switzerland
[c] Swiss Center of Applied Human Toxicology (SCAHT), Switzerland

ARTICLE INFO

Keywords:
COMT inhibitors
Uncoupling
Electron transport chain
Apoptosis
Necrosis

ABSTRACT

The catechol-*O*-methyltransferase inhibitor tolcapone causes hepatotoxicity and mitochondrial damage in animal models. We studied the interaction of tolcapone with mitochondrial respiration in comparison to entacapone in different experimental models. In HepaRG cells (human cell-line), tolcapone decreased the ATP content (estimated IC_{50} 100 ± 15 μM) and was cytotoxic (estimated IC_{50} 333 ± 45 μM), whereas entacapone caused no cytotoxicity and no ATP depletion up to 200 μM. Cytochrome P450 induction did not increase the toxicity of the compounds. In HepaRG cells, tolcapone (not entacapone) inhibited maximal complex I- and complex II-linked oxygen consumption. In intact mouse liver mitochondria, tolcapone stimulated state 2 complex II-linked respiration and both compounds inhibited state 3 respiration of complex IV. Mitochondrial uncoupling was confirmed for both compounds by stimulation of complex I-linked respiration in the presence of oligomycin. Inhibition of complex I, II and IV for tolcapone and of complex I and IV for entacapone was directly demonstrated in disrupted mouse liver mitochondria. In HepaRG cells, tolcapone-induced inhibition of mitochondrial respiration was associated with increased lactate and ROS production and hepatocyte necrosis. In conclusion, both compounds uncouple oxidative phosphorylation and inhibit mitochondrial enzyme complexes. Tolcapone is a more potent mitochondrial toxicant than entacapone. Mitochondrial toxicity is a possible mechanism for tolcapone-associated hepatotoxicity.

1. Introduction

Catechol-*O*-methyltransferase (COMT) inhibitors are important drugs for the treatment of patients with Parkinson syndrome. While the compounds of the first generation of COMT inhibitors were too toxic to reach the market, the two second generation COMT inhibitors tolcapone and entacapone represent an effective symptomatic treatment with an acceptable toxicity profile for specific patients with Parkinson syndrome (Benabou and Waters, 2003; Haasio, 2010; Kaakkola, 2000). Both of them are therefore currently on the market in many countries.

Tolcapone and entacapone inhibit both COMT mainly in the periphery and less in the central nervous system. Both compounds have shown to prolong the time of drug effect (ON time) and to decrease the time of no drug effect (OFF time) in patients with Parkinson syndrome (Kaakkola, 2000). Both drugs are nitrocatechol compounds (see Fig. 1) with a high lipophilicity. They are rapidly and almost completely absorbed but have a limited bioavailability due to hepatic first-pass metabolism (Kaakkola, 2000). While entacapone is metabolized mainly by glucuronidation (Kaakkola, 2000), the metabolism of tolcapone is more complex. Similar to entacapone, most of tolcapone is glucuronidated and the glucuronides are eliminated by the kidney and the bile (Jorga et al., 1999). In addition, a smaller portion can be hydroxylated by cytochrome P450 (CYP) 3A4 and another portion undergoes reduction of the nitro group. The amino metabolite of tolcapone has been shown to be an electrophile which can be detoxified by glutathione (Smith et al., 2003).

Clinically, the toxicity of the COMT inhibitors is mainly characterized by increased effects dopamine such as dyskinesia, nausea, and hallucinations (Haasio, 2010; Kaakkola, 2000). Non-dopaminergic adverse reactions mainly include diarrhea and abdominal pain. Elevated transaminases, indicating hepatocellular liver injury, have been

Abbreviations: COMT, catechol-*O*-methyltransferase; CYP, cytochrome P450; DMEM, Dulbecco's Modified Eagle Medium; FBS, Fetal bovine serum; PBS, phosphate buffered saline; BCA, bicinchoninic acid; FCCP, carbonyl cyanide 4-(trifluoromethoxy) phenylhydrazone; ROS, reactive oxygen species; SOD, superoxide dismutase

* Corresponding author at: Clinical Pharmacology & Toxicology, University Hospital, 4031 Basel, Switzerland.
E-mail address: kraehenbuehl@uhbs.ch (S. Krähenbühl).

[1] Contributed equally.

http://dx.doi.org/10.1016/j.tiv.2017.05.013
Received 8 February 2017; Received in revised form 26 April 2017; Accepted 15 May 2017
Available online 16 May 2017

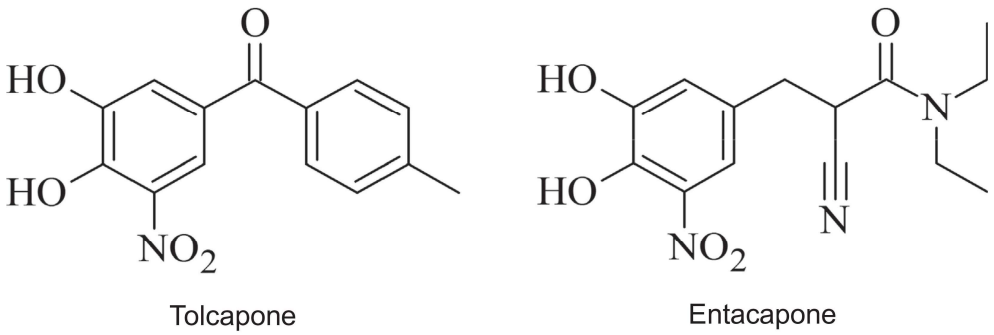

Fig. 1. Chemical structures of tolcapone and entacapone.

described in clinical studies in approximately 3% and 0.2% of patients treated with tolcapone and entacapone, respectively (Haasio, 2010; Kaakkola, 2000; Lew and Kricorian, 2007). Regarding tolcapone, hepatocellular injury is dose-dependent and normally occurs during the first six months of treatment (Olanow, 2000). Increased transaminases typically return rapidly to normal after stopping tolcapone and can also normalize when treatment is continued. Four patients with liver failure associated with tolcapone have been described, and 3 of these patients died (Olanow, 2000). In two of these patients, a liver biopsy is available. In one of them, the biopsy revealed centroacinar necrosis with an inflammatory infiltrate in the portal tracts and microvesicular steatosis in adjacent hepatocytes (Assal et al., 1998; Spahr et al., 2000). Electron microscopy of hepatocytes showed proliferation of swollen mitochondria, reduction in matrix density and loss of cristae (Borges, 2003; Spahr et al., 2000).

The electron microscopy findings suggested that tolcapone is a mitochondrial toxicant. The exact mechanism by which tolcapone damages hepatocyte mitochondria and how this is related to liver injury is currently not well understood. Previous studies have shown that tolcapone uncouples oxidative phosphorylation of liver mitochondria, leading to a drop in the mitochondrial membrane potential (Haasio et al., 2002), and to increased body temperature, weight loss, and hepatotoxicity in rats (Haasio et al., 2002; Haasio et al., 2001). Mitochondrial toxicity of tolcapone was also suggested in a capture compound mass spectrometry study, in which tolcapone interacted mostly with proteins of the mitochondrial respiratory chain and of β-oxidation (Fischer et al., 2010).

To the best of our knowledge, the functional consequences of the interaction of tolcapone with the enzyme complexes of the respiratory chain have so far not been described in detail and a comparison with the structural und functional analogue entacapone is lacking. The principle aim of the current study was therefore to investigate the interaction of tolcapone and entacapone with the function of the mitochondrial respiratory chain in HepaRG cells, a human liver cell line, and in freshly isolated mouse liver mitochondria.

2. Materials and methods

2.1. Chemicals

Entacapone was purchased from Toronto Research Chemicals Inc. (Toronto, Canada). All other chemicals were purchased from Sigma-Aldrich (Buchs, Switzerland) if not stated otherwise.

2.2. Cell culture

We used the human liver hepatocellular carcinoma cell line HepaRG, purchased from Bipredic International (Saint Grégoire, France). The cells were cultured in Dulbecco's Modified Eagle Medium (DMEM, no glutamine) supplemented with 10% FBS, 2 mM GlutaMAX, 50 µM hydrocortisone hemisuccinate, 5 µg/mL bovine insulin, and the antibiotics penicillin (100 Units/mL) and streptomycin (0.1 mg/mL). All products for cell culture were purchased from Life Technologies (Carlsbad, CA, USA). Cells were seeded at 10,000 cells per well for 96-well plates and at 300,000 for 6-well plates. They were kept at 37 °C in a humidified 5% CO_2 cell culture incubator and were passaged using trypsin. For differentiating, HepaRG cells were cultured as previously described (Guillouzo et al., 2007). For CYP induction differentiated HepaRG cells after differentiation were kept 3 days on low FBS medium (2% FBS), containing the CYP-inducers (CYP2E1: isoniazid 50 µM, CYP1A2: 3-methylcholanthrene 5 µM, CYP3A4 and others: rifampicin 20 µM) (Antherieu et al., 2010), with daily change of medium.

2.3. Cytotoxicity

We assessed cytotoxicity by the detection of adenylate kinase release, which results from the loss of cell membrane integrity. For adenylate kinase quantification, the ToxiLight assay kit (Lonza, Basel, Switzerland) was used accordingly to the manufacturer's protocol. Briefly, ToxiLight reaction buffer (100 µL) was mixed with 20 µL of supernatant from the treated cells in a new 96-well plate. After 5 min of incubation the luminescence was measured with a Tecan M200 Pro Infinity plate reader (Männedorf, Switzerland).

2.4. Intracellular ATP content

The intracellular ATP content, a marker for cell metabolic activity and viability, was determined using the CellTiter Glo kit (Promega, Madison, USA), following the manufacturers instruction. Briefly, 50 µL of assay buffer was added to each 96-well containing 50 µL culture medium. After incubation at room temperature for 15 min, luminescence was measured using a Tecan M200 Pro Infinity plate reader.

2.5. Protein content

The protein content was determined using the Pierce BCA Protein Assay Kit from Merck (Darmstadt, Germany) according to the manufacturer's manual as published earlier (Haegler et al., 2015).

2.6. Mitochondrial superoxide accumulation

We assessed mitochondrial superoxide anion production with the fluorogenic, mitochondria-specific dye MitoSOX Red reagent (Molecular Probes, Eugene, OR, USA) in a 96-well format. After drug treatment, we removed the medium and stained the cells with MitoSOX red (dissolved in Dulbecco's phosphate buffered saline (PBS) acquired from Life Technologies (Carlsbad, CA, USA), final concentration 2 µM). After 15 min of incubation at 37 °C in the dark, fluorescence was measured at 580 nm after excitation at a wavelength of 510 nm using a

Tecan Infinite pro 200 plate reader. Results were normalized to protein content.

2.7. Lactate production

Lactate concentrations in the cell culture supernatant were analyzed using an enzymatic assay (Olsen, 1971). Briefly, after drug treatment the supernatant was collected and diluted 1:1 with 6% (v/v) perchloric acid, vortexed for 5 s and centrifuged for 15 min at 16,000*g*. Lactate standards from 0 to 10 mM were prepared. 10 µL of sample was mixed with 100 µL of reagent mix containing 100 µL hydrazine buffer (6.8 mM EDTA, 100 mM hydrazine sulphate, 1 M hydrazine hydrate, pH 9) and 1 µL lactate dehydrogenase (5 mg/mL) and then incubated at room temperature for 30 min. The absorbance was measured at 340 nm using a Tecan M200 Pro Infinity plate reader.

2.8. mRNA expression

RNA was extracted and purified using the Qiagen RNeasy mini extraction kit (Qiagen, Hilden, Germany). The RNA quality was evaluated using NanoDrop 2000 (Thermo Scientific, Wohlen, Switzerland). For synthesizing cDNA from 1 µg RNA we used the Qiagen omniscript system. mRNA quantification was conducted using FastStart Universal SYBR Green Master from Roche (Basel, Switzerland) in a ViiA 7 Real Time PCR System from Applied Biosystems (Waltham, MA, USA). The relative quantity of specifically amplified cDNA was calculated using the comparative-threshold cycle method. GAPDH acted as endogenous reference and no-template and no-reverse-transcription controls ensured the absence of non-specific amplification. The primers used are listed in Supplementary Table 1.

2.9. Western blotting

After 24 h of incubation with the compounds indicated, cells were washed with ice-cold PBS and lysed with RIPA buffer (50 nM Tris-HCL, pH 7.4, 150 mM NaCl, 1% Triton X-100, 0.5% sodium deoxycholate, 0.1% sodium dodecylsulfate, and 1 mM EDTA in water) containing 1 tablet of complete Mini Protease inhibitor cocktail from Roche diagnostics (Indianapolis, USA) per 10 mL of buffer. Lysates were incubated with RIPA buffer under constant agitation for 20 min and then centrifuged at 15′700 g for 10 min at 4 °C. After determining the protein content with a Pierce BCA Protein Assay Kit, we separated 20 µg protein on 4–12% bis-tris gradient gels (Invitrogen, Carlsbad, CA, U.S.A), and transferred them to polyvinylidene difluoride membranes (Bio-rad, Hercules, CA, U.S.A) (Singh et al., 2015). To confirm uniform loading and for normalization, the GAPDH-content was used. For statistical image analysis, we used the BioImage Analysis unit Icy (v1.6.1.1) (Institute Pasteur, Paris, France), more specifically the package Fiji (fiji.sc/Fiji). Antibodies and dilutions can be found in Supplementary Table 1.

2.10. Mouse liver mitochondria

Male C57BL/6 mice were kept in the animal facility of the University Hospital Basel (Basel, Switzerland) in a temperature-controlled environment with a 12-h light/dark cycle and food and water ad libitum. Animal procedures were conducted in accordance with the institutional guidelines for the care and use of laboratory animals. Mice were sacrificed by cervical dislocation. Before the liver was removed, it was flushed with 5 mL of ice cold isolation buffer (200 mM mannitol, 50 mM sucrose, 1 mM Na_4EDTA, 20 mM HEPES, pH 7.4) and then immersed in ice-cold isolation buffer. After cutting half of the liver in small pieces it was isolated by differential centrifugation as described previously (Hoppel et al., 1979). The mitochondrial protein content was determined using the bicinchoninic acid (BCA) protein assay kit from Thermo Scientific (Wohlen, Switzerland).

2.11. Cellular oxygen consumption by HepaRG cells using the Seahorse XF24 analyzer

Cellular respiration was measured using a Seahorse XF24 analyzer (Seahorse Biosciences, North Billerica, MA, USA). HepaRG cells were seeded in Seahorse XF 24-well culture plates at 10,000 cells/well in DMEM growth medium and allowed to adhere overnight. Before the experiment, the medium was replaced with 750 µL unbuffered medium using a XF Prep Station (Seahorse Biosciences, North Billerica, MA, USA) and cells were equilibrated for 40 min at 37 °C in a CO_2-free incubator. Basal oxygen consumption was determined in the presence of glutamate and pyruvate (4 mM and 1 mM, respectively). After inhibition of mitochondrial phosphorylation by adding oligomycin (1 µM) to determine the oxidative leak, the mitochondrial electron transport chain was stimulated maximally by the addition of the uncoupler carbonyl cyanide p-(trifluoromethoxyl)-phenyl-hydrozone (FCCP, 1 µM). Finally, the extramitochondrial respiration was determined after the addition of the complex I inhibitor rotenone (1 µM). For the determination of the basal respiration, the oxidative leak and maximal respiration, extramitochondrial respiration was subtracted.

2.12. Function of the electron transport chain in HepaRG cells and in isolated liver mitochondria using high resolution respirometry

Mitochondrial respiration was measured in freshly isolated mouse liver mitochondria as well as in HepaRG cells treated with the compounds as indicated in the result section. Unless indicated otherwise, mitochondria were routinely preincubated for 15 min with the toxicants before substrates were added. We measured individual complex activities using an Oxygraph-2k high-resolution respirometer from Oroboros Instruments (Innsbruck, Austria), as described previously (Felser et al., 2013).

The activity of the enzyme complexes of the respiratory chain in HepaRG cells were determined using high resolution respirometry as described previously (Felser et al., 2013). For assessing the ability of coenzyme Q_{10} to rescue the decreased oxidation-capacity of complex I, we added increasing amounts of coenzyme Q_{10} (final concentration 1–20 µM) dissolved in DMSO at 37 °C after activating the complex using glutamate and malate (10 and 2 mM, respectively) followed by the addition of ADP (2.5 mM).

To confirm the integrity of the outer mitochondrial membrane, we showed the absence of a significant stimulatory effect of exogenous cytochrome *c* (10 µM) on respiration (maximally accepted increase of respiration < 20%).

2.13. Activity of enzyme complexes of the electron transport chain in isolated mitochondria

The individual activities of mitochondrial enzyme complexes (I–IV) were assessed by well-established spectrophotometric methods (Krahenbuhl et al., 1991; Krahenbuhl et al., 1994) in isolated mouse mitochondria, which had been kept frozen at −80 °C. Briefly, the activity of complex I was based on the conversion of NADH to NAD monitored at 340 nm using decylubiquinone as an electron acceptor. For complex II, we used succinate as a substrate and measured the conversion of oxidized dichloroindophenol to its reduced form at 600 nm. For complex III, we used decylubiquinol as a substrate and determined the conversion of ferricytochrome *c* to ferrocytochrome c at 550 nm. For complex IV we followed the conversion of ferrocytochrome c to ferricytochrome c at 550 nm. The activity of the respective enzyme complexes was determined as the difference in the presence of specific inhibitors (rotenone for complex I, thenoyltrifluoroacetone for complex II, antimycin A for complex III and sodium azide for complex IV).

2.14. Flow cytometry apoptosis

Apoptosis and necrosis were investigated using annexin V and propidium iodide (PI) staining (Invitrogen, Carlsbad, CA, U.S.A). Cells were treated with the test compounds for 24 h, then detached using trypsin-EDTA (0.25%) and, after washing with PBS, stained with 1 µL Alexa Fluor 488 annexin V and 1 µL propidium iodide 100 µg/mL in 100 µL annexin V binding buffer (10 mM HEPES, 140 mM NaCl, 2.5 mM $CaCl_2$ in H_2O, pH 7.4). Cells were incubated for 15 min at room temperature, then, after addition of 400 µL of binding buffer, they were analyzed by flow cytometry using a FACSCALIBUR (BD Biosciences, Franklin Lakes, New Jersey, U.S.). Data were analyzed using FlowJo 10.0.7 software (FlowJo LLC, Ashland, Oregon, US).

2.15. Caspases 3/7 activity

Caspase 3/7 activity was determined using the luminescent Caspase-Glo 3/7 Assay (Promega, Wallisellen, Switzerland). The assay was performed according to the manufacturer's protocol. Briefly, 100 µL assay reagent was added to each well in a 96-well plate containing the treated cells. After gentle agitation for 30 s, the plate was incubated at room temperature for 30 min. Luminescence was then measured in a Tecan M200 Pro Infinity plate reader.

2.16. Statistical methods

All results are expressed as mean ± standard deviation (SD). Statistical analysis and calculation of IC_{50} values were performed with the statistics program Prism 6 from GraphPad Software. For the calculation of the IC_{50} values Prism 6 uses a nonlinear regression model after transformation of the X-values (concentration) into the corresponding logarithms. Maximal effects (100% inhibition) were the value obtained for Triton X for AK release (cytotoxicity) and an ATP content of zero (cellular ATP content). Differences between groups were determined using one-way ANOVA followed by a Dunnett post-test. p-Values < 0.05 were considered as significant.

3. Results

3.1. Cytotoxicity and cellular ATP in HepaRG cells

To elucidate the toxic effects of tolcapone and entacapone, we first assessed cytotoxicity and cellular ATP content in HepaRG cells exposed at different concentrations for 24 h.

We found that tolcapone was cytotoxic (release of adenylate kinase) starting at 100 µM with an estimated IC_{50} of 333 µM and decreased the intracellular ATP content starting at 50 µM with an IC_{50} of 100 µM (Fig. 2A and B, Table 1). After 24 h of exposure almost all cells were dead when treated with 200 µM tolcapone. In order to find out if metabolites could be responsible for the observed cytotoxicity, we conducted cytotoxicity studies in HepaRG cells after CYP induction with rifampicin (mainly CYP3A4), isoniazid (CYP2E1) and 3-methylcholanthrene (CYP1A2) (Berger et al., 2016). Induction with isoniazid and 3-methylcholanthrene was only assessed for tolcapone and not for entacapone, since metabolism by CYP2E1 and CYP1A2 has only been demonstrated for tolcapone (Smith et al., 2003). As shown in Fig. 2A and B and as calculated in Table 1, CYP induction did not significantly increase the cytotoxicity or the effect on the cellular ATP content by tolcapone. In contrast to tolcapone, entacapone was not cytotoxic (release of adenylate kinase) under both non-induced and CYP 3A4 (treatment with rifampicin) induced conditions up to 200 µM (Fig. 2C). In addition, entacapone did not affect the cellular ATP content both under non-induced and CYP3A4-induced conditions up to 200 µM (Fig. 2D).

3.2. Effect on oxidative metabolism of HepaRG cells and of freshly isolated mouse liver mitochondria

Since the cellular ATP content of HepRG cells started to drop at clearly lower concentrations than cytotoxicity occurred (Table 1), we assumed mitochondrial toxicity for tolcapone. We therefore assessed oxidative metabolism in differentiated HepaRG cells. After treatment with tolcapone for 24 h, we observed a decrease in the presence of substrates linked to complex I (glutamate/malate) and to complex II (succinate) at 100 µM. However, we did not find any changes in the activity of complexes III (rotenone) or IV (TMPD/ascorbate) (Fig. 3A and B). The inhibitory effect of tolcapone was observable after stimulation of respiration with ADP (Fig. 3A) or after treatment with the F_0F_1-ATPase inhibitor oligomycin and uncoupling with FCCP (Fig. 3B). Exposure to 100 µM entacapone did not affect oxidative metabolism of HepaRG cells under the same conditions.

In order to investigate whether the effect on the enzyme complexes of the electron transport chain was directly associated with tolcapone or was dependent on long-term cellular reactions, we exposed freshly isolated mouse liver mitochondria acutely with 100 µM tolcapone and compared the findings to 100 µM entacapone. Under these conditions, both compounds decreased state 3 activity in the presence of complex I-linked substrates, but without reaching statistical significance (Fig. 3C). Moreover, tolcapone as well as entacapone significantly inhibited complex IV activity of the electron transport chain (Fig. 3D) but did not affect the activity of the other enzyme complexes. Both tolcapone and entocapone stimulated oxygen consumption in the presence of glutamate/malate (Fig. 3C) and succinate (Fig. 3D) before the addition of ADP (state 2 or leak state respiration), reaching statistical significance for tolcapone in the presence of succinate.

3.3. Effect on uncoupling of oxidative phosphorylation

Increased leak state respiration in the presence of tolcapone or entacapone suggested uncoupling of the respiratory chain. The uncoupling effect was not visible in the presence of ATP, probably because, as suggested by the results obtained in HepaRG cells, the inhibition of the electron transport chain was dominating under these conditions.

In order to further explore the interaction of tolcapone and entacapone with the respiratory chain, we assessed the concentration dependency of the effect of tolcapone and entacapone on phosphorylating mitochondria (state 3 condition) and on mitochondria in the presence of ADP and the F_0F_1-ATPase inhibitor oligomycin with glutamate/malate as substrates. Neither tolcapone nor entacapone significantly affected respiration in ADP-stimulated (state 3 condition) mitochondria (Fig. 4A). On the other hand, when phosphorylation was inhibited by oligomycin, uncoupling of the respiration could be observed with both compounds in a concentration-dependent manner, starting to be significant at 50 µM (Fig. 4B).

In a second step, we also assessed the time dependency of the inhibitory effect of tolcapone on oxidative metabolism of freshly isolated mouse liver mitochondria. As shown in Fig. 4C, the addition of tolcapone to mitochondria metabolizing glutamate/malate (state 2) increased oxygen consumption, indicating uncoupling. This increase was less, however, when mitochondria had been preincubated with tolcapone for 15 min before addition of the glutamate/malate, suggesting a combination of inhibition of the electron transport chain and uncoupling. Addition of ADP had no significant effect on respiration in tolcapone-preincubated mitochondria, but significantly increased oxygen consumption in incubations with immediate addition of tolcapone. A second addition of tolcapone to these incubations decreased oxidation rates (not reaching statistical significance). Cytochrome c was added to check the integrity of the mitochondria.

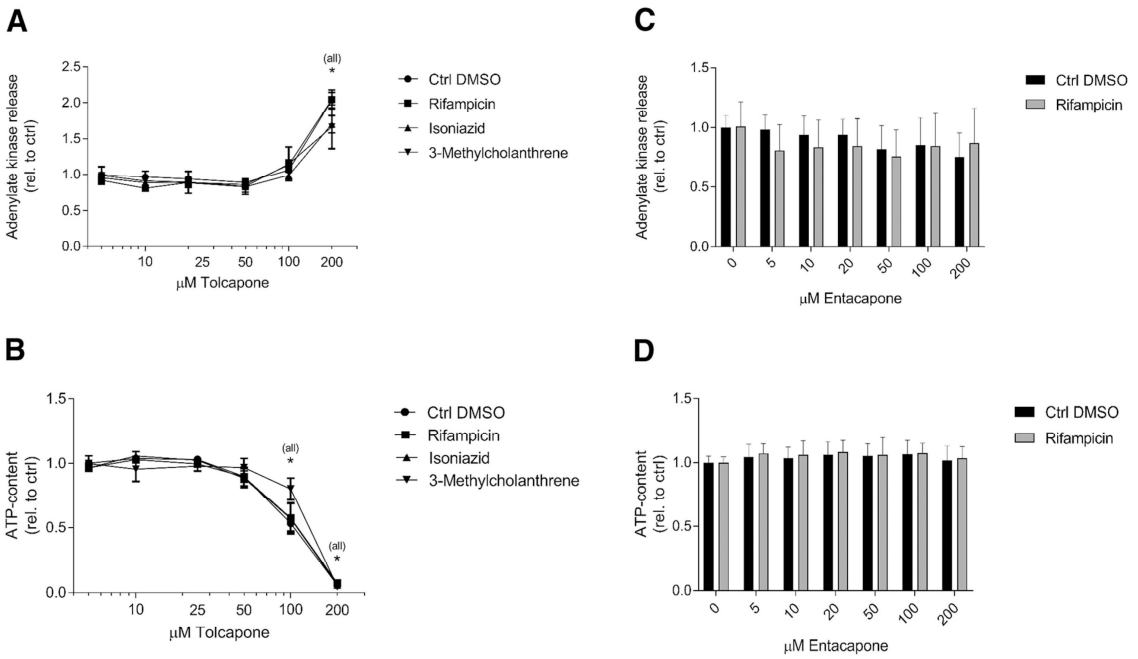

Fig. 2. Cytotoxicity and effect on intracellular ATP content. Cytotoxicity and intracellular ATP were assessed after drug exposure for 24 h in differentiated HepaRG cells (control) and in HepaRG cells pre-treated with rifampicin (induction of CYP3A4), isoniazid (induction of CYP2E1) or 3-methylcholanthrene (induction of CYP1A2). For CYP induction, differentiated HepaRG cells were treated for 72 h (rifampicin, isoniazid) or 24 h (3-methylcholanthrene) with the respective inducers before treatment with tolcapone or entacapone. (A) Cytotoxicity associated with tolcapone after exposure for 24 h. (B) Intracellular ATP content after exposure to tolcapone for 24 h. (C) Cytotoxicity associated with entacapone after exposure for 24 h. (D) Intracellular ATP content after treatment with entacapone for 24 h. Triton X was used as a positive control. Data are expressed as fold change (cytotoxicity) or remaining fraction (ATP) relative to DMSO 0.1% control (Ctrl DMSO) cells. Data are presented as mean ± SD of four independent experiments. Differences versus control values were determined using one-way ANOVA followed by a Dunnett post-test. *$p < 0.05$ vs. Ctrl DMSO 0.1%. The term (all) in Fig. 2B indicates that all groups at this concentration are different from the respective control values.

Table 1
IC_{50} values [µM] of tolcapone and entacapone calculated based on the experiments shown in Fig. 2A–D. 100% ATP content was defined as the ATP content in the absence of tolcapone or entacapone and 100% cytotoxicity as the AK activity in the cell supernatant after treatment with Triton X 0.2%. IC_{50} values were calculated using Prism 6 from at least 3 independent experiments and are presented as mean ± SD. N.d. not determined.

Inducer	Tolcapone		Entacapone	
	ATP	AK release	ATP	AK release
None (control)	100 ± 15	333 ± 45	> 200	> 200
Rifampicin	106 ± 14	406 ± 53	> 200	> 200
Isoniazid	104 ± 15	362 ± 52	n.d.	n.d.
3-Methylcholanthrene	123 ± 18	305 ± 44	n.d.	n.d.

3.4. Effect on activity of enzyme complexes of the electron transport chain in disrupted mouse liver mitochondria

In order to be able to measure the activities of the enzyme complexes of the electron transport chain without interference of uncoupling, we used established spectrophotometric methods in previously frozen mitochondria. The freezing process ruptures membranes and thus abolishes the functional integrity of the mitochondria, eliminating the possibility of building a transmembrane proton gradient and therefore uncoupling, but without affecting the activity of the individual enzyme complexes.

Under these conditions, tolcapone significantly and dose-dependently decreased activity of complex I, complex II and complex IV starting at 100 µM (Fig. 5A, B and D), but not of complex III (Fig. 5C). In comparison, entacapone did not affect complex II and III (Fig. 5B and C), but inhibited significantly the activity of complex I and IV at 200 µM and 100 µM, respectively (Fig. 5A and D).

3.5. Effect of coenzyme Q_{10} on the function of the electron transport chain

The enzyme complexes I and II transfer electrons from the electron-donors NADH and FADH, respectively, to coenzyme Q. Because the activity of complexes I and II were impaired by tolcapone, we hypothesized that tolcapone may interfere with the electron transfer, possibly by competing with coenzyme Q for electron uptake. In order to assess the ability of exogenous coenzyme Q_{10} to counteract the inhibitory effect of tolcapone on mitochondrial respiration, we investigated the effect of increasing concentrations of coenzyme Q_{10} on mitochondria preincubated with 100 µM tolcapone (Fig. 6). In control incubations not containing tolcapone, coenzyme Q_{10} did not significantly affect oxygen uptake. Compared to control incubations, tolcapone added 15 min before glutamate/malate inhibited mitochondrial respiration under state 3 conditions (in the presence of ADP). This inhibition could not be reversed by the addition of coenzyme Q_{10}, suggesting that the inhibition of the activity of complexes I and II by tolcapone was not caused by interaction with endogenous coenzyme Q.

3.6. Consequences of the inhibition of the electron transport chain

Inhibition of the electron transport chain is expected to be associated with increased glycolysis (Felser et al., 2013) and, in particular in the case of impaired activity of complex I and/or III (Balaban et al., 2005), with increased ROS production.

Accordingly, treatment with tolcapone induced a concentration-dependent lactate accumulation starting at 50 µM in HepaRG cells, indicating that cells are forced to switch to glycolysis and confirming that the mitochondrial electron transport chain is inhibited (Fig. 7A). In comparison, entacapone (up to 200 µM) did not increase the formation of lactate.

As complexes I and III of the electron transport chain are the main

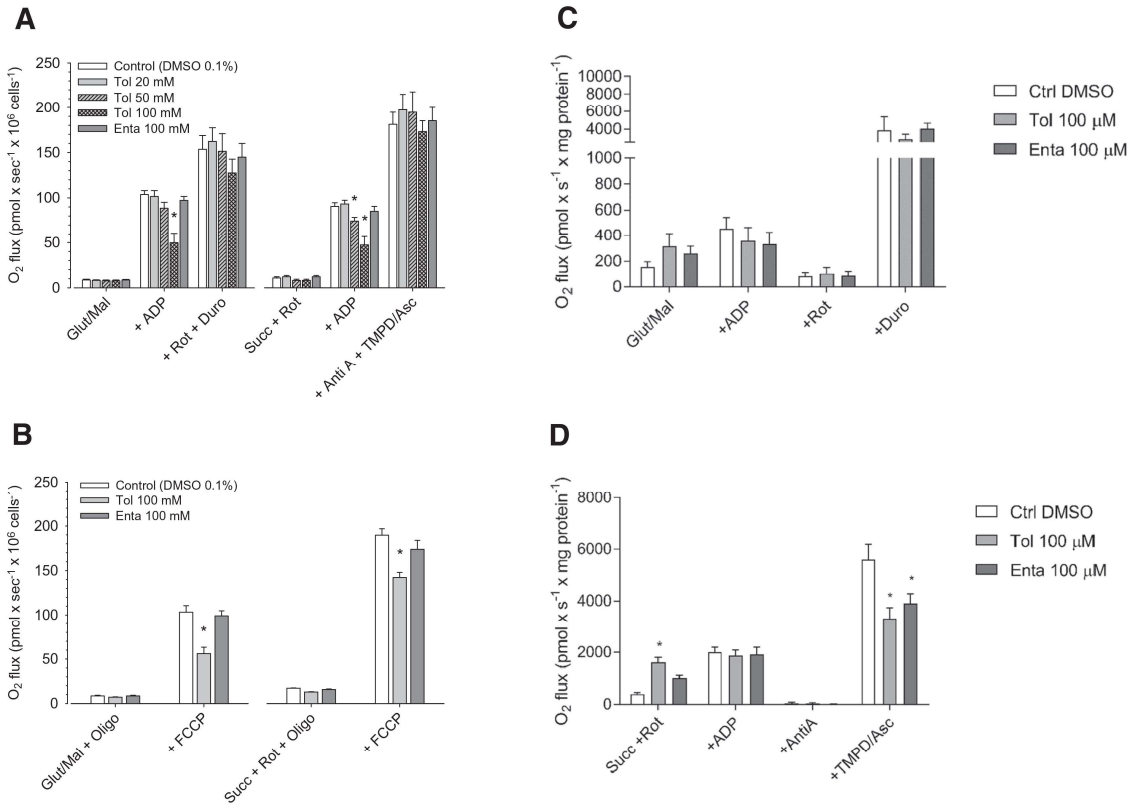

Fig. 3. Long-term and acute and effect of tolcapone and entacapone on oxidative metabolism in HepaRG cells and isolated mouse liver mitochondria. (A and B) HepaRG cells treated for 24 h with the compounds were permeabilized using digitonin, and oxygen consumption was measured using the Seahorse XF24 analyzer after addition of specific substrates and inhibitors of the enzyme complexes of the mitochondrial respiratory chain. (C and D) Freshly isolated mouse liver mitochondria were pretreated for 15 min with the drugs followed by determination oxygen consumption using high resolution respirometry after the addition of specific substrates and inhibitors of the complexes of the mitochondrial respiratory chain. Ctrl: control (DMSO 0.1%), Enta: entacapone, Tol: tolcapone, Glut/mal: glutamate/malate, Succ: succinate, Rot: rotenone, Duro: duroquinol, TMPD/Asc: tetramethyl-*p*-phenylenediamine/ascorbate, oligo: oligomycin, FCCP: Carbonyl cyanide 4-(trifluoromethoxy) phenylhydrazone. Differences versus control values were determined using one-way ANOVA followed by a Dunnett post-test. Data represent the mean ± SD of four independent experiments. *p < 0.05 versus control.

sites of mitochondrial superoxide anion generation (Balaban et al., 2005), we examined the accumulation of superoxide anion in HepaRG cells exposed to tolcapone and entacapone for 24 h. Exposure to tolcapone, which inhibited complex I, was associated with mitochondrial accumulation of superoxide anion, starting at 50 µM. In comparison, entacapone did not increase mitochondrial accumulation of superoxide anion (Fig. 7B).

As shown in Fig. 7C and D, treatment with tolcapone was associated with a concentration-dependent decrease in the mRNA expression of mitochondrial superoxide dismutase 1 (SOD1) and SOD2, reaching statistical significance at 200 µM. In contrast, treatment with entacapone did not significantly influence the mRNA expression of SOD1 and SOD2 up to 200 µM. A similar result was obtained for the mRNA expression of Nrf2 (Supplementary Fig. 1A). On the protein level, neither tolcapone nor entacapone affected the expression of SOD2 (Supplementary Fig. 1B), possibly because the exposure time (24 h) was too short.

3.7. Mechanisms of cell death in HepaRG cells

In order to investigate the mechanism of cell death, we measured externalization of phosphatidylserine (PS) using annexin V staining as a marker of apoptosis as well as staining of exposed nuclei by propidium iodine as a marker of late apoptosis/necrosis. As shown in Fig. 8A, entacapone, which was non-cytotoxic up to 200 µM (Fig. 2C), did not increase the number of apoptotic or necrotic cells. In comparison, tolcapone was associated with a minor (but statistically significant) increase in early apoptotic cells at 100 µM. At 200 µM, the number of early apoptotic cells did not exceed control values, but there was a 60% increase in late apoptotic and/or necrotic cells.

In order to further investigate the mechanisms of cell death associated with tolcapone, we assessed the activities of caspase 3 and 7. As shown in Fig. 8B, tolcapone inhibited caspase 3/7 activities, suggesting that apoptosis was not the responsible mechanism of cell death. In comparison, entacapone did not significantly affect the activities of caspase 3/7. These results were confirmed by investigating the cleavage of procaspase 3 (Fig. 8C). Neither entacapone nor tolcapone increased the cleavage of procaspase 3, whereas the positive control amiodarone was associated with increased production of cleaved caspase 3. Under the conditions investigated in the current study, tolcapone therefore caused cell death mainly by necrosis, not by apoptosis.

4. Discussion

In the current study, we showed that both tolcapone and entacapone inhibited several enzyme complexes of the electron transport chain after acute and long-term exposure and increase mitochondrial production of reactive oxygen species. We also showed that both compounds uncoupled oxidative phosphorylation of liver mitochondria. Tolcapone was a more potent toxicant than entacapone, eventually resulting in an increase in cellular lactate production, depletion of cellular ATP and hepatocyte necrosis.

The uncoupling effect of tolcapone has already been described in

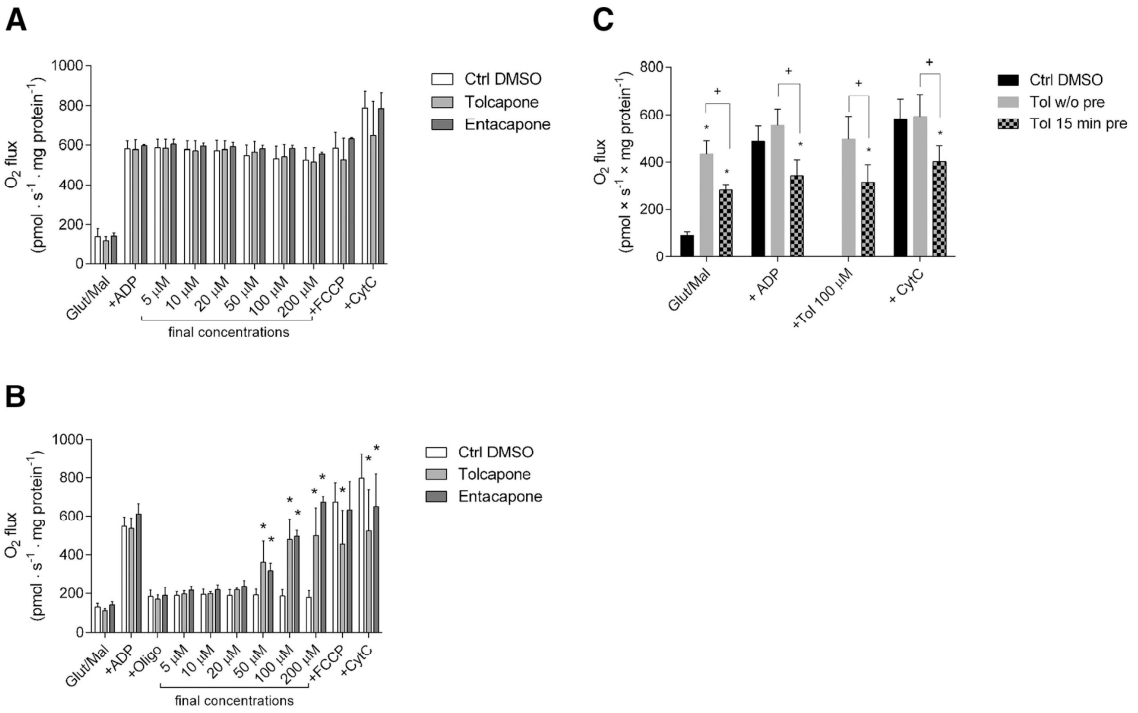

Fig. 4. Differentiation between uncoupling of oxidative phosphorylation and inhibition of the enzyme complexes of the electron transport chain by tolcapone in freshly isolated mouse liver mitochondria. Glutamate and malate were used as substrates for all incubations and oxidative metabolism was assessed by high resolution respirometry. (A) Acute effect of entacapone and tolcapone on state 3 respiration. (B) Effect of tolcapone and entacapone on leak respiration in the presence of oligomycin in order to inhibit ATP production. (C) Effect of pre-incubation with tolcapone for 15 min on state 2 and state 3 oxidation. Glut/Mal: glutamate and malate, Oligo: oligomycin, FCCP: Carbonyl cyanide 4-(trifluoromethoxy) phenylhydrazone, CytC: cytochrome c. Tol w/o pre: Oxidative metabolism was assessed immediately after the addition of tolcapone. Tol 15 min pre: Cells were preincubated for 15 min with tolcapone before assessing oxidative metabolism. Differences versus control values (Fig. 4A and B) and between the groups (Fig. 4C) were determined using one-way-ANOVA followed by a Dunnett post-test. Data are presented as mean ± SD of four independent experiments. *$p < 0.05$ vs. Control DMSO 0.1%, $^{+}p < 0.05$ vs. pre-incubation.

previous studies in vitro and in vivo (Haasio et al., 2002; Haasio et al., 2002). In the current study, the effect was not demonstrable in HepaRG cells exposed for 24 h, but could clearly be shown in isolated liver mitochondria exposed acutely to the toxicants. Since the uncoupling effect was present acutely after exposure of liver mitochondria, the uncoupling activity of tolcapone and entacapone depended most likely on the physicochemical properties of these compounds and was not a consequence of long-term effects such as increased expression of uncoupling proteins. It is important to realize that the incubation medium containing the toxicants was removed from HepaRG cells before the determination of oxygen consumption and that the cells were incubated in a suitable buffer not containing the toxicants. Cells were then permeabilized in order to render them accessible for the substrates and, as a consequence, allowing the toxicants to leave the cells. It can therefore be assumed that mitochondria in HepaRG cells were exposed to only low concentrations of the toxicants during the experiments assessing the electron transport chain. This contrasted with situation for isolated mitochondria, which were constantly exposed to the toxicant concentration indicated in the experiments. Both tolcapone and entacapone are weak acids with structural similarities to the well-established uncoupler dinitrophenol, suggesting that they can act as protonophores (McLaughlin and Dilger, 1980). Alternatively, as lipophilic substances, they may accumulate in the inner mitochondrial membrane and increase the permeability for protons (Sun and Garlid, 1992).

Considering the inhibition of the enzyme complexes of the electron transport chain, the situation appears to be different. The current study provides evidence that both tolcapone and entacapone inhibited the electron transport chain acutely; in disrupted mitochondria exposed to the toxicants, tolcapone inhibited complex I, II and IV and entacapone complex I and IV. On the other hand, after exposure of HepaRG cells for 24 h, only tolcapone inhibited complex I and II of the electron transport chain, whereas no inhibition was detectable for entacapone. Since coenzyme Q10 is important for the transport of electrons from complex I or II to complex III, inhibition of complexes I and II by tolcapone could have been due to interference with coenzyme Q10. We could exclude this possibility by adding exogenous coenzyme Q_{10} to mitochondria exposed to tolcapone, which did not attenuate the inhibition of complex I.

The current study does not answer the question how tolcapone and entacapone inhibited complexes I and II (and also complex IV by tolcapone) of the electron transport chain. Fischer et al. (Fischer et al., 2010) demonstrated the formation of adducts of tolcapone (or tolcapone metabolites) to protein subunits of complexes of the electron transport chain, which may be associated with inhibition of the electron transport chain. Taking into account that tolcapone was not immediately toxic but preincubation of the mitochondria with tolcapone was needed to achieve inhibition of the electron transport chain, this mechanism could explain the findings of the current study. In addition, it is possible that protein oxidation due to mitochondrial ROS accumulation may have impaired the function of mitochondrial proteins.

In order to be able to separate mitochondrial uncoupling from the inhibition of enzyme complexes of the electron transport chain, we examined the activity of enzyme complexes in disrupted mitochondria which cannot form a proton gradient. Using freshly isolated, intact mouse liver mitochondria, the inhibition of complexes I and II by tolcapone and entacapone could not be demonstrated, because the mitochondrial uncoupling and inhibition of the electron transport chain occurred at approximately the same concentrations. Similar findings have been reported previously for benzbromarone (Kaufmann et al., 2005) and for non-steroidal antiinflammatory drugs (Mahmud et al., 1996).

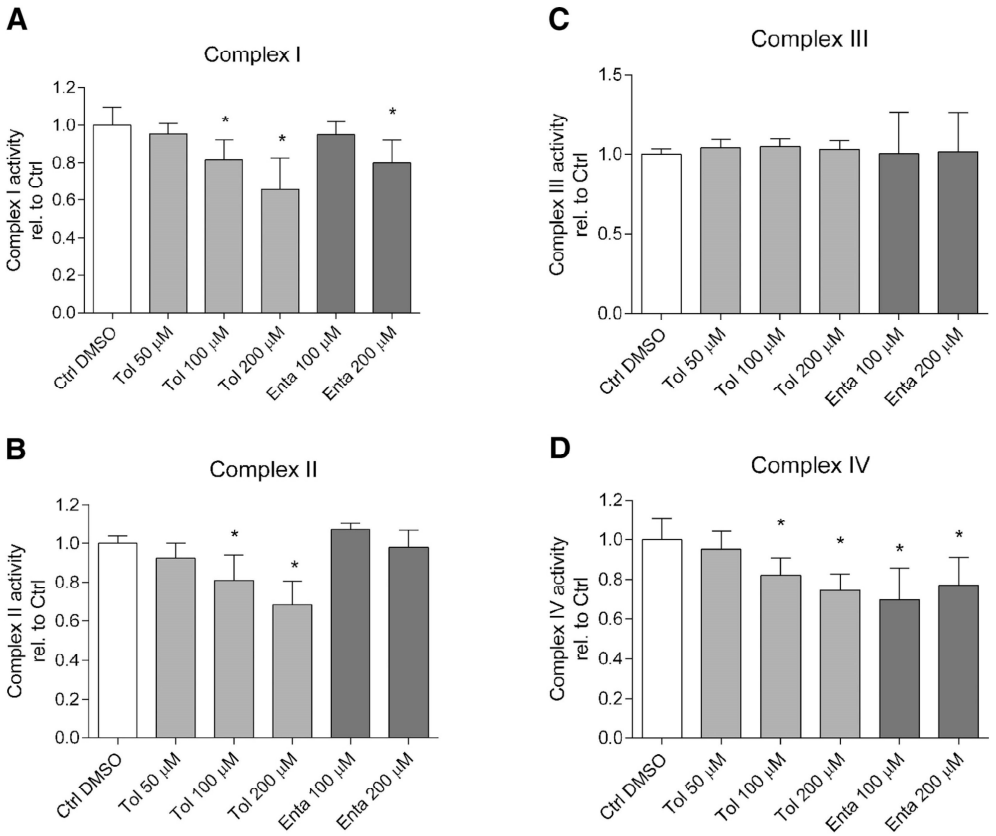

Fig. 5. Effect of tolcapone (Tol) and entacapone (Enta) on the activity of the enzyme complexes of the electron transport chain in frozen mouse liver mitochondria. Complex activities were determined using established spectrophotometric methods in frozen and re-thawed mouse liver mitochondria. Control activities (0.1% DMSO) for complex I, II, III, and IV were 41 ± 2.2, 51 ± 4.2, 86 ± 5.9, and 271 ± 12 nmol × min^{-1} × mg $protein^{-1}$ (mean ± SD), respectively. Differences versus control values were determined using one-way-ANOVA followed by a Dunnett post-test. Data are expressed as fold change to DMSO 0.1% control and are presented as mean ± SD of three independent experiments. *$p < 0.05$ versus control.

In a recent publication, tolcapone decreased the ATP content in HepG2 cells only in the presence of galactose, not of glucose (Kamalian et al., 2015) and was not cytotoxic under these conditions. This suggests that tolcapone's impairment of mitochondrial ATP production may be related to inhibition of enzyme complexes of the electron transport chain and to uncoupling of oxidative phosphorylation as shown in the current study. In the study of Kamalian et al. (Kamalian et al., 2015), entacapone was not cytotoxic and decreased the ATP content in HepG2 cells in the presence of galactose only at a concentration of 1 mM. In the current study, entacapone impaired mitochondrial functions (uncoupling, impairment of enzyme complexes of the electron transport chain) already at lower concentrations, but did not decrease the cellular ATP content and was not cytotoxic. While our results were qualitatively comparable, HepaRG cells appear to be more sensitive to entacapone than HepG2 cells.

Consequences of a significant inhibition of the electron transport chain are mainly increased glycolysis to maintain the cellular ATP content, increased mitochondrial production of ROS with oxidative

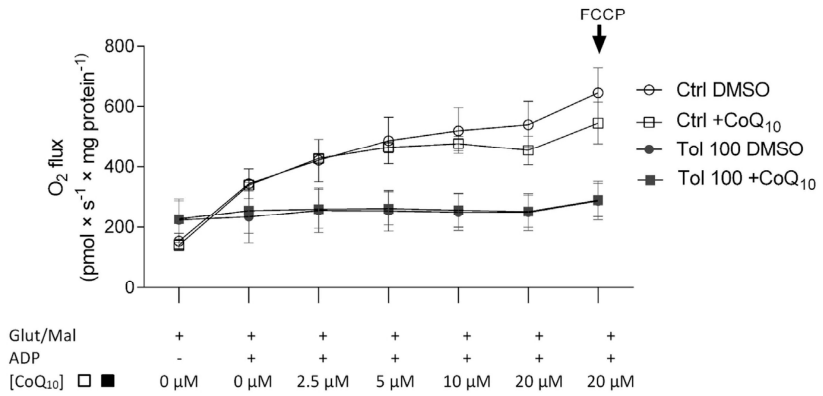

Fig. 6. Effect of coenzyme Q_{10} in freshly isolated mouse liver mitochondria on the inhibition of mitochondrial respiration by tolcapone in the presence of glutamate/malate/ADP. After 15 min of pretreatment with 100 µM tolcapone (Tol 100) or 0.1% DMSO (Ctrl), glutamate/malate and ADP were added followed by increasing amounts of coenzyme Q_{10} or 0.1% DMSO. Q_{10} concentrations represent final concentrations. Data represent the mean ± SD of three independent experiments.

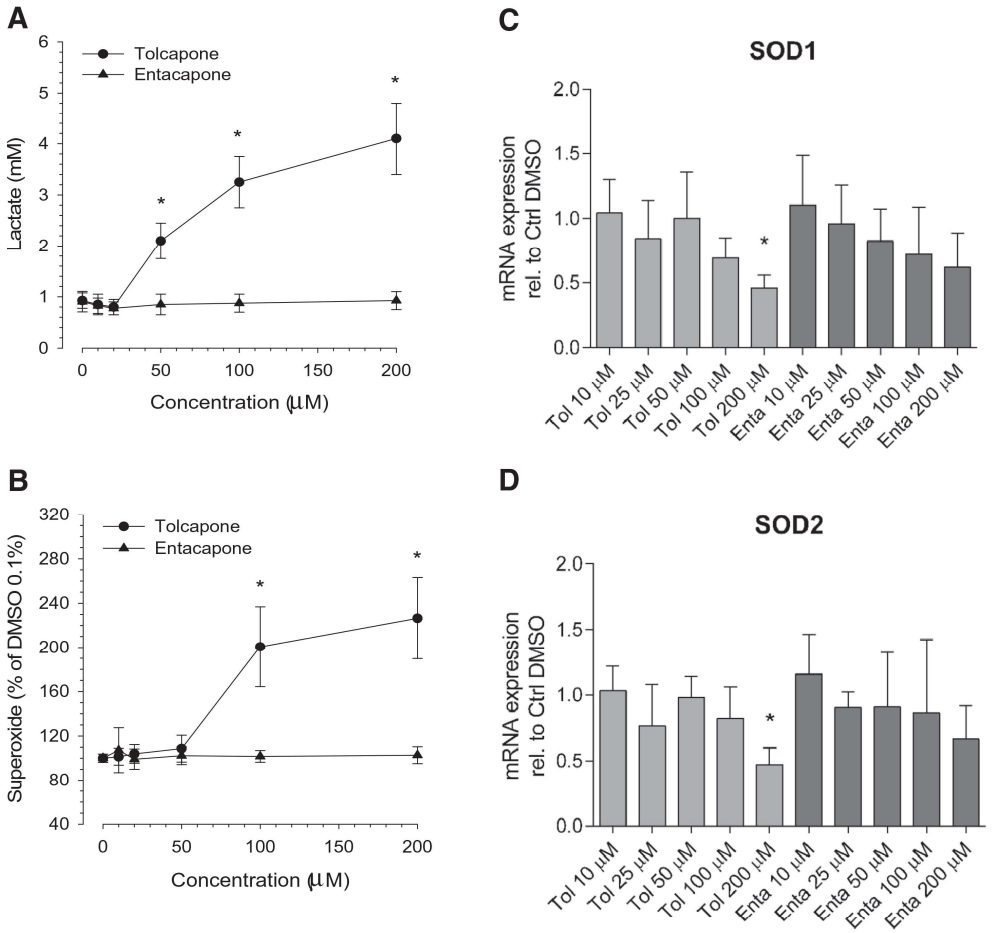

Fig. 7. Metabolic consequences of mitochondrial dysfunction in HepaRG cells treated with tolcapone or entacapone for 24 h. (A) Lactate production, (B) mitochondrial production of superoxide, (C) mRNA expression of superoxide dismutase 1 (SOD1) and (D) mRNA expression of SOD2. Numbers after T (tolcapone) and E (entacapone) in Fig. 7C and D reflect concentrations in µM. Data are presented as mean ± SD of three independent experiments. Differences versus control values were determined using one-way-ANOVA followed by a Dunnett post-test. *$p < 0.05$ versus control incubations containing 0.1% DMSO.

damage to proteins, lipids and mtDNA and mitochondrial membrane permeabilization, leading to a drop in the mitochondrial membrane potential and to hepatocyte apoptosis and/or necrosis (Felser et al., 2013; Kaufmann et al., 2005). Although both tolcapone and entacapone inhibited enzyme complexes of the electron transport chain (tolcapone complexes I, II and IV and entacapone complexes I and II), increased lactate production, production of ROS and necrosis were only observed for tolcapone, but not for entacapone. The current study demonstrates that tolcapone was a stronger inhibitor of the electron transport chain activity than entacapone at equal concentrations, which is compatible with the findings described above. In line with this statement, tolcapone, but not entacapone, was associated hepatocyte necrosis at 200 µM. These findings are in agreement with the cellular ATP content, which had dropped by 50% at 100 µM and to basically 0 at 200 µM tolcapone. Apoptosis has been shown to be dependent on ATP (Dorn, 2013; Eguchi et al., 1997) and does not occur in the absence of ATP. This contrasts with necrosis which does not rely on the cellular ATP content.

In clinical investigations, maximal plasma concentrations attained following the single oral administration of 200 mg entacapone or 200 mg tolcapone (the usually ingested single doses) were approximately 10 µM and 20 µM, respectively (Kaakkola, 2000). Assuming that the hepatic concentrations correspond approximately to the plasma concentrations, the concentration of entacapone and tolcapone would be below the minimal toxic concentration associated with the uncoupling and/or inhibition of the electron transport chain for entacapone (100 µM) and tolcapone (50 µM). Considering the extensive first-pass metabolism of the compounds, the hepatic concentration may be higher, however, than the plasma concentration after oral ingestion.

Regarding entacapone, the low frequency of clinically relevant hepatotoxicity in humans may be explained by the fact that the hepatic exposure is too low after a single dose 200 mg and that, as shown in the current study, entacapone is less toxic to mitochondria than tolcapone at the same concentration. Hepatotoxicity associated with tolcapone has been described to be dose-dependent, and to occur in only approximately 3% of patients when the recommended doses are not exceeded (Haasio, 2010; Kaakkola, 2000). Patients affected at therapeutic doses may therefore have susceptibility factors, which, taking into account the mechanism of toxicity, may be factors associated with mitochondrial dysfunction. Similar findings have been reported for other drugs with mitochondrial toxicity, e.g. valproate. Severe liver disease with valproate has been associated with mutations in the DNA polymerase-γ (Stewart et al., 2010), which is responsible for mitochondrial DNA synthesis.

In conclusion, both tolcapone and entacapone uncouple oxidative phosphorylation and inhibit enzyme complexes of the respiratory chain. At similar concentrations, tolcapone exhibits a more pronounced mitochondrial toxicity, resulting in increased lactate and ROS production, ATP depletion and hepatocyte apoptosis and necrosis. The more pronounced clinical hepatotoxicity of tolcapone compared to entaca-

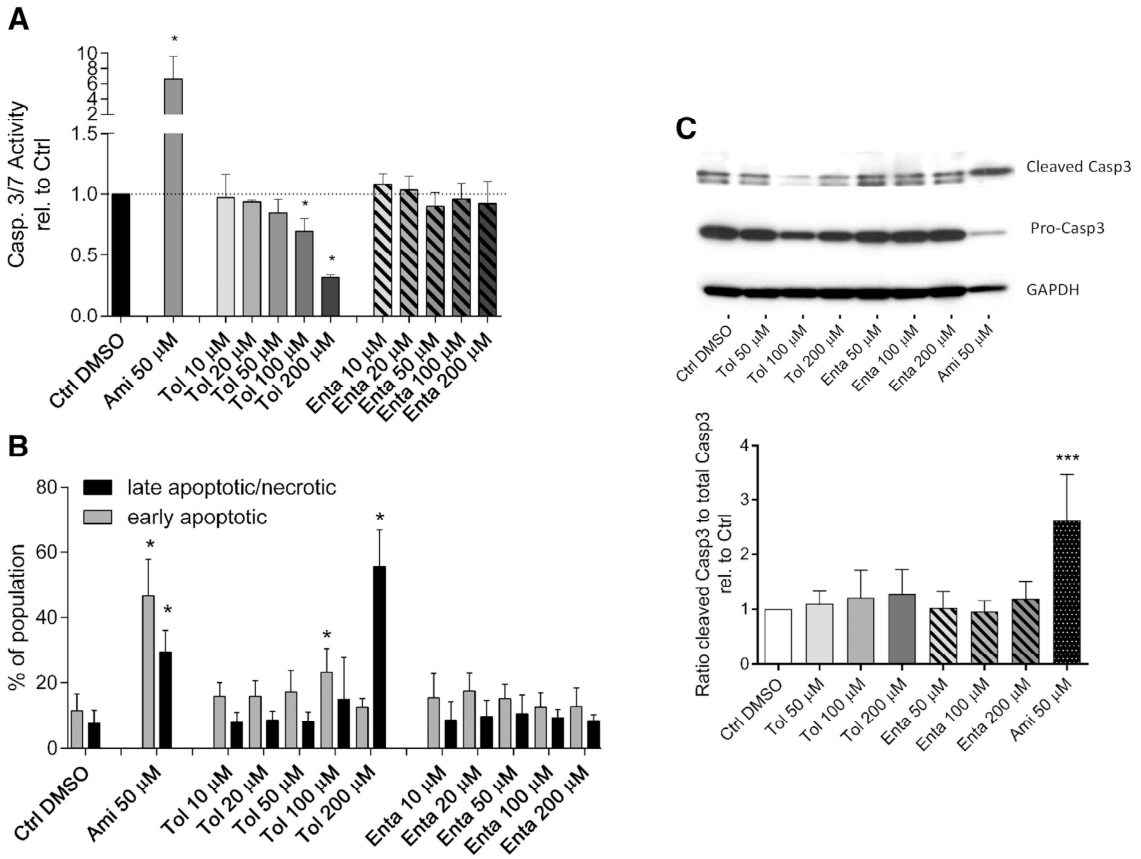

Fig. 8. Mechanisms of cell death associated with tolcapone (Tol) and entacapone (Enta). (A) Activity of caspase (casp) 3/7 in HepaRG cells treated with the drugs for 24 h. Amiodarone (Ami) was used as a positive control. Data are given relative to control (Ctrl DMSO) values. (B) Annexin V binding and PI uptake by HepaRG cells exposed to the drugs for 24 h and analyzed using flow cytometry. Early apoptotic populations are stained with annexin V only, late apoptotic and/or necrotic cells are positive for PI. Amiodarone was used as a positive control for apoptosis. Data are presented as a percentage of the total cell count. (C) Ratio of cleaved (active) to pro-caspase 3 (inactive) expressed relative to control incubations containing 0.1% DMSO determined by western blotting. Amiodarone was used as positive control for caspase 3 cleavage. Data present the mean ± SD of at last three independent experiments. *p < 0.05 versus control DMSO.

pone can be explained by higher systemic exposure levels at maximal single doses and by a higher intrinsic mitochondrial toxicity.

Supplementary data to this article can be found online at http://dx.doi.org/10.1016/j.tiv.2017.05.013.

Financial support

This study was supported by a grant from the Swiss National Science Foundation to SK (SNF 31003A-132992).

Conflict of interest statement

None of the authors reports any conflict of interest regarding the paper.

Transparency document

The http://dx.doi.org/10.1016/j.tiv.2017.05.013 associated with this article can be found, in online version.

References

Anthérieu, S., Chesne, C., Li, R., Camus, S., Lahoz, A., Picazo, L., Turpeinen, M., Tolonen, A., Uusitalo, J., Guguen-Guillouzo, C., Guillouzo, A., 2010. Stable expression, activity, and inducibility of cytochromes P450 in differentiated HepaRG cells. Drug Metab. Dispos. 38, 516–525.

Assal, F., Spahr, L., Hadengue, A., Rubbia-Brandt, L., Burkhard, P.R., 1998. Tolcapone and fulminant hepatitis. Lancet 352, 958.

Balaban, R.S., Nemoto, S., Finkel, T., 2005. Mitochondria, oxidants, and aging. Cell 120, 483–495.

Benabou, R., Waters, C., 2003. Hepatotoxic profile of catechol-*O*-methyltransferase inhibitors in Parkinson's disease. Expert Opin. Drug Saf. 2, 263–267.

Berger, B., Donzelli, M., Maseneni, S., Boess, F., Roth, A., Krahenbuhl, S., Haschke, M., 2016. Comparison of liver cell models using the basel phenotyping cocktail. Front. Pharmacol. 7, 443.

Borges, N., 2003. Tolcapone-related liver dysfunction: implications for use in Parkinson's disease therapy. Drug Saf. 26, 743–747.

Dorn 2nd, G.W., 2013. Molecular mechanisms that differentiate apoptosis from programmed necrosis. Toxicol. Pathol. 41, 227–234.

Eguchi, Y., Shimizu, S., Tsujimoto, Y., 1997. Intracellular ATP levels determine cell death fate by apoptosis or necrosis. Cancer Res. 57, 1835–1840.

Felser, A., Blum, K., Lindinger, P.W., Bouitbir, J., Krahenbuhl, S., 2013. Mechanisms of hepatocellular toxicity associated with dronedarone–a comparison to amiodarone. Toxicol. Sci. 131, 480–490.

Fischer, J.J., Michaelis, S., Schrey, A.K., Graebner, O.G., Glinski, M., Dreger, M., Kroll, F., Koester, H., 2010. Capture compound mass spectrometry sheds light on the molecular mechanisms of liver toxicity of two Parkinson drugs. Toxicol. Sci. 113, 243–253.

Guillouzo, A., Corlu, A., Aninat, C., Glaise, D., Morel, F., Guguen-Guillouzo, C., 2007. The human hepatoma HepaRG cells: a highly differentiated model for studies of liver metabolism and toxicity of xenobiotics. Chem. Biol. Interact. 168, 66–73.

Haasio, K., 2010. Toxicology and safety of COMT inhibitors. Int. Rev. Neurobiol. 95, 163–189.

Haasio, K., Sopanen, L., Vaalavirta, L., Linden, I.B., Heinonen, E.H., 2001. Comparative toxicological study on the hepatic safety of entacapone and tolcapone in the rat. J. Neural. Transm. (Vienna) 108, 79–91.

Haasio, K., Koponen, A., Penttila, K.E., Nissinen, E., 2002a. Effects of entacapone and tolcapone on mitochondrial membrane potential. Eur. J. Pharmacol. 453, 21–26.

Haasio, K., Nissinen, E., Sopanen, L., Heinonen, E.H., 2002b. Different toxicological profile of two COMT inhibitors in vivo: the role of uncoupling effects. J. Neural. Transm. (Vienna) 109, 1391–1401.

Haegler, P., Grünig, D., Berger, B., Krähenbühl, S., Bouitbir, J., 2015. Impaired

mitochondrial function in HepG2 cells treated with hydroxy-cobalamin[c-lactam]: a cell model for idiosyncratic toxicity. Toxicology 336, 48–58.
Hoppel, C., DiMarco, J.P., Tandler, B., 1979. Riboflavin and rat hepatic cell structure and function. Mitochondrial oxidative metabolism in deficiency states. J. Biol. Chem. 254, 4164–4170.
Jorga, K., Fotteler, B., Heizmann, P., Gasser, R., 1999. Metabolism and excretion of tolcapone, a novel inhibitor of catechol-O-methyltransferase. Br. J. Clin. Pharmacol. 48, 513–520.
Kaakkola, S., 2000. Clinical pharmacology, therapeutic use and potential of COMT inhibitors in Parkinson's disease. Drugs 59, 1233–1250.
Kamalian, L., Chadwick, A.E., Bayliss, M., French, N.S., Monshouwer, M., Snoeys, J., Park, B.K., 2015. The utility of HepG2 cells to identify direct mitochondrial dysfunction in the absence of cell death. Toxicol. in Vitro 29, 732–740.
Kaufmann, P., Torok, M., Hanni, A., Roberts, P., Gasser, R., Krahenbuhl, S., 2005. Mechanisms of benzarone and benzbromarone-induced hepatic toxicity. Hepatology 41, 925–935.
Krahenbuhl, S., Chang, M., Brass, E.P., Hoppel, C.L., 1991. Decreased activities of ubiquinol:ferricytochrome c oxidoreductase (complex III) and ferrocytochrome c:oxygen oxidoreductase (complex IV) in liver mitochondria from rats with hydroxycobalamin[c-lactam]-induced methylmalonic aciduria. J. Biol. Chem. 266, 20998–21003.
Krahenbuhl, S., Talos, C., Wiesmann, U., Hoppel, C.L., 1994. Development and evaluation of a spectrophotometric assay for complex III in isolated mitochondria, tissues and fibroblasts from rats and humans. Clin. Chim. Acta 230, 177–187.
Lew, M.F., Kricorian, G., 2007. Results from a 2-year centralized tolcapone liver enzyme monitoring program. Clin. Neuropharmacol. 30, 281–286.
Mahmud, T., Rafi, S.S., Scott, D.L., Wrigglesworth, J.M., Bjarnason, I., 1996. Nonsteroidal antiinflammatory drugs and uncoupling of mitochondrial oxidative phosphorylation. Arthritis Rheum. 39, 1998–2003.
McLaughlin, S.G., Dilger, J.P., 1980. Transport of protons across membranes by weak acids. Physiol. Rev. 60, 825–863.
Olanow, C.W., 2000. Tolcapone and hepatotoxic effects. Tasmar advisory panel. Arch. Neurol. 57, 263–267.
Olsen, C., 1971. An enzymatic fluorimetric micromethod for the determination of acetoacetate, β-hydroxybutyrate, pyruvate and lactate. Clin. Chim. Acta 33, 293–300.
Singh, F., Charles, A.L., Schlagowski, A.I., Bouitbir, J., Bonifacio, A., Piquard, F., Krahenbuhl, S., Geny, B., Zoll, J., 2015. Reductive stress impairs myoblasts mitochondrial function and triggers mitochondrial hormesis. Biochim. Biophys. Acta 1853, 1574–1585.
Smith, K.S., Smith, P.L., Heady, T.N., Trugman, J.M., Harman, W.D., Macdonald, T.L., 2003. In vitro metabolism of tolcapone to reactive intermediates: relevance to tolcapone liver toxicity. Chem. Res. Toxicol. 16, 123–128.
Spahr, L., Rubbia-Brandt, L., Burkhard, P.R., Assal, F., Hadengue, A., 2000. Tolcapone-related fulminant hepatitis: electron microscopy shows mitochondrial alterations. Dig. Dis. Sci. 45, 1881–1884.
Stewart, J.D., Horvath, R., Baruffini, E., Ferrero, I., Bulst, S., Watkins, P.B., Fontana, R.J., Day, C.P., Chinnery, P.F., 2010. Polymerase gamma gene POLG determines the risk of sodium valproate-induced liver toxicity. Hepatology 52, 1791–1796.
Sun, X., Garlid, K.D., 1992. On the mechanism by which bupivacaine conducts protons across the membranes of mitochondria and liposomes. J. Biol. Chem. 267, 19147–19154.

Supplementary data

The catechol-O-methyltransferase inhibitors tolcapone and entacapone uncouple and inhibit the mitochondrial respiratory chain in HepaRG cells

Running title: Mitochondrial toxicity of COMT inhibitors

[1,2]Andrea Felser*, [1,2]David Grünig*, [1,2,3]Jamal Bouitbir, [1,2,3]Stephan Krähenbühl

*contributed equally

[1]Division of Clinical Pharmacology & Toxicology, University Hospital Basel, Switzerland;

[2]Department of Biomedicine, University of Basel, Switzerland;

[3]Swiss Center of Applied Human Toxicology (SCAHT)

Correspondence

Stephan Krähenbühl, MD, PhD

Clinical Pharmacology & Toxicology

University Hospital

4031 Basel

Switzerland

Phone: +41 61 265 4715

Fax: +41 61 265 4560

E-mail: kraehenbuehl@uhbs.ch

Table

Supplementary Table 1

The following primers were used for mRNA quantification:

GAPDH	fwd: 5'-AGCCACATCGCTCAGACA-3'
	rev: 5'-GCCCAATACGACCAAATC-3'
SOD1	fwd: 5′-TGGCCGATGTGTCTATTGAA-3′
	rev: 5′-ACCTTTGCCCAAGTCATCTG-3′
SOD2	fwd: 5′-GGTTGTTCACGTAGGCCG-3′
	rev: 5′-CAGCAGGCAGCTGGCT-3′
NRF2	fwd: 5'-AGCCCAGCACATCCAGTCAG-3'
	rev: 5'-TGCATGCAGTCATCAAAGTACAAAG-3'

Suppl. Fig. 1

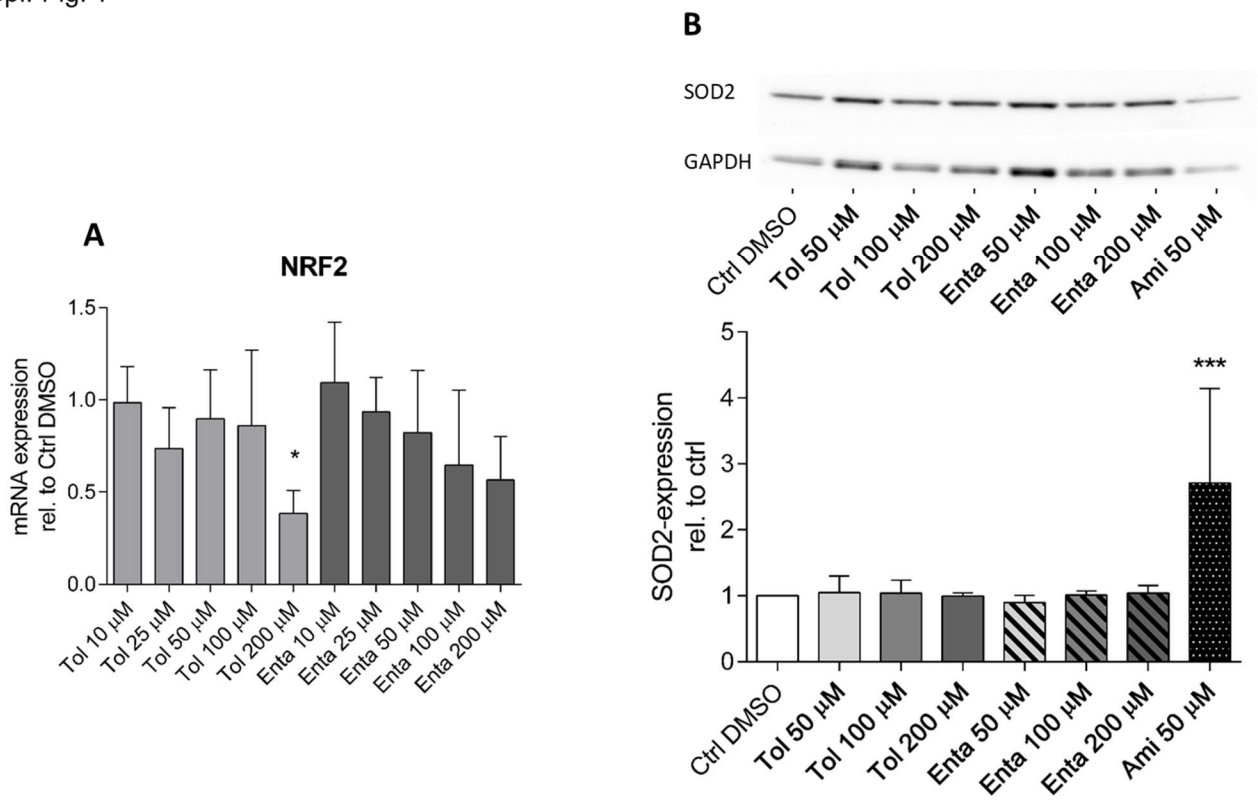

3. DISCUSSION

Drug-induced adverse reactions are not only agonizing for patients but also challenging for clinicians. Adverse reactions, aside from monetary consequences for the healthcare system, also represent a crucial challenge to the industry in the success of bringing and maintaining a drug on the market. DILI is the main reason for drug withdrawal from the market [215] and is, especially in the case of idiosyncratic reactions, rarely detected in preclinical or even clinical development [124]. Additional to withdrawal, marketed drugs can also receive black box warnings or restricted use assignments. An improved preclinical detectability of such adverse reactions would therefore be highly appreciated in the industry.

The low incidence of idiosyncratic DILI, coupled with unpredictability and the incomplete understanding of various mechanisms of action, documents the need of additional investigations on this topic. In recent years, research has shown that DILI is not only dependent on the drug itself, but also on several environmental and host factors [108]. Particularly, preexisting or acquired mitochondrial predispositions have increasingly been identified as susceptibility factor for the development of idiosyncratic adverse reactions [216].

With our newly established method for the measurement of changes in FA metabolism by analyzing the acylcarnitine pattern, we aimed to provide a sensitive biomarker to improve the detection and investigation of drug-induced hepatic steatosis.

3.1 Acylcarnitine Measurement

Liquid chromatography-tandem mass spectrometry (LC-MS/MS) is a highly sensitive method for the specific analysis of multiple compounds in one sample. The analysis of acylcarnitines for the investigation of FA metabolism has been used since many years [217]. Relying on radioenzymatic assays at first, it was promptly adopted in clinics for the diagnosis of organic acidurias and FA oxidation defects after development of respective LC-MS/MS methods [218]. Nowadays, most countries adopted the measurement of medium-chain acylcarnitines in the routine-screening of newborns, in order to test for MCAD deficiency [219].

Since acylcarnitines are known to reflect the cellular acyl-CoA pattern [64], we aimed to use the identification of altered acylcarnitine profiles to make interpretations based on specific intermediate metabolites. In Paper 1, we included C2-, C4-, C5-, C6-, C8-, C10-, C12-, C14-, C16 carnitines in our LC-MS/MS method, giving us insight into chain-length specificity of FA oxidation inhibition. Furthermore, we included a specific intermediary metabolite, 3-oxo palmitoyl-CoA, in order to get information about the last step of β-oxidation.

To develop and simultaneously test the method, we included three well specified inhibitors of FA oxidation. For the most part, we found anticipated changes, showing nicely the applicability of this effective method.

This is nicely visible by the intense increase of medium-, but not long-chain acylcarnitines after treatment with MCPA, a strong MCAD inhibitor. The rise of medium-chain acylcarnitines is well known in patients lacking a functional MCAD [220,221]. Furthermore, acetylcarnitine, as well as long-chain acylcarnitines were significantly suppressed by MCPA, indicating the lack of substrate for the β-oxidation of short-chain FAs. For the cell, acetyl-CoA is not only important for anabolic reactions, but is also a central messenger for the fine tuning of energy metabolism and can be interpreted as part of the overall energy-status of the cell [222]. Since part of the acetyl-CoA pool is constantly converted to acetylcarnitine [223], the cellular content thereof could also be understood in this way.

Interestingly, however, the decline in acetylcarnitine was not reflected in the intracellular ATP content. This could be explained by the fact that the cells are grown in culture medium, containing 5.5 mM glucose, and therefore able to compensate deficient energy production by acetyl-CoA usage, by an increase in the use of glucose. This effect can be caused by the depletion of cytosolic acetyl-CoA, which activates AMPK, and thereby stimulates katabolic reactions, such as stimulation of glycolysis [222,224].

In the case of etomoxir-induced changes, we observed a decrease in C8- to C16 acylcarnitines in the supernatant, with normal levels of acylcarnitines shorter than C6. This pattern was expected, due to the inability of the cell to convert activated long-chain FAs into acylcarnitines as a result of CPT1 inhibition. Indeed, there is also an acyltransferase form present, which is not associated with mitochondria, the carnitine-octanoyl transferase (COT). This microsomal- and peroxisomal-associated enzyme, although having a preference for medium-chain acyl-CoAs, is also able to transfer long-chain acyl-CoAs to carnitine. Studies by Lilly et al. showed that etomoxiryl-CoA also reversibly inhibits COT, however, at 100 times the concentration it needs for CPT1 inhibition [165].

Triacsin C induced similar changes to the acylcarnitine profile of treated cells as etomoxir. The suppression of all acylcarnitines, but acetyl- and C4-acylcarnitines, can be explained through a similar mechanism as the one of etomoxir. When FAs cannot be activated to the CoA-form, it is impossible for carnitine acyltransferases to interact with them, thus leading to a decreased overall content of acylcarnitines. Since there are up to 26 isoforms of acetyl-CoA synthetases, with eleven of them responsible for medium-chain and long-chain FA activation [39], it also seems comprehensible that acylcarnitines were less suppressed than in etomoxir-treated cells, as triacsin C reportedly only inhibits certain isoforms, and not the whole activation process [180].

Treatment with 4-bromocrotonic acid led to a somewhat unexpected acylcarnitine pattern. The 3-oxo-palmitoylcarnitine accumulation was induced, as expected from long-chain 3-ketothiolase inhibition. However, we also found an accumulation of C5- and C4-carnitines. This suggests that 4-bromocrotonic acid is not specific for the long-chain form of the β-ketothiolases, but that it also inhibits the short-chain form (acetoacetyl-CoA thiolase). This effect could be deduced from the structure of this compound, as it has the same form as butanoyl-CoA (C4-CoA), with an additional bromine at the fourth carbon. Furthermore, 4-bromocrotonic acid first has to be hydroxylated and then dehydrogenated to 4-bromo-3hydroxybutanoic acid

and 4-bromo-3oxobutanoic acid, respectively, to finally yield the form, which is responsible for the inhibition of the thiolases [172,173] . As these conversions are carried out by enzymes of the β-oxidation chain, namely enoyl-CoA hydratase and 3-hydroxy acyl-CoA dehydrogenase, it would be plausible that 4-bromocrotonic acid also could inhibit at these steps. Studies on isolated enzymes by Olowe and Schulz, however, found no inhibitory activity on the 3-hydroxyacyl CoA-dehydrogenase and only a minor (8%) inhibition of the long-chain enoyl-CoA hydratase with concentrations of 4-bromocrotonic acid, which inhibited 100% of both short- and long-chain 3-ketothiolases [173]. Taken together, these findings are in agreement with our interpretation of the acylcarnitine pattern and the conclusion that 4-bromocrotonic acid inhibits both forms of mitochondrial acyl-CoA thiolases.

Regarding these four model compounds, the established LC-MS/MS method proved to supply valuable and discriminative information on the location of inhibition. Furthermore, the method repeatedly turned out to be a more sensitive approach to identify drugs inhibiting FA oxidation.

Of the ten compounds, on which this method was applied, the acylcarnitine method proved to show significant findings at lower concentrations in half of the cases (tamoxifen, WIN55, tolcapone, entacapone, and valproic acid). For two compounds (MCPA and amiodarone) the method was equally sensitive as the radioenzymatic assay and for two (etomoxir and triacsin C) the tested concentrations did not allow to make this comparison. Only 4-bromocrotonic acid was more potent in β-oxidation inhibition studies, using isolated mitochondria, than in producing significant changes in the acylcarnitine pattern. The LC-MS/MS method, however, was still more sensitive than the determination of 4-bromocrotonic acid-induced inhibition of β-oxidation in cells. In all cases, measurement of β-oxidation inhibition by radioenzymatic- or acylcarnitine determinations was more sensitive than lipid accumulation results.

As stated above, it is of desire for the pharmaceutical industry to have tools, which can predict drug-induced hepatic steatosis during preclinical development. Indeed, several steatogenic drug candidates could be identified preclinically in animal models [225]. However, considering the high costs of animal studies, as well as the "three R" principle, new *in vitro* systems are of high interest. Additionally, *in vitro* systems can be applied in high-throughput screenings, allowing for the testing of large numbers of drug candidates.

In light of the multiple hit theory, there are four basic pathways in which a "hit" has to occur for the development of hepatic steatosis, which is uptake, degradation, synthesis, or excretion. Since all these pathways are very complex and underlie various regulatory and compensatory factors, tests, which give more information of what exactly is affected, would be of advantage. The acylcarnitine profile measurement, obviously, is only focused on the breakdown of FAs.

Since many years, information about the FA-breakdown capacity of cells or tissues is acquired using radioenzymatic assays [226-228]. By incubation with radioactive-labelled FAs and subsequent measurement of radioactive products by liquid scintillation, this method allows for precise and quantitative results of the oxidation capacity of nearly every tissue or cells. The assay can also be adapted to various situations by using

differently labelled FAs or FA-metabolites. One can for example supply ^{14}C-palmitate to investigate general β-oxidation capacity. By using ^{14}C-palmitoylcarnitine, the activation step, as well as the influence of CPT1 are omitted. By using ^{14}C-octanoate, results will give information about enzymes with medium-chain specificity. Also the location of the label can influence the outcome of results. ^{14}C-label on the position C-16 allows for the measurement of complete oxidation of the FA, while label on the C-1 position is more readily available, only showing the first cycle of oxidation. Today, this type of assay is still the standard method to show inhibition of β-oxidation [229].

The drawbacks, however, of these well-established and popular assays are obvious. First of all, although relatively safe, ^{14}C is radioactive and requires special safety conditions, such as special allocated working spaces and waste management [230]. Furthermore, radio-labelled substrates are considerably more expensive than their "normal" counterparts. Especially, when in need of different substrates for the evaluation of different single-reaction steps, or partial reactions, this can be of significance.

With the determination of the acylcarnitine-pattern by LC-MS/MS several of these drawbacks are avoided. The acylcarnitine method presented in this thesis is not only considerably cheaper per sample, but also safer and much faster. Since the assay was optimized for the use in 96-well format, it uses a limited amount of cells, and therefore cell culture products, as well as less amount of drugs for treatment. Also the sample workup is fast and uncomplicated, as the method was developed without derivatization processes, which are often needed in other protocols [231-233]. But most importantly, the acylcarnitine-profile gives information about several aspects of FA breakdown within one measurement, compared to the radioenzymatic assays. This LC-MS/MS method, however, cannot always replace the determinations with radioactive-labelled substrates, as it is only semi-quantitative. An additional advantage of the acylcarnitine measurement is that it only needs a small amount of supernatant, leaving cells, as well as remaining supernatant available for separate investigations. This makes it possible to link several assays together with the use of only one 96-well plate.

To this date, a limited, but slowly increasing number of quantifiable *in vitro* models of steatosis for the use of early screening of potential pharmaceuticals have been proposed [109,225,234]. All of them rely on the colorimetric or fluorescent detection of intracellular lipids within treated hepatocytes. Most of these systems use HepG2 cells for the testing and quantification of lipids, which is done with either Nile red [235], Oil red O [236], or BODIPY493/503 [147,237] staining. The fluorescent dye BODIPY proofed to be the most sensitive for the detection of lipid accumulation in these studies.

Taking these considerations together, the acylcarnitine-profile analysis seems to be highly suitable for the application in research and industry for a detailed assessment of drug-induced FA-oxidation defects.

3.2 Mechanisms of Hepatic Steatosis

The main goal of this thesis was the elucidation of steatogenic mechanisms exerted by the drugs of interest. Regarding the compounds, which were chosen for the mechanistic investigations, all of them showed dose-dependent lipid accumulation in our *in vitro* models, providing first and important evidence and demonstrating the principle usability of the models.

Concerning the model inhibitors discussed above, we did not find induction of steatosis with etomoxir nor with MCPA treatment. This was surprising at first, as these compounds are strong and irreversible inhibitors of β-oxidation, and were also applied on cells in concentrations much higher than their EC_{50} values for FA oxidation inhibition. This finding, however, is in line with the multiple hit hypothesis of steatosis-induction, which states that multiple factors are necessary for the induction of excess LD formation. In our studies, triacsin C even reduced lipid accumulation, determined by flow cytometry and fluorescence microscopy. These findings were less surprising, as triacsin C is reportedly inhibiting acyl-CoA synthetases mainly involved in lipogenesis [181]. Dechandt et al. made similar findings, showing triacsin C to reduce LD formation in rat hepatocytes [238]. Importantly, these findings mean that impairment of hepatic FA metabolism can be missed, if LD accumulation is used as the only assay of FA metabolism.

Of the model compounds, only 4-bromocrotonic acid showed accumulation of neutral lipids in treated cells. Since our data consistently supported the multiple hit theory, it seems obvious that 4-bromocrotonic acid is exerting an additional pro-steatogenic effect to its irreversible inhibition of β-oxidation. Explanation thereof could be taken from studies by the group of Jim Fong with 4-bromocrotonic treated adipocytes. They found an increase in glucose uptake, as well as inhibition of hormone-sensitive lipase, after treatment with the compound. Both mechanisms are reportedly independent from FA-oxidation inhibition [239,240]. They argue that the active metabolite of 4-bromocrotonic acid, 3-keto-4-bromobutyryl-CoA, is accumulating within mitochondria, and through either conversion into its carnitine derivate (by the mitochondrial carnitine acetyltransferase) and subsequent translocation by the carnitine shuttle, or by diffusion of the free acid (formed by short-chain acyl-CoA hydrolase), it reaches the cytosolic compartment, where it inhibits the lipase. The hormone-sensitive lipase is also expressed in hepatocytes, where it contributes to lipolysis, which is carried out on the surface of LDs [241]. The steatogenic effect of 4-bromocrotonic acid in hepatocytes could therefore be attributed to β-oxidation inhibition coupled with decreased breakdown of stored TGs.

3.3.1 Mechanisms of Amiodarone

Amiodarone is a well-known hepatotoxic compound with high steatogenic potential in patients. Since its introduction it has been extensively studied on its adverse reactions on the liver. Accumulation in liver tissue [242], as well as in mitochondria [243], due to its high lipophilicity, leads to multiple toxic responses in cells. This toxicity is attributed to the benzofuran moiety of the molecule [244].

Amiodarone is a strong inhibitor of FA oxidation, leading to microvesicular steatosis [245] . It was shown to decrease the activities of CPT1 and long-chain acyl-CoA dehydrogenase [187,243,244]. Furthermore, it is also a known mitochondrial uncoupler, as well as an inhibitor of Complex I and II [243,244], which aggravates the effects of β-oxidation inhibition. As inhibition of the ETC, especially at Complex I, leads to increased accumulation of ROS, toxicity of accumulating FAs may be further enhanced through the formation of lipid peroxidation products. In fact, increased lipid peroxidation is a reported consequence of amiodarone treatment [246].

The acylcarnitine pattern of amiodarone-treated cells showed a dose-dependent decrease in medium-chain to long-chain acylcarnitines (C6-C14), with only a small decrease in palmitoyl-carnitine. CPT1 inhibition, however, should yield significant lower levels of palmitoyl-carnitine, as apparent in etomoxir-treated cells. This could be explained by the inhibition of long-chain acyl-CoA dehydrogenase by amiodarone, leading to a less pronounced decrease of this long-chain variant due to limited accumulation of palmitoyl-CoA. In our studies, contrary to an earlier study [187], we also observed inhibition of MCAD, which should result in higher content of medium-chain acylcarnitines. Since C6 – C14 acylcarnitines were decreased, it appears that CPT1 inhibition, decreasing all long- and medium-chain acylcarnitines, is of greater influence on the pattern of acylcarnitines than the downstream inhibition of MCAD.

In a study in mice treated with amiodarone, it was found that amiodarone inhibits the activity of MTTP [247], leading to a decreased VLDL export of the liver, with corresponding lower TG concentration in the serum. In our study, we also found a decrease in VLDL export in HepG2 cells, which was, however, not significant.

An additional mechanism of amiodarone augmented hepatic steatosis, reported in literature, is the upregulation of many lipogenic genes [248], explained in part by the triple PPARα/β/γ agonism of amiodarone [249].

Lastly, we also found a decrease in thapsic acid formation in cells treated with amiodarone. Thapsic acid represents an intermediate in the peroxisomal breakdown of palmitic acid by ω-oxidation, which can be used by the cell as alternative pathway, if mitochondrial breakdown is disturbed [40]. This inhibition is not surprising, as FAs are metabolized to dicarboxylic acid by the CYP4A and 4F family, and amiodarone and its metabolites are known inhibitors of multiple other CYPs [188].

Altogether, the adverse effects of amiodarone presented from research show remarkably consistently a conclusive picture of multiple impacts of the drug on the development of hepatic steatosis.

3.3.2 Mechanisms of Tamoxifen

We found tamoxifen to induce lipid accumulation in HepG2 cells, like it is seen in 43% of patients as hepatocellular steatosis within the first two years of treatment [194]. It inhibited dose-dependently the β-oxidation of the cells, at the location of CPT1. This can also be seen in the pattern of acylcarnitines, where acetyl-carnitine and C6 – C16 acylcarnitines were decreased, consistent with the inhibition of mitochondrial FA

import. Measurements of intracellular acyl-CoAs in MCF7 cells (mammary epithelium cells) also revealed decreased content of a medium chain acyl-CoA, however, with additional increase in C16-CoA. The study, however, showed no effect on acetyl-CoA levels [250], while slightly reduced acetyl-CoA levels were observed in the liver of tamoxifen treated rats [251]. In addition to β-oxidation inhibition, we also found tamoxifen to decrease ω-oxidation, as thapsic acid formation was inhibited. Lastly, further increasing lipid accumulation, also VLDL export was decreased by tamoxifen treatment.

The few *in vitro* studies on tamoxifen consent on one mechanism leading to steatosis of the cells used, namely increased FA and TG synthesis, mediated by the transcription factor SREPB-1c [250,252-254]. Furthermore, in one of the studies, it was found that tamoxifen increases glycolysis and inhibits Complex I [250].

The majority of toxicity studies of tamoxifen on the liver were carried out in animal experiments, using mainly rats, as this model was shown to be superior to the mouse model [255]. The findings and propositions of tamoxifen studies vary greatly between research groups [104]. For example, the hypothesized steatogenic mechanism mediated by SREBP-1c from *in vitro* experiments was partially confirmed in one study in mice [256], while four other groups found the opposite, namely a downregulation of FAS [251,257-259], which is regulated by SREBP-1c [260].

In rat liver mitochondria, it was observed that tamoxifen (or metabolites) uncouple mitochondria and compromise the ETC [261,262], with the specific location of Complex I, found a few years later [263]. Complex I inhibition was also seen in mice, in which also Complex IV was inhibited by tamoxifen [257]. An investigation in isolated rat liver mitochondria, furthermore, showed only inhibition of Complex III and not of Complex I or IV [264]. For the most part it seems clear, that tamoxifen is disturbing the oxphos pathway, with most reports agreeing on Complex I as the affected site.

Since Complex I regenerates NAD^+, which is a cofactor needed for the second dehydrogenation step in β-oxidation [42], it was hypothesized that the β-oxidation in mitochondria is compromised as well [104]. Indeed, we found inhibition of CPT1, which is also proposed by other authors [104]. One author found CPT1 inhibition with a joint decrease of its mRNA [257], while other authors, however, did not find FA oxidation reduction in mice [256], or an influence on CPT1 activity in rats [251]. Also no difference in genes relating β-oxidation in mice was reported [256,258], suggesting no inhibition of β-oxidation *in vivo*.

Tamoxifen reduced VLDL export in our study, which can also be observed in patients [265]. It was argued by the authors of this study that this observed change in patients was due to decreased release of growth hormone, which in turn decreases ApoB expression. Also one study in mice reported lower serum TG and slightly lower ApoB concentrations [257]. The state of data concerning ApoB, however, is equally complex as the topics above, as also opposite reports can be found. A case report of a woman showed high VLDL and high ApoB in plasma [266], while other studies report no differences in VLDL levels [267-270]. These studies also reported no significant change in serum TG levels. In contrast, there are reports saying otherwise, as for example a recent meta-analysis of five studies with 215 participants, showing an increase in serum TG [271]. Another study, showing a

significant elevation of serum TG, states that the changes in the vast majority of patients were not clinically important, while in a small number of patients, who already presented high TG levels prior to treatment, tamoxifen therapy led to further elevations, necessitating dose reduction [272]. The significant elevation of serum TG could therefore be an adverse effect only affecting a specific population. A study in support of this showed a specific ApoE phenotype (ApoE4) to be a determining factor for serum TG elevation in Greek women [269]. Tamoxifen was also shown to reduce the activity of LPL in several investigations [266,273,274], implicating decreased VLDL metabolism in the periphery as a culprit of elevated serum TG.

The discussion above shows the complex and diverse findings of studies with tamoxifen and suggest numerous effects leading to hepatic steatosis. The mostly coherent findings of complex inhibition, with possible reduction in FA oxidation, coupled with upregulation of lipogenic genes and reduced VLDL catabolism in the periphery, could be taken as mechanisms leading to hepatic steatosis.

Lastly, the question of metabolite formation in our cell model remains, as tamoxifen, although quite potent itself for ESR binding (IC_{50} around 420 nM [275]), is considered as prodrug and needs activation to its metabolite 4-hydroxy tamoxifen (endoxifen), which possesses a 100 times higher activity [103,276]. Since HepG2 cells have almost no activity of CYP2D6 [137], which is responsible for this transformation, effects observed *in vivo* or in PHH could be missed. Endoxifen has not only a higher ESR-binding capacity but also behaves differently in uncoupling and Complex inhibition studies [261], questioning the translatability of *in vitro* studies with tamoxifen.

3.3.3 Mechanisms of WIN55, 212-2

The endocannabinoid system has substantially gained recognition in terms of energy homeostasis. Cannabinoids, endogenous and exogenous, modulate appetite behavior, promote adipogenesis, block energy expenditure, and regulate peripheral energy metabolism [277,278]. Some of the effects originate from the central nervous system over tissue innervations, other effects are direct, through binding of CB receptors, present in numerous tissues.

In regard to the liver, it is now widely accepted that CB1 activation promotes hepatic steatosis, while CB2 activation is considered protective [85,88,90,199,278,279]. CB2 is mainly expressed in neuronal cells and immune cells. The protective effect on the liver by CB2 is believed to be carried out by anti-fibrotic effects on stellate cells, as well as by an anti-inflammatory effect through modulation of Kupffer- and endothelial cells [88]. Since CB2 is not expressed in hepatocytes [280,281], the steatogenic effect of cannabinoids is mediated over hepatic CB1, as this receptor is shown to be overexpressed in steatogenic tissue [282].

For the most part, the nature of cannabinoid mediated lipid accumulation, is not well elucidated, but rather shown through inverted mechanistic studies, namely through knockout or inhibition of CB1, as this modulation has been considered as possible treatment target [87]. Knockout of CB1 in animals or specific inhibition of CB1,

consistently led to an increased FA oxidation capacity and also to a resistance to diet-induced hepatic steatosis [90,91,278,280,283-285].

The synthetic cannabinoid WIN55 showed β-oxidation inhibition in our study with a decrease in C2-C10 acylcarnitines, with normal concentrations of C12-C16 acylcarnitines. This pattern could be explained by inhibition of mitochondrial import combined with impaired long-chain FA metabolism. We, however, did not find direct inhibitory effects of WIN on CPT1 or long-chain acyl-CoA dehydrogenase. In the literature, on the other hand, it is reported that there is a downregulation of CPT1 after treatment with THC [92]. Other authors showed the negative regulation of CB1 on CPT1 by knockout models [91,285,286]. Also long-chain acyl-CoA dehydrogenase was shown to be upregulated upon antagonism of CB1 [285]. Since the measurements of acylcarnitines, as well as of β-oxidation, were done in an *in vitro* system over 24 hours and enzyme inhibition studies in acutely treated mitochondria, it could be that decreased activities of CPT1 and LCAD were missed in our study.

Cannabinoids act inhibitory on the adenylate cyclase, resulting in reduced cAMP levels, which results in a decreased activity of protein kinase A (PKA) [287]. This leads to less phosphorylated, and thus less active CPT1 [288]. The same mechanism can also derive from decreased activity of AMPK, which is also negatively controlled by cannabinoids [96]. Enzyme complexes of the ETC are also affected by this decrease in phosphorylation and are shown to have decreased activity after treatment with cannabinoids in different tissues [95,97,98,289-291], which can also lead to increased formation of ROS [292]. This reduced activity of the ETC can therefore also be a factor contributing to the decreased FA oxidation, observed with the treatment of WIN55. Furthermore, elevated ROS levels in hepatocytes can worsen the development of hepatic steatosis as well. The cell upregulates mitochondrial biogenesis under circumstances of mitochondrial stress, to promote a healthy, functional mitochondrial pool [293]. Studies in adipocytes showed a clear negative effect on mitochondrial biogenesis through down modulation of PGC1α [294,295], which further fuels mitochondrial dysfunction, as seen with treatment of CB1 agonists.

Another contributing mechanism for lipid accumulation is the induction of lipogenic factors, such as SREBP-1c, ACC or FAS. Upregulation, higher expression, and also higher activities of these factors are reported in almost every study investigating cannabinoid-induced changes in lipid synthesis [92,200,277,280,285].

Moreover, it was shown that CB1 activation contributes to diet-induced insulin resistance through inhibition of insulin signaling. This insulin resistance impairs suppression of hepatic glucose production, while *de novo* lipogenesis stays the same or even increases due to compensatory hyperinsulinemia [296].

Additional to the ubiquitous actions of cannabinoids in the body, a circumstance that makes it difficult to draw conclusions from literature and to translate *in vitro* findings, is that studies are done in numerous species and tissues, mostly focusing on neuronal implications. In this discussion references contain studies carried out in tissue samples of cells from brain, adipose tissue, muscle, pancreas, and liver from humans, mice, rats, pigs, and dogs.

Lastly, WIN significantly reduced the export of VLDL in our cell model. There is, however no report in literature about cannabinoids affecting this pathway.

Given all these points, it implies that WIN55, as a potent CB1 agonist, induces hepatic steatosis through many individual effects. Together with our study, it seems that CB1 activation leads to the observed lipid accumulation in hepatocytes by decreasing FA oxidation, upregulation of lipid synthesis, and a decrease of TG excretion.

3.3.4 Mechanisms of Tolcapone and Entacapone

Tolcapone and entacapone are two valuable drugs for the treatment of Parkinson disease. Since tolcapone, and not entacapone, was associated with rare [297], but severe, hepatotoxicity, it has been the focus of numerous studies to elucidate its mechanism of toxicity. After reaching the market in 1997, it was shown early on that tolcapone is a mitochondrial toxicant.

Initial investigations by a finnish group reveiled the strong mitochondrial uncoupling potential of tolcapone *in vitro* and *in vivo* [206-208,298,299]. These thorough studies showed tolcapone to be even more potent than the model-uncoupler 2,4-dinitrophenol and produced corresponding adverse effects, such as swollen mitochondria with loss of cristae, elevation of body temperature, increased metabolic rate, diminished ATP/ADP ratio, and thus fast onset of rigor mortis. Entacapone, structurally very similar to tolcapone, did also show uncoupling potential, however, at higher concentrations than tolcapone. Albeit, it was consistently shown that entacapone was safe in even high, but still pharmacologically relevant doses. This trend pervades through all studies comparing tolcapone and entacapone, thus in the following sections only consequences of tolcapone treatment will be discussed. The discrepancies of the toxic effects of the two drugs will, however, be still discussed at the end.

In agreemant with the finnish group, our study could also show the uncoupling potential of tolcapone, showing a direct, protonophoric effect of the drug. The effective uncoupling concentration, however, was higher in our studies, explainable by the presence of bovine serum albumin in the respiration medium and the high protein binding of tolcapone (99% [206]), while Haasio et al. did not have additional protein in their respiration medium.

We observed an increase in ROS formation after treatment with tolcapone, which is in agreement with the finding in literature that tolcapone enhances ROS formation and drastically reduces the antioxidant GSH [300]. This is somewhat surprising, as nitrocatecholamines, specifically also tolcapone, have intrinsic antioxidant properties [301], and it is also postulated that mitochondrial uncoupling reduces the formation of ROS [302]. It is well-known that inhibition of the respiratory chain is an important mechanism for the production of ROS. In a capture compound mass spectrometry study, it was reveiled that tolcapone binds to proteins of the ETC [211]. We therefore studied the inhibition of individual complexes, which can be challenging, when inhibition and uncoupling occurs concominantly. In order to exclude the effects of uncoupling, we spectrophotometrically

measured the activity of Complex I – IV in previously frozen mitochondrial isolations, which abolishes the integrity of the mitochondrial membrane. Indeed, we found tolcapone to inhibit Complexes I, II, and IV and were the first to show this bivalent effect, effectively explaining the ROS accumulation. Additionally, tolcapone was reported to induce oxidative stress through its amine- and acetylamine metabolites, which can be bioactivated to the *o*-quinone or quinone-imine form by CYPs 3A4, 2E1, and 1A2, exerting toxicity similar to the well-known paracetmaol-NAPQI mechanism [303]. We, however, could not observe increased toxicity after induction of said enzymes in our cell model.

Important for our motivation to study tolcapone was the finding of microvesicular steatosis in a patient who delevoped tolcapone-related fulminant hepatitis [209]. Considering that induction of hepatic steatosis requires more than one "hit", according to the multiple hit theory, it seemed logical to look for an additional mechanism to the harsh effects of tolcapone on the oxphos pathway. Furthermore, the capture compound mass spectrometry study also showed the binding of tolcapone to enzymes of the FA oxidation pathways [211]. This study by Fisher et al. prooved itself once again, as we found β-oxidation inhibition in HepaRG cells on the level of FA activation and long-chain acyl-CoA dehydrogense. These inhbitions are also represented in the acylcarnitine profile of tolcapone treated HepaRG cells, where we saw a decrease in medium-chain acylcarnitines and an increase in long-chain acylcarnitines, consistent with a inhibition of overall acylcarnitine formation, as seen with triacsin C, the model-ACSL inhibitor, with a simultanious accumulation of long-chain acylcarnitines because of the inhibition of long-chain acyl-CoA dehydrogenase. 3-oxo-palmitoylcarnitine was increased as well, which was also predicted from the study of Fisher et al. [211], reporting tolcapone binding to the 3-keto-acyl-CoA thiolase. Furthermore, this capture compound mass spectrometry study also implemented one of the multiple ACSLs, namely ACSL1, in the tolcapone mediated effects, which we also could show with the decreased content of this enzyme in our cells. Lastly, Fisher et al. also identified one more enzyme of the mitochondrial β-oxidation pathway, the enoyl-CoA hydratase, which we, however, did not investigate.

In our study, we found even more negative effects, fueling the progression of hepatic steatosis, as we saw an upregulation of genes related to the uptake of FAs (CD36 and FATP5), as well as a decreased excretion of VLDL, resulting from decreased synthesis of ApoB100. It could be, that the upregulation of CD36 and FATP5 is a compensatory mechanism to the inhibiton of ACSL1 (or others), as these FA transporters also exert FA activation, besides their cellular uptake [304,305]. Furthermore, it is also reported in literature that tolcapone can inhibit the export of bile acids in hepatocytes [306]. This finding is of importance, as it is known that the accumulation of bile acids can have multiple inhibitory effects on the energy metabolism in hepatocytes. Studies by Krähenbühl et al. have shown that accumulating lipophilic bile acids exert toxicity on mitochondria, such as inhibition of respiratory complexes [154], decrease of antioxidative capacity [307], and inhibition of FA oxidation [65,308].

Lastly, the question remains why entacapone, structurally very similar, as well as in its molecular effects, does not show clinical toxicity to a similar extent like tolcapone. After all, entacapone showed many of the effects like tolcapone. It uncouples mitochondria, increases lipid accumulation in HepG2 cells, is also reported to

inhibit bile acid excretion [306], depresses medium-chain acylcarnitines with an increase in palmitoylcarnitine, and inhibits Complex I and IV. In the capture compound mass spectrometry study, it was also shown to bind to similar proteins, as tolcapone does [211]. Suprisingly, however, entacapone is consistently shown to be untoxic [214], also until high concentrations [208]. Toxic effects of entacapone always occur at significant higher doses as with tolcapone. Since pharmacological concentrations in plasma, after ingestion of the normal dose of 200 mg of either drug, reach maximal concentrations of 21 μM and 6 μM for tolcapone and entacapone, respectively[202], the almost non-existent hepatotoxicity of entacapone in patients makes sense. Furthermore, entacapone has a higher clearance and is less lipophilic than tolcapone, thus less likely to accumulate in membranes.

As shown above, tolcapone has manifold effects on hepatic energy metabolism, explaining the induction of microvesicular steatosis, as seen in patients. Taken together, the hits leading to this adverse reactions are mitochondrial dysfunction on the level of respiration and FA oxidation, as well as decreased TG excretion. The disturbed energy production is nicely visible by the increase of lactate in our treated cells, showing a shift to glycolysis to restore the decreased ATP production by mitochondria. Furthermore, the increase in ROS with concominant decrease in antioxidative capacity, also shown by decrease in SOD1 and SOD2, further signifies the toxic insult of tolcapone on the liver. Moreover, the importance of FA oxidation inhibition for the toxic effect of the drug was shown by the fact that tolcapone decreases energy production of cells even in the absence of the influence on the ETC[309], as well as underlying mitochondrial dysfunction was shown to be a susceptebility factor for tolcapone-induced liver injury [310]. All the effects, discussed above, decisively explain the finding of necrosis, rather than apoptosis, which would rely on ATP, of which the cell is devoided, as well as the induction of steatosis and shed new light on the mechanism of tolcapone-associated DILI.

3.3 Concluding Remarks and Outlook

During our studies on the mechanisms of drug-induced hepatic steatosis, we applied the acylcarnitine method, as well as old and well-known methods, to assess inhibitions of mitochondrial β-oxidation. We could constantly show that the results of the acylcarnitine pattern were in agreement with the findings obtained with established, direct determinations of enzyme activities. Using the acylcarnitine types, included in our measurement, we could make clear predictions about inhibition of import or activation, general chain-length specificity of FA breakdown, acetyl-CoA content, as well as long-chain β-keto thiolase inhibition. Unquestionably, this gave us valuable insight into the mechanism of the drugs included in our studies, however, not to the full extent possible. The breakdown of FAs involves several more enzymes, worth including in the method. Therefore, it would be of value to supplement the LC-MS/MS method with intermediates, such as enoyl-carnitines and 3-hydroxyacyl-carnitines. Furthermore, of the aforementioned intermediates, as well as of the 3-ketoacyl-carnitine, of which we only have the C16 form, additional determination of short- and medium-chain forms would be of value.

This, however, would require specific inhibitors of corresponding enzymes, which is, to the best of our knowledge, not existing for all of them. Indeed, certain inhibitors, such as MCPA, could be altered to be more specific for different FA chain-lengths. In the case of MCPA this was shown by synthesis of C6-MCPA (**Fig. 25a**), which provided an inhibitor more specific to long-chain acyl-CoA dehydrogenase [168]. The same approach could be used for generating C12-MCPA (**Fig. 25b**), which should be specific only for the long-chain acyl-CoA dehydrogenase. Likewise, increasing the chain-length of 4-bromocrotonic acid to 16-bromohexadec-2-enoic acid (**Fig. 25c**) for specific inhibition of the long-chain β-keto thiolase could be possible. In the same fashion, other brominated FAs and FA breakdown intermediate analogs have been shown to irreversibly inhibit enzymes in the β-oxidation, by forming covalent adducts to a lysine, cysteine, or serine residue within the active site [311]. The specificity of these inhibitors to one enzyme, however, remains questionable, considering the studies with 4-bromocrotonic acid. Also inhibitors for the enoyl-CoA hydratase[312] (**Fig. 25d**), short-chain-[313] (**Fig. 25e**), and long-chain 3-hydroxyacyl-CoA dehydrogenase[314] (**Fig. 25f**) have been identified. Clear data on their specificity, however, is lacking.

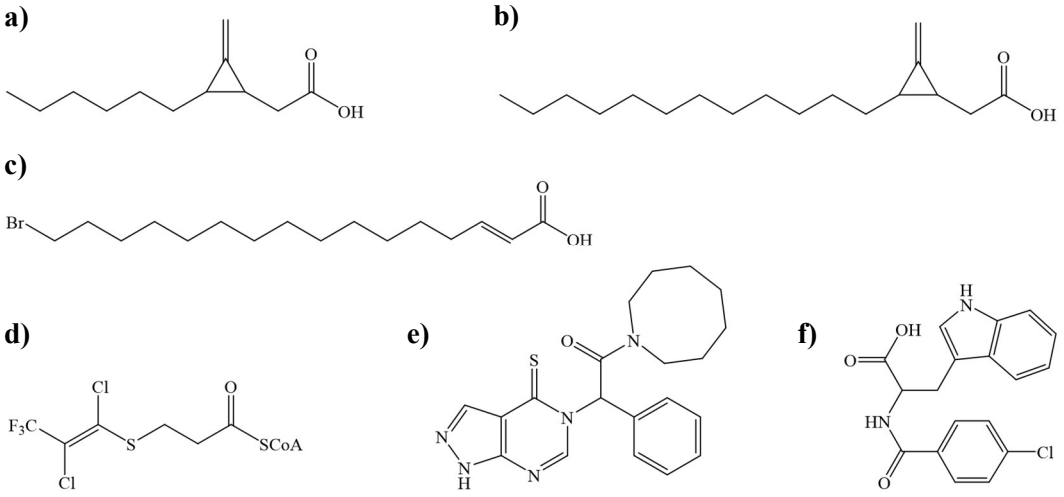

Fig. 25. Chemical structures of the proposed specific inhibitors of fatty acid oxidation. a) C6-MCPA, b) C12-MCPA, c) 16-bromohexadec-2-enoic acid, d) 5,6-dichloro7,7,7-trifluoro-4-thia-5-heptenoyl-CoA, e) AG18051 and f) benzotript.

We fed our cells with palmitic- and oleic acid, for studying the effects and consequences of the inhibitors we used, with attention to enzymes involved in metabolism of saturated FAs. Inclusion of branched-chain, multiple unsaturated, or very-long-chain FAs and inhibitors of enzymes involved in their metabolism, therefore, could also be considered.

As illustrated above, the acylcarnitine method has a great potential to be adapted to various domains of FA metabolism research. Due to the possibility to link the assay with multiple others, using various well-plate systems, as well as its fast and simple workup and analysis, this method represents a relevant possibility to use for investigators. In our case, especially the conjunction with lipid accumulation, cell viability/apoptosis, and VLDL export would represent an improved and streamlined approach to determinations, which are already established in our laboratory. This would be possible by using the supernatants of cells for acylcarnitine

analysis and determination of excreted VLDL, then using trypsinized cells for simultaneous and semi-automatic analysis by flow cytometric of lipid accumulation with a BODIPY dye, as well as determination of cell viability and apoptosis with the AnnexinV/PI staining, in 96-well format. Particularly, this would reduce time and costs for the screening of drugs with possible steatogenic effects, which would also serve the need of the industry of preclinical high-throughput screening methods for the early detection of possible adverse effects of drug candidates.

In conclusion, we could show the value and applicability of the analysis of acylcarnitine pattern in our work. Together with an additional battery of assessments, we were successful in confirming, as well as in shedding new light on the molecular mechanisms of drug-induced steatosis of several compounds. Therefore, the acylcarnitine method, as well as our findings, will hopefully improve the investigation and understanding of adverse reactions on the liver for academia as well as for the industry, ultimately improving the work of clinicians and more importantly the life of patients.

4. BIBLIOGRAPHY

1 Pawlak, M., Lefebvre, P. & Staels, B. Molecular mechanism of PPARalpha action and its impact on lipid metabolism, inflammation and fibrosis in non-alcoholic fatty liver disease. *J Hepatol* **62**, 720-733, doi:10.1016/j.jhep.2014.10.039 (2015).

2 Liu, S.-L. *et al.* Discovery of serum biomarkers of alcoholic fatty liver in a rodent model: C-reactive protein. *Journal of Biomedical Science* **18**, 52-52, doi:10.1186/1423-0127-18-52 (2011).

3 Abumrad, N. A. & Davidson, N. O. Role of the gut in lipid homeostasis. *Physiological reviews* **92**, 1061-1085, doi:10.1152/physrev.00019.2011 (2012).

4 Stevenson, A. *Oxford Dictionary of English*. (OUP Oxford, 2010).

5 Hussain, M. M. Intestinal lipid absorption and lipoprotein formation. *Curr Opin Lipidol* **25**, 200-206, doi:10.1097/MOL.0000000000000084 (2014).

6 Cordain, L. *et al.* Origins and evolution of the Western diet: health implications for the 21st century. *The American journal of clinical nutrition* **81**, 341-354, doi:10.1093/ajcn.81.2.341 (2005).

7 Green, P. H. & Riley, J. W. Lipid absorption and intestinal lipoprotein formation. *Aust N Z J Med* **11**, 84-90 (1981).

8 Monsivais, P. & Drewnowski, A. The rising cost of low-energy-density foods. *Journal of the American Dietetic Association* **107**, 2071-2076, doi:10.1016/j.jada.2007.09.009 (2007).

9 Eyster, K. M. The membrane and lipids as integral participants in signal transduction: lipid signal transduction for the non-lipid biochemist. *Advances in physiology education* **31**, 5-16, doi:10.1152/advan.00088.2006 (2007).

10 Mattes, R. D. Oral fatty acid signaling and intestinal lipid processing: support and supposition. *Physiol Behav* **105**, 27-35, doi:10.1016/j.physbeh.2011.02.016 (2011).

11 Frazer, A. C. Normal and defective fat absorption in man. *Schweizerische medizinische Wochenschrift* **76**, 903-908 (1946).

12 Nhavi, N. G. & Patwardhan, V. N. The absorption of fats from the human intestine. *The Indian journal of medical research* **34**, 49-58 (1946).

13 Wang, T. Y., Liu, M., Portincasa, P. & Wang, D. Q. New insights into the molecular mechanism of intestinal fatty acid absorption. *Eur J Clin Invest* **43**, 1203-1223, doi:10.1111/eci.12161 (2013).

14 Feingold, K. R. & Grunfeld, C. in *Endotext* (eds L. J. De Groot *et al.*) (2000).

15 Cohen, D. E. & Fisher, E. A. Lipoprotein metabolism, dyslipidemia, and nonalcoholic fatty liver disease. *Seminars in liver disease* **33**, 380-388, doi:10.1055/s-0033-1358519 (2013).

16 van der Vusse, G. J. Albumin as fatty acid transporter. *Drug Metab Pharmacokinet* **24**, 300-307 (2009).

17 Fruhbeck, G., Mendez-Gimenez, L., Fernandez-Formoso, J. A., Fernandez, S. & Rodriguez, A. Regulation of adipocyte lipolysis. *Nutr Res Rev* **27**, 63-93, doi:10.1017/S095442241400002X (2014).

18 Furuhashi, M., Saitoh, S., Shimamoto, K. & Miura, T. Fatty Acid-Binding Protein 4 (FABP4): Pathophysiological Insights and Potent Clinical Biomarker of Metabolic and Cardiovascular Diseases. *Clinical Medicine Insights. Cardiology* **8**, 23-33, doi:10.4137/cmc.s17067 (2014).

19 Vorum, H., Brodersen, R., Kragh-Hansen, U. & Pedersen, A. O. Solubility of long-chain fatty acids in phosphate buffer at pH 7.4. *Biochimica et biophysica acta* **1126**, 135-142 (1992).

20 Fujiwara, S. & Amisaki, T. Fatty acid binding to serum albumin: molecular simulation approaches. *Biochimica et biophysica acta* **1830**, 5427-5434, doi:10.1016/j.bbagen.2013.03.032 (2013).

21 Sear, J. Anatomy and physiology of the liver. *Baillière's Clinical Anaesthesiology* **6**, 697-727, doi:10.1016/S0950-3501(05)80304-6 (1992).

22 Sendensky, A. & Dufour, J.-F. *Liver Physiology*. (2011).

23 Fukao, T. *et al.* Ketone body metabolism and its defects. *Journal of inherited metabolic disease* **37**, 541-551, doi:10.1007/s10545-014-9704-9 (2014).

24 Gray, M. W. Mitochondrial evolution. *Cold Spring Harbor perspectives in biology* **4**, a011403, doi:10.1101/cshperspect.a011403 (2012).

25 Schon, E. A., DiMauro, S. & Hirano, M. Human mitochondrial DNA: roles of inherited and somatic mutations. *Nature reviews. Genetics* **13**, 878-890, doi:10.1038/nrg3275 (2012).

26 Palikaras, K. & Tavernarakis, N. Mitochondrial homeostasis: the interplay between mitophagy and mitochondrial biogenesis. *Experimental gerontology* **56**, 182-188, doi:10.1016/j.exger.2014.01.021 (2014).

27 Lopez-Lluch, G. Mitochondrial activity and dynamics changes regarding metabolism in ageing and obesity. *Mechanisms of ageing and development* **162**, 108-121, doi:10.1016/j.mad.2016.12.005 (2017).

28 Else, P. L. & Hulbert, A. J. An allometric comparison of the mitochondria of mammalian and reptilian tissues: the implications for the evolution of endothermy. *Journal of comparative physiology. B, Biochemical, systemic, and environmental physiology* **156**, 3-11 (1985).

29 Wojtczak, L. & Zabłocki, K. *Basic Mitochondrial Physiology in Cell Viability and Death*. (2008).

30 Cazeneuve, P. & Lépine, R. Sur les effets produits par l'ingestion et l'infusion intra-veineuse de trois colorants jaunes, derives de la houille. *Compt Rend Soc Biol* **101**, 1167-1169 (1885).

31 Horner, W. D. A Study of Dinitrophenol and Its Relation to Cataract Formation. *Transactions of the American Ophthalmological Society* **39**, 405-437 (1941).

32 Muriel, P. *Liver pathophysiology : therapies and antioxidants*. 393.

33 Rinaldo, P. Fatty acid transport and mitochondrial oxidation disorders. *Seminars in liver disease* **21**, 489-500, doi:10.1055/s-2001-19037 (2001).

34 Leonardi, R., Zhang, Y. M., Rock, C. O. & Jackowski, S. Coenzyme A: back in action. *Progress in lipid research* **44**, 125-153, doi:10.1016/j.plipres.2005.04.001 (2005).

35 Koo, S. H. Nonalcoholic fatty liver disease: molecular mechanisms for the hepatic steatosis. *Clinical and molecular hepatology* **19**, 210-215, doi:10.3350/cmh.2013.19.3.210 (2013).

36 Kawano, Y. & Cohen, D. E. Mechanisms of hepatic triglyceride accumulation in non-alcoholic fatty liver disease. *Journal of gastroenterology* **48**, 434-441, doi:10.1007/s00535-013-0758-5 (2013).

37 Yan, S. *et al.* Long-chain acyl-CoA synthetase in fatty acid metabolism involved in liver and other diseases: an update. *World journal of gastroenterology : WJG* **21**, 3492-3498, doi:10.3748/wjg.v21.i12.3492 (2015).

38 Van Horn, C. G. *et al.* Characterization of recombinant long-chain rat acyl-CoA synthetase isoforms 3 and 6: identification of a novel variant of isoform 6. *Biochemistry* **44**, 1635-1642, doi:10.1021/bi0477211 (2005).

39 Watkins, P. A. & Ellis, J. M. Peroxisomal acyl-CoA synthetases. *Biochimica et biophysica acta* **1822**, 1411-1420, doi:10.1016/j.bbadis.2012.02.010 (2012).

40 Wanders, R. J., Komen, J. & Kemp, S. Fatty acid omega-oxidation as a rescue pathway for fatty acid oxidation disorders in humans. *The FEBS journal* **278**, 182-194, doi:10.1111/j.1742-4658.2010.07947.x (2011).

41 Eaton, S., Bartlett, K. & Pourfarzam, M. Mammalian mitochondrial beta-oxidation. *The Biochemical journal* **320 (Pt 2)**, 345-357 (1996).

42 Houten, S. M. & Wanders, R. J. A general introduction to the biochemistry of mitochondrial fatty acid beta-oxidation. *Journal of inherited metabolic disease* **33**, 469-477, doi:10.1007/s10545-010-9061-2 (2010).

43 Watmough, N. J. & Frerman, F. E. The electron transfer flavoprotein: Ubiquinone oxidoreductases. *Biochimica et Biophysica Acta (BBA) - Bioenergetics* **1797**, 1910-1916, doi:https://doi.org/10.1016/j.bbabio.2010.10.007 (2010).

44 Reddy, J. K. & Hashimoto, T. Peroxisomal beta-oxidation and peroxisome proliferator-activated receptor alpha: an adaptive metabolic system. *Annual review of nutrition* **21**, 193-230, doi:10.1146/annurev.nutr.21.1.193 (2001).

45 Lazarow, P. B. Rat liver peroxisomes catalyze the beta oxidation of fatty acids. *Journal of Biological Chemistry* **253**, 1522-1528 (1978).

46 Coleman, R. A. & Lee, D. P. Enzymes of triacylglycerol synthesis and their regulation. *Progress in lipid research* **43**, 134-176 (2004).

47 Nguyen, P. *et al.* Liver lipid metabolism. *Journal of animal physiology and animal nutrition* **92**, 272-283, doi:10.1111/j.1439-0396.2007.00752.x (2008).

48 Berg JM, T. J., Stryer L. in *Biochemistry. 5th edition* (ed W H Freeman) Ch. 22.5, (2002).

49 Wakil, S. J. Fatty acid synthase, a proficient multifunctional enzyme. *Biochemistry* **28**, 4523-4530 (1989).

50 Lupu, R. & Menendez, J. A. Targeting Fatty Acid Synthase in Breast and Endometrial Cancer: An Alternative to Selective Estrogen Receptor Modulators? *Endocrinology* **147**, 4056-4066, doi:10.1210/en.2006-0486 (2006).

51 Schroeder, F., Jolly, C. A., Cho, T. H. & Frolov, A. Fatty acid binding protein isoforms: structure and function. *Chemistry and physics of lipids* **92**, 1-25 (1998).

52 Schroeder, F. *et al.* Fatty Acid Binding Protein-1 (FABP1) and the Human FABP1 T94A Variant: Roles in the Endocannabinoid System and Dyslipidemias. *Lipids* **51**, 655-676, doi:10.1007/s11745-016-4155-8 (2016).

53 Storch, J. & Corsico, B. The emerging functions and mechanisms of mammalian fatty acid-binding proteins. *Annual review of nutrition* **28**, 73-95, doi:10.1146/annurev.nutr.27.061406.093710 (2008).

54 Welte, M. A. Fat on the move: intracellular motion of lipid droplets. *Biochemical Society transactions* **37**, 991-996, doi:10.1042/bst0370991 (2009).

55 Yamaguchi, T., Omatsu, N., Omukae, A. & Osumi, T. Analysis of interaction partners for perilipin and ADRP on lipid droplets∗. *Molecular and Cellular Biochemistry* **284**, 167-173, doi:10.1007/s11010-005-9045-y (2006).

56 Masuda, Y. *et al.* ADRP/adipophilin is degraded through the proteasome-dependent pathway during regression of lipid-storing cells. *Journal of lipid research* **47**, 87-98, doi:10.1194/jlr.M500170-JLR200 (2006).

57 Xu, W. *et al.* Differential Roles of Cell Death-inducing DNA Fragmentation Factor-alpha-like Effector (CIDE) Proteins in Promoting Lipid Droplet Fusion and Growth in Subpopulations of Hepatocytes. *The Journal of biological chemistry* **291**, 4282-4293, doi:10.1074/jbc.M115.701094 (2016).

58 Zhou, L. *et al.* Cidea promotes hepatic steatosis by sensing dietary fatty acids. *Hepatology* **56**, 95-107, doi:10.1002/hep.25611 (2012).

59 Gordon, D. A. & Jamil, H. Progress towards understanding the role of microsomal triglyceride transfer protein in apolipoprotein-B lipoprotein assembly. *Biochimica et biophysica acta* **1486**, 72-83 (2000).

60 Tiwari, S. & Siddiqi, S. A. Intracellular trafficking and secretion of VLDL. *Arteriosclerosis, thrombosis, and vascular biology* **32**, 1079-1086, doi:10.1161/atvbaha.111.241471 (2012).

61 Fisher, E. A. & Ginsberg, H. N. Complexity in the secretory pathway: the assembly and secretion of apolipoprotein B-containing lipoproteins. *The Journal of biological chemistry* **277**, 17377-17380, doi:10.1074/jbc.R100068200 (2002).

62 Sundaram, M. & Yao, Z. Recent progress in understanding protein and lipid factors affecting hepatic VLDL assembly and secretion. *Nutrition & metabolism* **7**, 35, doi:10.1186/1743-7075-7-35 (2010).

63 Ramasamy, I. Recent advances in physiological lipoprotein metabolism. *Clinical chemistry and laboratory medicine* **52**, 1695-1727, doi:10.1515/cclm-2013-0358 (2014).

64 Morand, R., Donzelli, M., Haschke, M. & Krahenbuhl, S. Quantification of plasma carnitine and acylcarnitines by high-performance liquid chromatography-tandem mass spectrometry using online solid-phase extraction. *Analytical and bioanalytical chemistry* **405**, 8829-8836, doi:10.1007/s00216-013-7309-z (2013).

65 Krahenbuhl, S. & Brass, E. P. Fuel homeostasis and carnitine metabolism in rats with secondary biliary cirrhosis. *Hepatology* **14**, 927-934 (1991).

66 Scarpulla, R. C. Metabolic control of mitochondrial biogenesis through the PGC-1 family regulatory network. *Biochimica et biophysica acta* **1813**, 1269-1278, doi:10.1016/j.bbamcr.2010.09.019 (2011).

67 Lee, H. C. & Wei, Y. H. Mitochondrial biogenesis and mitochondrial DNA maintenance of mammalian cells under oxidative stress. *The international journal of biochemistry & cell biology* **37**, 822-834, doi:10.1016/j.biocel.2004.09.010 (2005).

68 Sanderson, L. M. *et al.* Effect of synthetic dietary triglycerides: a novel research paradigm for nutrigenomics. *PloS one* **3**, e1681, doi:10.1371/journal.pone.0001681 (2008).

69 Kersten, S. Integrated physiology and systems biology of PPARα. *Molecular Metabolism* **3**, 354-371, doi:10.1016/j.molmet.2014.02.002 (2014).

70 Contreras, A. V., Torres, N. & Tovar, A. R. PPAR-α as a Key Nutritional and Environmental Sensor for Metabolic Adaptation. *Advances in Nutrition* **4**, 439-452, doi:10.3945/an.113.003798 (2013).

71 Morillas, M. *et al.* Structural Model of a Malonyl-CoA-binding Site of Carnitine Octanoyltransferase and Carnitine Palmitoyltransferase I: MUTATIONAL ANALYSIS OF A MALONYL-CoA AFFINITY DOMAIN. *Journal of Biological Chemistry* **277**, 11473-11480, doi:10.1074/jbc.M111628200 (2002).

72 Hirschey, M. D. *et al.* SIRT3 regulates fatty acid oxidation via reversible enzyme deacetylation. *Nature* **464**, 121-125, doi:10.1038/nature08778 (2010).

73 Fernandez-Marcos, P. J. & Auwerx, J. Regulation of PGC-1alpha, a nodal regulator of mitochondrial biogenesis. *The American journal of clinical nutrition* **93**, 884s-890, doi:10.3945/ajcn.110.001917 (2011).

74 Horton, J. D., Goldstein, J. L. & Brown, M. S. SREBPs: activators of the complete program of cholesterol and fatty acid synthesis in the liver. *The Journal of clinical investigation* **109**, 1125-1131, doi:10.1172/JCI15593 (2002).

75 Moon, Y. A. The SCAP/SREBP Pathway: A Mediator of Hepatic Steatosis. *Endocrinology and metabolism (Seoul, Korea)* **32**, 6-10, doi:10.3803/EnM.2017.32.1.6 (2017).

76 Marion-Letellier, R., Savoye, G. & Ghosh, S. Fatty acids, eicosanoids and PPAR gamma. *European journal of pharmacology* **785**, 44-49, doi:10.1016/j.ejphar.2015.11.004 (2016).

77 Kroker, A. J. & Bruning, J. B. Review of the Structural and Dynamic Mechanisms of PPARγ Partial Agonism. *PPAR Research* **2015**, 816856, doi:10.1155/2015/816856 (2015).

78 Cui, J., Shen, Y. & Li, R. Estrogen synthesis and signaling pathways during aging: from periphery to brain. *Trends in molecular medicine* **19**, 197-209, doi:10.1016/j.molmed.2012.12.007 (2013).

79 Barros, R. P. & Gustafsson, J. A. Estrogen receptors and the metabolic network. *Cell metabolism* **14**, 289-299, doi:10.1016/j.cmet.2011.08.005 (2011).

80 Murphy, E. & Korach, K. S. Actions of estrogen and estrogen receptors in nonclassical target tissues. *Ernst Schering Foundation symposium proceedings*, 13-24 (2006).

81 Hayashi, S. & Yamaguchi, Y. Estrogen signaling pathway and hormonal therapy. *Breast cancer (Tokyo, Japan)* **15**, 256-261, doi:10.1007/s12282-008-0070-z (2008).

82 Ponnusamy, S. *et al.* An estrogen receptor beta-selective agonist inhibits non-alcoholic steatohepatitis in preclinical models by regulating bile acid and xenobiotic receptors. *Experimental biology and medicine (Maywood, N.J.)* **242**, 606-616, doi:10.1177/1535370216688569 (2017).

83 Wang, X. *et al.* Hepatic estrogen receptor alpha improves hepatosteatosis through upregulation of small heterodimer partner. *J Hepatol* **63**, 183-190, doi:10.1016/j.jhep.2015.02.029 (2015).

84 Bisogno, T. & Maccarrone, M. Endocannabinoid signaling and its regulation by nutrients. *BioFactors* **40**, 373-380, doi:10.1002/biof.1167 (2014).

85 Alswat, K. A. The role of endocannabinoids system in fatty liver disease and therapeutic potentials. *Saudi journal of gastroenterology : official journal of the Saudi Gastroenterology Association* **19**, 144-151, doi:10.4103/1319-3767.114505 (2013).

86 Scuderi, C. *et al.* Cannabidiol in medicine: a review of its therapeutic potential in CNS disorders. *Phytotherapy research : PTR* **23**, 597-602, doi:10.1002/ptr.2625 (2009).

87 Pertwee, R. G. Cannabinoid receptor ligands: clinical and neuropharmacological considerations, relevant to future drug discovery and development. *Expert opinion on investigational drugs* **9**, 1553-1571, doi:10.1517/13543784.9.7.1553 (2000).

88 Pacher, P. & Mechoulam, R. Is lipid signaling through cannabinoid 2 receptors part of a protective system? *Progress in lipid research* **50**, 193-211, doi:10.1016/j.plipres.2011.01.001 (2011).

89 Hezode, C. *et al. Daily cannabis use: a novel risk factor of steatosis severity in patients with chronic hepatitis C* 134 thesis, (2008).

90 Purohit, V., Rapaka, R. & Shurtleff, D. Role of cannabinoids in the development of fatty liver (steatosis). *The AAPS journal* **12**, 233-237, doi:10.1208/s12248-010-9178-0 (2010).

91 Osei-Hyiaman, D. *et al.* Hepatic CB1 receptor is required for development of diet-induced steatosis, dyslipidemia, and insulin and leptin resistance in mice. *The Journal of clinical investigation* **118**, 3160-3169, doi:10.1172/jci34827 (2008).

92 Zhang, Y. F., Yuan, Z. Q., Song, D. G., Zhou, X. H. & Wang, Y. Z. Effects of cannabinoid receptor 1 (brain) on lipid accumulation by transcriptional control of CPT1A and CPT1B. *Animal genetics* **45**, 38-47, doi:10.1111/age.12078 (2014).

93 Biswas, K. K. *et al.* Membrane cholesterol but not putative receptors mediates anandamide-induced hepatocyte apoptosis. *Hepatology (Baltimore, Md.)* **38**, 1167-1177, doi:10.1053/jhep.2003.50459 (2003).

94 Sarker, K. P. & Maruyama, I. Anandamide induces cell death independently of cannabinoid receptors or vanilloid receptor 1: possible involvement of lipid rafts. *Cellular and molecular life sciences : CMLS* **60**, 1200-1208, doi:10.1007/s00018-003-3055-2 (2003).

95 Benard, G. *et al.* Mitochondrial CB(1) receptors regulate neuronal energy metabolism. *Nature neuroscience* **15**, 558-564, doi:10.1038/nn.3053 (2012).

96 Lipina, C., Irving, A. J. & Hundal, H. S. Mitochondria: a possible nexus for the regulation of energy homeostasis by the endocannabinoid system? *American journal of physiology. Endocrinology and metabolism* **307**, E1-13, doi:10.1152/ajpendo.00100.2014 (2014).

97 Fisar, Z., Singh, N. & Hroudova, J. Cannabinoid-induced changes in respiration of brain mitochondria. *Toxicology letters* **231**, 62-71, doi:10.1016/j.toxlet.2014.09.002 (2014).

98 Zaccagnino, P., Corcelli, A., Baronio, M. & Lorusso, M. Anandamide inhibits oxidative phosphorylation in isolated liver mitochondria. *FEBS letters* **585**, 429-434, doi:10.1016/j.febslet.2010.12.032 (2011).

99 Catanzaro, G., Rapino, C., Oddi, S. & Maccarrone, M. Anandamide increases swelling and reduces calcium sensitivity of mitochondria. *Biochemical and biophysical research communications* **388**, 439-442, doi:10.1016/j.bbrc.2009.08.037 (2009).

100 Krahenbuhl, S., Fischer, S., Talos, C. & Reichen, J. Ursodeoxycholate protects oxidative mitochondrial metabolism from bile acid toxicity: dose-response study in isolated rat liver mitochondria. *Hepatology* **20**, 1595-1601 (1994).

101 Giannini, E. G., Testa, R. & Savarino, V. Liver enzyme alteration: a guide for clinicians. *CMAJ : Canadian Medical Association journal = journal de l'Association medicale canadienne* **172**, 367-379, doi:10.1503/cmaj.1040752 (2005).

102 Gowda, S. *et al.* A review on laboratory liver function tests. *The Pan African medical journal* **3**, 17 (2009).

103 Murdter, T. E. *et al.* Activity levels of tamoxifen metabolites at the estrogen receptor and the impact of genetic polymorphisms of phase I and II enzymes on their concentration levels in plasma. *Clinical pharmacology and therapeutics* **89**, 708-717, doi:10.1038/clpt.2011.27 (2011).

104 Ribeiro, M. P., Santos, A. E. & Custodio, J. B. Mitochondria: the gateway for tamoxifen-induced liver injury. *Toxicology* **323**, 10-18, doi:10.1016/j.tox.2014.05.009 (2014).

105 He, K. *et al.* Lacteal secretion, fetal and maternal tissue distribution of dasatinib in rats. *Drug metabolism and disposition: the biological fate of chemicals* **36**, 2564-2570, doi:10.1124/dmd.108.022764 (2008).

106 Lau, C. L. *et al.* Sunitinib-ibuprofen drug interaction affects the pharmacokinetics and tissue distribution of sunitinib to brain, liver, and kidney in male and female mice differently. *Fundamental & clinical pharmacology* **29**, 404-416, doi:10.1111/fcp.12126 (2015).

107 Devarbhavi, H. An Update on Drug-induced Liver Injury. *Journal of clinical and experimental hepatology* **2**, 247-259, doi:10.1016/j.jceh.2012.05.002 (2012).

108 Fontana, R. J. Pathogenesis of idiosyncratic drug-induced liver injury and clinical perspectives. *Gastroenterology* **146**, 914-928, doi:10.1053/j.gastro.2013.12.032 (2014).

109 Amacher, D. E. The mechanistic basis for the induction of hepatic steatosis by xenobiotics. *Expert opinion on drug metabolism & toxicology* **7**, 949-965, doi:10.1517/17425255.2011.577740 (2011).

110 Hassan, K., Bhalla, V., El Regal, M. E. & HH, A. K. Nonalcoholic fatty liver disease: a comprehensive review of a growing epidemic. *World journal of gastroenterology : WJG* **20**, 12082-12101, doi:10.3748/wjg.v20.i34.12082 (2014).

111 Schwenger, K. J. & Allard, J. P. Clinical approaches to non-alcoholic fatty liver disease. *World journal of gastroenterology : WJG* **20**, 1712-1723, doi:10.3748/wjg.v20.i7.1712 (2014).

112 Rabinowich, L. & Shibolet, O. Drug Induced Steatohepatitis: An Uncommon Culprit of a Common Disease. *BioMed research international* **2015**, 168905, doi:10.1155/2015/168905 (2015).

113 Mahler, H. *et al.* Fulminant liver failure in association with the emetic toxin of Bacillus cereus. *The New England journal of medicine* **336**, 1142-1148, doi:10.1056/nejm199704173361604 (1997).

114 Machado, M. V. & Cortez-Pinto, H. Non-alcoholic fatty liver disease: what the clinician needs to know. *World journal of gastroenterology : WJG* **20**, 12956-12980, doi:10.3748/wjg.v20.i36.12956 (2014).

115 Dyson, J. & Day, C. Treatment of non-alcoholic fatty liver disease. *Digestive diseases (Basel, Switzerland)* **32**, 597-604, doi:10.1159/000360511 (2014).

116 Niki, E., Yoshida, Y., Saito, Y. & Noguchi, N. Lipid peroxidation: mechanisms, inhibition, and biological effects. *Biochemical and biophysical research communications* **338**, 668-676, doi:10.1016/j.bbrc.2005.08.072 (2005).

117 Murphy, M. P. How mitochondria produce reactive oxygen species. *The Biochemical journal* **417**, 1-13, doi:10.1042/BJ20081386 (2009).

118 Thomas, C., Mackey, M. M., Diaz, A. A. & Cox, D. P. Hydroxyl radical is produced via the Fenton reaction in submitochondrial particles under oxidative stress: implications for diseases associated with iron accumulation. *Redox report : communications in free radical research* **14**, 102-108, doi:10.1179/135100009x392566 (2009).

119 Abdelmagid, S. A. *et al.* Comprehensive Profiling of Plasma Fatty Acid Concentrations in Young Healthy Canadian Adults. *PloS one* **10**, e0116195, doi:10.1371/journal.pone.0116195 (2015).

120 Slotte, J. P. Biological functions of sphingomyelins. *Progress in lipid research* **52**, 424-437, doi:10.1016/j.plipres.2013.05.001 (2013).

121 Buzzetti, E., Pinzani, M. & Tsochatzis, E. A. The multiple-hit pathogenesis of non-alcoholic fatty liver disease (NAFLD). *Metabolism: clinical and experimental* **65**, 1038-1048, doi:10.1016/j.metabol.2015.12.012 (2016).

122 Njølstad, P. R. *et al.* Medium chain acyl-CoA dehydrogenase deficiency and fatal valproate toxicity. *Pediatric Neurology* **16**, 160-162, doi:10.1016/S0887-8994(96)00318-9 (1997).

123 Krahenbuhl, S., Brandner, S., Kleinle, S., Liechti, S. & Straumann, D. Mitochondrial diseases represent a risk factor for valproate-induced fulminant liver failure. *Liver* **20**, 346-348 (2000).

124 Regev, A. Drug-induced liver injury and drug development: industry perspective. *Seminars in liver disease* **34**, 227-239, doi:10.1055/s-0034-1375962 (2014).

125 Chang, C.-W. *et al.* Identification and Categorization of Liver Toxicity Markers Induced by a Related Pair of Drugs. *International journal of molecular sciences* **12**, 4609-4624, doi:10.3390/ijms12074609 (2011).

126 Franco, N. H. Animal Experiments in Biomedical Research: A Historical Perspective. *Animals (Basel)* **3**, 238-273, doi:10.3390/ani3010238 (2013).

127 Parasuraman, S. Toxicological screening. *Journal of Pharmacology & Pharmacotherapeutics* **2**, 74-79, doi:10.4103/0976-500X.81895 (2011).

128 Ringer, S. & Buxton, D. W. Upon the Similarity and Dissimilarity of the behaviour of Cardiac and Skeletal Muscle when brought into relation with Solutions containing Sodium, Calcium and Potassium Salts. *The Journal of physiology* **8**, 288-295 (1887).

129 Roux, W. Beiträge zur Entwickelungsmechanik des Embryo. *Archiv für pathologische Anatomie und Physiologie und für klinische Medicin* **114**, 246-291, doi:10.1007/bf01882630 (1888).

130 Doelle, H. W., Rokem, J. S. & Berovic, M. *BIOTECHNOLOGY - Volume I: Fundamentals in Biotechnology*. (Eolss Publishers, 2009).

131 Lucey, B. P., Nelson-Rees, W. A. & Hutchins, G. M. Henrietta Lacks, HeLa cells, and cell culture contamination. *Archives of pathology & laboratory medicine* **133**, 1463-1467, doi:10.1043/1543-2165-133.9.1463 (2009).

132 Zeilinger, K., Freyer, N., Damm, G., Seehofer, D. & Knospel, F. Cell sources for in vitro human liver cell culture models. *Experimental biology and medicine (Maywood, N.J.)* **241**, 1684-1698, doi:10.1177/1535370216657448 (2016).

133 Gomez-Lechon, M. J., Donato, M. T., Castell, J. V. & Jover, R. Human hepatocytes in primary culture: the choice to investigate drug metabolism in man. *Current drug metabolism* **5**, 443-462 (2004).

134 Hewitt, N. J. *et al.* Studies comparing in vivo:in vitro metabolism of three pharmaceutical compounds in rat, dog, monkey, and human using cryopreserved hepatocytes, microsomes, and collagen gel immobilized hepatocyte cultures. *Drug metabolism and disposition: the biological fate of chemicals* **29**, 1042-1050 (2001).

135 Ullrich, A. *et al.* Long term cultures of primary human hepatocytes as an alternative to drug testing in animals. *Altex* **26**, 295-302 (2009).

136 Jigorel, E., Le Vee, M., Boursier-Neyret, C., Bertrand, M. & Fardel, O. Functional expression of sinusoidal drug transporters in primary human and rat hepatocytes. *Drug metabolism and disposition: the biological fate of chemicals* **33**, 1418-1422, doi:10.1124/dmd.105.004762 (2005).

137 Berger, B. *et al.* Comparison of Liver Cell Models Using the Basel Phenotyping Cocktail. *Frontiers in pharmacology* **7**, 443, doi:10.3389/fphar.2016.00443 (2016).

138 Castell, J. V., Jover, R., Martinez-Jimenez, C. P. & Gomez-Lechon, M. J. Hepatocyte cell lines: their use, scope and limitations in drug metabolism studies. *Expert opinion on drug metabolism & toxicology* **2**, 183-212, doi:10.1517/17425255.2.2.183 (2006).

139 Hengstler, J. G. *et al.* Cryopreserved primary hepatocytes as a constantly available in vitro model for the evaluation of human and animal drug metabolism and enzyme induction. *Drug metabolism reviews* **32**, 81-118, doi:10.1081/dmr-100100564 (2000).

140 Gomez-Lechon, M. J., Tolosa, L. & Donato, M. T. Upgrading HepG2 cells with adenoviral vectors that encode drug-metabolizing enzymes: application for drug hepatotoxicity testing. *Expert opinion on drug metabolism & toxicology* **13**, 137-148, doi:10.1080/17425255.2017.1238459 (2017).

141 Donato, M. T., Lahoz, A., Castell, J. V. & Gomez-Lechon, M. J. Cell lines: a tool for in vitro drug metabolism studies. *Current drug metabolism* **9**, 1-11 (2008).

142 Gomez-Lechon, M. J., Tolosa, L., Conde, I. & Donato, M. T. Competency of different cell models to predict human hepatotoxic drugs. *Expert opinion on drug metabolism & toxicology* **10**, 1553-1568, doi:10.1517/17425255.2014.967680 (2014).

143 Donato, M. T., Tolosa, L. & Gomez-Lechon, M. J. Culture and Functional Characterization of Human Hepatoma HepG2 Cells. *Methods Mol Biol* **1250**, 77-93, doi:10.1007/978-1-4939-2074-7_5 (2015).

144 Javitt, N. B. Hep G2 cells as a resource for metabolic studies: lipoprotein, cholesterol, and bile acids. *FASEB journal : official publication of the Federation of American Societies for Experimental Biology* **4**, 161-168 (1990).

145 Knowles, B. B., Howe, C. C. & Aden, D. P. Human hepatocellular carcinoma cell lines secrete the major plasma proteins and hepatitis B surface antigen. *Science (New York, N.Y.)* **209**, 497-499 (1980).

146 Dongiovanni, P. *et al.* Iron Depletion by Deferoxamine Up-Regulates Glucose Uptake and Insulin Signaling in Hepatoma Cells and in Rat Liver. *The American Journal of Pathology* **172**, 738-747, doi:10.2353/ajpath.2008.070097 (2008).

147 Donato, M. T. *et al.* Cytometric analysis for drug-induced steatosis in HepG2 cells. *Chemico-biological interactions* **181**, 417-423, doi:10.1016/j.cbi.2009.07.019 (2009).

148 Gomez-Lechon, M. J. *et al.* A human hepatocellular in vitro model to investigate steatosis. *Chemico-biological interactions* **165**, 106-116, doi:10.1016/j.cbi.2006.11.004 (2007).

149 International, B. *Origins of the HepaRG cell line*, <https://www.heparg.com/rubrique-origins-of-the-heparg-cell-line> (2018).

150 Antherieu, S., Chesne, C., Li, R., Guguen-Guillouzo, C. & Guillouzo, A. Optimization of the HepaRG cell model for drug metabolism and toxicity studies. *Toxicol In Vitro* **26**, 1278-1285, doi:10.1016/j.tiv.2012.05.008 (2012).

151 Antherieu, S. *et al.* Stable expression, activity, and inducibility of cytochromes P450 in differentiated HepaRG cells. *Drug metabolism and disposition: the biological fate of chemicals* **38**, 516-525, doi:10.1124/dmd.109.030197 (2010).

152 Rogue, A., Lambert, C., Spire, C., Claude, N. & Guillouzo, A. Interindividual variability in gene expression profiles in human hepatocytes and comparison with HepaRG cells. *Drug metabolism and disposition: the biological fate of chemicals* **40**, 151-158, doi:10.1124/dmd.111.042028 (2012).

153 Guillouzo, A. *et al.* The human hepatoma HepaRG cells: a highly differentiated model for studies of liver metabolism and toxicity of xenobiotics. *Chemico-biological interactions* **168**, 66-73, doi:10.1016/j.cbi.2006.12.003 (2007).

154 Krahenbuhl, S., Stucki, J. & Reichen, J. Reduced activity of the electron transport chain in liver mitochondria isolated from rats with secondary biliary cirrhosis. *Hepatology* **15**, 1160-1166 (1992).

155 Grunig, D., Felser, A., Bouitbir, J. & Krahenbuhl, S. The catechol-O-methyltransferase inhibitors tolcapone and entacapone uncouple and inhibit the mitochondrial respiratory chain in HepaRG cells. *Toxicol In Vitro* **42**, 337-347, doi:10.1016/j.tiv.2017.05.013 (2017).

156 Grunig, D., Felser, A., Duthaler, U., Bouitbir, J. & Krahenbuhl, S. Effect of the catechol-O-methyltransferase inhibitors tolcapone and entacapone on fatty acid metabolism in HepaRG cells. *Toxicological sciences : an official journal of the Society of Toxicology*, doi:10.1093/toxsci/kfy101 (2018).

157 Felser, A., Blum, K., Lindinger, P. W., Bouitbir, J. & Krahenbuhl, S. Mechanisms of hepatocellular toxicity associated with dronedarone--a comparison to amiodarone. *Toxicological sciences : an official journal of the Society of Toxicology* **131**, 480-490, doi:10.1093/toxsci/kfs298 (2013).

158 Haegler, P. *et al.* Hepatic Effects of Pharmacological Doses of Hydroxy-Cobalamin[c-lactam] in Mice. *PloS one* **12**, e0171026, doi:10.1371/journal.pone.0171026 (2017).

159 Felser, A. *et al.* Hepatic toxicity of dronedarone in mice: Role of mitochondrial β-oxidation. *Toxicology* **323**, 1-9, doi:http://dx.doi.org/10.1016/j.tox.2014.05.011 (2014).

160 Hornig-Do, H. T. *et al.* Isolation of functional pure mitochondria by superparamagnetic microbeads. *Analytical biochemistry* **389**, 1-5, doi:10.1016/j.ab.2009.02.040 (2009).

161 Krahenbuhl, S., Stucki, J. & Reichen, J. Mitochondrial function in carbon tetrachloride-induced cirrhosis in the rat. Qualitative and quantitative defects. *Biochemical pharmacology* **38**, 1583-1588 (1989).

162 Kappler, L. *et al.* Purity matters: A workflow for the valid high-resolution lipid profiling of mitochondria from cell culture samples. *Sci Rep* **6**, 21107, doi:10.1038/srep21107 (2016).

163 Grünig, D., Duthaler, U. & Krähenbühl, S. Effect of Toxicants on Fatty Acid Metabolism in HepG2 Cells. *Frontiers in pharmacology* **9**, doi:10.3389/fphar.2018.00257 (2018).

164 Agius, L., Peak, M. & Sherratt, S. A. Differences between human, rat and guinea pig hepatocyte cultures. A comparative study of their rates of beta-oxidation and esterification of palmitate and their sensitivity to R-etomoxir. *Biochemical pharmacology* **42**, 1711-1715 (1991).

165 Lilly, K., Chung, C., Kerner, J., VanRenterghem, R. & Bieber, L. L. Effect of etomoxiryl-CoA on different carnitine acyltransferases. *Biochemical pharmacology* **43**, 353-361 (1992).

166 Holubarsch, C. J. *et al.* A double-blind randomized multicentre clinical trial to evaluate the efficacy and safety of two doses of etomoxir in comparison with placebo in patients with moderate congestive heart failure: the ERGO (etomoxir for the recovery of glucose oxidation) study. *Clinical science (London, England : 1979)* **113**, 205-212, doi:10.1042/cs20060307 (2007).

167 Tanaka, K., Kean, E. A. & Johnson, B. Jamaican vomiting sickness. Biochemical investigation of two cases. *The New England journal of medicine* **295**, 461-467, doi:10.1056/nejm197608262950901 (1976).

168 Broadway, N. M. & Engel, P. C. Novel methylenecyclopropyl-based acyl-CoA dehydrogenase inhibitor. *FEBS letters* **437**, 122-126 (1998).

169 Ikeda, Y. & Tanaka, K. Selective inactivation of various acyl-CoA dehydrogenases by (methylenecyclopropyl)acetyl-CoA. *Biochimica et biophysica acta* **1038**, 216-221 (1990).

170 Tserng, K. Y., Jin, S. J. & Hoppel, C. L. Spiropentaneacetic acid as a specific inhibitor of medium-chain acyl-CoA dehydrogenase. *Biochemistry* **30**, 10755-10760 (1991).

171 Yao, K. W., Mao, L. F., Luo, M. J. & Schulz, H. The relationship between mitochondrial activation and toxicity of some substituted carboxylic acids. *Chemico-biological interactions* **90**, 225-234 (1994).

172 el-Aleem, S. A. & Schulz, H. Evaluation of inhibitors of fatty acid oxidation in rat myocytes. *Biochemical pharmacology* **36**, 4307-4312 (1987).

173 Olowe, Y. & Schulz, H. 4-Bromocrotonic acid, an effective inhibitor of fatty acid oxidation and ketone body degradation in rat heart mitochondria. On the rate-determining step of beta-oxidation and ketone body degradation in heart. *The Journal of biological chemistry* **257**, 5408-5413 (1982).

174 Omura, S., Tomoda, H., Xu, Q. M., Takahashi, Y. & Iwai, Y. Triacsins, new inhibitors of acyl-CoA synthetase produced by Streptomyces sp. *The Journal of antibiotics* **39**, 1211-1218 (1986).

175 Tomoda, H., Igarashi, K. & Omura, S. Inhibition of acyl-CoA synthetase by triacsins. *Biochimica et biophysica acta* **921**, 595-598 (1987).

176 Chegary, M. *et al.* Characterization of L-aminocarnitine, an inhibitor of fatty acid oxidation. *Molecular genetics and metabolism* **93**, 403-410, doi:10.1016/j.ymgme.2007.11.001 (2008).

177 Igal, R. A., Wang, P. & Coleman, R. A. Triacsin C blocks de novo synthesis of glycerolipids and cholesterol esters but not recycling of fatty acid into phospholipid: evidence for functionally separate pools of acyl-CoA. *The Biochemical journal* **324 (Pt 2)**, 529-534 (1997).

178 Tomoda, H., Igarashi, K., Cyong, J. C. & Omura, S. Evidence for an essential role of long chain acyl-CoA synthetase in animal cell proliferation. Inhibition of long chain acyl-CoA synthetase by triacsins caused inhibition of Raji cell proliferation. *The Journal of biological chemistry* **266**, 4214-4219 (1991).

179 Bu, S. Y. & Mashek, D. G. Hepatic long-chain acyl-CoA synthetase 5 mediates fatty acid channeling between anabolic and catabolic pathways. *Journal of lipid research* **51**, 3270-3280, doi:10.1194/jlr.M009407 (2010).

180 Kim, J. H., Lewin, T. M. & Coleman, R. A. Expression and characterization of recombinant rat Acyl-CoA synthetases 1, 4, and 5. Selective inhibition by triacsin C and thiazolidinediones. *The Journal of biological chemistry* **276**, 24667-24673, doi:10.1074/jbc.M010793200 (2001).

181 Lewin, T. M., Kim, J. H., Granger, D. A., Vance, J. E. & Coleman, R. A. Acyl-CoA synthetase isoforms 1, 4, and 5 are present in different subcellular membranes in rat liver and can be inhibited independently. *The Journal of biological chemistry* **276**, 24674-24679, doi:10.1074/jbc.M102036200 (2001).

182 Prior, A. M. *et al.* Inhibition of long chain fatty acyl-CoA synthetase (ACSL) and ischemia reperfusion injury. *Bioorganic & medicinal chemistry letters* **24**, 1057-1061, doi:10.1016/j.bmcl.2014.01.016 (2014).

183 Mason, J. W. Amiodarone. *The New England journal of medicine* **316**, 455-466, doi:10.1056/nejm198702193160807 (1987).

184 Olszewska, A. & Szewczyk, A. Mitochondria as a pharmacological target: magnum overview. *IUBMB life* **65**, 273-281, doi:10.1002/iub.1147 (2013).

185 Lewis, J. H. *et al.* Histopathologic analysis of suspected amiodarone hepatotoxicity. *Human pathology* **21**, 59-67 (1990).

186 Lewis, J. H. *et al.* Amiodarone hepatotoxicity: prevalence and clinicopathologic correlations among 104 patients. *Hepatology* **9**, 679-685 (1989).

187 Felser, A. *et al.* Hepatic toxicity of dronedarone in mice: role of mitochondrial beta-oxidation. *Toxicology* **323**, 1-9, doi:10.1016/j.tox.2014.05.011 (2014).

188 McDonald, M. G., Au, N. T. & Rettie, A. E. P450-Based Drug-Drug Interactions of Amiodarone and its Metabolites: Diversity of Inhibitory Mechanisms. *Drug metabolism and disposition: the biological fate of chemicals* **43**, 1661-1669, doi:10.1124/dmd.115.065623 (2015).

189 Pirovino, M., Muller, O., Zysset, T. & Honegger, U. Amiodarone-induced hepatic phospholipidosis: correlation of morphological and biochemical findings in an animal model. *Hepatology* **8**, 591-598 (1988).

190 Lafuente-Lafuente, C. *et al.* Amiodarone concentrations in plasma and fat tissue during chronic treatment and related toxicity. *British Journal of Clinical Pharmacology* **67**, 511-519, doi:10.1111/j.1365-2125.2009.03381.x (2009).

191 Shagufta & Ahmad, I. Tamoxifen a pioneering drug: An update on the therapeutic potential of tamoxifen derivatives. *European journal of medicinal chemistry* **143**, 515-531, doi:10.1016/j.ejmech.2017.11.056 (2017).

192 Yang, G., Nowsheen, S., Aziz, K. & Georgakilas, A. G. Toxicity and adverse effects of Tamoxifen and other anti-estrogen drugs. *Pharmacology & therapeutics* **139**, 392-404, doi:10.1016/j.pharmthera.2013.05.005 (2013).

193 Schweizerische Gesellschaft für Chemische Industrie. (Documed, Basel).

194 Nishino, M., Hayakawa, K., Nakamura, Y., Morimoto, T. & Mukaihara, S. Effects of tamoxifen on hepatic fat content and the development of hepatic steatosis in patients with breast cancer: high

frequency of involvement and rapid reversal after completion of tamoxifen therapy. *AJR. American journal of roentgenology* **180**, 129-134, doi:10.2214/ajr.180.1.1800129 (2003).

195 United States Department of, H., Human Services. Substance, A., Mental Health Services Administration. Center for Behavioral Health, S. & Quality. (Inter-university Consortium for Political and Social Research (ICPSR) [distributor], 2014).

196 Schweiz Sektion Kriminalität und Strafrecht & Schweiz Bundesamt für Statistik. *Polizeiliche Kriminalstatistik (PKS) Jahresbericht 2014*. (Office fédéral de la statistique (OFS), 2014).

197 Gmel, G. *Veränderungen im Cannabiskonsum 2004-2007 Ergebnisse des Schweizerischen Cannabismonitorings*. (Schweizerische Eidgenossenschaft, Eidgenössisches Departement des Innern EDI, 2008).

198 Guzman, M. *et al.* Oleoylethanolamide stimulates lipolysis by activating the nuclear receptor peroxisome proliferator-activated receptor alpha (PPAR-alpha). *The Journal of biological chemistry* **279**, 27849-27854, doi:10.1074/jbc.M404087200 (2004).

199 Yang, Y.-Y. & Lin, H.-C. Cross-regulation of cannabinoid CB1 and CB2 receptors governs hepatic steatosis. *Liver International* **30**, 1397-1399, doi:10.1111/j.1478-3231.2010.02352.x (2010).

200 De Gottardi, A., Spahr, L., Ravier-Dall'Antonia, F. & Hadengue, A. Cannabinoid receptor 1 and 2 agonists increase lipid accumulation in hepatocytes. *Liver international : official journal of the International Association for the Study of the Liver* **30**, 1482-1489, doi:10.1111/j.1478-3231.2010.02298.x (2010).

201 de Lau, L. M. & Breteler, M. M. Epidemiology of Parkinson's disease. *The Lancet. Neurology* **5**, 525-535, doi:10.1016/s1474-4422(06)70471-9 (2006).

202 Kaakkola, S. Clinical pharmacology, therapeutic use and potential of COMT inhibitors in Parkinson's disease. *Drugs* **59**, 1233-1250 (2000).

203 Muller, T. Catechol-O-methyltransferase inhibitors in Parkinson's disease. *Drugs* **75**, 157-174, doi:10.1007/s40265-014-0343-0 (2015).

204 Kaakkola, S. Problems with the present inhibitors and a relevance of new and improved COMT inhibitors in Parkinson's disease. *International review of neurobiology* **95**, 207-225, doi:10.1016/b978-0-12-381326-8.00009-0 (2010).

205 Eggert, K., Oertel, W. H. & Lees, A. J. Safety and efficacy of tolcapone in the long-term use in Parkinson disease: an observational study. *Clinical neuropharmacology* **37**, 1-5, doi:10.1097/wnf.0000000000000008 (2014).

206 Haasio, K., Koponen, A., Penttila, K. E. & Nissinen, E. Effects of entacapone and tolcapone on mitochondrial membrane potential. *European journal of pharmacology* **453**, 21-26 (2002).

207 Haasio, K., Nissinen, E., Sopanen, L. & Heinonen, E. H. Different toxicological profile of two COMT inhibitors in vivo: the role of uncoupling effects. *Journal of neural transmission (Vienna, Austria : 1996)* **109**, 1391-1401, doi:10.1007/s00702-002-0748-x (2002).

208 Nissinen, E., Kaheinen, P., Penttila, K. E., Kaivola, J. & Linden, I. B. Entacapone, a novel catechol-O-methyltransferase inhibitor for Parkinson's disease, does not impair mitochondrial energy production. *European journal of pharmacology* **340**, 287-294 (1997).

209 Spahr, L., Rubbia-Brandt, L., Burkhard, P. R., Assal, F. & Hadengue, A. Tolcapone-related fulminant hepatitis: electron microscopy shows mitochondrial alterations. *Digestive diseases and sciences* **45**, 1881-1884 (2000).

210 McBurney, R. N. *et al.* The liver toxicity biomarker study phase I: markers for the effects of tolcapone or entacapone. *Toxicologic pathology* **40**, 951-964, doi:10.1177/0192623312444026 (2012).

211 Fischer, J. J. *et al.* Capture compound mass spectrometry sheds light on the molecular mechanisms of liver toxicity of two Parkinson drugs. *Toxicological sciences : an official journal of the Society of Toxicology* **113**, 243-253, doi:10.1093/toxsci/kfp236 (2010).

212 Assal, F., Spahr, L., Hadengue, A., Rubbia-Brandt, L. & Burkhard, P. R. Tolcapone and fulminant hepatitis. *Lancet (London, England)* **352**, 958 (1998).

213 Rouru, J. *et al.* Pharmacokinetics of oral entacapone after frequent multiple dosing and effects on levodopa disposition. *European journal of clinical pharmacology* **55**, 461-467 (1999).

214 Haasio, K. Toxicology and safety of COMT inhibitors. *International review of neurobiology* **95**, 163-189, doi:10.1016/b978-0-12-381326-8.00007-7 (2010).

215 Bakke, O. M., Manocchia, M., de Abajo, F., Kaitin, K. I. & Lasagna, L. Drug safety discontinuations in the United Kingdom, the United States, and Spain from 1974 through 1993: a regulatory perspective. *Clinical pharmacology and therapeutics* **58**, 108-117, doi:10.1016/0009-9236(95)90078-0 (1995).

216 Tujios, S. & Fontana, R. J. Mechanisms of drug-induced liver injury: from bedside to bench. *Nature reviews. Gastroenterology & hepatology* **8**, 202-211, doi:10.1038/nrgastro.2011.22 (2011).

217 Brass, E. P. & Hoppel, C. L. Carnitine metabolism in the fasting rat. *The Journal of biological chemistry* **253**, 2688-2693 (1978).

218 Vreken, P. *et al.* Quantitative plasma acylcarnitine analysis using electrospray tandem mass spectrometry for the diagnosis of organic acidaemias and fatty acid oxidation defects. *Journal of inherited metabolic disease* **22**, 302-306 (1999).

219 Wilcken, B. & Wiley, V. Fifty years of newborn screening. *Journal of paediatrics and child health* **51**, 103-107, doi:10.1111/jpc.12817 (2015).

220 Minkler, P. E. & Hoppel, C. L. Quantification of free carnitine, individual short- and medium-chain acylcarnitines, and total carnitine in plasma by high-performance liquid chromatography. *Analytical biochemistry* **212**, 510-518, doi:10.1006/abio.1993.1361 (1993).

221 Rinaldo, P., Cowan, T. M. & Matern, D. Acylcarnitine profile analysis. *Genetics in medicine : official journal of the American College of Medical Genetics* **10**, 151-156, doi:10.1097/GIM.0b013e3181614289 (2008).

222 Pietrocola, F., Galluzzi, L., Bravo-San Pedro, J. M., Madeo, F. & Kroemer, G. Acetyl coenzyme A: a central metabolite and second messenger. *Cell metabolism* **21**, 805-821, doi:10.1016/j.cmet.2015.05.014 (2015).

223 Farrell, S., Vogel, J. & Bieber, L. L. Entry of acetyl-L-carnitine into biosynthetic pathways. *Biochimica et biophysica acta* **876**, 175-177 (1986).

224 Viollet, B. *et al.* Activation of AMP-activated protein kinase in the liver: a new strategy for the management of metabolic hepatic disorders. *The Journal of physiology* **574**, 41-53, doi:10.1113/jphysiol.2006.108506 (2006).

225 Amacher, D. E. & Chalasani, N. Drug-induced hepatic steatosis. *Seminars in liver disease* **34**, 205-214, doi:10.1055/s-0034-1375960 (2014).

226 Krahenbuhl, S., Talos, C. & Reichen, J. Mechanisms of impaired hepatic fatty acid metabolism in rats with long-term bile duct ligation. *Hepatology* **19**, 1272-1281 (1994).

227 Brass, E. P. Effect of alpha-ketobutyrate on palmitic acid and pyruvate metabolism in isolated rat hepatocytes. *Biochimica et biophysica acta* **888**, 18-24 (1986).

228 Brass, E. P., Fennessey, P. V. & Miller, L. V. Inhibition of oxidative metabolism by propionic acid and its reversal by carnitine in isolated rat hepatocytes. *The Biochemical journal* **236**, 131-136 (1986).

229 Huynh, F. K., Green, M. F., Koves, T. R. & Hirschey, M. D. Measurement of fatty acid oxidation rates in animal tissues and cell lines. *Methods in enzymology* **542**, 391-405, doi:10.1016/b978-0-12-416618-9.00020-0 (2014).

230 Eckerman, K., Wolbarst, A. & Richardson, A. C. B. *Limiting values of radionuclide intake and air concentration and dose conversion factors for inhalation, submersion, and ingestion: Federal guidance report No. 11.* (1988).

231 Chace, D. H., Hillman, S. L., Van Hove, J. L. & Naylor, E. W. Rapid diagnosis of MCAD deficiency: quantitative analysis of octanoylcarnitine and other acylcarnitines in newborn blood spots by tandem mass spectrometry. *Clin Chem* **43**, 2106-2113 (1997).

232 Minkler, P. E. *et al.* Quantification of carnitine and acylcarnitines in biological matrices by HPLC electrospray ionization-mass spectrometry. *Clin Chem* **54**, 1451-1462, doi:10.1373/clinchem.2007.099226 (2008).

233 Millington, D. S. & Stevens, R. D. Acylcarnitines: analysis in plasma and whole blood using tandem mass spectrometry. *Methods Mol Biol* **708**, 55-72, doi:10.1007/978-1-61737-985-7_3 (2011).

234 Amacher, D. E. Strategies for the early detection of drug-induced hepatic steatosis in preclinical drug safety evaluation studies. *Toxicology* **279**, 10-18, doi:10.1016/j.tox.2010.10.006 (2011).

235 McMillian, M. K. *et al.* Nile Red binding to HepG2 cells: an improved assay for in vitro studies of hepatosteatosis. *In vitro & molecular toxicology* **14**, 177-190, doi:10.1089/109793301753407948 (2001).

236 Amacher, D. E. & Martin, B. A. Tetracycline-induced steatosis in primary canine hepatocyte cultures. *Fundamental and applied toxicology : official journal of the Society of Toxicology* **40**, 256-263 (1997).

237 Fujimura, H., Murakami, N., Kurabe, M. & Toriumi, W. In vitro assay for drug-induced hepatosteatosis using rat primary hepatocytes, a fluorescent lipid analog and gene expression analysis. *Journal of applied toxicology : JAT* **29**, 356-363, doi:10.1002/jat.1420 (2009).

238 Dechandt, C. R. P. *et al.* Triacsin C reduces lipid droplet formation and induces mitochondrial biogenesis in primary rat hepatocytes. *Journal of bioenergetics and biomembranes* **49**, 399-411, doi:10.1007/s10863-017-9725-9 (2017).

239 Fong, J. C., Leu, S. J. & Chai, S. P. Differential inhibition of lipolysis by 2-bromopalmitic acid and 4-bromocrotonic acid in 3T3-L1 adipocytes. *Biochimica et biophysica acta* **1344**, 65-73 (1997).

240 Leu, S. J., Chai, S. P., Kwok, C. F. & Fong, J. C. 4-Bromocrotonic acid enhances basal but inhibits insulin-stimulated glucose transport in 3T3-L1 adipocytes. *Biochemical and biophysical research communications* **244**, 11-14, doi:10.1006/bbrc.1998.8207 (1998).

241 Schott, M. B. *et al.* beta-Adrenergic induction of lipolysis in hepatocytes is inhibited by ethanol exposure. *The Journal of biological chemistry* **292**, 11815-11828, doi:10.1074/jbc.M117.777748 (2017).

242 Brien, J. F., Jimmo, S., Brennan, F. J., Ford, S. E. & Armstrong, P. W. Distribution of amiodarone and its metabolite, desethylamiodarone, in human tissues. *Canadian journal of physiology and pharmacology* **65**, 360-364 (1987).

243 Fromenty, B. *et al.* Dual effect of amiodarone on mitochondrial respiration. Initial protonophoric uncoupling effect followed by inhibition of the respiratory chain at the levels of complex I and complex II. *The Journal of pharmacology and experimental therapeutics* **255**, 1377-1384 (1990).

244 Spaniol, M., Bracher, R., Ha, H. R., Follath, F. & Krahenbuhl, S. Toxicity of amiodarone and amiodarone analogues on isolated rat liver mitochondria. *J Hepatol* **35**, 628-636 (2001).

245 Fromenty, B. *et al.* Amiodarone inhibits the mitochondrial beta-oxidation of fatty acids and produces microvesicular steatosis of the liver in mice. *The Journal of pharmacology and experimental therapeutics* **255**, 1371-1376 (1990).

246 Letteron, P., Fromenty, B., Terris, B., Degott, C. & Pessayre, D. Acute and chronic hepatic steatosis lead to in vivo lipid peroxidation in mice. *J Hepatol* **24**, 200-208 (1996).

247 Letteron, P., Sutton, A., Mansouri, A., Fromenty, B. & Pessayre, D. Inhibition of microsomal triglyceride transfer protein: another mechanism for drug-induced steatosis in mice. *Hepatology* **38**, 133-140, doi:10.1053/jhep.2003.50309 (2003).

248 Antherieu, S., Rogue, A., Fromenty, B., Guillouzo, A. & Robin, M. A. Induction of vesicular steatosis by amiodarone and tetracycline is associated with up-regulation of lipogenic genes in HepaRG cells. *Hepatology* **53**, 1895-1905, doi:10.1002/hep.24290 (2011).

249 Szalowska, E., van der Burg, B., Man, H. Y., Hendriksen, P. J. & Peijnenburg, A. A. Model steatogenic compounds (amiodarone, valproic acid, and tetracycline) alter lipid metabolism by different mechanisms in mouse liver slices. *PloS one* **9**, e86795, doi:10.1371/journal.pone.0086795 (2014).

250 Daurio, N. A. *et al.* AMPK Activation and Metabolic Reprogramming by Tamoxifen through Estrogen Receptor-Independent Mechanisms Suggests New Uses for This Therapeutic Modality in Cancer Treatment. *Cancer research* **76**, 3295-3306, doi:10.1158/0008-5472.can-15-2197 (2016).

251 Gudbrandsen, O. A., Rost, T. H. & Berge, R. K. Causes and prevention of tamoxifen-induced accumulation of triacylglycerol in rat liver. *Journal of lipid research* **47**, 2223-2232, doi:10.1194/jlr.M600148-JLR200 (2006).

252 Fleischmann, M. & Iynedjian, P. B. Regulation of sterol regulatory-element binding protein 1 gene expression in liver: role of insulin and protein kinase B/cAkt. *The Biochemical journal* **349**, 13-17 (2000).

253 Porstmann, T. *et al.* PKB/Akt induces transcription of enzymes involved in cholesterol and fatty acid biosynthesis via activation of SREBP. *Oncogene* **24**, 6465-6481, doi:10.1038/sj.onc.1208802 (2005).

254 Zhao, F. *et al.* The effect and mechanism of tamoxifen-induced hepatocyte steatosis in vitro. *International journal of molecular sciences* **15**, 4019-4030, doi:10.3390/ijms15034019 (2014).

255 Robinson, S. P., Langan-Fahey, S. M., Johnson, D. A. & Jordan, V. C. Metabolites, pharmacodynamics, and pharmacokinetics of tamoxifen in rats and mice compared to the breast cancer patient. *Drug metabolism and disposition: the biological fate of chemicals* **19**, 36-43 (1991).

256 Cole, L. K., Jacobs, R. L. & Vance, D. E. Tamoxifen induces triacylglycerol accumulation in the mouse liver by activation of fatty acid synthesis. *Hepatology* **52**, 1258-1265, doi:10.1002/hep.23813 (2010).

257 Larosche, I. *et al.* Tamoxifen inhibits topoisomerases, depletes mitochondrial DNA, and triggers steatosis in mouse liver. *The Journal of pharmacology and experimental therapeutics* **321**, 526-535, doi:10.1124/jpet.106.114546 (2007).

258 de Conti, A. *et al.* Genotoxic, epigenetic, and transcriptomic effects of tamoxifen in mouse liver. *Toxicology* **325**, 12-20, doi:10.1016/j.tox.2014.08.004 (2014).

259 Lelliott, C. J. *et al.* Transcript and metabolite analysis of the effects of tamoxifen in rat liver reveals inhibition of fatty acid synthesis in the presence of hepatic steatosis. *FASEB journal : official publication of the Federation of American Societies for Experimental Biology* **19**, 1108-1119, doi:10.1096/fj.04-3196com (2005).

260 Roder, K., Zhang, L. & Schweizer, M. SREBP-1c mediates the retinoid-dependent increase in fatty acid synthase promoter activity in HepG2. *FEBS letters* **581**, 2715-2720, doi:10.1016/j.febslet.2007.05.022 (2007).

261 Cardoso, C. M., Moreno, A. J., Almeida, L. M. & Custodio, J. B. 4-Hydroxytamoxifen induces slight uncoupling of mitochondrial oxidative phosphorylation system in relation to the deleterious effects of tamoxifen. *Toxicology* **179**, 221-232 (2002).

262 Cardoso, C. M., Custodio, J. B., Almeida, L. M. & Moreno, A. J. Mechanisms of the deleterious effects of tamoxifen on mitochondrial respiration rate and phosphorylation efficiency. *Toxicology and applied pharmacology* **176**, 145-152, doi:10.1006/taap.2001.9265 (2001).

263 Moreira, P. I., Custodio, J., Moreno, A., Oliveira, C. R. & Santos, M. S. Tamoxifen and estradiol interact with the flavin mononucleotide site of complex I leading to mitochondrial failure. *The Journal of biological chemistry* **281**, 10143-10152, doi:10.1074/jbc.M510249200 (2006).

264 Tuquet, C., Dupont, J., Mesneau, A. & Roussaux, J. Effects of tamoxifen on the electron transport chain of isolated rat liver mitochondria. *Cell biology and toxicology* **16**, 207-219 (2000).

265 Birzniece, V., Barrett, P. H. R. & Ho, K. K. Y. Tamoxifen reduces hepatic VLDL production and GH secretion in women: a possible mechanism for steatosis development. *European journal of endocrinology* **177**, 137-143, doi:10.1530/eje-17-0151 (2017).

266 Brun, L. D., Gagne, C., Rousseau, C., Moorjani, S. & Lupien, P. J. Severe lipemia induced by tamoxifen. *Cancer* **57**, 2123-2126 (1986).

267 Gupta, S. *et al.* Effects of tamoxifen therapy on plasma lipid profile in patients of breast cancer. *The Journal of the Association of Physicians of India* **54**, 183-186 (2006).

268 Bruning, P. F. *et al.* Tamoxifen, serum lipoproteins and cardiovascular risk. *British journal of cancer* **58**, 497-499 (1988).

269 Liberopoulos, E. *et al.* Are the effects of tamoxifen on the serum lipid profile modified by apolipoprotein E phenotypes? *Oncology* **62**, 115-120, doi:10.1159/000048256 (2002).

270 Bagdade, J. D., Wolter, J., Subbaiah, P. V. & Ryan, W. Effects of tamoxifen treatment on plasma lipids and lipoprotein lipid composition. *The Journal of clinical endocrinology and metabolism* **70**, 1132-1135, doi:10.1210/jcem-70-4-1132 (1990).

271 Sahebkar, A. *et al.* The Effects of Tamoxifen on Plasma Lipoprotein(a) Concentrations: Systematic Review and Meta-Analysis. *Drugs* **77**, 1187-1197, doi:10.1007/s40265-017-0767-4 (2017).

272 Liu, C. L. & Yang, T. L. Sequential changes in serum triglyceride levels during adjuvant tamoxifen therapy in breast cancer patients and the effect of dose reduction. *Breast cancer research and treatment* **79**, 11-16 (2003).

273 Hozumi, Y., Kawano, M., Hakamata, Y., Miyata, M. & Jordan, V. C. Tamoxifen inhibits lipoprotein activity: in vivo and in vitro studies. *Hormone research* **53**, 36-39, doi:10.1159/000023511 (2000).

274 Kawano, M., Hozumi, Y. & Itoh, K. Tamoxifen might influence the affinity of LPL for heparin-sepharose. *Clin Chim Acta* **337**, 141-145 (2003).

275 Geiser, A. G. *et al.* A new selective estrogen receptor modulator with potent uterine antagonist activity, agonist activity in bone, and minimal ovarian stimulation. *Endocrinology* **146**, 4524-4535, doi:10.1210/en.2005-0024 (2005).

276 Weng, S. C. *et al.* Sensitizing estrogen receptor-negative breast cancer cells to tamoxifen with OSU-03012, a novel celecoxib-derived phosphoinositide-dependent protein kinase-1/Akt signaling inhibitor. *Molecular cancer therapeutics* **7**, 800-808, doi:10.1158/1535-7163.mct-07-0434 (2008).

277 Osei-Hyiaman, D. *et al.* Endocannabinoid activation at hepatic CB1 receptors stimulates fatty acid synthesis and contributes to diet-induced obesity. *The Journal of clinical investigation* **115**, 1298-1305, doi:10.1172/jci23057 (2005).

278 Vettor, R. & Pagano, C. The role of the endocannabinoid system in lipogenesis and fatty acid metabolism. *Best Practice & Research Clinical Endocrinology & Metabolism* **23**, 51-63, doi:10.1016/j.beem.2008.10.002 (2009).

279 Aso, E. & Ferrer, I. Cannabinoids for treatment of Alzheimer's disease: moving toward the clinic. *Frontiers in pharmacology* **5**, 37, doi:10.3389/fphar.2014.00037 (2014).

280 Shi, D. *et al.* Inhibiting CB1 receptors improves lipogenesis in an in vitro non-alcoholic fatty liver disease model. *Lipids in health and disease* **13**, 173, doi:10.1186/1476-511x-13-173 (2014).

281 Mallat, A., Teixeira-Clerc, F. & Lotersztajn, S. Cannabinoid signaling and liver therapeutics. *Journal of Hepatology* **59**, 891-896, doi:10.1016/j.jhep.2013.03.032 (2013).

282 Zduniak, K. *et al.* Immunohistochemical analysis of cannabinoid receptor 1 expression in steatotic rat livers. *Experimental and therapeutic medicine* **11**, 1227-1230, doi:10.3892/etm.2016.3036 (2016).

283 Parfieniuk, A. & Flisiak, R. Role of cannabinoids in chronic liver diseases. *World journal of gastroenterology : WJG* **14**, 6109-6114 (2008).

284 Jourdan, T. *et al.* Antagonism of peripheral hepatic cannabinoid receptor-1 improves liver lipid metabolism in mice: evidence from cultured explants. *Hepatology* **55**, 790-799, doi:10.1002/hep.24733 (2012).

285 Kabir, M. *et al.* CB1R antagonist increases hepatic insulin clearance in fat-fed dogs likely via upregulation of liver adiponectin receptors. *American Journal of Physiology - Endocrinology and Metabolism* **309**, E747-E758, doi:10.1152/ajpendo.00196.2015 (2015).

286 Jeong, W. I. *et al.* Paracrine activation of hepatic CB1 receptors by stellate cell-derived endocannabinoids mediates alcoholic fatty liver. *Cell metabolism* **7**, 227-235, doi:10.1016/j.cmet.2007.12.007 (2008).

287 Melck, D. *et al.* Involvement of the cAMP/protein kinase A pathway and of mitogen-activated protein kinase in the anti-proliferative effects of anandamide in human breast cancer cells. *FEBS letters* **463**, 235-240 (1999).

288 Kerner, J. *et al.* Phosphorylation of Rat Liver Mitochondrial Carnitine Palmitoyltransferase-I: EFFECT ON THE KINETIC PROPERTIES OF THE ENZYME. *Journal of Biological Chemistry* **279**, 41104-41113, doi:10.1074/jbc.M406570200 (2004).

289 Singh, N., Hroudova, J. & Fisar, Z. Cannabinoid-Induced Changes in the Activity of Electron Transport Chain Complexes of Brain Mitochondria. *Journal of molecular neuroscience : MN* **56**, 926-931, doi:10.1007/s12031-015-0545-2 (2015).

290 Athanasiou, A. *et al.* Cannabinoid receptor agonists are mitochondrial inhibitors: a unified hypothesis of how cannabinoids modulate mitochondrial function and induce cell death. *Biochemical and biophysical research communications* **364**, 131-137, doi:10.1016/j.bbrc.2007.09.107 (2007).

291 Hebert-Chatelain, E. *et al.* Cannabinoid control of brain bioenergetics: Exploring the subcellular localization of the CB1 receptor. *Mol Metab* **3**, 495-504, doi:10.1016/j.molmet.2014.03.007 (2014).

292 Wolff, V. *et al.* Tetrahydrocannabinol induces brain mitochondrial respiratory chain dysfunction and increases oxidative stress: a potential mechanism involved in cannabis-related stroke. *BioMed research international* **2015**, 323706, doi:10.1155/2015/323706 (2015).

293 Jornayvaz, F. R. & Shulman, G. I. Regulation of mitochondrial biogenesis. *Essays in biochemistry* **47**, 69-84, doi:10.1042/bse0470069 (2010).

294 Tedesco, L. *et al.* Cannabinoid type 1 receptor blockade promotes mitochondrial biogenesis through endothelial nitric oxide synthase expression in white adipocytes. *Diabetes* **57**, 2028-2036, doi:10.2337/db07-1623 (2008).

295 Tedesco, L. *et al.* Cannabinoid receptor stimulation impairs mitochondrial biogenesis in mouse white adipose tissue, muscle, and liver: the role of eNOS, p38 MAPK, and AMPK pathways. *Diabetes* **59**, 2826-2836, doi:10.2337/db09-1881 (2010).

296 Liu, J. *et al.* Hepatic Cannabinoid Receptor-1 Mediates Diet-Induced Insulin Resistance via Inhibition of Insulin Signaling and Clearance in Mice. *Gastroenterology* **142**, 1218-1228.e1211, doi:10.1053/j.gastro.2012.01.032 (2012).

297 Lew, M. F. & Kricorian, G. Results from a 2-year centralized tolcapone liver enzyme monitoring program. *Clinical neuropharmacology* **30**, 281-286, doi:10.1097/WNF.0b013e318149f290 (2007).

298 Haasio, K., Sopanen, L., Vaalavirta, L., Linden, I. B. & Heinonen, E. H. Comparative toxicological study on the hepatic safety of entacapone and tolcapone in the rat. *J Neural Transm (Vienna)* **108**, 79-91, doi:10.1007/s007020170099 (2001).

299 Haasio, K., Lounatmaa, K. & Sukura, A. Entacapone does not induce conformational changes in liver mitochondria or skeletal muscle in vivo. *Experimental and toxicologic pathology : official journal of the Gesellschaft fur Toxikologische Pathologie* **54**, 9-14, doi:10.1078/0940-2993-00228 (2002).

300 Tafazoli, S., Spehar, D. D. & O'Brien, P. J. Oxidative stress mediated idiosyncratic drug toxicity. *Drug metabolism reviews* **37**, 311-325, doi:10.1081/dmr-55227 (2005).

301 Bertolini, F., Novaroli, L., Carrupt, P. A. & Reist, M. Novel screening assay for antioxidant protection against peroxyl radical-induced loss of protein function. *Journal of pharmaceutical sciences* **96**, 2931-2944, doi:10.1002/jps.20881 (2007).

302 Korshunov, S. S., Skulachev, V. P. & Starkov, A. A. High protonic potential actuates a mechanism of production of reactive oxygen species in mitochondria. *FEBS letters* **416**, 15-18 (1997).

303 Smith, K. S. *et al.* In vitro metabolism of tolcapone to reactive intermediates: relevance to tolcapone liver toxicity. *Chemical research in toxicology* **16**, 123-128, doi:10.1021/tx025569n (2003).

304 Doege, H. *et al.* Targeted deletion of FATP5 reveals multiple functions in liver metabolism: alterations in hepatic lipid homeostasis. *Gastroenterology* **130**, 1245-1258, doi:10.1053/j.gastro.2006.02.006 (2006).

305 Coburn, C. T., Hajri, T., Ibrahimi, A. & Abumrad, N. A. Role of CD36 in membrane transport and utilization of long-chain fatty acids by different tissues. *Journal of Molecular Neuroscience* **16**, 117-121, doi:10.1385/JMN:16:2-3:117 (2001).

306 Morgan, R. E. *et al.* A multifactorial approach to hepatobiliary transporter assessment enables improved therapeutic compound development. *Toxicological sciences : an official journal of the Society of Toxicology* **136**, 216-241, doi:10.1093/toxsci/kft176 (2013).

307 Krahenbuhl, S., Talos, C., Lauterburg, B. H. & Reichen, J. Reduced antioxidative capacity in liver mitochondria from bile duct ligated rats. *Hepatology* **22**, 607-612 (1995).

308 Lang, C. *et al.* Impaired hepatic fatty acid oxidation in rats with short-term cholestasis: characterization and mechanism. *Journal of lipid research* **42**, 22-30 (2001).

309 Korlipara, L. V., Cooper, J. M. & Schapira, A. H. Differences in toxicity of the catechol-O-methyl transferase inhibitors, tolcapone and entacapone to cultured human neuroblastoma cells. *Neuropharmacology* **46**, 562-569, doi:10.1016/j.neuropharm.2003.10.015 (2004).

310 Longo, D. M., Yang, Y., Watkins, P. B., Howell, B. A. & Siler, S. Q. Elucidating Differences in the Hepatotoxic Potential of Tolcapone and Entacapone With DILIsym((R)), a Mechanistic Model of Drug-Induced Liver Injury. *CPT: pharmacometrics & systems pharmacology* **5**, 31-39, doi:10.1002/psp4.12053 (2016).

311 Coleman, R. A., Rao, P., Fogelsong, R. J. & Bardes, E. S. G. 2-Bromopalmitoyl-CoA and 2-bromopalmitate: Promiscuous inhibitors of membrane-bound enzymes. *Biochimica et Biophysica Acta (BBA) - Lipids and Lipid Metabolism* **1125**, 203-209, doi:https://doi.org/10.1016/0005-2760(92)90046-X (1992).

312 Agnihotri, G. & Liu, H.-w. Enoyl-CoA hydratase: Reaction, mechanism, and inhibition. *Bioorganic & Medicinal Chemistry* **11**, 9-20, doi:https://doi.org/10.1016/S0968-0896(02)00333-4 (2003).

313 Kissinger, C. R. *et al.* Crystal structure of human ABAD/HSD10 with a bound inhibitor: implications for design of Alzheimer's disease therapeutics. *Journal of molecular biology* **342**, 943-952, doi:10.1016/j.jmb.2004.07.071 (2004).

314 Hashimoto, T., Shindo, Y., Souri, M. & Baldwin, G. S. A new inhibitor of mitochondrial fatty acid oxidation. *Journal of biochemistry* **119**, 1196-1201 (1996).

5. ACKNOWLEDGMENT

First, I would like to express my sincerest thanks and gratitude to my doctoral advisor **Prof. Stephan Krähenbühl**. He granted me not only the possibility of two master degrees and a PhD position but also motivated me throughout the years in my scientific achievements. I am deeply thankful for learning from your extensive knowledge and always enjoyed the sometimes lengthy discussions about difficult scientific problems. Thank you for your encouragement and advice!

My deepest gratitude, of course, also goes to the outstanding scientists of the Labs 410 and 411. Thank you so much **Jamal**, for always having an ear and advice about mitochondrial problems, as well as on various other topics from work or life. The time with you was always better than Eschguet! It was always a pleasure stopping by for a coffee in the Postdoc cubicle, which was of course also thanks to **Urs.** Although you replaced me as the tallest person in the lab, I could never be mad at you, as you also became a cherished friend of mine. I am also sincerely thankful that you introduced me to the mystical topics of LC-MS, and trusted me to tamper with your machines.

My friend **Riccardo** with two c's, also to you, I send my great thanks, not only for answering every question about flow-cytometry or immunology, but mostly for the wild, silly, funny, but also serious discussions during the probably thousands of coffees we had.

During my time as PhD student, I had the pleasure to supervise two master students, who could not have been more different in character, however both greatly valuable for my work. Thank you very much **Martina** for your exemplary work and contributions. Also thank you **Leonora** for your excellent work, I greatly enjoyed the discussions and fun times we had, during our time together in 410.

I really had a wonderful time in this lab, which would have not been possible without my lab neighbor **Deborah**, as well as **Dino**, it was always a pleasure to spend time with you two. A person, I also will never forget is of course **Gerda**. I hope we will have many dance battles in the future to come. **Fabio** also deserves my great thanks, you brought a whole bucket of fun into the lab and you were always there for the infamous after-work beer. And of course, let's not forget **Miljenko, Bea, Patrizia, Benji, Franziska, Anna, Noëmi, Karolina, Xun, and Evelyne**. You all contributed to my fabulous time, working in Clinical Pharmacology and Toxicology!

Last, but certainly not least, my thanks goes out to all my **loved ones**, who supported me in all the years. Danke viel mohl vor allem minere **Familie**! Das ihr mich immer so guet unterstützt hend über die viele Johr vo minere Usbildig und fürs Verständniss dasi so selte zrugg in schöne Ottoberg cho bin. Jetzt bini halt doch nöd Koch worde…

Grünig